Institut für Nutzpflanzenwissenschaften

und Ressourcenschutz (INRES)

Responses of the root-associated microbiota to pathogen infection and pest management strategies

Dissertation

zur Erlangung des Grades

Doktor der Agrarwissenschaften (Dr. agr.)

der Agrar-, Ernährungs- und Ingenieurwissenschaftlichen Fakultät

der Rheinischen Friedrich-Wilhelms-Universität Bonn

von

Maximilian Fernando Becker

aus

Herten, Deutschland

Bonn, 2026

Angefertigt mit Genehmigung der Agrar-, Ernährungs- und Ingenieurwissenschaftlichen Fakultät der Rheinischen Friedrich-Wilhelms-Universität Bonn.

Referentin: Prof. Dr. Claudia Knief

Korreferentin: PD Dr. Ulrike Steiner

Korreferent: Prof. Dr. Michael Schloter

Tag der mündlichen Prüfung: 15.01.2026

„Nothing in life is to be feared, it is only to be understood. Now is the time to understand more, so that we may fear less.“ – Marie Curie

Teile der in dieser Dissertation beschriebenen Ergebnisse sind in folgenden Originalpublikationen veröffentlicht:

Becker, M., Hellmann, M. & Knief, C. Spatio-temporal variation in the root-associated microbiota of orchard-grown apple trees. *Environmental Microbiome* **17**, 31 (2022). https://doi.org/10.1186/s40793-022-00427-z

Becker, M.F., Klueken, A.M. & Knief, C. Effects of above ground pathogen infection and fungicide application on the root-associated microbiota of apple saplings. *Environmental Microbiome* **18**, 43 (2023). https://doi.org/10.1186/s40793-023-00502-z

Becker, M. F., Deichmann, M., Klueken, A. M., & Knief, C. Effects of plant health protecting product applications on the root-associated microbiota of apple saplings and strawberries. *Phytobiomes Journal*, ja (2024). https://doi.org/10.1094/PBIOMES-04-24-0040-R

Table of Contents

Summary

The microbes living in and in close proximity to plant roots are subject to host-driven selection and can confer substantial benefits to the plant such as growth promotion and stress tolerance. Studying this root-associated microbiota and the factors shaping its composition holds substantial potential to improve plant health and crop yield, thereby contributing to sustainable agriculture. At the same time, population growth and climate change necessitate increasing agricultural output while minimizing environmental impacts. Pathogen infections threaten yields, raising the need for frequent applications of plant health protecting products to minimize their impact. Yet, little is known about the impact of both infections and plant health protecting product applications on the root-associated microbiota. Even when these perturbations occur only above ground, they may alter plant metabolism and root exudation, leading to downstream effects on the below ground microbiota. Clarifying such plant-mediated effects will improve our understanding of the factors influencing the root-associated microbiota and could ultimately help support plant health.

Accordingly, I addressed four questions: (i) whether the root-associated microbiota of apple exhibits intrinsic spatial and temporal variation related to root phenology and seasonality; (ii) how foliar fungal infection of apple saplings alters the root-associated microbiota; (iii) how above ground applications of plant health protecting products with different modes of action affect the root-associated microbiota in two crop systems; and (iv) how the combined pathogen infection and product application influence the root-associated microbiota. I used greenhouse and field experiments and profiled the bacterial root-associated microbiota by next-generation sequencing of 16S rRNA gene amplicons.

The root-associated microbiota showed spatial variation on various scales. On a smaller scale, the rhizosphere effect was observed with distinct community compositions in the rhizosphere and endosphere in all trials. On larger scales, the root-associated bacterial communities of fully grown apple trees shifted along a root size gradient and along spatial distances in the field and were furthermore subject to seasonal and annual variation. Such heterogeneity should be accounted for in future microbiome studies. Foliar pathogen infections induced plant-mediated changes in the root-associated microbiota upon severe leaf infection. Community changes did not differ between the two inoculated pathogens but scaled with disease severity. Naturally occurring root infections in mature trees elicited even stronger community shifts, indicating that infections exert the strongest impact on the associated microbiota in the affected region.

Above ground applications of plant protection products did not elicit consistent, treatment-specific plant-mediated responses in the root-associated microbiota. Only systemic products induced mild, transient effects that were no longer detectable two weeks after the final application. Nevertheless, product applications often increased within-treatment variability in community compositions, consistent with the “Anna Karenina principle” (AKP). Under this principle, changes in the root-associated microbiota by a perturbation can be deterministically, but the extent of the alteration is stochastic depending on the severity of the stressor. In this context, foliar pathogen infection represented a more severe perturbation than product application. Moreover, a curative product application even mitigated pathogen-induced stress and helped reestablish the plant’s preferred bacterial community in both the rhizosphere and endosphere. No differences in plant morphological and physiological characteristics were observed, suggesting that product application and mild AKP effects had no negative impacts on plant health. Thus, besides their direct protective and curative properties, the responsible use of plant health protecting products may support microbiome management and therefore potentially contribute to sustainable agriculture.

Zusammenfassung

Die Mikroben, die in und direkt um Pflanzenwurzeln herum leben, unterliegen einer wirtsgesteuerten Selektion, die der Pflanze erhebliche Vorteile wie Wachstumsförderung und Stressresistenz bieten kann. Die Untersuchung dieser wurzelassoziierten Mikrobiota und der Faktoren, die ihre Zusammensetzung beeinflussen, birgt großes Potenzial zur Verbesserung der Pflanzengesundheit und ihres Ertrags. Gleichzeitig erfordert eine wachsenden Weltbevölkerung und der Klimawandel eine Steigerung der landwirtschaftlichen Produktion bei gleichzeitiger Minimierung ihrer Umweltauswirkungen. Pathogeninfektionen gefährden Erträge, wodurch regelmäßige Pflanzenschutzmittelanwendungen nötig sind. Dennoch ist wenig über die Auswirkungen sowohl von Infektionen als auch von Pflanzenschutzmittelanwendungen auf die wurzelassoziierte Mikrobiota bekannt. Selbst wenn diese Störungen nur oberirdisch auftreten, können sie den Pflanzenstoffwechsel und die Wurzelausscheidung verändern und zu nachgelagerten Effekten auf die unterirdische Mikrobiota führen. Die Analyse dieser pflanzenvermittelten Effekte wird unser Verständnis der Faktoren verbessern, die die wurzelassoziierte Mikrobiota beeinflussen, und könnte letztlich zu einer Verbesserung der Pflanzengesundheit führen.

Deshalb habe ich in dieser Dissertation vier Fragen untersucht: (i) ob die wurzelassoziierte Mikrobiota des Apfels eine intrinsische räumliche und zeitliche Variation in Bezug auf Wurzelphänologie und Saisonalität aufweist; (ii) wie sich Blattpilzinfektionen auf die wurzelassoziierte Mikrobiota von Apfeljungpflanzen auswirkt; (iii) wie oberirdische Pflanzenschutzmittelanwendungen mit unterschiedlichen Wirkmechanismen die wurzelassoziierte Mikrobiota in zwei Anbausystemen beeinflussen; und (iv) wie die Kombination von Pathogeninfektion und Produktanwendung die wurzelassoziierte Mikrobiota beeinflussen. Ich habe Gewächshaus- und Feldexperimente durchgeführt und die bakterielle wurzelassoziierte Mikrobiota durch Next-Generation-Sequenzierung von 16S rRNA-Genamplikons analysiert.

Die wurzelassoziierte Mikrobiota wies räumliche Variation auf verschiedenen Skalen auf. Auf der kleinsten Skala wurde der Rhizosphäreneffekt mit individuellen Gemeinschaften in Rhizosphäre und Endosphäre in allen Versuchen beobachtet. In größerem Maßstab verschoben sich die wurzelassoziierten Gemeinschaften von ausgewachsenen Apfelbäumen entlang eines Wurzelgrößengradienten und entlang räumlicher Distanzen im Feld und unterlagen zudem saisonaler und jährlicher Variation. Diese Heterogenität sollte in zukünftigen Mikrobiomstudien berücksichtigt werden. Schwere Blattpilzinfektionen induzierten pflanzenvermittelte Veränderungen in der wurzelassoziierten Mikrobiota. Die Unterschiede in der Gemeinschaftszusammensetzung hingen dabei nicht vom Pathogen ab, sondern korrelierte mit Krankheitsintensität. Natürlich vorkommende Wurzelinfektionen in Apfelbäumen führten zu noch stärkeren Gemeinschaftsveränderungen, was darauf hinweist, dass Infektionen den stärksten Einfluss auf die assoziierte Mikrobiota in der betroffenen Region ausüben.

Oberirdische Pflanzenschutzmittelanwendungen führten nicht zu konsistenten, behandlungsspezifischen pflanzenvermittelten Reaktionen in der wurzelassoziierten Mikrobiota. Lediglich systemische Produkte induzierten milde, vorübergehende Effekte, die zwei Wochen nach der letzten Anwendung nicht mehr nachweisbar waren. Dennoch erhöhten Produktanwendungen häufig die Variabilität der Gemeinschaftszusammensetzungen innerhalb einer Behandlung, was mit dem „Anna-Karenina-Prinzip“ (AKP) übereinstimmt. Nach diesem Prinzip können Veränderungen in der wurzelassoziierten Mikrobiota durch eine Störung deterministisch sein, aber das Ausmaß der Veränderung ist stochastisch und hängt von der Intensität des Stressors ab. In diesem Kontext stellte die Blattpathogeninfektion eine schwerere Störung dar als die Produktanwendung. Darüber hinaus hat eine kurative Produktanwendung sogar den von Pathogenen induzierten Stress reduziert und half, die bevorzugte bakterielle Gemeinschaft der Pflanze sowohl in Rhizosphäre als auch in Endosphäre wiederherzustellen. Es wurden keine Unterschiede in den morphologischen und physiologischen Eigenschaften der Pflanze beobachtet, was darauf hindeutet, dass Produktanwendungen und milde AKP-Effekte keine negativen Auswirkungen auf die Pflanzengesundheit hatten. Somit könnte die verantwortungsvolle Verwendung von Pflanzenschutzmitteln neben ihren direkten protektiven und kurativen Eigenschaften das Mikrobiomanagement unterstützen und somit potenziell zu einer nachhaltigen Landwirtschaft beitragen.

List of Figures

Fig. II-6: Variation in the apple root-associated bacterial community structure due to spatial (root section), temporal and tree-to-tree effects. **A** Constrained analysis of principal coordinates (CAP, based on DEICODE distance matrices, constrained by the variables tree, root section, and timepoint) shown for the L-compartment (left) and T-compartment (right). A color gradient differentiates the four sampling timepoints and symbol shapes the root section. **B** Statistical evaluation of differences in bacterial beta diversity in the L- and T-compartment. Effect sizes were assessed by PERMANOVA based on DEICODE distance matrices.

Fig. III-1: Timeline of the temporal (**A**) and mixed trial (**B**) with inoculation, fungicide application and sampling dates (TP) of apple saplings being indicated. Timelines are labelled with plant age on top and days after infection (DAI) below. The temporal trial consisted of *V. inaequalis* or *P. leucotricha* infected plants and a control treatment without infection. The mixed trial included a treatment with *P. leucotricha* infection without fungicide treatment (inoculated untreated, IU), a treatment with *P. leucotricha* infection and fungicide treatment (inoculated treated, IT), and a non-inoculated untreated control (NC).

Fig. III-2: Disease severity of apple saplings infected by *V. inaequalis* or *P. leucotricha*. Disease severity was rated per plant at a 0–5 scale with 0 = healthy and 5 = multiple leaves entirely covered with mycelium and leaves close to senescence. Mean values and standard deviation are displayed based on 11–52 replicates. Significant differences in disease severity were evaluated between different timepoints based on Dunn's test with Benjamini–Hochberg correction for multiple testing. Lower case letters indicate differences at $p = 0.05$. DAI = days after inoculation.

Fig. III-3: Principal Coordinate Analysis (PCoA) calculated from DEICODE distance matrices, showing variation in the root-associated bacterial community composition of differently inoculated apple saplings over time. Variation in the L-compartment (upper panel) and T-compartment (lower panel) is shown.

Fig. III-4: Temporal dynamics in the root-associated bacterial community composition of differently inoculated apple saplings. **A**-**C** Principal Coordinate Analysis (PCoA) based on DEICODE distance matrices, showing variation in the L-compartment (left) and T-compartment (right). **A** Untreated control plants. **B** *P. leucotricha* inoculated plants. **C** *V. inaequalis* inoculated plants. A color code illustrates the different sampling timepoints, point size indicates disease severity based on a 0–5 scale with 0 = plant with healthy leaves and 5 = plant having multiple leaves entirely covered with mycelium and with leaves close to senescence. **D**–**F** PERMANOVA results for pairwise comparisons between timepoints in the three treatment groups: **D** untreated control plants, **E** *P. leucotricha* inoculated plants. **F** *V. inaequalis* inoculated plants. Results for the L-compartment (upper right side) and the T-compartment (lower left side) are shown. R^2-values are color coded and Benjamini–Hochberg adjusted *p*-values indicated by asterisks, i.e., "*" represents $p \leq 0.01$ and "." represents $0.05 \geq p > 0.01$. The significance threshold was set at $\alpha = 0.01$.

Fig. III-5: Development of disease severity over three timepoints (TP1–TP3) on *P. leucotricha* infected apple saplings. One inoculated group (IT) was treated with a synthetic fungicide at TP2, the other remained untreated (IU). Both treatments were compared to an uninoculated control group (NC). Disease severity was rated on a 0–5 scale and the mean values and standard deviation of 9–35 replicates are shown. Significant differences in disease severity between the three groups at TP2 and TP3 were assessed by Dunn's test with Benjamini–Hochberg correction for multiple testing.

Fig. III-6: Variation in the root-associated bacterial community of apple saplings linked to treatment and sampling timepoint (TP). The variation in alpha diversity presented based on the Shannon index in the L-compartment (left panel) and T-compartment (right panel). Differences in Shannon diversity were analyzed based on linear models (LM). Different letters represent significant changes according to Tukey's HSD post hoc tests performed between all seven groups of samples.

Fig. III-7: Variation in beta diversity of differently treated apple saplings at three distinct timepoints (TP) in the L-compartment (upper panel) and T-compartment (lower panel). Variation is presented based on constrained analysis of principal coordinates (CAP) using DEICODE distance matrices; it is constrained by the variables sampling timepoint, treatment and disease severity. Plants were either inoculated with *P. leucotricha* and left untreated (IU) or were additionally treated with a synthetic fungicide (IT), or they underwent a treatment with water as control (NC). The different treatments are shown in different colors, and disease severity is illustrated by different symbol sizes, rated on a 0–5 scale with 0 = healthy plants and 5 = plants having multiple leaves entirely covered with mycelium and with leaves close to senescence.

Fig. III-8: Pairwise PERMANOVA results comparing bacterial community composition in the L- and T-compartment of apple saplings at different timepoints (TP) of three differently treated groups (IU, IT, NC). R^2-values are illustrated using a color scale with the Benjamini–Hochberg adjusted *p*-values indicated by asterisks, i.e., "*" represents $p \leq 0.01$ and "." represents $0.05 \geq p > 0.01$. Results for the L-compartment are shown in the upper right side of the figure and for the T-compartment in lower left side. The significance threshold was set at $\alpha = 0.01$.

Fig. III-9: Differential abundance analysis performed at genus level by ANCOM-BC of differently treated apple saplings at the last sampling timepoint (TP3). Results are shown for the L- and T-associated bacterial communities (upper and lower panel, respectively). Plants were inoculated with *P. leucotricha* and then left untreated (IU) or treated with a synthetic fungicide (IT) or remained uninoculated and treated with water as control (NC). The heatmap shows the coefficients obtained from the ANCOM-BC log-linear model divided by their standard error (called W-value). The color code indicates differential abundances between two treatments with red indicating enrichment in the last value of the column name. A "*" is shown if ANCOM-BC showed significant differences based on adjusted *p*-values in this comparison. In addition, the mean relative abundances of the taxa are displayed and only taxa with a mean relative abundance of > 0.1% are shown.

Fig. IV-1: Variation in alpha diversity in the root-associated bacterial community of strawberry plants upon application of different plant health protecting products (PHPPs). Boxplots show variation in Shannon`s diversity index between treatments and in comparison to bulk soil samples. Mean values and standard deviations (SD) are indicated below the figure (A). Differences in Shannon`s diversity index between treatments and in interaction with other factors are reported based on linear regression analysis (B). Two root compartments were separately analysed, representing bacteria loosely attached to the roots (L-compartment) and bacteria tightly attached to and inside the roots (T-compartment). Within the root compartments, two different root sections were considered: fine and thick roots. PHPPs were applied in two different application modes: Aliette, Luna, Movento and Bactiva were either applied at the recommended (r.) or doubled rate (d.). Serenade was applied at the recommended rate with either a felt mat (w.Serenade) covering the soil or without (w/o.Serenade). Results with significant differences are printed in bold.

Fig. IV-2: Variation in the root-associated bacterial community of apple plants due to the application of plant health protecting products (PHPP) in the concentration trial. (A) Principal Coordinate Analysis (PCoA) based on DEICODE distance matrices. (B) Differences in community composition and dispersion assessed by PERMANOVA and PERMDISP, respectively. Responses were analysed in the two root compartments (L and T). Each PHPP was applied in two different application modes (Application). The products Aliette, Luna and Movento were either applied at the recommended rate or twice the rate. Serenade was applied at the recommended rate but in case of the "without felt mat" treatment, the felt mat covering the soil of all samples was taken off and the product was thus in direct contact with the soil.

Fig. IV-3: Principal Coordinate Analysis (PCoA) based on DEICODE distance matrices showing variation in the root-associated bacterial community composition of apple plants in the temporal trial upon application of different plant health protecting products (PHPP). The individual PCoA plots display the variation in the root-associated bacterial community composition at the early and late sampling timepoint (one and two weeks after final PHPP application, respectively) in L- and T-compartments, representing the loosely (L) and tightly (T) root-associated bacteria.

Fig. IV-4: Principal Coordinate Analysis (PCoA) based on DEICODE distance matrices showing variation in the root-associated bacterial community composition of apple plants in the temporal trial upon application of different plant health protecting products (PHPP). The individual PCoA plots display the variation in the root-associated bacterial community composition at the early and late sampling timepoint (one and two weeks after final PHPP application, respectively) in L- and T-compartments, representing the loosely (L) and tightly (T) root-associated bacteria.

Suppl. Fig. VII-1: Photographs showing the root system of a fully grown commercial apple tree (top) and two rows of an apple orchard (bottom).

Suppl. Fig. VII-2: Differential abundance analysis of the loosely (L) and tightly (T) associated bacteria in the three experimental field trials using ANCOM-BC. The heatmap shows the coefficients obtained from the ANCOM-BC log-linear model divided by their standard error (called W-value) with red indicating enrichment in the T-compartment. A "*" is shown if ANCOM-BC showed significant differences using the adjusted *p*-value in this comparison. The mean abundance of the families in their respective trial are shown in the adjacent barplot as % and only families with mean abundances ≥ 0.5% are shown (ST refers to the spatio-temporal trial). A greyed-out field means that this family is below the 0.5% threshold in a trial. The families in the heatmap rows are separated by the phylum they belong to and displayed in different colors.

Suppl. Fig. VII-3: Root-associated bacterial community composition of the loosely (L) and tightly (T) associated bacteria in four different root size sections and the bulk soil (b) of four apple trees analyzed in the spatial trial. Constrained analysis of principal coordinates (CAP; based on DEICODE distance matrices and the variables compartment, tree and root quadrant) to assess the relevance of those variables on variation in bacterial community composition.

Suppl. Fig. VII-4: Root-associated bacterial community composition of bulk soil near the apple trees analyzed in the spatial trial. Constrained analysis of principal coordinates (CAP; based on DEICODE distance matrices and the variables tree and root quadrant) to assess the relevance of those variables on variation in bacterial community composition.

Suppl. Fig. VII-5: Differential abundance analysis of the loosely (L) and tightly (T) associated bacteria and the bulk soil (b) in four different trees (T1 to T4) of the spatial trial using ANCOM-BC. The heatmap shows the coefficients obtained from the ANCOM-BC log-linear model divided by their standard error (called W-value). A "*" is shown if ANCOM-BC showed significant differences using the adjusted *p*-value in this comparison. The color code indicates differential abundances between two samples with red indicating enrichment in the larger root sections. A grey color indicates that this ASV was not detected in the respective compartment. The mean relative abundance of the ASVs in the entire compartment is shown as % and ASVs with mean abundances ≥0.1% in either compartment are displayed. The ASVs in the rows of the heatmap are separated according to phylum.

Suppl. Fig. VII-6: Pairwise PERMANOVA for comparison of timepoints in the temporal trial in the L- and T-compartment in the upper (A) and lower (B) panel, respectively. The color codes for the R^2-value and `.` indicates a *p*-value between 0.05 and 0.1, `*` indicates a *p*-value between 0.01 and 0.05, `**` a *p*-value between 0.01 and 0.001. The adjusted *p*-values using Benjamini-Hochberg correction for multiple testing are not displayed as they were all non-significant.

Suppl. Fig. VII-7: Comparison of the T-compartment of six tree individuals in the temporal trial. Trees 1 to 3 and trees 4 to 6 were standing adjacently in separate opposite rows. (A) Pairwise PERMANOVA with *p*-values adjusted using Benjamini-Hochberg correction for multiple testing. The color codes for the R^2-value and `.` indicates a p_{adj} -value between 0.05 and 0.1, `*` indicates a p_{adj} -value between 0.01 and 0.05. (B) Differentially abundant ASVs identified by ANCOM-BC. The heatmap shows the coefficients obtained from the ANCOM-BC log-linear model divided by their standard error (called W-value). A "*" is shown if ANCOM-BC showed significant differences using the p_{adj}-value in this comparison. The color code indicates differential abundances between two samples with red indicating enrichment in the tree with the higher identifier number. The mean relative abundance of the ASVs in the T- compartment is shown as % and ASVs with mean abundances ≥ 0.3% are displayed. The ASVs in the rows of the heatmap are separated according to phylum.

Suppl. Fig. VII-8: Differentially abundant ASVs in the L- and T-compartment (upper and lower panel, respectively) for two different root size sections at four different timepoints according to ANCOM-BC. Fine roots had a diameter between 1 and 3 mm and thick roots between 3 and 6 mm. Samples were taken at four timepoints (TP1: 21.03.2019; TP2: 15.04.2019; TP3: 05.06.2019 and TP4: 20.08.2019). The first four columns compare the fine to the thick roots at each timepoint, the next three the different timepoints in the fine roots and the last three columns compare the thick roots at each timepoint. The heatmap shows the coefficients obtained from the ANCOM-BC log-linear model divided by their standard error (called W-value). The colour code indicates differential abundances between two factors with red indicating enrichment in the second mentioned factor. A "*" is shown if ANCOM-BC showed significant differences using p_{adj}-values in this comparison. The mean abundance of the ASVs in the entire compartment is shown as % and only ASVs with mean abundances ≥ 0.3% are shown.

Suppl. Fig. VIII-1: Composition of the root-associated bacterial community of apple plants as revealed by 16S rRNA gene amplicon sequencing in the temporal trial. The relative abundance of bacterial families in samples from three different treatments (*P. leucotricha*, *V. inaequalis* and a negative control) sampled at different days after inoculation (DAI) in the loosely associated (L, upper panel) and tightly associated (T, lower panel) compartment is shown. Phyla and their families with < 2% relative abundance in the respective treatment were grouped as "Other".

Suppl. Fig. VIII-2: Differential abundance analysis of genera in the L- and T-compartment (panel A and B, respectively) in dependence on pathogen infection 40 days after inoculation (DAI) compared to 0 DAI based on ANCOM-BC. Plants were either inoculated with *V. inaequalis* (V) or *P. leucotricha* (L) and are shown besides an uninoculated control treatment (C). The heatmap shows the coefficients obtained from the ANCOM-BC log-linear model divided by their standard error (called W-value). The colour code indicates differential abundances of genera between the two timepoints with red indicating an increase in relative abundance at 40 DAI compared to 0 DAI. A "*" is shown if ANCOM-BC showed significant differences using the adjusted *p*-value in this comparison. The mean relative abundances of the taxa are displayed at 40 DAI in percent. In the L-compartment, most identified genera of the pathogen inoculated plants belong to the phylum *Proteobacteria*, e.g., unclassified members of the *Comamonadaceae*, *Moraxellaceae*, *Morganellaceae*, *Sphingomonadaceae* and *Xanthomonadaceae*. In the control plants, several *Acidobacteriota* such as *Acidipila*, *Bryobacter* or *Bryocella* were significantly decreased in relative abundance at 40 DAI, though not in the inoculated plants. Only few observations like these were made in the T-compartment with *Edaphobacter*, *Acidibacter* and unclassified members of *Methylophilaceae* and *Micropepsaceae* being significantly increased in the inoculated plants 40 DAI, but not in the control plants.

Suppl. Fig. VIII-3: Composition of the root-associated bacterial community of apple plants as revealed by 16S rRNA gene amplicon sequencing in the mixed trial. The relative abundance of bacterial families in samples from three different treatments (IU: inoculated & untreated, IT: inoculated & treated, and NC: negative control) at three different timepoints (TP) in the loosely associated (L, upper panel) and tightly associated (T, lower panel) compartment is shown. Phyla and their families with < 2% relative abundance in the respective treatment were grouped as "Other".

Suppl. Fig. VIII-4: Variation in beta diversity of differently treated apple saplings at timepoint (TP) 3 in the L-compartment (upper panel) and T-compartment (lower panel). Variation is presented based on constrained analysis of principal coordinates (CAP) using DEICODE distance matrices; it is constrained by the variables treatment and disease severity. Plants were either inoculated with *P. leucotricha* and left untreated (IU) or were additionally treated with a synthetic fungicide (IT), or they underwent a treatment with water as control (NC). The different treatments are shown in different colors, and disease severity is illustrated by different symbol sizes, rated on a 0-5 scale with 0 = healthy plants and 5 = plants having multiple leaves entirely covered with mycelium and with leaves close to senescence.

Suppl. Fig. VIII-5: Boxplots showing the differences between two different treatments (IT and IU) to an untreated control group (NC group) for the (A) L-compartment and (B) T-compartment at TP3 based on DEICODE distances. Significant differences were calculated with pairwise Kruskal-Wallis tests ("***"" = *p*-value of < 0.001, ns = non significant).

Suppl. Fig. IX-1: Separation of the strawberry root system into fine (right) and thick (left) roots.

Suppl. Fig. IX-2: Patterns of the beta Nearest Taxon Index (betaNTI) in the concentration trial. Patterns between different treatments (**A**) in the L-compartment and (**B**) the T-compartment are shown. Specifically, a betaNTI or betaNRI between –2 and 2 reveals dominance of stochastic processes, whereas |betaNRI| or |betaNTI| >2 reveals the significant dominance of deterministic processes. The products Aliette, Luna and Movento were either applied at the recommended rate (r) or twice the rate (double: d). Serenade was applied at the recommended rate but with (w felt) or without a felt mat (w/o felt) to cover the soil.

Suppl. Fig. IX-3: Patterns of beta Nearest Taxon Index (betaNTI) in the bacterial community of the temporal trial upon different plant health protecting product (PHPP) treatments in the L-compartment (**A** and **C**) and the T-compartment (**B** and **D**) at two different timepoints (early and late).

Suppl. Fig. IX-4: Patterns of the beta Nearest Taxon Index (betaNTI) in the bacterial community of the strawberry trial upon different plant health protecting product (PHPP) treatments in the L-compartment (panels **A** and **C**) and the T-compartment (**B** and **D**) in two different root sections (fine and thick roots). The products Aliette, Bactiva, Luna and Movento were either applied at the recommended rate (r) or twice the rate (double: d). Serenade was applied at the recommended rate but with (w felt) or without a felt mat (w/o felt) to cover the soil.

Suppl. Fig. IX-5: Community assembly process measurements by taxonomic normalized stochasticity ratios (tNST) based on Jaccard's distance in the concentration trial. Ratios for bacterial communities upon different PHPP treatments in the L-compartment (**A**) and the T-compartment (**B**) are shown. The products Aliette, Luna and Movento were either applied at the recommended rate (r) or twice the rate (double: d). Serenade was applied at the recommended rate but with (w felt) or without a felt mat (w/o felt) to cover the soil.

Suppl. Fig. IX-6: Community assembly process measurements by taxonomic normalized stochasticity ratios (tNST) based on Jaccard's distance in the temporal trial. Ratios for bacterial communities upon different PHPP treatments in the L-compartment (**A** and **C**) and the T-compartment (**B** and **D**) at two different sampling timepoints (early and late) are shown.

Suppl. Fig. IX-7: Community assembly process measurements by taxonomic normalized stochasticity ratios (tNST) based on Jaccard's distance in the strawberry trial. Ratios for bacterial communities upon different PHPP treatments in the L-compartment (**A** and **C**) and the T-compartment (**B** and **D**) in two different root sections (fine and thick roots) are shown. The products Aliette, Bactiva, Luna and Movento were either applied at the recommended rate (r) or twice the rate (double: d). Serenade was applied at the recommended rate but with (w felt) or without a felt mat (w/o felt) to cover the soil.

Suppl. Fig. IX-8: Differential abundance analysis of bacterial communities in the L- and T-compartment of PHPP treated apple plants versus control plants in the concentration trial using ANCOM-BC at genus level resolution. Plants were treated with one of four different plant health protecting products with different application modes or water as control. The products Aliette, Luna and Movento were either applied at the recommended rate (r.) or twice the rate (d.). Serenade was applied at the recommended rate, but in case of the "w/o felt" treatment the felt mat covering the soil of all samples was taken off and the product was thus in direct contact with the soil. Individual models were calculated for each compartment (L and T). The heatmap shows the coefficients obtained from the ANCOM-BC log-linear model divided by their standard error (called W-value). The colour code indicates differential abundances between a treatment and control with red indicating enrichment in the last value of the column name (i.e. the respective PHPP treatment). A "*" is shown if ANCOM-BC showed significant differences using the adjusted *p*-value in this comparison ($p_{adj} < 0.05$). The mean relative abundances of the taxa across all treatments but in their respective compartment are shown in the right horizontal barplot in percent.

Suppl. Fig. IX-9: Differential abundance analysis of bacterial communities in the L- and T-compartment (**A** and **B**, respectively) of PHPP treated young apple plants at two different timepoints in the temporal trial using ANCOM-BC at genus level resolution. Plants were treated with one of four different plant health protecting products or water as control and sampled either one (early) or two weeks (late) after the last PHPP application. The heatmap shows the coefficients obtained from the ANCOM-BC log-linear model divided by their standard error (called W-value). The colour code indicates differential abundances between two compartments with red indicating enrichment as given at the last position in the column name. A "*" is shown if ANCOM-BC showed significant differences using the adjusted *p*-value in this comparison ($p_{adj} < 0.05$). The mean relative abundances of the taxa across all treatments is shown in the right horizontal barplot in percent.

Suppl. Fig. IX-10: Differential abundance analysis of bacterial communities in the L- and T-compartment of PHPP treated young strawberry plants at genus level using ANCOM-BC. The root system was divided into fine and thick roots. Plants were treated with one of five different plant health protecting products with different application modes or water as control. The products Aliette, Luna Movento and Bactiva were either applied at the recommended rate (r.) or twice the rate (d.). Serenade was applied at the recommended rate but in case of the "w/o felt" treatment, the felt mat covering the soil of all samples was taken off before product application and the product was thus in direct contact with the soil. Individual models were calculated for each compartment and root type. The heatmap shows the coefficients obtained from the ANCOM-BC log-linear model divided by their standard error (called W-value). The colour code indicates differential abundances between respective PHPP treatments and control with red indicating enrichment in PHPP treated plants. A "*" is shown if ANCOM-BC showed significant differences using the adjusted *p*-value in this comparison ($p_{adj} < 0.05$). The mean relative abundances of the taxa across all treatments is shown in the right horizontal barplot in percent. Scaling of colour code and relative abundance is adjusted for each plot independently.

Suppl. Fig. IX-11: Relative abundance of bacterial orders in samples from three different greenhouse trials (Temporal, Concentration, and Strawberry) in the bulk soil (B), loosely associated (L) and tightly associated (T) compartment. Phyla and their orders with < 2 % relative abundance in the respective trial were grouped as "Other".

Suppl. Fig. IX-12: Differential abundance analysis of bacterial orders obtained from bulk soil (B) and root compartments with loosely (L) and tightly (T) associated bacteria in the three experimental trials (Temporal, Concentration, Strawberry) using ANCOM-BC. The heatmap shows the coefficients obtained from the ANCOM-BC log-linear model divided by their standard error (called W-value). The colour code indicates differential abundances between two compartments with red indicating enrichment in the last value of the column name. A "*" is shown if ANCOM-BC showed significant differences using the adjusted *p*-value in this comparison ($p_{adj} < 0.05$). The mean abundance of the orders over all trials is shown in the adjacent barplot in percent and only orders with an overall mean abundance ≥ 0.5 % are shown. The orders in the heatmap rows are sorted and separated by the phylum they belong to and are displayed in different colours.

Suppl. Fig. X-1: Community assembly process measurements by taxonomic normalized stochasticity ratios (tNST) based on Jaccard's distance in the combined trial. Ratios for bacterial communities upon different treatments in the rhizosphere and endosphere are shown. The IT group received a preventative treatment with the fungicide Aliette. After two weeks, both the IU and IT group received an inoculation with the foliar pathogen *P. leucotricha*. When disease symptoms became severe, the IT group received a curative Aliette application. The NC group was treated with water instead of a fungicide application or pathogen suspension.

List of Tables

Suppl. Table VII-1: The sampling timepoints of the temporal trial (left) and the spatio-temporal (ST) trial (right).

Suppl. Table VII-2: Sequences of barcoded forward primers targeting the 16S rRNA gene. Primers include a barcode (8 bp) and the primer sequence itself. The reverse primer was not modified.

Suppl. Table VII-3: The hierarchies in each of the trials with the number of samples. Total read number after quality filtering, mean number of reads per sample and the number of samples remaining after quality filtering.

Suppl. Table VII-4: The ten most prominent genera in each trial with their mean relative abundance and standard deviation (SD).

Suppl. Table VII-5: Differences in bacterial beta diversity in dependence on tree individual and root size section in the loosely (L) and tightly (T) associated root microbiota in the spatial trial. Effect sizes in beta diversity were assessed by pairwise PERMANOVA based on DEICODE distance matrices and p_{adj}-values calculated using Bonferroni's algorithm.

Suppl. Table VII-6: Significant differences in the apple root-associated bacterial community structure due to temporal, root size and spatial effects. The spatial effects in terms of tree-to-tree variation, longitudinal position of the tree and row of the tree were analyzed separately. Effect sizes were analyzed by PERMANOVA based on DEICODE distance matrices. Significant results are printed bold.

Suppl. Table VIII-1: The hierarchies in each of the trials with the number of samples. Total read number after quality filtering, mean number of reads per sample and the number of samples remaining after quality filtering.

Suppl. Table VIII-2: Differences in beta diversity of the root-associated bacterial community of apple saplings in the L- and T-compartment inoculated with two different pathogens (*V. inaequalis* or *P.leucotricha*, additionally a negative control) and sampled at different timepoints. The disease severity, the height of the plant and the number of leaves was measured at each timepoint. Effect sizes were assessed by ANOSIM based on DEICODE distance matrices. Significant results ($p < 0.05$) are printed bold.

Suppl. Table VIII-3: Differences in beta diversity of the root-associated bacterial community of apple saplings in the L- and T-compartment treated with two different pathogens and sampled at different timepoints (TP). Effect sizes were assessed by PERMANOVA based on DEICODE distance matrices. Significant results ($p < 0.05$) are printed bold.

Suppl. Table VIII-4: Dispersion of the root-associated bacterial community of young apple plants between different treatments at different timepoints (DAI) in the L- and T-compartment. The different treatments included inoculations with either *V. inaequalis* (V) or *P. leucotricha* (L) and an uninoculated control (C). Effect sizes were assessed by PERMDISP and Tukey's test based on DEICODE distance matrices and p-values adjusted after multiple comparison. Significant results are printed in bold.

Suppl. Table IX-1: Overview of the used plant health protecting products (PHPP) with their active ingredients, the standard field application rate and applied concentrations.

Suppl. Table IX-2: The hierarchies in each of the trials with the number of samples. Total read number, mean number of reads per sample and the number of samples remaining after quality filtering.

Suppl. Table IX-3: Compositional variation in the root associated bacterial communities in the strawberry trial due to the application of different plant health protecting products (PHPP) and their different modes of application. The evaluation was performed independently for both root compartments (Comp.: loosely (L) and tightly (T) fraction). The significant influence of the different root sections (fine and thick roots) resulted in further data subsetting. Five different products were applied, each with two different application modes, and those treatments were grouped as "PHPP Application". Differences in composition and dispersion were assessed by PERMANOVA and PERMDISP, respectively, applied to DEICODE distance matrices. Results with significant differences are printed in bold.

Suppl. Table IX-4: Table of pairwise PERMDISP results comparing different product applications in the strawberry trial. PHPP application occurred at the recommended application rate (r) and twice the rate (d) in comparison to a control group in the L- and T-compartment (Comp.) in different root sections (RS): fine roots (FR) or thick roots (TR). In case of Serenade both applications were at the recommended rate but with (w) or without (w/o) a felt mat covering the soil surface. Results with significant differences are printed in bold.

List of Abbreviations

AKP:	Anna Karenina Principle
ASV:	Amplicon sequence variant
betaNRI:	Beta net relatedness index
betaNTI:	Beta nearest taxon index
CAP:	Constrained analysis of principal coordinates
d.:	Double the recommended rate
DAI:	Days after inoculation
dH^2O:	Distilled water
DNA:	Deoxyribonucleic acid
DLR:	Dienstleistungszentrum Ländlicher Raum
DS:	Disease severity
FDR:	False discovery rate
FR:	Fine roots
IT:	Inoculated treated
IPM:	Integrated pest management
IU:	Inoculated untreated
L:	Loosely associated
LNA:	Locked nucleic acid
LMM:	Linear mixed-effects models
NC:	Uninoculated untreated control
p_{adj}:	Adjusted *p*-values
PCoA:	Principal coordinate analysis
PCR:	Polymerase chain reaction
PERMANOVA:	Permutational multivariate analysis of variance
PERMDISP:	Permutational analysis of multivariate dispersions
PGPR:	Plant growth promoting rhizobacteria
PHPP:	Plant health protecting product
r.:	The recommended rate
rRNA:	Ribosomal RNA
SD:	Standard deviation
T:	Tightly associated
TP:	Timepoint
tNST:	Taxonomic normalized stochasticity ratio
TR:	Thick roots
w felt:	With felt map
w/o felt:	Without felt map

I. Introduction

1. The root-associated microbiome

Soil harbors one of the most diverse and complex microbiomes on Earth and is a huge natural reservoir for numerous microorganisms (Fierer 2017). One gram of soil from temperate regions may harbor between 10^7 and 10^{10} microbial cells and up to 10,000 to 50,000 microbial species (Raynaud and Nunan 2014; Blakemore 2018). However, microbial activity here is often limited, especially by carbon availability (German et al. 2011). In contrast to this, the soil in immediate proximity of plant roots is one of the most dynamic microbial hotspots (Tian et al. 2020) with reports of up 10^{11} microbial cells per gram of root (Ali et al. 2017) and over 30,000 prokaryotic species (Mendes et al. 2011). The stimulation of microbial growth and activity is due to the release of carbon-rich deposits by plant roots into the surrounding soil with a roughly estimated 11% of the net fixed carbon (or 27% of carbon allocated to roots) being secreted by the plant (Jones et al. 2009; Pausch and Kuzyakov 2018). The resulting biological changes in the soil caused by rhizodeposition, along with chemical and physical changes, have been named the rhizosphere effect, a term first coined in 1904 by the German agronomist Lorenz Hiltner (Hiltner 1904). By adjusting the composition of the root exudates, plants are capable to actively recruit specific microbes in the rhizosphere as an adaptation strategy in cases of biotic or abiotic stresses (Berg and Smalla 2009; Hartmann et al. 2009; Berendsen et al. 2012; Rizaludin et al. 2021). Some rhizospheric microbes undergo an even closer relationship and attach to the root surface, the rhizoplane, or even enter the root and establish an endophytic lifestyle (Frank et al. 2017; Araujo et al. 2019; White et al. 2019). This process has been described as a dynamic process in which microbes in the rhizosphere are first recruited from the surrounding soil, and subject to further selection by the host in order to colonize the central cylinder, where they must survive under the vastly different internal conditions (Bulgarelli et al. 2013; Bulgarelli et al. 2012; Edwards et al. 2015). This bottleneck results in compartment-specific microbial communities with decreased microbial diversity and an expected higher level of interaction along the soil-endosphere continuum (Beckers et al. 2017; Bulgarelli et al. 2013; Deyett and Rolshausen 2020). The collective communities in the rhizosphere, rhizoplane and endosphere make up the root-associated microbiota and

their collective genomes are referred to the root microbiome, also called the second genome of the plant (Berendsen et al. 2012).

The assembly of the root microbiome does not only depend on the root compartment but also on several deterministic factors such as plant species, host genotype, soil properties, plant cultivation practices, geographical location, and stochastic factors (Bonkowski et al. 2021; Rüger et al. 2021; Garbeva et al. 2008; Micallef et al. 2009). Additionally, temporal variation has been shown due to the developmental stage of the plant and due to seasonal changes (Bonkowski et al. 2021; Wei et al. 2022; Chaparro et al. 2014; Dove et al. 2021). In herbaceous and annual plants, temporal dynamics in the structure of the associated microbial community are considered to be closely linked to the plant development stage (Bonkowski et al. 2021; Donn et al. 2015; Li et al. 2014; Maarastawi et al. 2018; Munoz-Ucros et al. 2021; Shi et al. 2015). The temporal dynamics of trees on the other hand likely results from seasonal shifts in carbon allocation into the roots and the surrounding soil due to differences in photosynthetic activity (Epron et al. 2011). Spatial variation has been shown for annual plants from a larger scale such as geographical location to smaller scales such as the location along the root axis (Bonkowski et al. 2021; Rüger et al. 2021). The deterministic assembly process is mostly driven by the plant via rhizodeposition, which itself depends on various factors, including abiotic and biotic influence factors (Haichar et al. 2008; Zhalnina et al. 2018). Abiotic factors include light intensity and temperature (Pramanik et al. 2000), water supply (Henry et al. 2007), high salt concentrations (Lombardi et al. 2018), the mechanistics of carbon and nitrogen flow into the rhizosphere (Jones et al. 2009), or the presence of chemical pesticides (Qu et al. 2021), whereas biotic factors include the presence of other organisms (reviewed in Dessaux et al. 2016), and root or even foliar pathogens (Yuan et al. 2018; Wen et al. 2021). Thus, the plant is able to respond to many external stress factors both above and below ground and change the root microbiome community composition to evade some of those stress factors.

Due to the range of biotic and abiotic stresses and the necessity of the wide range of resources the plant needs to acquire from soil, the root-soil interface has been shown to be a highly complex and dynamic ecosystem (Jones and Hinsinger 2008) in which plant roots must compete with various soil organisms for space, water and mineral nutrients (Haichar et al. 2014). Besides competition, the interactions between the plant

and its root-associated microbiome can also be negative in case of parasitism or pathogenesis (Bais et al. 2006). However, they can also be positive, such as the mutualistically beneficial mycorrhizal colonization of roots or the recruitment of so-called plant growth-promoting rhizobacteria (PGPR). Positive effects of the root-associated microbiome for the plant include effects on seed germination, seedling vigor, plant growth and development, nutrition, diseases, and productivity (Ali et al. 2017; Mendes et al. 2013). The root-associated microbiome can directly affect root architecture and morphology, promote hormone synthesis or metabolism, facilitate nutrient uptake and mobilization, and modulate the plant's defense responses against pathogens and environmental stresses (Berendsen et al. 2012; Bulgarelli et al. 2013; Hacquard and Schadt 2015). Thus, the root-associated communities have been of special interest in recent years due to their potential contribution to sustainable agriculture (Busby et al. 2017; Santoyo et al. 2016; White et al. 2019).

2. The root microbiome in agriculture

The rapid increase of the human population under challenging conditions has led to an urgent need for an increased but sustainable production of food in the near future. Climate change, land and resource limitations, along with other abiotic and biotic stresses, pose serious threats to crop production (Kumar and Dubey 2020). At the same time, environmental and public concerns raise the need to reduce the use of agrochemicals. Recently, targeted modifications of the root-associated microbiome have been of particular interest as a sustainable alternative to improve crop health and yield (reviewed in Vries and Wallenstein 2017). As previously stated, the microbial communities are largely influenced by the composition, quality, and quantity of rhizodeposits, which on the other hand affect plant growth and productivity (Dessaux et al. 2016). This phenomenon is called rhizosphere feedback and exploiting or manipulating this process allows to improve overall plant growth and health with a reduced use of agrochemicals. One approach is the genetic engineering of plants to alter the root exudate composition or root architecture and thereby optimize the functions of the root associated microbiota. This was already shown for different genotypes of the same host plant (reviewed in Berg and Smalla 2009) and for several transgenic plants (Wei et al. 2020; Zhang et al. 2019). However, plant genome editing techniques lack public acceptance, especially in Western countries, and thus their application remain low due

(Hakim et al. 2021; Ma et al. 2018). Another approach and one frequently exploited is the targeted application with artificially reproduced microbes. One of the most intensely studied group of microbes with plant beneficial properties are the plant growth promoting rhizobacteria (PGPR). They have been shown to induce their beneficial effects via a huge array of different mechanisms. They can increase plant resistance to various abiotic stress factors such as high salinity (Schmitz et al. 2022), drought (Vries et al. 2020), heat (Issa et al. 2018) and improve overall adaptation to changing environments (Berendsen et al. 2012; Trivedi et al. 2020). Furthermore, they are able to enhance the capacity of plants to obtain nutrients from the soil by solubilization of micro-nutrients or increasing phosphorous availability (Backer et al. 2017) and by biological nitrogen fixation (Herridge et al. 2008). Biological nitrogen fixation is the largest single global input of reactive nitrogen and its importance will likely increase due to a predicted doubling in demand by 2050 (Fowler et al. 2015), thus highlighting the need to include PGPRs in crop production systems. Furthermore, PGPRs are able to secrete various organic acids, siderophores or enzymes like phytases for an increased uptake of inorganic phosphates and metal ions, such as zinc or iron, which are often growth-limiting factors (Maitra et al. 2022). A wide range of PGPR can produce phytohormones such as auxins, gibberellins, and cytokinins that are potentially affecting plant growth and development (Ali et al. 2017). Those hormones have been shown to have beneficial effects such as increasing root growth and overall biomass, enhancement of plant shoots or reducing inhibitory growth factors or stress hormones (Ahmed and Hasnain 2014; Ruzzi and Aroca 2015; Maitra et al. 2022; Glick 2015). Furthermore, they can reduce biotic stresses such as herbivory or pathogenic microorganisms (Bulgarelli et al. 2013). PGPR can actively antagonize soil-borne pathogens by competition, predation, and parasitism or through the production of antifungal or antibactericidal compounds. Also, they can elicit the basal defense response in plants by activating the induced systemic resistance responses (Kumar and Dubey 2020; Hacquard and Schadt 2015). Thereby, they can precondition the plant's defense systems and thus lead to faster plant responses upon pathogen attacks (Compant et al. 2005; Maitra et al. 2022). Thus, through the potential increase in yield and plant nutrient content, protection against pathogens and abiotic stresses, the management and application of PGPR has been shown to be a potential effective and environmentally friendly approach to improve sustainable crop production.

3. Plant pathogens and their effects on the root-associated microbiota

Plant pathogens are a major threat to global food supply as they cause losses between 20% to 40% of crop production annually with an estimated value of around $220 billion (National Institute of Food and Agriculture 2023; Oerke and Dehne 2004). Additionally, climate change is predicted to have a progressively negative effect on the yield of food crops (Luck et al. 2011) and the number of effective pesticides is decreasing due to resistances as well as public concerns about potential environmental and health impacts of agrochemicals (Corkley et al. 2022). Thus, implementing integrated pest management strategies and developing non-chemical control measures are vital for sustaining high crop yields (Birch et al. 2011; Pertot et al. 2017).

A wide range of organisms can be plant pathogenic, including bacteria, fungi, nematodes, viruses and insects (Dangl and Jones 2001). They can attack a large host range at numerous developmental stages, organs, and under different environmental conditions. Fungi are considered to be among the most severe pathogens, as they can sporulate prolifically and can thus rapidly infect large populations such as monocultures (Strange 2003). Their spores may be spread by water, wind or vectors (such as insects or machinery) and can often survive over several growing seasons, thus complicating disease control. They can also often produce toxins and/or an array of enzymes that can destroy plant cell structures. Furthermore, most fungal pathogens can quickly form resistances against chemical fungicides, an increasingly problematic issue as studies show (Corkley et al. 2022; Weber and Hahn 2019; Leroch et al. 2011). They often infect plants through their stomata, wounds or can penetrate plant structures such as leaves, stems or roots (Termorshuizen 2016). Fungal pathogens are often differentiated between soil, air and seed-borne pathogens, though not all pathogens fit into this classification. Whereas some of them infect only root or leaf tissues, others become systemic pathogens and can infect the entire plant (Termorshuizen 2016). Common disease symptoms are necrosis of plant organs, wilting, root rot, wounding, and the development of fungal structures that could ultimately lead to cell and plant death. Those symptoms usually lead to decreased overall plant health, yield and crop quality losses. Besides those direct effects on the plant, it is becoming increasingly clear that different root, above ground or systemic pathogens can impact the plant-associated microbiota. Examples of pathogens affecting the root-associated microbiome are the

soil-borne oomycete *Phytophthora* spp. causing root rot (Solís-García et al. 2020), or the above ground fungal pathogens *Botrytis cinerea* (Tender et al. 2016) and *Podosphaera aphanis* (Yang et al. 2020). Exemplary systemic bacterial pathogens are *Erwinia amylovora*, causing fireblight in several *Rosaceae*, or the phloem-limited bacterial Huanglongbing citrus disease (Trivedi et al. 2012). Additionally, the phyllosphere microbiome, defined as microbial community in the aerial region of the plant, has been shown to shift after infection with the foliar fungal pathogen *Diaporthe citri* (Li et al. 2022). Thus, there are first indications that pathogen infections not only affect the plant but the holobiont, the plant host and its associated microbiota. However, detailed knowledge about this process and the implications for an integrated pest management system is limited and there are currently no comparative studies using several host-pathogen systems under varying environmental conditions (Busby et al. 2017). Furthermore, all studies have investigated either specific root compartments or sampled the entire root system at a single timepoint past infection and thus did not account for the temporal and spatial variability of the root-associated microbiota. Furthermore, it is unknown whether localized pathogen infections can induce changes in the microbiome of distant plant parts, such as foliar pathogens on the rhizosphere. Due to the potential of PGPR to antagonize pathogens (Finkel et al. 2017; Liu et al. 2021b), understanding the effects of pathogen infections onto the feedback system between plants and the root-associated microbiota has the potential to be a vital component of biological pest control.

4. Pest management strategies and their effects on the root-associated microbiota

Due to the major threat of plant pests to global food supply, plant protection is of vital importance in agricultural systems. There are numerous methods for agricultural crop protection such as using resistant cultivars, application of agrochemicals, culture rotation, removal of litter residues (Jeschke et al. 2013; Michalecka et al. 2018). The modern and universally endorsed paradigm for crop protection is the concept of integrated pest management (IPM), which combines different management strategies and practices to combat plant pests with minimal applications of chemical pesticides (Stenberg 2017). However, the application of synthetic pesticides and newer biological products for disease prevention and reduction is still common practice (Jeschke et al. 2013).

Pesticides can be differentiated into different groups, mostly depending on their target organisms: herbicides (against weeds und unwanted vegetation), insecticides (against insects), fungicides (fungal agents), the relatively new class of biopesticides (defined as a natural product either containing microbes or compounds derived from living organisms including plants, nematodes, and microbes that limit or reduce disease severity) and others (e.g. acaricides or virucides). They can be further differentiated into protectant and penetrant pesticides: whereas protectant pesticides are active on the plant surface they are applied on, penetrant pesticides are absorbed into the plant after the application. There, they act as protectant pesticide but can also move throughout the plant and are also labeled systemic pesticides. Depending on their movement, they are further differentiated into locally systemic (only short distances, e.g. within the leaf it was absorbed into), translaminar systemic (movement from one surface of a leaf to the opposite side), xylem mobile pesticides (move upwards the plant through the xylem) and amphimobile or truly systemic pesticides (move both upward through the xylem and downward through the phloem). Another classification of pesticides is by the chemical structure of their active ingredients. They can be differentiated either by the physical location within an organism where pesticides act, known as the target site, or the biochemical process in which the pesticides interfere, also known as the mode of action. The extensive and prolonged use of synthetic pesticides with similar modes of action coupled with the over-simplification of cropping systems has led to widespread resistance to pesticides (Busi et al. 2013). Furthermore, environmental and public health effects and concerns, along with regulatory restrictions, have led to a decrease of approved active substances. While there were more than 500 active substances registered in the EU in 2017, the number has dropped to 451 in 2023, despite numerous biopesticides and a few chemicals being approved (Marchand 2023). Biopesticides are nowadays often used in combination or rotation with synthetic pesticides to reduce the use of synthetic pesticides, while also decreasing the risk of pesticide resistance, and thereby extending the longevity of new and existing chemicals (Dara 2016; Chandler et al. 2011; Damalas and Koutroubas 2018; Ayer et al. 2021). Synthetic pesticides are generally considered to be more target-specific and pose fewer environmental risks and thus have gained an important role in sustainable agriculture (Riaz et al. 2021; Samada and Tambunan 2020).

Similar to infections with plant pathogens, there are first indications that the application of pesticides has a potential impact on the holobiont, especially on the root-associated microbiota (reviewed in Ramakrishnan et al. 2021). Most studies have analyzed the effects of direct pesticide applications into the soil or as seed treatment (Huang et al. 2021; Nettles et al. 2016; Kusstatscher et al. 2020; Deng et al. 2019; Qian et al. 2018), whereas little is known about possible plant mediated effects on the root-associated microbiota when pesticides are applied above ground. However, in commercial horticulture most pesticides are applied as foliar sprays and less as drench application or seed coating (Dara 2016; Thompson et al. 2023). Also similar to the analyses of pathogen effects on the root-associated microbiota, the temporal and spatial variability has not been accounted for in the present studies. In addition, the effects of pesticides on the root-associated microbiota have been studied on healthy plants, while the combined effects resulting from pathogen infections and pesticides applications remain unknown. Due to the high prevalence of pathogen infections, coupled with the high usage of pesticides, understanding their effects on the holobiont of healthy and diseased plants is essential for promoting plant health and growth and has thereby potential to contribute to sustainable agriculture (Lynch and Leij 2001; Busby et al. 2017).

5. Apple and strawberry cultivation

Apple (*Malus* X *domestica* Borkh.) is one of the most important fruit crops globally in terms of production and consumption with around 93 Mt of apples produced in 2021 and an economic value of around $45 billion (Ritchie and Roser 2020; FAOSTAT 2022). The cultivated apple is thought to originate in Eurasia as the result of hybridization among different *Malus* species (Khajuria et al. 2018; Spengler 2019). It is nowadays grown in all temperate zones in more than a hundred countries with China and USA being the largest producers (FAOSTAT 2020). Sustainable apple production is challenged by numerous factors such as climate change, high reliance on chemical fertilizers and pesticides, as well as the threat by various pathogens (Morales-Quintana et al. 2020; Lang 2019). More than 90 fungal pathogens can cause different diseases from the field to fruit storage, resulting in inferior quality of fruit and drastic reduction in overall yield (Khajuria et al. 2018). Two of the most important and prominent foliar diseases worldwide are apple scab and powdery mildew caused by the fungi *Venturia inaequalis* (Cke.) Wint. and *Podosphaera leucotricha*, respectively (Bowen et al. 2011;

Tian et al. 2019). Apple scab is the biggest challenge faced by apple growers globally as production losses in highly infected orchards can go up to 70% (MacHardy 1996; Khajuria et al. 2018). The most prominent disease symptoms are premature leaf and fruit fall, as well as deformations in shape and size of the fruits, making the fruit unacceptable for the market (Jha et al. 2009). In contrast, powdery mildew mainly infects young green tissues of the plant, as well as developing blossoms and flower buds (Strickland et al. 2020). Infected leaves tend to curl or roll upwards along the edges and may drop prematurely during summer. This leads to overall reduced plant vitality and lower assimilation rates, thereby resulting in yield losses (Urbanietz and Dunemann 2005). For both diseases, the most effective management method is to avoid planting highly susceptible varieties. The susceptible varieties and, under extreme pathogen favorable conditions, even resistant varieties need to be treated with short interval routine fungicide sprays, applied from budburst to harvest and later at storage (Eurostat 2007; Berrie and Xu 2003). However, with increasing pest resistance, public concern, environmental risks and rising chemical costs, such practices have generally become less acceptable (Damos et al. 2015).

Another major fruit crop, strawberry (*Fragaria* X *ananassa* Duch.), covers an important place in the horticultural industry with around 9.0 Mt produced annually and an economic value of around $25 billion (FAOSTAT 2020). They are widely produced in almost all regions of the world with China, USA and Mexico being the main producers (Simpson 2018; Husaini and Neri 2016). Similarly to apple, its sustainable production is challenged by various pathogens and rising pesticide resistances (Husaini and Neri 2016; Dara 2016; Weber and Hahn 2019). Grey mold caused by *Botrytis* spp. is the principal fruit disease in most strawberry-growing areas worldwide (Sutton 1998). It is a well-known high-risk pathogen with respect to its ability to develop resistance to various fungicide classes and there are currently no fully resistant strawberry cultivars (Weber and Hahn 2019). Thus, high synthetic pesticide use for production and protection of the crop is needed and lead to the fact that strawberries are the most pesticide contaminated fruits (Rahman et al. 2018; El-Sheikh et al. 2023).

6. Aims of the study

Both apple and strawberry production are threatened by numerous plant pests and non-pesticide interventions are often not sufficient for effective plant protection. Thus, in modern agricultural systems, frequent applications of pesticides are necessary to obtain high yields with high quality fruits (Eurostat 2007, 2022). In recent years, understanding and engineering the root-associated microbiota has become a potentially important and more sustainable approach to improve plant growth and health (Dessaux et al. 2016). However, the responses of the root-associated microbiota to specific agricultural management practices are still largely unknown. Understanding the feedback system between the plant and its associated microbiota under various conditions and the responses of this microbiota upon plant pathogen infection or pesticide application is essential and holds potential to improve plant health by more effective treatment or support of beneficial microorganisms.

The overall aim of this thesis is the evaluation of the impact of foliar pathogen infection and above ground pesticide application on the root-associated microbiota and on above and below ground plant development. For this, a number of hypotheses arose:

I. **The root-associated microbiota of apple plants has an intrinsic spatial and temporal variation related to root phenology and seasonal variation.** As a prerequisite for evaluating pathogen and pesticide related effects, understanding the intrinsic variation of the root-associated microbiota is vital. Small-scale differences within individual orchard-grown tree root systems are likely to be related to rhizodeposition and seasonal and annual variation (manuscript 1). I hypothesize to observe those distinct differences between the root compartments also in greenhouse-grown apple saplings (manuscript 2 and 3).

II. **The infection of apple saplings with above ground fungal pathogens leads to changes in the bacterial community composition in the root-associated microbiota.** Foliar infections are known to induce significant effects on plant physiology. I hypothesize that those infections lead to pathogen species dependent and independent responses on the root-associated microbiota with distinct response differences between the root compartments (manuscript 2). Furthermore, I hypothesize these plant mediated responses to have a temporal dynamic in dependence on disease severity.

III. **The application of pesticides leads to application specific responses in the root-associated microbiota.** These changes depend on the product, the application mode and vary between different root compartments (manuscript 2 and 3). Beyond, I hypothesize that there are universal effects independent of conditions such as the used soil or model organism.

IV. **The combined effect of pathogen infection and pesticide application leads to distinct changes in the root-associated microbiota** (manuscript 2). The curative application of pesticides might lead to a new stable community composition, or it might aid the return of the microbiota to that of a healthy plant after a pathogen infection event.

II. Spatio-temporal variation in the root-associated microbiota of orchard-grown apple trees

Modified on the basis of

Maximilian Fernando Becker[1], Manfred Hellmann[2] and Claudia Knief[1], 2022. Environmental Microbiome 17, 31.
DOI: https://doi.org/10.1186/s40793-022-00427-z

[1] University of Bonn, Institute of Crop Science and Resource Conservation, Molecular Biology of the Rhizosphere, Nussallee 13, 53115 Bonn

[2] Dienstleistungszentrum Ländlicher Raum (DLR) Rheinpfalz, Kompetenzzentrum Gartenbau Klein-Altendorf, 53359, Rheinbach

Author contributions:

CK and MFB designed the study. MFB performed field and laboratory work, the bioinformatic and statistical analyses. MH supported the field work. MFB drafted the manuscript, CK and MFB further reviewed and edited. All authors read and approved the final manuscript.

Abstract

The root-associated microbiome has been of keen research interest especially in the last decade due to the large potential for increasing overall plant performance in agricultural systems. Studies about spatio-temporal variation of the root-associated microbiome focused so far primarily on community-compositional changes of annual plants, while little is known about their perennial counterparts. The aim of this work was to get deep insight into the spatial patterns and temporal dynamics of the root associated microbiota of apple trees.

The bacterial community structure in rhizospheric soil and endospheric root material from orchard-grown apple trees was characterized based on 16S rRNA gene amplicon sequencing. At the small scale, the rhizosphere and endosphere bacterial communities shifted gradually with increasing root size diameter (PERMANOVA R^2-values up to 0.359). At the larger scale, bulk soil heterogeneity introduced variation between tree individuals, especially in the rhizosphere microbiota, while the presence of a root pathogen was contributing to tree-to-tree variation in the endosphere microbiota. Moreover, the communities of both compartments underwent seasonal changes and displayed year-to-year variation (PERMANOVA R^2-values of 0.454 and 0.371, respectively).

The apple tree root-associated microbiota can be spatially heterogeneous at field scale due to soil heterogeneities, which particularly influence the microbiota in the rhizosphere soil, resulting in tree-to-tree variation. The presence of pathogens can contribute to this variation, though primarily in the endosphere microbiota. Smaller-scale spatial heterogeneity is observed in the rhizosphere and endosphere microbiota related to root diameter, likely influenced by root traits and processes such as rhizodeposition. The microbiota is also subject to temporal variation, including seasonal effects and annual variation. As a consequence, responses of the tree root microbiota to further environmental cues should be considered in the context of this spatio-temporal variation.

1. Introduction

The rhizosphere is defined as the narrow region of soil around plant roots in which the roots, the biota and the soil interact with each other (Lynch and Leij 2001). It harbors a specific microbiome, which influences plant growth and development and has potential to contribute to sustainable agriculture (Busby et al. 2017; Santoyo et al. 2016; White et al. 2019). Plants enrich microbial taxa from the surrounding soil, which then thrive in the root-associated soil and eventually establish a closer relationship by entering the root to pursue an endophytic lifestyle (Bulgarelli et al. 2013; Frank et al. 2017). This results in compartment-specific microbial communities with decreased microbial diversity and an expected higher level of interaction of root endophytes compared to the rhizosphere microbiome (Beckers et al. 2017; Bulgarelli et al. 2013). The assembly of the plant root-associated microbiome depends on several deterministic factors such as plant host genotype and developmental stage, soil properties, plant cultivation practices, geographical location, possible presence of root pathogens and stochastic factors (Bonkowski et al. 2021). The impact of these factors on the root-associated microbiome has been studied in different herbaceous and annual plants (Bulgarelli et al. 2013; Carrión et al. 2019; Chapelle et al. 2016; Edwards et al. 2015; Lundberg et al. 2012; Munoz-Ucros et al. 2021), but less in perennials and in particular in tree species (Beckers et al. 2016; Cregger et al. 2018; Mazzola et al. 2015; Padhi et al. 2019; Pervaiz et al. 2020).

In herbaceous and annual plants, temporal dynamics in the structure of the associated microbial community are considered to be closely linked to the plant development stage (Bonkowski et al. 2021; Donn et al. 2015; Li et al. 2014; Maarastawi et al. 2018; Munoz-Ucros et al. 2021; Shi et al. 2015). Previous studies on temporal dynamics of the root associated microbiota in trees have either focused on the early assembly or on pathogen infection (Blaustein et al. 2017; Dove et al. 2021; Wang and Mazzola 2019), and it remains unclear to what extent the root associated microbiota of trees is subject to seasonal changes and annual (year-to-year) variation.

Temporal dynamics in the root-associated microbiota of trees may result from seasonal shifts in carbon allocation into the roots and the surrounding soil (Epron et al. 2011). This release of predominantly photosynthetic assimilates into the rhizosphere soil mainly occurs at root tips and in the elongation zone (Epron et al. 2011; Hoffland et al.

1989; Zhalnina et al. 2018). Older root sections become suberized and are considered to be less relevant compared to fine roots concerning carbon release into the rhizosphere and nutrient uptake. As rhizodeposition provides a major source of nutrients for microorganisms in the rhizosphere (Hassan et al. 2019; Jacoby and Kopriva 2019; Zhalnina et al. 2018), the assembly of specific microbial communities likely varies between different root sections along the root axis. Such differences have been reported for some herbaceous monocots, e.g. along the root axis of maize (Rüger et al. 2021) or between root tips and bases of *Brachypodium* (Kawasaki et al. 2016), but remain to be assessed in the tree rhizosphere microbiota.

The root-associated microbiota of trees has so far predominantly been studied in poplar and orchard trees, especially in citrus and apple (Beckers et al. 2017; Blaustein et al. 2017; Cregger et al. 2018; Padhi et al. 2019; Pervaiz et al. 2020). Most studies with apple focused on apple replant disease, a worldwide phenomenon causing growth reductions and losses in fruit yield and quality (Rumberger et al. 2007; Franke-Whittle et al. 2015; Jiang et al. 2017; Mahnkopp-Dirks et al. 2021; van Horn et al. 2021). The poplar studies mainly addressed the variability of bacterial communities between tree individuals and between plant compartments such as root, rhizosphere, leaf or stem (Beckers et al. 2017; Cregger et al. 2018). For a detailed study of the spatio-temporal variation in the tree-root associated microbiota, we chose mature apple trees (*Malus* X *domestica* Borkh.) as model organism, because of its high importance as perennial fruit crop with a worldwide production of 86 million tonnes in 2018 (FAOSTAT 2019). Commercially grown apple trees have a particular root architecture with very compact root growth (Suppl. Fig. VII-1), which facilitates a systematic spatial analysis of all parts of the root system.

Aim of this study was to systematically investigate spatio-temporal patterns in the root-associated microbiota of commercially grown apple trees. We hypothesized that i) small-scale differences exist in the structure of the microbiota within individual tree root systems, with a successional gradient in relation to root diameter, as rhizodeposition is considered to decrease with increasing root size, ii) the root-associated microbiota undergoes temporal succession, related to the phenological development of the plant, and shows annual variation, iii) spatial patterns and temporal dynamics differ between the rhizosphere and endosphere microbiota, resulting from specific impacts of different

factors on these microbiotas. To test these hypotheses, we analyzed the root-associated microbiota of orchard-grown apple trees based on three field trials. Focus of the first trial (referred to as “spatial trial”) was the spatial variation within the root system of individual trees, while the second “temporal trial” addressed variation over time. In a third “spatio-temporal trial”, performed a year later, the small-scale spatial variation within the root system and the temporal patterns were further elucidated and directly compared. Moreover, larger-scale spatial variation from tree to tree resulting from field heterogeneity was assessed for trees between and along two rows, i.e. along an 80-m longitudinal transect in the field. We studied the spatio-temporal patterns comparatively in two compartments according to the concept of Donn et al. (2015) by analysis of the loosely associated root microbiota (L-compartment), which primarily represents microorganisms residing in the rhizosphere, and the tightly associated microbiota (T-compartment), which primarily represents endophytes and microorganisms being very tightly associated to the root surface. Focus was on the bacterial community composition, which was analyzed by amplicon sequencing of the 16S rRNA gene.

2. Material and methods

2.1 Study site and root sampling

Three field trials were conducted at the research facility “DLR Rheinpfalz” in Mecken-heim, Germany. For the spatial trial, the entire root systems of four healthy adjacently grown apple trees (in order from tree 1 to tree 4) of the variety “Welland” were dug out and divided into four quadrants around the stem. In each quadrant, roots were divided into four sections depending on their root diameter (1: ≤ 1 mm, 2: 1 – 2 mm, 3: 2 – 4 mm, 4: ≥ 4 mm root diameter) as a proxy for root age and rhizodeposition. Triplicate samples were taken from each size category within a quadrant. One bulk soil sample was taken for each quadrant of each tree nearby the respective tree root system. For the temporal trial, root systems of six healthy trees of the variety “Topaz” were sampled at twelve time points over the course of one year from May 2018 to April 2019 (Suppl. Table VII-1). Trees were located in two opposing rows and in each row three adjacent trees at approximately 1.5 m spacing were sampled, thus all standing in close proximity to each other. Root samples were collected at each timepoint from each tree using a custom-made metal corer (Ø = 4.5 cm), which was inserted approx. 50 cm into the soil at a distance of around 20-30 cm from the tree trunk. Care was taken to sample from a new position within the tree root system at each time point. Roots with a size between 1 to 6 mm were collected from the drill core, primarily from 30 to 40 cm soil depth. In the spatio-temporal trial, nine healthy apple trees of the variety “Topaz”, located in the same two rows as the trees of the temporal trial were sampled four times between March and end of August 2019 (Suppl. Table VII-1). The timepoints reflect phenologi-cal stages from initial emergence of leaves in spring until shortly before fruit harvest, during which we expected to find the strongest temporal dynamics in the community composition. Nine trees were analyzed within two opposing tree rows, respectively, spanning a distance of roughly 80 m. The rows were divided into three equally large clusters and three trees were sampled in each cluster, i.e. every third tree was sampled in each cluster. Root samples were collected with a metal corer and separated into two different size fractions in this trial: fine roots (FR) with a diameter between 1 to 3 mm and thick roots (TR) with 3 to 6 mm diameter.

2.2 Sample processing

All samples were collected in 50-ml falcon tubes, stored on ice and frozen at -80°C within six hours of sampling. Upon thawing for further processing, loosely attached soil was shaken off and the roots cut into the different root size fractions. Loosely and tightly root-associated microorganisms were collected according to the protocol of Donn et al. (2015). For the L-compartment, around 45 ml of 0.2 mM sterile $CaCl_2$ solution was added to the root samples in 50-ml falcon tubes and vortexed three times for 30 seconds to loosen adhering soil and microorganisms from the roots. After 10 min of sedimentation the root material was transferred into a fresh 15-ml falcon tube, which was immediately frozen in liquid nitrogen for analysis of the T-compartment. The suspension containing the microorganisms of the L-compartment was centrifuged at 4255 x g for 15 min at 5 °C in a swing-bucket rotor to pellet all microbial cells. The supernatant was discarded up to 15 ml, the pellet resuspended in this remaining liquid by vortexing, the suspension transferred to a 15-ml falcon tube and centrifuged again. The supernatant was decanted and the pellet immediately frozen in liquid nitrogen. Both L- and T-samples were stored at -80 °C until further processing. To improve comparability, the bulk soil samples were processed in a similar way as the root samples by adding 45 ml of 0.2 mM sterile $CaCl_2$ solution to the soil, vortexing three times for 30 s, followed by 10 min of sedimentation and centrifugation at 4255 x g for 15 min at 5 °C. The supernatant was discarded and the sample frozen in liquid nitrogen. All samples were freeze dried using a Heto PowerDry PL6000 freeze dryer (Thermo Fisher Scientific, Waltham, MA) and vortexed afterwards to homogenize the sample material. The frozen root material of the T-compartment was ground using a Retsch Mixer Mill MM 400 (Haan, Germany) and Retsch 25-ml grinding jars with 15-mm steel balls for 2 min at 25 Hz.

2.3 DNA extraction and 16S rRNA gene PCR

A detailed description of the DNA extraction and subsequent 16S rRNA gene targeted PCR is given in the supplement (Suppl. VII). In brief, DNA extractions were performed using the NucleoSpin® Soil DNA extraction kit (Macherey Nagel, Düren, Germany) and DNA concentrations were quantified using the QuantiFluor®dsDNA System (Promega Corporation, Fitchburg, WI). For bacterial community analysis, the 16S rRNA gene was amplified using an LNA PCR protocol to suppress the amplification of plant organelle derived 16S rRNA genes (Ikenaga and Sakai 2014). The bacterial

genes were amplified using the modified primer set 63f-1492r, followed by a nested PCR using primer set 799f-1193r (V5 - V7 region) to obtain PCR products of adequate length for sequencing. The forward primer in this nested PCR contained an 8-bp sample-specific barcode (Suppl. Table VII-2), similarly as used in Frindte et al. (Frindte et al. 2019). PCR products were pooled at equimolar concentrations and purified with the HighPrep™PCR Clean-up System kit (MagBio Genomics, Gaithersburg, MD). Library preparation and sequencing on a HiSeq system (Illumina, San Diego, CA) was performed by the Max Planck-Genome-centre Cologne and generated paired-end reads (2 × 250 bp).

2.4 Sequence data analysis

The raw sequence reads were processed using a custom bash script with Cutadapt version 2.10 to demultiplex the samples (Martin 2011). Primer removal and further processing was done with QIIME2 version 2021.02 (Bolyen et al. 2019). Denoising was performed using DADA2, likewise as forward and reverse read trimming and truncation after inspecting the quality profiles according to the developer's recommendations (Callahan et al. 2016). Amplicon sequence variants (ASVs) of each trial were defined using a custom classify-sklearn plugin classifier against the SILVA 138 database, which was subsetted to the amplicon region and using the last common ancestor method (Bokulich et al. 2018; Quast et al. 2013; Yilmaz et al. 2014). For each trial, the classified reads were quality filtered separately by removing rare ASVs that appeared less than 20 times and in less than 5 samples within a trial. Likewise, samples with less than 10.000 reads were excluded. The total number of samples, the hierarchical structures of the trials, the read numbers and the number of samples remaining after quality filtering are displayed in Suppl. Table VII-3. After quality filtering a minimum of 28 samples remained in the spatial trial for each root section in each compartment. In the temporal trial, between three and six samples were available for each timepoint in each compartment and between four and nine samples in the spatio-temporal trial for each timepoint in each root section and compartment.

Statistical analyses were performed in the QIIME2 environment and in R version 4.0.2 (R Core Team 2021) using the packages "phyloseq" (McMurdie and Holmes 2013), "microbiome" (Lahti et al. 2017) and "qiime2R" (Jordan E Bisanz 2018), while figures were generated using the "ggplot2" package (Wickham 2016). All further statistical

analyses were done separately for the two root compartments and the bulk soil by dividing the datasets. Alpha diversity was estimated by Shannon`s diversity index using a feature table rarefied to 10.000 reads per sample. Linear mixed-effects models were constructed to assess differences in alpha diversity using the “lmer” function of the lme4 package for the spatial and spatio-temporal trial, while the “lme” function of the nlme package was used for the temporal trial. For the spatial trial, the Shannon values of the pseudo-replicates were averaged. The variables root section and plant individual were used as fixed factors and their interaction was included, while the root quadrant was added as random effect. In the temporal trial, tree individual and season (season defined as shown in Suppl. Table VII-1) were used as fixed factors, the tree individual as random factor and the date of sampling was integrated to adjust the temporal autocorrelation using the “corAR1” constructor. In the spatio-temporal trial, the root sections and sampling timepoints were used as fixed factors and their interaction included, while the tree individual was added as random factor. Significance was determined using the “anova” function and pairwise comparisons were performed by estimated marginal means using the “emmeans” function of the emmeans package.

Differences in the bacterial community composition were determined based on the non-rarefied dataset using the q2-plugin “DEICODE”, a form of Aitchison Distance (Martino et al. 2019), and constrained analysis of principal coordinates (CAP) using “capscale” in the “vegan” package (Jari Oksanen et al. 2019). Statistical differences were calculated using “adonis”, a form of one-way permutational multivariate analysis of variance (PERMANOVA), followed by a pairwise PERMANOVA with Benjamini-Hochberg correction for multiple testing using the “pairwise.adonis” function, resulting in adjusted *p*-values (p_{adj}). All explanatory variables were coded as categorical factors. In the spatial trial, the effects of tree individual and root section were evaluated and permutations constrained by the factor root quadrant due to the nested design. In the temporal trial, variation due to sampling timepoint and tree individual were assessed, whereby permutations were constrained by the factor tree individual due to the repeated sample collection from the same individuals over time. This was also done in the spatio-temporal trial, where the effects of timepoint, root section and tree individual were analyzed. To assess whether gradual changes between or along tree rows contribute to tree-to-tree variation the factor tree was replaced by row or longitudinal position and the results were compared. Pairwise differential abundance analysis at ASV

level was performed for all trials using ANCOM-BC with detection for structural zeros turned on (Lin and Peddada 2020). Conservative variance estimates of the test statistic were used and *p*-values were adjusted using Holm's correction. While ASVs with a mean abundance of ≥ 0.1% in either the L- or T-compartment were included in the analysis of the spatial trial, a threshold of ≥ 0.3% mean relative abundance was applied in the analysis of the second and third trial, because of the slightly lower sample number and thus an increased false discovery rate (FDR) for low abundant ASVs. Similarly, differential abundance analysis was performed at family and phylum level comparing the L- and T-compartment in the different trials.

3. Results

3.1 Differences in the root microbiota between compartments at phylum and family level

Bacterial community composition was clearly dominated by members of the phylum *Proteobacteria* (mean relative abundance of 59.0%) in all samples, mostly followed by *Actinobacteriota* (12.7%), *Bacteroidota* (9.5%) and *Acidobacteriota* (6.9%) (Fig. II-1 A). Clear differences were seen in the community composition between L- and T-compartment in all three trials by one-way PERMANOVA on DEICODE distances (spatial trial: $R^2 = 0.483$, $p = 0.001$ | temporal trial: $R^2 = 0.449$, $p = 0.001$ | spatio-temporal trial: $R^2 = 0.458$, $p = 0.001$). Most consistent was a strong increase in the relative abundance of *Actinobacteriota* and the low-abundant *Myxococcota* in the T-compartment according to a differential abundance analysis by ANCOM-BC (Fig. II-1 B). The corresponding analysis at family level revealed that 13 members of *Actinobacteriota* were enriched in the T-compartment in one or more trials. Phyla with significant enrichment in the L-compartment included the *Acidobacteriota* (Fig. II-1 B) with eight responsive families in at least one trial (Suppl. Fig. VII-2). Similar patterns were observed for the phyla *Bacteroidota* and *Dependentiae*. Moreover, individual families within the *Desulfobacterota*, *Gemmatimonadota*, *Firmicutes* and *Nitrospirota* responded in this way. In contrast, the proteobacterial families showed differential responses with 13 families being enriched and 14 being depleted in the T-compartment, which explains the mostly non-significant change at phylum level (Fig. II-1 B). Differences between the two compartments were also evident among the ten most abundant genera in each compartment

(Suppl. Table VII-4). Due to these profound differences, which were also evident in CAP plots of individual trials (exemplarily shown in Suppl. Fig. VII-3) all further analyses were conducted separately for each compartment.

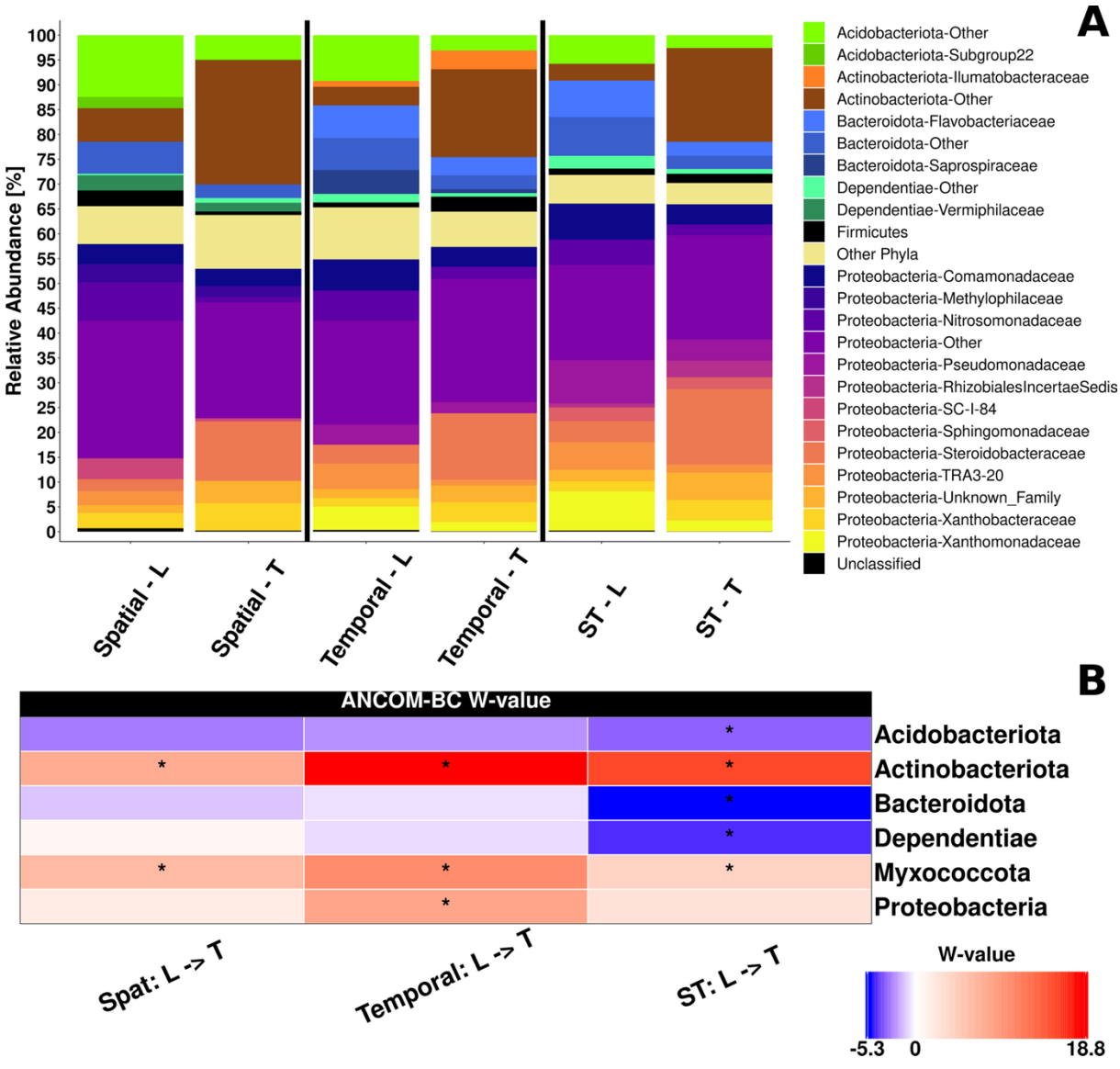

Fig. II-1: Root-associated bacterial community composition of apple trees as revealed by 16S rRNA gene amplicon sequencing. **A** Relative abundance of bacterial families in samples from three different field trials (Spatial, Temporal and ST: spatio-temporal) in the loosely associated (L) and tightly associated (T) compartment. Phyla and their families with < 2% relative abundance in the respective trial were grouped as "Other". **B** Differential abundance analysis of L- and T-communities at phylum level using ANCOM-BC. The heatmap shows the coefficients obtained from the ANCOM-BC log-linear model divided by their standard error (called W-value). The colour code indicates differential abundances between two compartments with red indicating enrichment in the T-compartment. A "*" is shown if ANCOM-BC showed significant differences using the adjusted *p*-value in this comparison.

3.2 Analysis of spatial patterns in the root-associated microbiota

Spatial variation in the bacterial community structure within tree-root systems was assessed based on four adjacently grown apple trees. The root system of each tree was divided into four quadrants around the trunk and roots were separated into four size sections according to diameter. The mean Shannon diversity index of the bacterial community was significantly ($p < 0.001$) reduced in the T-compartment (7.61 ± 0.39) compared to the L-compartment (8.28 ± 0.43), where it was similar to the bulk soil diversity (8.22 ± 0.25). In the L-compartment, variation in diversity was observed between the individual trees ($p < 0.001$), while neither root section nor its interaction with individual trees caused significant changes (Fig. II-2 A, C). Pairwise comparisons showed that trees 1 and 2 had a slightly lower diversity estimate than trees 3 and 4 ($p < 0.001$). In the T-compartment, no factor showed effects on alpha diversity (p-values > 0.05) (Fig. II-2 C). Only the factor root section was close to the significance threshold ($p = 0.058$), with roots with the largest diameter tending to have a more diverse bacterial community than those of the other three size sections (Fig. II-2 A).

Analyzing beta diversity by PERMANOVA and CAP (Fig. II-2 B, C) showed that tree-to-tree variation was the predominant factor explaining variation in bacterial community composition in the L-compartment ($R^2 = 0.354$; $p < 0.001$), reflected by its separation along the first CAP axis, which explained 28% of the variation. Similar to alpha diversity results, the adjacent trees 1 and 2 as well as the adjacent trees 3 and 4 were more similar in their bacterial community composition to each other compared to the other two trees. This is supported by pairwise PERMANOVA, where all trees except tree 1 versus tree 2 were shown to be significantly different from each other (R^2-values between 0.317 and 0.365, $p_{adj} = 0.006$) and with tree 3 versus tree 4 having a neglectable small R^2-value (0.075, $p_{adj} = 0.006$) (Suppl. Table VII-5). Besides tree individuality, the root section had a significant impact on the bacterial community in the L-compartment ($R^2 = 0.200$; $p = 0.001$), resulting in a successive separation of samples in CAP according to root size along the second axis with 19.8% explained variation. This gradual shift was most clearly seen in trees 3 and 4, which showed in general larger variation in community composition compared to trees 1 and 2 (Fig. II-2 B). Pairwise PERMANOVA performed over all four trees supported this, with strongest differences

C

Com-partment	Variable	PERMANOVA				LMM	
		Df	F. Model	R^2	*p*	F.Model	*p*
L	Tree	3	26.766	0.354	0.001	35.111	< 0.001
	Root Section	3	47.411	0.200	0.001	0.235	0.872
	Tree * Root Section	9	4.121	0.092	0.001	1.442	0.200
T	Tree	3	12.731	0.124	0.001	1.929	0.139
	Root Section	3	36.720	0.359	0.001	2.684	0.058
	Tree * Root Section	9	3.986	0.117	0.001	1.233	0.301

Fig. II-2: Spatial variation in the root-associated bacterial community of apple trees linked to root section, tree individual and root quadrant. **A** Variation in alpha diversity presented based on the Shannon index in the L-compartment (left) and T-compartment (right) of four different trees. The different colours in the boxplots indicate different root sections according to their root diameter. **B** Variation in beta diversity presented based on constrained analysis of principal coordinates (CAP; using DEICODE distance matrices, constrained by the variables tree, root section and root quadrant) shown for the L-compartment (left) and T-compartment (right). Different colours were used for different root size sections and symbol shapes for the four individual trees sampled. **C** Statistical evaluation of differences in alpha and beta diversity in the L- and T-compartment. Effect sizes in beta diversity were assessed by PERMANOVA based on DEICODE distance matrices, while differences in Shannon diversity were analysed based on Linear Mixed-Effects Models (LMM).

between the smallest and the two largest root sections (Suppl. Table VII-5). In the T-compartment, root section was the strongest explanatory factor ($R^2 = 0.359$; $p = 0.001$), and a gradual shift in community composition in relation to root size section was evident in the CAP plot along the first axis, explaining 29% of the variation (Fig. II-2 B). Pairwise PERMANOVA showed that all root sections were indeed significantly different from each other (R^2-values between 0.096 and 0.318; $p_{adj} \leq 0.012$, Suppl. Table VII-5).

ASVs with differential abundance between root size sections were identified based on ANCOM-BC. Interestingly, most ASVs with consistent changes across root size sections in the L-compartment showed a similar trend in the T-compartment (Fig. II-3). Overall, the majority of responsive ASVs decreased in relative abundance with increasing root diameter in both compartments, e.g., *Actinobacteriota*, *Bacteroidota*, *Myxococcota* and *Patescibacteria*. In contrast, no phylum showed consistent increases with root size, rather some specific ASVs. In particular ASVs of the *Proteobacteria*, which was the most responsive phylum, showed differential responses. Most of the significant differences were observed between the largest and the two smallest root sections. In the L-compartment, this was seen for ASVs representing potential nitrogen fixing taxa (*Azovibrio*, *Mesorhizobium*, *Noviherbaspirillum*), methylotrophs (*Methylibium*, *Methylotenera*, unclassified *Methylophilaceae*), and other unclassified ASVs (e.g. *Rhizobiaceae*, *Sphingomonadaceae*, *Xanthomonadaceae*), which decreased in relative abundance in the largest root size fraction. ASVs that were in contrast more abundant in the largest size fraction included primarily *Acidobacteriota*, *Nocardia* and some *Proteobacteria* (*Acidibacter*, *Pseudolabrys*, one of the ASVs assigned to *Methylotenera* and unclassified *Halieaceae* and *Moraxellaceae*). In the T-compartment, the distinction of the largest root size fraction was even more prominent than in the L-compartment in all major responsive groups. Especially among the *Actinobacteriota* in the T-compartment, most ASVs decreased along the root section gradient towards the largest one with only *Nocardia*, *Mycobacterium* and one *Streptomyces* ASV being an exception, which increased along the size gradient. Furthermore, different *Proteobacteria* such as rhizobia, some methylotrophs, sphingomonads, or ammonium oxidizers tended to decrease in relative abundance in the larger root sections, while only few *Proteobacteria* increased (*Pseudolabrys*, *Reyranella*, unclassified *Halieceae* and *Methyloligellaceae*).

Seeing substantial tree-to-tree variation especially in the L-compartment, we assessed whether the bulk soil samples collected within the root quadrants showed a similar pattern. PERMANOVA and CAP (Suppl. Fig. VII-4) revealed indeed a grouping of the bulk soil samples according to tree location ($R^2 = 0.515$; $p < 0.05$). Similar as seen in the L-compartment, samples taken nearby trees 1 and 2 tended to cluster more closely together compared to trees 3 and 4. Despite a rather low number of bulk soil samples being available, differential abundance analysis allowed us to identify 26 responsive ASVs with a mean relative abundance of ≥ 0.1% (Suppl. Fig. VII-5). Of these, 42.4% showed a similar response pattern in the L-compartment, while only 11.5% responded similarly in the T-compartment. Thus, tree-to-tree variation, especially in the L-compartment, appears to be influenced by spatial patterns in the bulk soil.

3.3 Succession of the microbial community composition over time

The temporal dynamics in the loosely and tightly root-associated bacterial communities were studied based on six apple trees that were repeatedly sampled twelve times over the course of one year (Suppl. Table VII-1). The alpha diversity estimates of both compartments showed comparable fluctuations over time with highest Shannon indices in the summer months June until August (Fig. II-4 A). Afterwards, diversity decreased with the exception of the December samples until around March/April, when a steep increase followed in spring around the time when leaves and first buds emerged. The statistical analysis showed significant results between seasons in both compartments (both *p*-values = 0.002) with the winter season having a significantly reduced diversity compared to the summer season in both compartments (both *p*-values = 0.001), even though the December timepoint showed an intermediate increase. Regarding beta diversity, the factor time showed a significant impact on the bacterial communities in both compartments according to PERMANOVA (L: $R^2 = 0.454$; $p = 0.001$ | T: $R^2 = 0.371$; $p = 0.001$). CAP plots revealed that fluctuations in the L-compartment occurred primarily in summer 2018, followed by a continuous though weaker succession in the following months until the end of the experiment in spring 2019 (Fig. II-4 B). In the T-compartment successional changes were likewise mostly seen between May and September 2018, while less changes occurred in the cold months. In PERMANOVA no pairwise comparison remained significant after adjusting for multiple

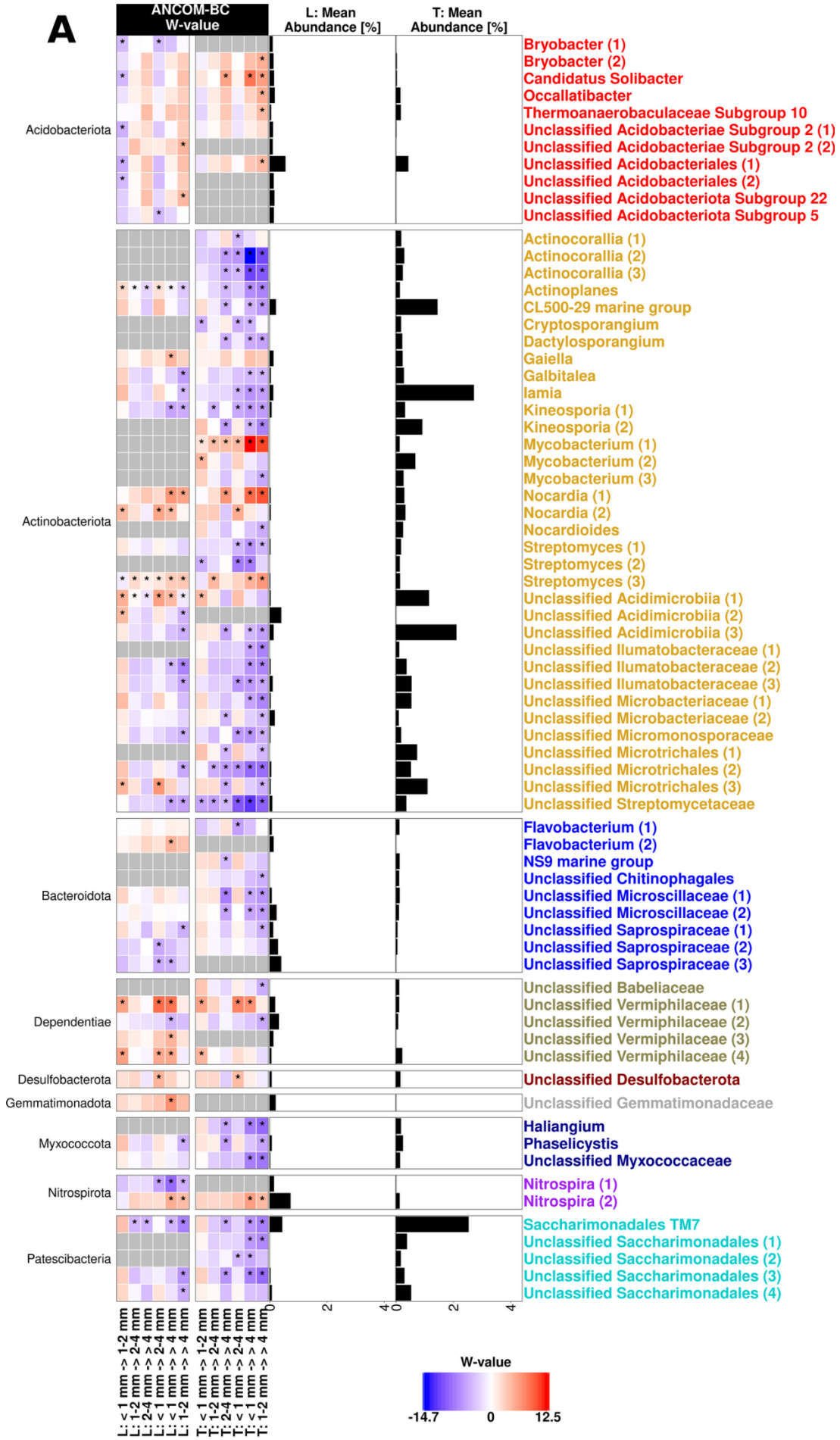
A
ANCOM-BC W-value
L: Mean Abundance [%]
T: Mean Abundance [%]
Acidobacteriota
Actinobacteriota
Bacteroidota
Dependentiae
Desulfobacterota
Gemmatimonadota
Myxococcota
Nitrospirota
Patescibacteria
Bryobacter (1)
Bryobacter (2)
Candidatus Solibacter
Occallatibacter
Thermoanaerobaculaceae Subgroup 10
Unclassified Acidobacteriae Subgroup 2 (1)
Unclassified Acidobacteriae Subgroup 2 (2)
Unclassified Acidobacteriales (1)
Unclassified Acidobacteriales (2)
Unclassified Acidobacteriota Subgroup 22
Unclassified Acidobacteriota Subgroup 5
Actinocorallia (1)
Actinocorallia (2)
Actinocorallia (3)
Actinoplanes
CL500-29 marine group
Cryptosporangium
Dactylosporangium
Gaiella
Galbitalea
Iamia
Kineosporia (1)
Kineosporia (2)
Mycobacterium (1)
Mycobacterium (2)
Mycobacterium (3)
Nocardia (1)
Nocardia (2)
Nocardioides
Streptomyces (1)
Streptomyces (2)
Streptomyces (3)
Unclassified Acidimicrobiia (1)
Unclassified Acidimicrobiia (2)
Unclassified Acidimicrobiia (3)
Unclassified Ilumatobacteraceae (1)
Unclassified Ilumatobacteraceae (2)
Unclassified Ilumatobacteraceae (3)
Unclassified Microbacteriaceae (1)
Unclassified Microbacteriaceae (2)
Unclassified Micromonosporaceae
Unclassified Microtrichales (1)
Unclassified Microtrichales (2)
Unclassified Microtrichales (3)
Unclassified Streptomycetaceae
Flavobacterium (1)
Flavobacterium (2)
NS9 marine group
Unclassified Chitinophagales
Unclassified Microscillaceae (1)
Unclassified Microscillaceae (2)
Unclassified Saprospiraceae (1)
Unclassified Saprospiraceae (2)
Unclassified Saprospiraceae (3)
Unclassified Babeliaceae
Unclassified Vermiphilaceae (1)
Unclassified Vermiphilaceae (2)
Unclassified Vermiphilaceae (3)
Unclassified Vermiphilaceae (4)
Unclassified Desulfobacterota
Unclassified Gemmatimonadaceae
Haliangium
Phaselicystis
Unclassified Myxococcaceae
Nitrospira (1)
Nitrospira (2)
Saccharimonadales TM7
Unclassified Saccharimonadales (1)
Unclassified Saccharimonadales (2)
Unclassified Saccharimonadales (3)
Unclassified Saccharimonadales (4)
L: 1-2 mm > 1 mm
L: 2-4 mm > 1-2 mm
L: > 4 mm > 2-4 mm
L: 1-2 mm > 1 mm
L: 2-4 mm > 1-2 mm
L: > 4 mm > 2-4 mm
T: 1-2 mm > 1 mm
T: 2-4 mm > 1-2 mm
T: > 4 mm > 2-4 mm
T: 1-2 mm > 1 mm
T: 2-4 mm > 1-2 mm
T: > 4 mm > 2-4 mm
0
2
4
0
2
4
W-value
-14.7
0
12.5

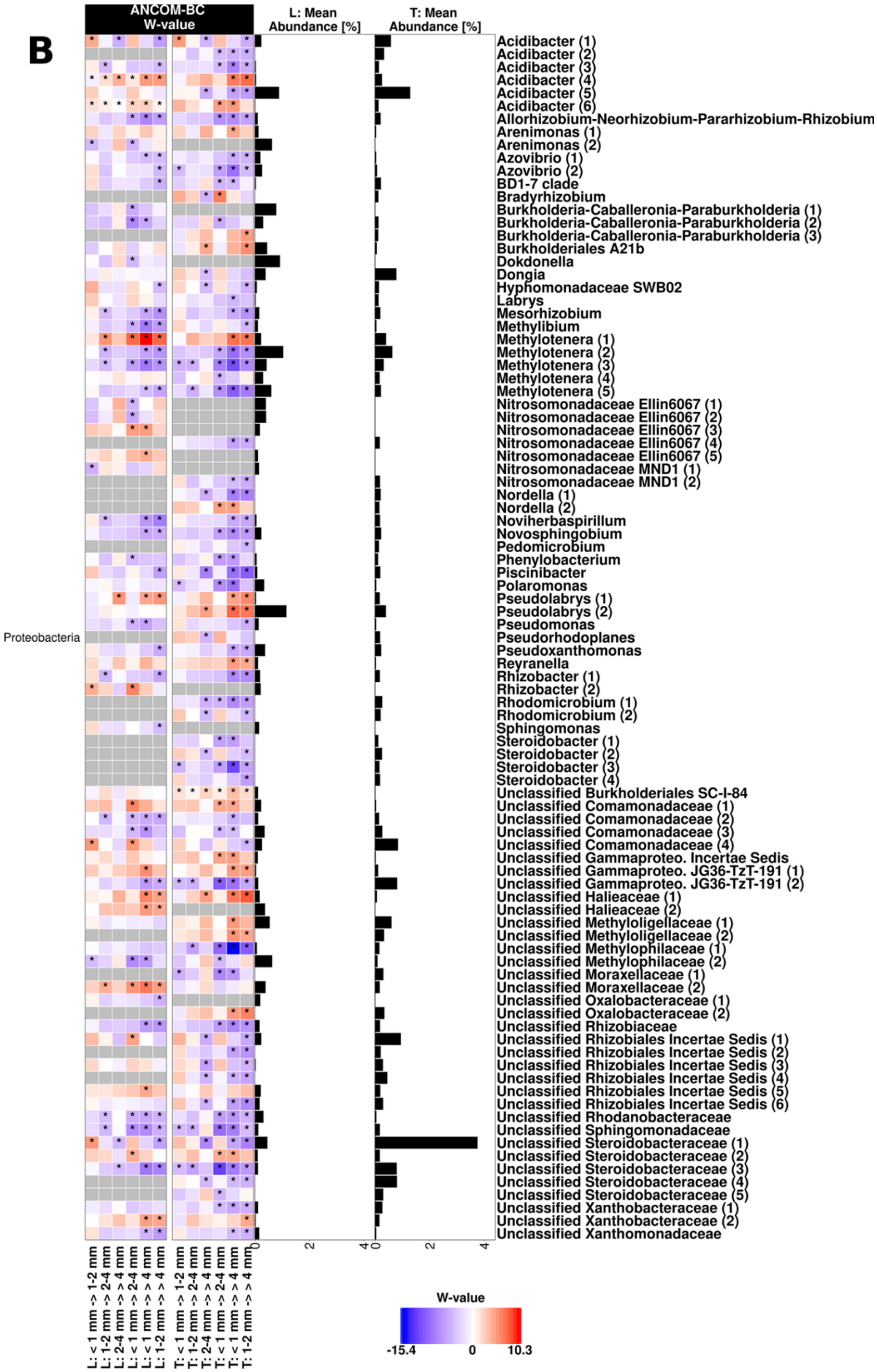
B
ANCOM-BC W-value
L: Mean Abundance [%]
T: Mean Abundance [%]
Proteobacteria
Acidibacter (1)
Acidibacter (2)
Acidibacter (3)
Acidibacter (4)
Acidibacter (5)
Acidibacter (6)
Allorhizobium-Neorhizobium-Pararhizobium-Rhizobium
Arenimonas (1)
Arenimonas (2)
Azovibrio (1)
Azovibrio (2)
BD1-7 clade
Bradyrhizobium
Burkholderia-Caballeronia-Paraburkholderia (1)
Burkholderia-Caballeronia-Paraburkholderia (2)
Burkholderia-Caballeronia-Paraburkholderia (3)
Burkholderiales A21b
Dokdonella
Dongia
Hyphomonadaceae SWB02
Labrys
Mesorhizobium
Methylibium
Methylotenera (1)
Methylotenera (2)
Methylotenera (3)
Methylotenera (4)
Methylotenera (5)
Nitrosomonadaceae Ellin6067 (1)
Nitrosomonadaceae Ellin6067 (2)
Nitrosomonadaceae Ellin6067 (3)
Nitrosomonadaceae Ellin6067 (4)
Nitrosomonadaceae Ellin6067 (5)
Nitrosomonadaceae MND1 (1)
Nitrosomonadaceae MND1 (2)
Nordella (1)
Nordella (2)
Noviherbaspirillum
Novosphingobium
Pedomicrobium
Phenylobacterium
Piscinibacter
Polaromonas
Pseudolabrys (1)
Pseudolabrys (2)
Pseudomonas
Pseudorhodoplanes
Pseudoxanthomonas
Reyranella
Rhizobacter (1)
Rhizobacter (2)
Rhodomicrobium (1)
Rhodomicrobium (2)
Sphingomonas
Steroidobacter (1)
Steroidobacter (2)
Steroidobacter (3)
Steroidobacter (4)
Unclassified Burkholderiales SC-I-84
Unclassified Comamonadaceae (1)
Unclassified Comamonadaceae (2)
Unclassified Comamonadaceae (3)
Unclassified Comamonadaceae (4)
Unclassified Gammaproteo. Incertae Sedis
Unclassified Gammaproteo. JG36-TzT-191 (1)
Unclassified Gammaproteo. JG36-TzT-191 (2)
Unclassified Halieaceae (1)
Unclassified Halieaceae (2)
Unclassified Methyloligellaceae (1)
Unclassified Methyloligellaceae (2)
Unclassified Methylophilaceae (1)
Unclassified Methylophilaceae (2)
Unclassified Moraxellaceae (1)
Unclassified Moraxellaceae (2)
Unclassified Oxalobacteraceae (1)
Unclassified Oxalobacteraceae (2)
Unclassified Rhizobiaceae
Unclassified Rhizobiales Incertae Sedis (1)
Unclassified Rhizobiales Incertae Sedis (2)
Unclassified Rhizobiales Incertae Sedis (3)
Unclassified Rhizobiales Incertae Sedis (4)
Unclassified Rhizobiales Incertae Sedis (5)
Unclassified Rhizobiales Incertae Sedis (6)
Unclassified Rhodanobacteraceae
Unclassified Sphingomonadaceae
Unclassified Steroidobacteraceae (1)
Unclassified Steroidobacteraceae (2)
Unclassified Steroidobacteraceae (3)
Unclassified Steroidobacteraceae (4)
Unclassified Steroidobacteraceae (5)
Unclassified Xanthobacteraceae (1)
Unclassified Xanthobacteraceae (2)
Unclassified Xanthomonadaceae
0
2
4
0
2
4
L: < 1 mm -> 1-2 mm
L: 1-2 mm -> 2-4 mm
L: 2-4 mm -> > 4 mm
L: < 1 mm -> 2-4 mm
L: < 1 mm -> > 4 mm
L: 1-2 mm -> > 4 mm
T: < 1 mm -> 1-2 mm
T: 1-2 mm -> 2-4 mm
T: 2-4 mm -> > 4 mm
T: < 1 mm -> 2-4 mm
T: < 1 mm -> > 4 mm
T: 1-2 mm -> > 4 mm
W-value
-15.4
0
10.3

Fig. II-3: Differentially abundant ASVs in different root size sections of the L- and T-compartment based on ANCOM-BC. The heatmap shows the coefficients obtained from the ANCOM-BC log-linear model divided by their standard error (called W-value). A "*" is shown if ANCOM-BC showed significant differences using adjusted *p*-values in this comparison. The colour code indicates differential abundances between two root size sections with red indicating enrichment in the respective larger root section. A grey colour indicates that this ASV was not detected in the respective compartment. The mean relative abundance of the ASVs in the entire compartment is shown as % and ASVs with mean abundances ≥ 0.1% in either compartment are displayed. Names of ASVs are coloured according to phylum. **A** All phyla but *Proteobacteria*, which are displayed in (**B**). (See figure on previous pages).

testing considering all sample combinations. However, based on non-adjusted *p*-values revealed some trends, i.e. that changes developed primarily between summer (23.05.2018 to 16.7.2018) and autumn/winter timepoints (25.10.2018 to 17.4.2019) (Suppl. Fig. VII-6). In particular for the L-compartment, the bacterial community composition did not (yet) return to its initial pattern after one year, as seen in the CAP plot (Fig. II-4 B) and the non-adjusted *p*-values of the PERMANOVA, where the last timepoint (17.04.2019) was different from nearly all earlier timepoints.

Temporal dynamics of abundant ASVs (mean relative abundance ≥ 0.3%) between successive timepoints were evaluated by ANCOM-BC (Fig. II-5). Changes were primarily evident for *Proteobacteria*, while *Actinobacteriota* responded primarily in the T-compartment, where they occurred more abundantly (Fig. II-1). In both compartments, we observed several taxa with recurrent fluctuations in relative abundance over one season, whereby a significant increase was quite often immediately followed by a significant decrease or vice versa (e.g. *Burkholderiales* TR3-20, *Nitrosomadaceae* MND1, *Lysobacter* or *Pseudoxanthomonas*). These changes correspond to the fluctuations observed in the CAP plot during summer (Fig. II-4 B, left panel). In the L-compartment, less significant changes were detected in autumn/winter (25.10.2018 to 17.04.2019; TP8 to TP12) than in spring/summer (Fig. II-5, upper panel). The responsive taxa and their patterns in the T-compartment were mostly different from those in the L-compartment and most changes were seen between the first and last sampling timepoint (TP1 and TP12), where twelve significantly differentially abundant ASVs were identified.

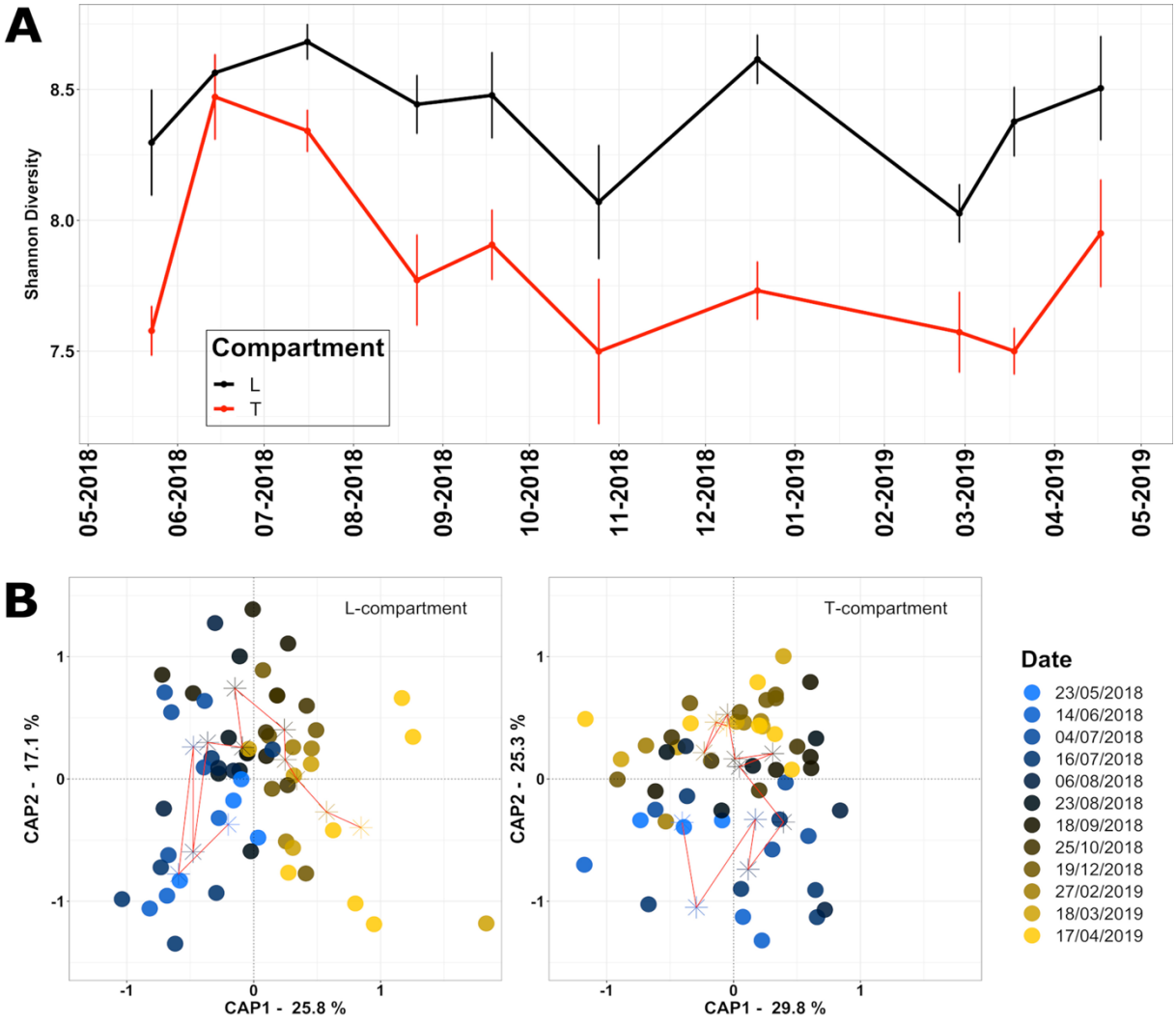

C

Com-partment	Variable	PERMANOVA				LMM	
		Df	F. Model	R^2	*p*	F.Model	*p*
L	Tree	5	1.472	0.083	0.001		
	Timepoint	11	3.657	0.454	0.001		
	Season	3				5.878	0.002
T	Tree	5	7.025	0.311	0.001		
	Timepoint	11	3.807	0.371	0.001		
	Season	3				5.737	0.002

Fig. II-4: Temporal variation in the root-associated bacterial community of apple trees. **A** Changes in alpha diversity based on the Shannon index in the two root compartments over time. Error bars indicate the standard error. **B** Constrained analysis of principal coordinates (based on DEICODE distance matrices and constrained by the variables tree and timepoint) to assess the relevance of time on variation in bacterial community composition in the L-compartment (left) and T-compartment (right). A colour gradient differentiates the twelve sampling timepoints. The stars are the calculated centroids of the samples from each timepoint and are connected with a red line along the timeline. **C** Statistical evaluation of differences in bacterial alpha and beta diversity in the L- and T-compartment. Effect sizes in beta diversity were assessed by PERMANOVA based on DEICODE distance matrices, while differences in Shannon diversity were analysed based on linear mixed models.

Tree-to-tree variation in beta diversity was mainly seen in the T-compartment ($R^2 = 0.311$; $p = 0.001$) (Fig. II-4 C). Pairwise PERMANOVA as well as ANOM-BC revealed that mainly tree individual 2 and partially tree 1 were distinct from the rest (Suppl. Fig. VII-7). Interestingly, the most responsive abundant ASV (mean relative abundance in the T-compartment 2.2%, SD: 5.1) belonged to the genus "*Candidatus* Phytoplasma", a plant pathogen. It was significantly enriched in tree 2 and to a lower degree in tree 1 compared to all other trees (Suppl. Fig. VII-7 A) reaching 24.4% relative abundance in tree 2 at the final sampling timepoint.

3.4 Comparative analysis of temporal and differently scaled spatial variation in the rhizosphere microbiota

In the spatio-temporal trial we focused on four time points in spring and summer, i. e. during the growing season, and on two relevant root size classes to assess small-scale spatial variation. In addition, larger-scale tree-to-tree variation was assessed along a longitudinal transect following two adjacent tree rows in the orchard (Suppl. Fig. VII-1) and evaluated between individual trees, trees between rows and along rows. Alpha diversity of the bacterial communities was not changed by any factor in this trial, likewise as in the temporal trial. Beta diversity analysis based on a PERMANOVA model with root section, timepoint and tree individual as explanatory variables revealed that all three factors were significant in both compartments with tree-to-tree variation being most relevant (L: $R^2 = 0.292$; $p = 0.001$ | T: $R^2 = 0.345$; $p = 0.002$) (Fig. II-6 B). This was followed by root size in the L-compartment and time in the T-compartment. To evaluate whether tree-to-tree variation was following a spatial pattern between or along rows, these factors were used alternatively in the PERMANOVA model instead of tree. In the L-compartment, the position of a tree in the row as well as its interaction with the factors timepoint and root section was explaining a considerable part of the variation (Suppl. Table VII-6), while this was not evident in the T-compartment. To analyze variation comparatively in the two root size sections, the data were divided according to root section. PERMANOVA showed that time and tree individual explained variation only in the thick root section of both, the L- and T-compartment, but not in the fine root fraction (Table II-1).

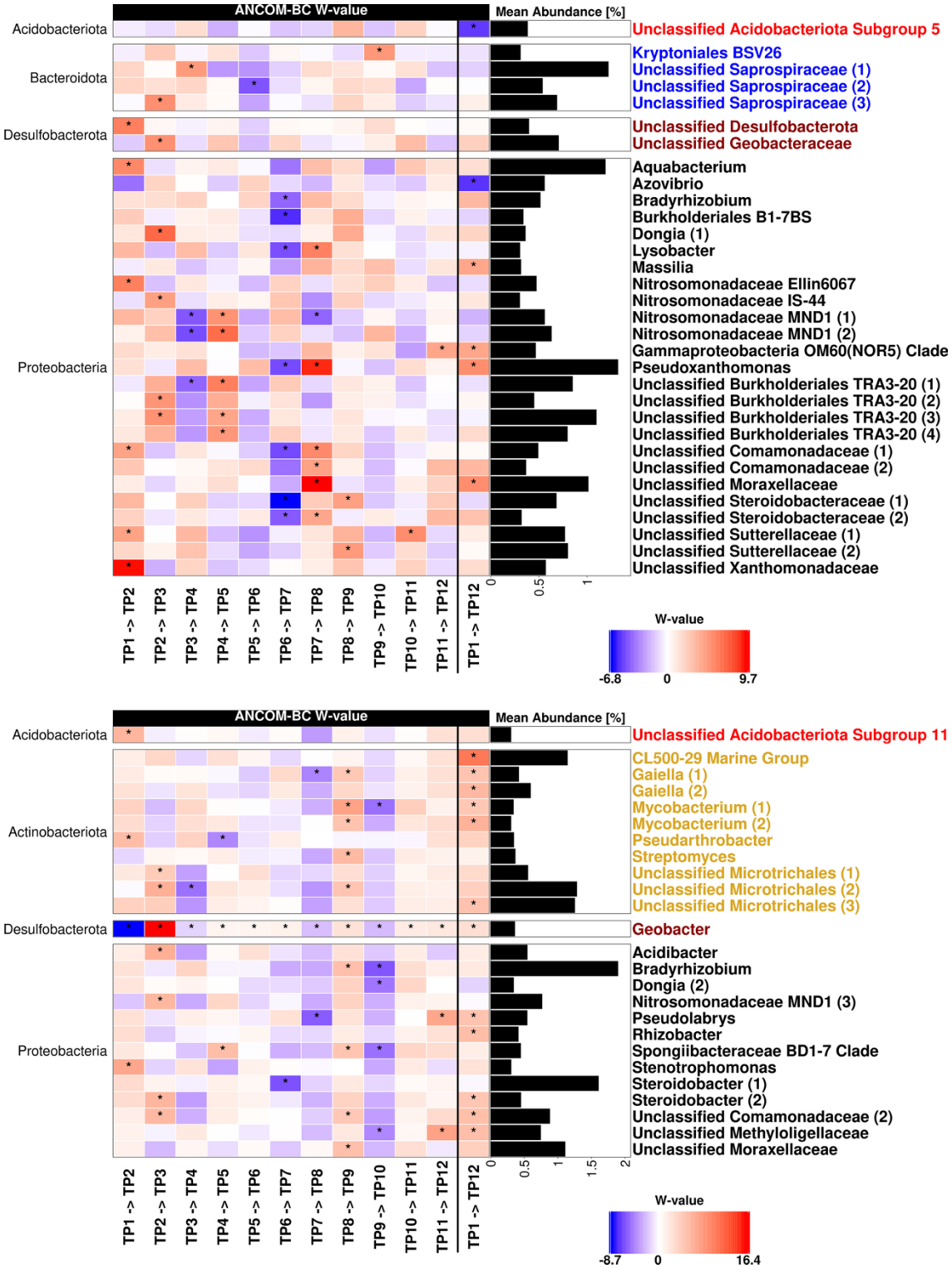

Fig. II-5: Differentially abundant ASVs between twelve successive timepoints in the L-compartment (upper) and T-compartment (lower panel) according to ANCOM-BC. The dates of the timepoints (TP) are listed in Suppl. Table VII-1. The heatmap shows the coefficients obtained from the ANCOM-BC log-linear model divided by their standard error (called W-value). A "*" is shown if ANCOM-BC showed significant differences using the adjusted *p*-value. The colour code indicates differential abundances between two samples with red indicating enrichment at the later timepoint. The mean relative abundance of the ASVs in the entire compartment is shown as % and ASVs with mean abundances ≥ 0.3% are displayed. The ASVs in the rows of the heatmap are separated according to phylum. Besides the comparisons between successive timepoints, differences between the first and last timepoint are shown.

A

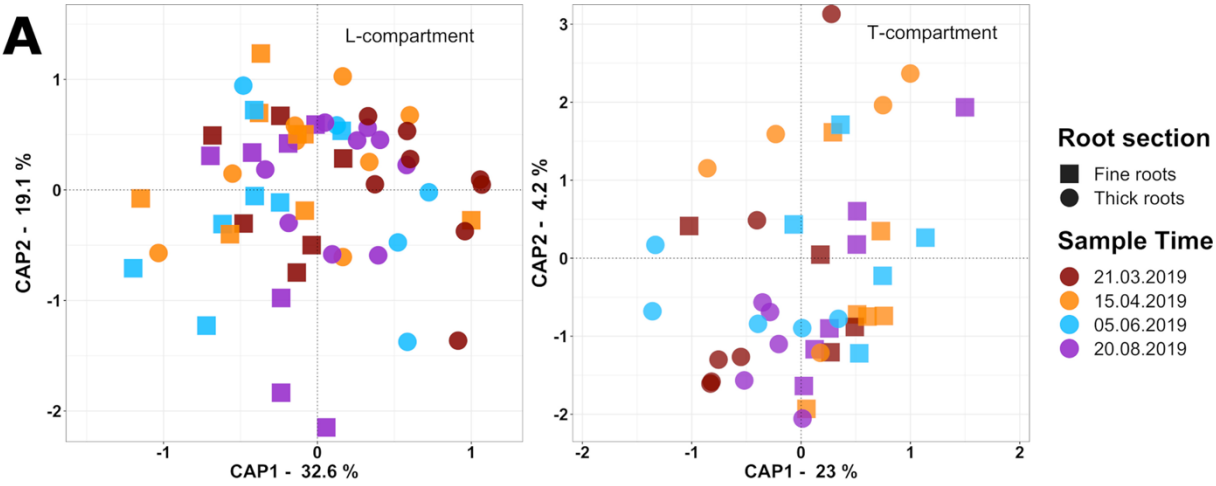

B

Compartment	Variable	PERMANOVA		
		F. Model	R^2	*p*
L	Timepoint	2.978	0.090	0.006
	Root section	13.681	0.137	0.001
	Tree	3.637	0.292	0.001
	Timepoint * Root section	1.935	0.058	0.076
T	Timepoint	2.980	0.119	0.018
	Root section	7.259	0.096	0.001
	Tree	3.248	0.345	0.002
	Timepoint * Root section	1.680	0.067	0.112

Fig. II-6: Variation in the apple root-associated bacterial community structure due to spatial (root section), temporal and tree-to-tree effects. **A** Constrained analysis of principal coordinates (CAP, based on DEICODE distance matrices, constrained by the variables tree, root section, and timepoint) shown for the L-compartment (left) and T-compartment (right). A color gradient differentiates the four sampling timepoints and symbol shapes the root section. **B** Statistical evaluation of differences in bacterial beta diversity in the L- and T-compartment. Effect sizes were assessed by PERMANOVA based on DEICODE distance matrices.

Table II-1: Significant differences in the apple root-associated bacterial community structure due to spatial (longitudinal position in field), temporal and tree-to-tree effects. Differences in bacterial diversity in the L- and T-compartment of fine (FR) and thick (TR) roots were assessed. Effect sizes were analyzed by PERMANOVA based on DEICODE distance matrices. Significant results are printed in bold.

Compartment - Section	Variable	PERMANOVA		
		F.Model	R^2	*p*
L-FR	Timepoint	1.880	0.148	0.101
	Tree	2.052	0.431	0.365
L-TR	**Timepoint**	**4.903**	**0.244**	**0.001**
	Tree	**3.441**	**0.457**	**0.001**
T-FR	Timepoint	1.385	0.127	0.625
	Tree	2.311	0.566	0.763
T-TR	**Timepoint**	**2.947**	**0.279**	**0.012**
	Tree	**1.610**	**0.406**	**0.005**

In ANCOM-BC, we evaluated differences of highly abundant ASVs (mean abundance ≥ 0.3%) in samples of different root diameter or time (Suppl. Fig. VII-8). Significant root-section related differences were primarily seen at the first timepoint, with similar trends being mostly maintained at all other timepoints. As in the spatial trial (Fig. II-3), most responsive ASVs were detected among the *Proteobacteria*. These included in the L-compartment ASVs of *Methylotenera*, *Pseudoxanthomonas*, and *Xanthomonadaceae*, which decreased in relative abundance in the thicker roots, while *Pseudolabrys* increased. In the T-compartment, ASVs identified as *Methylotenera* and several members of *Steroidobacter* and *Steroidobacteraceae* decreased in the thicker root sections consistently in both trials. Lastly, temporal dynamics were assessed independently in the two root size sections (Suppl. Fig. VII-8), revealing that temporal dynamics were mostly seen in the thick root fraction of the L-compartment. Changes were predominantly detected among the *Proteobacteria*, as in the temporal trial (Fig. II-5). This included ASVs such as *Dongia*, *Pseudoxanthomonas*, *Burkholderiales* TRA3-20, *Nitrosomonadaceae* MND1 and unclassified members of *Saprospiraceae*, *Moraxellaceae* and *Comamonadaceae*, which were all responsive in both trials, though at different timepoints.

4. Discussion

4.1 Compartment-specific differences in the apple tree rhizosphere

Based on knowledge from annual crops (Donn et al. 2015; Kawasaki et al. 2016), we expected clear differences between the loosely and tightly associated bacterial communities. Indeed, consistent differences in relative abundances were observed for the dominant families and phyla in all three experimental trials (Fig. II-1 and Suppl. Fig. VII-2). This is largely in accordance with differences reported for annual crops including maize, rice, wheat or *Arabidopsis*, where *Proteobacteria* and *Actinobacteriota* were more prevalent in the T-compartment or endosphere, while *Acidobacteriota* were more prevalent in the L-compartment or rhizosphere (Donn et al. 2015; Bulgarelli et al. 2013; Lundberg et al. 2012; Edwards et al. 2015; Fan et al. 2017). Moreover, our findings are in agreement with results from citrus and olive trees (Fernández-González et al. 2019; Zhang et al. 2017), while they are partially different to the findings reported for poplar trees, which showed a significantly higher relative abundance of *Actinobacteriota* in the rhizosphere soil compared to the root endosphere, while *Proteobacteria* responded similarly as in our work (Beckers et al. 2017; Gottel et al. 2011). Overall, it appears that trees enrich similar phyla in the endosphere as many of their annual herbaceous counterparts, pointing towards analogous selection mechanisms.

By far the most abundant taxon (11 – 16%) in the T-compartment in all three trials was the genus *Steroidobacter* (or *Steroidobacteraceae* in the spatial trial) (Suppl. Table VII-4). This genus has been reported to be associated with apple roots in an earlier study (Bulgari et al. 2012), but not as the dominant taxon, and has been found abundantly in Marchantia liverworts, indicating a possible long co-evolutionary history with plants (Alcaraz et al. 2018). Growth of *Steroidobacter agariperforans* can be stimulated in vitro by diffusible metabolites of *Rhizobiales* (Sakai et al. 2014), another typical group of plant root colonizers that were abundantly present in the apple tree root endosphere (Suppl. Table VII-4). Moreover, the genus is known from *Pinus* roots growing in subsoil or from the subsoil itself, with positive effects on nutrient cycling (Gu et al. 2017; Marupakula et al. 2017). Most of our sampled root material was located in the subsoil, which may promote the dominance of *Steroidobacter* in the T-compartment. Several other dominant taxa in the T-compartment in all three trials (e.g. *Acidibacter*, *Flavobacterium*, *Pseudomonas*, *Bradyrhizobium*, *Bacillus*, as well as unidentified

ASVs in the families *Burkholderiaceae*, *Microtrichales* or Rhizobiales *incertae sedis*) have frequently been found in other rhizosphere studies and many of those are known to have plant beneficial traits, e.g. stimulation of plant defense, or have been reported to reduce the abundance of soil-borne pathogens in apple orchards (e.g. *Alternaria mali*) and may thus play an important role in the apple root microbiome (Caputo et al. 2015; Deakin et al. 2018; Kolton et al. 2014; Li et al. 2017).

In contrast, only few of the dominant taxa in the L-compartment have potentially plant beneficial traits such as *Pseudomonas*, *Flavobacterium*, members of *Burkholderiales*, *Comamonadaceae* or *Saprospiraceae*. They have been shown to utilize root metabolites, degrade (lignin-derived) aromatic compounds, produce anti-microbial substances, partake in sulfonate cycling in the wheat rhizosphere or break down complex organic compounds (Coenye and Vandamme 2003; Kawasaki et al. 2016; Li et al. 2017; McIlroy and Nielsen 2014; Schmalenberger et al. 2008; Vandenkoornhuyse et al. 2007; Vacheron et al. 2013). Other dominant ASVs found here were *Nitrospira* and *Nitrosomonadaceae* MND1, capable of nitrification (Prosser et al. 2014; Deng et al. 2019; Wang et al. 2020a) and possibly important for nutrient cycling in the rhizosphere.

To conclude, both compartments harbor specific microbial communities with possible abilities to benefit the plant. Predominant taxa in the L-compartment are primarily known to be associated with the conversion of plant-derived organic compounds, are involved in the nitrogen cycle or may have growth-promoting traits, while several taxa in the T-compartment have been shown to harbor strains being involved in biocontrol or possess plant-growth promoting abilities.

4.2 Bacterial community shifts along a root size gradient

We observed successive changes in beta diversity with increasing root diameter in the first and third trial in both compartments (Figs. II-2 and II-6). This indicates that apple trees selectively shape their bacterial communities along the root axis. Differences between root sections were recently also reported for the maize rhizosphere microbiota, though the community did not show a gradual transition in beta diversity along the axis (Rüger et al. 2021). However, in that work the focus was on very early assembly processes and the analyzed root regions were younger. In the apple rhizosphere, several ASVs showed similar trends of increasing or decreasing abundance in both

compartments along the root size gradient (Fig. II-3), suggesting that similar selection processes contribute to these differences along the root axis in both compartments.

In the L-compartment, the selective process is likely primarily driven by rhizodeposition, including processes such as organic carbon exudation, which changes and decreases with increasing root diameter as larger roots become suberized (Badri and Vivanco 2009; Keel et al. 2012; Proctor and He 2017). This is supported by our finding that rhizosphere-associated taxa, which are known to be frequent colonizers and relative abundant at early growth stages in other plants or to profit from root exudates, decreased towards the largest root section, e.g. *Allorhizobium-Neorhizobium-Pararhizobium-Rhizobium*, *Pseudoxanthomonas*, *Methylibium* or other unclassified *Rhizobiaceae* (Araujo et al. 2019; Mao et al. 2014; Spaink et al. 1998; Wang et al. 2017).

That carbon source availability can drive differentiation along the root axis in both compartments can also be nicely exemplified by focusing on methylotrophic bacteria. Several methylotrophic taxa occurred with higher relative abundance in the smaller root size sections in the two trials, such as *Methylotenera*, *Methylibium* or members of the family *Methylophilaceae* (Fig. II-3 and Suppl. Fig. VII-8). These organisms can grow on methanol, which is a waste metabolic by-product of growing plant tissue (Miliute et al. 2016; Macey et al. 2020). Using methanol likely provides a selective advantage for methylotrophs during plant colonization, as demonstrated earlier (Sy et al. 2005). Since root growth occurs predominantly at the root tips and in the elongation zone, this is likely the area with the highest release of methanol and corresponding very well to the enrichment of methylotrophs in thinner root sections. Noteworthy, not all ASVs representing methylotrophs were enriched towards these thinner root sections, few taxa showed an opposite pattern (ASVs identified as *Methylotenera* or *Methyloligellaceae*), which may indicate further niche differentiation within the population of methylotrophs. It is likely that other taxa respond to other carbon compounds in the L- and T-compartment in a similar way, but these specific dependencies, which may involve more than one carbon compound a taxon is responding to, remain to be identified in future studies.

4.3 Temporal changes in the loosely and tightly bound root microbiota

The temporal trial, which focused on differences throughout an entire year, showed that a succession in community composition took place in both compartments with more changes occurring during spring and summer than in winter (Figs. II-4 and II-5). This resulted in a higher alpha diversity during the summer months (Fig. II-4 A) and in community compositional differences primarily between summer and winter (Suppl. Fig. VII-6). It is likely that the changes in the root-associated microbiota were related to plant phenological processes. Apple root growth in mature trees has been reported to occur unevenly during the year with a possible bimodal pattern with substantial root growth ("root flush") around full bloom and either mid-summer or harvest (Eissenstat et al. 2006). This coincides with the increasing Shannon diversity observed during spring and early summer in 2018 and 2019 (Fig. II-4 A) (Macey et al. 2020). Likewise, changes in community composition were stronger during the growing season, especially in the L-compartment, i.e. at the time when photosynthesis and rhizodeposition were most relevant (Wingate et al. 2010).

Interestingly, the bacterial communities of the L-compartment at the last analyzed timepoint shifted further away from most other timepoints rather than returning to its initial state (Fig. II-4 B and Suppl. Fig. VII-6), indicating that the loosely associated microbial community does not necessarily return to a highly season-specific state after one year. This is underlined by the fact that no taxon that was responsive to season in the temporal trial showed a highly reproducible pattern in the spatio-temporal trial, though the identity of the responsive taxa was at least partially overlapping in the two trials. Microorganisms in the L-compartment are known to be less protected against abiotic influences compared to the T-associated microbiota (Lumibao et al. 2020), which suggests that further factors besides tree phenology are inducing changes. Variations in weather conditions are likely contributing to these year-to-year alterations. We encountered quite unordinary weather conditions in 2018 with high temperatures during summer with little precipitation and a warm December with intensive precipitation (Kraska 2019). The latter may have caused the spike in alpha diversity in the L-compartment in December 2018 (Fig. II-4 A) and perhaps also the intermediately higher number of responsive taxa in the T-compartment (Fig. II-5, T8 to T9 and T9 to T10). Besides a direct impact of weather conditions on microorganisms, higher

temperatures increase the rate of photosynthesis and thus likely the rate of rhizodeposition, as shown for perennial plants and trees (Amos and Walters 2006; Uselman et al. 2000). An increased carbon flux due to higher temperatures is thus likely contributing to seasonal dynamics in bacterial communities. Water availability is also strongly weather related, but drought was probably not a major limiting factor in this study even during the exceptionally warm summer, because the trees were drip-irrigated. It may primarily have affected the dynamics in December 2018. Taken together, our results suggest that the temporal dynamics in the root-associated microbiota are related to plant phenology as well as abiotic factors such as weather conditions, which can act directly on the microbiota or indirectly via modulating plant physiological processes.

In the third trial, we additionally evaluated temporal differences in the root-associated microbiota individually for different root size fractions. Seasonal dynamics were detected in both compartments (L and T) (Fig. II-6 B), but largely restricted to the thicker root fraction (Table II-1). Likewise, tree-to-tree variation was limited to the thicker root fraction. These findings indicate that tree-specific communities may develop with increasing root thickness/age, which are then more responsive to seasonal dynamics compared to the microbial communities in finer roots. That no significant differences were observed in the fine roots in either compartment indicates that other factors than seasonal dynamics influence the microbiota there.

4.4 Field scale gradients and pathogen infection as underlying causes for tree-to-tree variation

In all three trials we observed a significant impact of the individual trees on the bacterial community structure (Figs. II-2, II-4 and II-6), with varying effect sizes on the L- versus T-compartment. In the spatial trial, tree-to-tree variation was primarily seen in the bacterial community of the L-compartment. This was likely caused by underlying variation in the bulk soil microbiota, because the microbiota in the bulk soil samples showed similar community patterns as in the L-compartment (Suppl. Fig. VII-4), and because the rhizosphere microbiota is known to be drafted from the surrounding bulk soil (Vries and Wallenstein 2017). Similarly, the observed variation along rows in the spatio-temporal trial points to field-scale heterogeneity in the bulk soil that causes shifts especially in the loosely associated microbiota (Fig. II-6 B and Suppl. Fig. VII-6). A previous study analyzing the spatial structuring of soil microbial communities in an apple orchard also

found that spatial (1-5 m) variability was present within an orchard, though it did not follow a predictable pattern (Deakin et al. 2018). Such variability can be explained either by physio-chemical differences in the soil or by the fact that the distribution of soil microorganisms relies on passive mechanisms of dispersal in the soil, even in the absence of environmental gradients (Bahram et al. 2016).

In all trials, tree-to-tree variation was observed. In the temporal and spatio-temporal trial, this variation was more relevant in the T-compartment than in the L-compartment (Figs. II-4C and II-6B). Moreover, it was of higher relevance in the thicker than in the thinner root size fractions (Table II-1). Similar differences were also seen in the first trial (data not shown) and indicate that tree-specific influences may predominantly affect closely associated endophytes in older root regions. We identified pathogen infection as likely cause for tree-to-tree variation in the temporal trial, as two trees showed high relative abundance of an ASV classified as "*Candidatus* Phytoplasma". This genus includes the apple specific root pathogen "*Candidatus* Phytoplasma mali", the causal agent of apple proliferation and a BLAST search of the sequence resulted in 100% query cover (Bulgari et al. 2012; Seemüller and Schneider 2004). We did not detect any signs of infection when sampling, but infected trees may be asymptomatic. Tree-to-tree variation of the tightly associated bacterial community is likely caused by restructuring the native community in infected trees, as seen in previous studies (Bulgari et al. 2014; Trivedi et al. 2012; Trivedi et al. 2016), and it highlights the impact of a pathogen infection in the root system on the root-associated microbiome. This pathogen was not found or in marginally small abundances in the other two trials, which leads to the conclusion that further tree-specific traits cause tree-to-tree variation. Observing tree-to-tree variation in a comparable range as seen for the impact of root section and temporal variation indicates the need for a sufficiently high number of replicate trees in future orchard studies.

5. Conclusion

Our study demonstrates that the root-associated bacterial microbiome of apple trees is compartment-specific and shows spatio-temporal patterns. Genera being associated with the conversion of organic carbon compounds or being involved in the nitrogen cycle were more frequently enriched in the L-compartment, while several genera in the T-compartment are known to include strains being involved in biocontrol or with plant-growth promoting abilities. Spatial patterns were shown to exist at different scales, ranging from variation within the root system of an individual tree over tree-to-tree variation between adjacent trees to variation relevant to field scale. We identified root diameter, which served as proxy for root age and therewith differences in root physiology and rhizodeposition processes, as a relevant factor for variation within the tree root system. Factors leading to tree-to-tree variation act compartment specific, with soil properties introducing spatial patterns primarily in the loosely associated rhizosphere microbiota, while tree-specific traits such as pathogen infection level introduced more variation in the tightly associated microbiota. Seasonal variation is also present in the microbiota of both compartments of apple trees, most evident between summer and winter, likely linked to tree phenology, weather conditions, and climatic differences between years. This temporal variation may modulate microbiome responses to other environmental factors and deserves careful attention in future field studies. Besides, the observed tree-to-tree variation, which was often as relevant as the spatio-temporal variation, points to the need for sufficiently large sample sizes even within one orchard. Variation in microbiome data due to root region or time can be reduced by collecting homogenous samples, e.g. with a consistent representation of root regions. Such strategies will help to identify further influence factors of the tree root microbiome in future studies.

III. Effects of above ground pathogen infection and fungicide application on the root-associated microbiota of apple saplings

Modified on the basis of

Maximilian Fernando Becker[1], A. Michael Klueken[2] and Claudia Knief[1], 2023.
Environmental Microbiome 18, 43.
DOI: https://doi.org/10.1186/s40793-023-00502-z

[1] University of Bonn, Institute of Crop Science and Resource Conservation, Molecular Biology of the Rhizosphere, Nussallee 13, 53115 Bonn

[2] Bayer AG, Crop Science Division, Disease Control Biology, Alfred-Nobel-Str. 50, 40789 Monheim am Rhein, Germany

Author contributions:

CK and MFB designed the study. MFB performed the field and laboratory work, as well as the bioinformatic and statistical analyses. MFB drafted the manuscript, CK, AMK and MFB further reviewed and edited. All authors discussed the results and agreed on the final version.

Abstract

The root-associated microbiome has been of keen research interest especially in the last decade due to the large potential for increasing overall plant performance in agricultural systems. Knowledge about the impact of above ground plant disturbances on the root-associated microbiome remains limited. We addressed this by focusing on two potential impacts, foliar pathogen infection alone and in combination with the application of a plant health protecting product. We hypothesized that these lead to plant-mediated responses in the rhizosphere microbiota.

The effects of an infection of greenhouse grown apple saplings with either *Venturia inaequalis* or *Podosphaera leucotricha* as foliar pathogen, as well as the combined effect of *P. leucotricha* infection and foliar application of the synthetic plant health protecting product Aliette (active ingredient: fosetyl-aluminum), were studied on the root-associated microbiota. The bacterial community structure of rhizospheric soil and endospheric root material was characterized post-infection, using 16S rRNA gene amplicon sequencing. With increasing disease severity both pathogens led to changes in the rhizosphere and endosphere bacterial communities in comparison to uninfected plants (explained variance up to 17.7%). While the preventive application of Aliette on healthy plants two weeks prior inoculation did not induce changes in the root-associated microbiota, a second later application on the diseased plants decreased disease severity and resulted in differences of the rhizosphere bacterial community between infected and several of the cured plants, though differences were overall not statistically significant.

Foliar pathogen infections can induce plant-mediated changes in the root-associated microbiota, indicating that above ground disturbances are reflected in the below-ground microbiome, even though these become evident only upon severe leaf infection. The application of the fungicide Aliette on healthy plants itself did not induce any changes, but the application to diseased plants helped the plant to regain the microbiota of a healthy plant. These findings indicate that above ground agronomic management practices have implications for the root-associated microbiome, which should be considered in the context of microbiome management strategies.

1. Introduction

The term rhizosphere was first coined in 1904 by the German agronomist and plant physiologist Lorenz Hiltner and is now defined as the narrow region of soil around plant roots, which harbors a specific microbiome with potential benefits for plant health (Hiltner 1904; Ali et al. 2017; Mendes et al. 2013). Some rhizosphere microbes have capabilities to enter the root and establish an endophytic lifestyle, thereby undergoing an even closer association and with further possibilities to influence root health and plant growth (Frank et al. 2017; Araujo et al. 2019; White et al. 2019). This root-associated microbiome is mostly recruited from the surrounding soil and is considered to be crucial for healthy agricultural soils and thus for food production (reviewed in Vries and Wallenstein 2017). Its composition has been shown to depend on various factors such as the biophysical and biogeochemical environment, but is also actively shaped by the plant (Costa et al. 2006; La Fuente Cantó et al. 2020). The plant species (Garbeva et al. 2008; Berg and Smalla 2009), its genotype (Micallef et al. 2009), spatial heterogeneity within the root system related to root age and differentiation (Bonkowski et al. 2021; Becker et al. 2022) and nutrient acquisition strategies (Guyonnet et al. 2018) are considered some of the main drivers behind microbiome assembly and dynamics. More specifically, its composition is shaped by the plant via rhizodeposition (Haichar et al. 2008; Zhalnina et al. 2018), which itself depends on various factors, including abiotic and biotic influence factors. Abiotic factors include light intensity and temperature (Pramanik et al. 2000), the mechanistics of carbon and nitrogen flow into the rhizosphere (Jones et al. 2009), water supply (Henry et al. 2007), or the application of plant health protecting products (PHPPs) such as pesticides (Dinelli et al. 2007), while biotic factors include the presence of other organisms (reviewed in Dessaux et al. 2016, and root or even foliar pathogens to which the plant responds (Yuan et al. 2018; Wen et al. 2021; Becker et al. 2022).

The root-associated microbiome is known to be able to protect plants against stresses such as pathogen infections (Finkel et al. 2017) and has been shown to be actively recruited to suppress soilborne pathogens (Liu et al. 2021b). Various studies in recent years have shown that different root, above ground or systemic pathogens can impact the root-associated microbiota. Devastating root pathogens such as *Phytophthora* causing root rot (Solís-García et al. 2020), above ground fungal pathogens such as

Botrytis cinerea (Tender et al. 2016) or *Podosphaera aphanis* on strawberry (Yang et al. 2020), as well as the phloem-limited bacterial Huanglongbing citrus disease (Trivedi et al. 2012) have been shown to induce changes in the microbial rhizosphere community to varying degrees. Beyond this, Gu et al. (2022) have recently suggested that small changes in the rhizosphere microbiome can be an early indicator for the presence of a soilborne pathogen. The effects of a pathogen infection can be plant compartment specific as a recent study by Kim et al. (2021) shows. Here, the systemic bacterial pathogen *Erwinia amylovora* causing fireblight in several *Rosaceae* was shown to induce significant changes in the apple root endosphere bacterial community composition, whereas the rhizosphere communities remained unchanged. Thus, evidence exists that above ground or systemic pathogens can impact the root-associated microbiota. However, detailed knowledge about this process remains limited; it is in particular unknown how early during the above ground infection process changes become evident in the root-associated microbiota and whether responses are pathogen-specific. Understanding the composition and responses of the root-associated microbial communities of healthy and diseased plants is essential for promoting plant health and growth and has thereby potential to contribute to sustainable agriculture (Lynch and Leij 2001; Busby et al. 2017).

Currently, disease control relies predominantly on repeated PHPP applications and the integration of non-pesticidal control measures, such as removing litter residues or using resistant plant varieties (Carisse and Bernier 2002; Michalecka et al. 2018). The application of synthetic and biological products for disease prevention and reduction is common practice and has recently been found to influence the root-associated microbiota (reviewed in Ramakrishnan et al. 2021). Depending on the product group and application mode, different effects on the root-associated microbiota have been observed by pesticide applications. PHPPs with direct contact of the compound with the root-associated microbiota have been shown to induce significant effects. For example, soil or seed treatments such as seed coatings, as well as systemic PHPPs have been shown to affect bacterial and fungal rhizosphere communities in maize, soybean, rice, strawberry and sugar cane (Huang et al. 2021; Nettles et al. 2016; Kusstatscher et al. 2020; Deng et al. 2019; Qian et al. 2018). Similarly, spray applications of the systemic herbicide haloxyfop-R-methyl have been shown to dissipate into the rhizosphere soil upon application and consecutive plant death to influence the soil and

rhizosphere bacterial richness and diversity (Liang et al. 2020). However, little is known about possible plant mediated effects on the root-associated microbiota when PHPPs are applied above ground. The only currently available study about the effects of spray application of a mixture of the systemic fungicides fosetyl-aluminum and propamocarb-hydrochloride has been shown to have a rather weak and only transient impact on the root-associated microbiota (Fournier et al. 2020). Thus, effects of PHPPs in direct or close contact with the root-associated microbiome in form of seed/soil treatment or as systemic products have been shown, whereas the effects of above ground product applications and thereby plant mediated responses on the root-associated microbiota are currently largely unknown. However, in commercial fruit tree orchards most pesticides are applied as foliar sprays and less as drench application or seed coating (Thompson et al. 2023). Moreover, the effects of PHPPs on the root-associated microbiome have been studied on healthy plants, while the combined effects resulting from pathogen infections and PHPP applications remain unknown. This may have additive effects, leading to an even more distinct root-associated microbiota of infected, PHPP treated plants, or may to some extent reduce the infection impact, if plants and their associated microbiota are cured by PHPP treatment.

Aim of this study was to investigate the effects of two above ground fungal pathogens and the interaction with a synthetic fungicide on the root-associated bacterial microbiota. We chose apple (*Malus* X *domestica* Borkh.) as a model organism due to its economic relevance, its susceptibility to several severe pathogens, and the current disease control methods. It is the third most important fruit in terms of production and consumption worldwide with around 83 Mt of apples produced annually (Khajuria et al. 2018; Ritchie and Roser 2020). Sustainable apple production is threatened by both, above and below ground pathogens, causing substantial yield and economic losses. Two of the most important and prominent foliar diseases worldwide are apple scab and powdery mildew caused by the fungi *Venturia inaequalis* and *Podosphaera leucotricha*, respectively (Bowen et al. 2011; Tian et al. 2019). Infections by these pathogens are minimized and plant health is maintained in apple orchards by frequent pesticide applications with high dosages (Eurostat 2007).

We hypothesized that i) foliar pathogen infection changes the apple sapling root-associated bacterial community structure depending on disease severity and pathogen

species and ii) the application of PHPPs promotes the return of the microbiota to that of a healthy plant after a pathogen infection event. To test these hypotheses, we analyzed the root-associated microbiota of young apple plants based on two greenhouse trials. Focus of the first trial (referred to as temporal trial) were pathogen-infection induced changes over time in the root-associated bacterial community of plants, either inoculated with the apple pathogen *V. inaequalis* or *P. leucotricha* in comparison to healthy plants. Focus of the second trial (mixed trial) was to analyze the effect of a *P. leucotricha* infection followed by the application of the synthetic fungicide Aliette (containing fosetyl-aluminum). This locally systemic product was chosen as it is effective against *P. leucotricha* (Petré et al. 2015) and because it has been shown to only induce weak transient changes in the root-associated microbiota (Fournier et al. 2020). Its active ingredient, fosetyl-aluminum, is considered to have a low mammalian toxicity and to be rapidly degraded in soil to non-toxic components (Lewis et al. 2016). In both trials we divided the root-associated microbiota into the “loosely associated” (L-compartment, primarily the rhizosphere) and “tightly associated” (T-compartment, primarily the endosphere) microbiota according to the concept of Donn et al. (2015) to study responses compartment-specifically. The bacterial community composition was analyzed by amplicon sequencing of the 16S rRNA marker gene.

2. Material and Methods

2.1 Soil substrate preparation

For both the temporal and mixed trial, soil in proximity of apple trees was taken from a commercial apple orchard in Buxtehude, Germany. The soil was air dried and sieved through a 2-mm mesh. As growth substrate, 45% of this soil was mixed with 45% sterile silica sand and 10% perlite to improve soil texture and therewith seedling growth. The soil mixture was remoistened two days before use and the watered soil transferred into growing trays or pots.

2.2 Plant cultivation

Commercially available apple seeds (*Malus* X *domestica* Borkh., cv. Pink Lady) were stored for at least two months at -20 °C for stratification. For use, the seeds were then incubated in sterile distilled water (dH^2O) for four days at 6 °C. Before the seeds were placed into silica sand for germination, the sand was autoclaved, placed into boxes and wetted with sterile dH^2O overnight. Germination occurred for two weeks at 4 °C with the lid of the tray closed. Individual seedlings were further cultivated in the prepared soil mixture in growing trays, slightly covered with soil, and left for 17 days with 14-hour light phase (> 300 µmol m−2 s−1, Philips SGR 140, Hamburg, Germany) at 16 °C ± 2 °C and 10-hour dark phase at 14 °C ± 2 °C in a glasshouse with 50-70% relative air humidity. Healthy 40-day old seedlings were transferred to 13-cm round pots containing pre-moistured soil mixture together with 0.25 g Basacote 6 M controlled-release fertilizer (Compo Expert, Germany). During the following cultivation period, pest control was conducted by using commercially available beneficial organisms in release sachets (*Neoseiulus cucumeris*, *N. barkeri*, *Phytoseiulus persimilis*, *Amblyseius cucumeris*, *Encarsia formosa*, *Chrysoperla carnea*; Sautter & Stepper, Germany) as biocontrol agents and fungal disease control by weekly sulphur fumigation. To protect the soil from contamination with sulphur, it was covered with felt maps. The pots were drip-irrigated with approximately 10 ml of water per pot per day and their position was randomly changed every week. For both trials, plants were grown under these conditions for five weeks until further treatment.

2.3 Pathogen infection

Prior pathogen inoculation, plant leaves were rinsed with water to remove sulphur residues. *V. inaequalis* infection of 75-day old apple plants was performed by the method of Steiner and Oerke (2007). Briefly, a *V. inaequalis* spore solution with 10^6 conidia ml^{-1} was prepared from frozen detached apple leaves (cultivar Pink Lady) with sporulating lesions of strain HS1, which were taken from the strain collection at the INRES Department for Plant Diseases and Plant Protection at the University of Bonn. The spore solution was evenly sprayed onto the plant leaf surfaces. For the untreated control, sterile dH^2O was sprayed onto the plant surface. Powdery mildew infection was achieved using fresh *P. leucotricha* spores from propagation apple plants (cultivar Pink Lady), as plant material with spores cannot be processed for storage. Diseased apple

plants with sporulating colonies on leaves were evenly shaken over the plants. Plants from all three treatments were kept for 48 hours in sealable plastic containers filled with roughly 1 cm of water in order to create a humid environment and thus ensure a successful infection with *V. inaequalis* (while maintaining similar conditions between treatments). Additionally, a dark panel was put on top of the boxes for 24 hours to decrease light intensity. Afterwards, all plants were placed into climate chambers, whereby the *P. leucotricha* inoculated plants were transferred to a separate chamber to prevent cross-infections. Cross-infection of the control plants by *P. leucotricha* could be excluded because this pathogen requires wet leaf surfaces to germinate. Water supply of the plants was ensured by manually watered mats and both climate chambers were configured to have the same climate conditions (14-hour light / 10-hour dark cycle with 18 °C during daytime and 16 °C during night-time for increased pathogen infection). *V. inaequalis* infected plants were inoculated a second time with the pathogen at 16 days after inoculation (DAI) as described above to achieve an infection of newly developed leaves. To establish the infection, all plants (including *P. leucotricha* treated and control plants without second inoculation) were placed in plastic boxes for 48 h as described above. Samples were taken at different timepoints: 0, 3, 6, 12, 16, 28, 40 and 48 DAI (Fig. III-1). At 0 DAI, just before infection, 20 plants were destructively sampled to have a large baseline of untreated plants. Seven to eight replicate plants per treatment were sampled at each timepoint between 3 and 40 DAI with the exception of *P. leucotricha* inoculated plants at 40 DAI. Due to severe disease symptoms all remaining 22 plants were sampled at this timepoint. At 48 DAI, the remaining 15 and 11 replicate plants of the *V. inaequalis* and control group, respectively, were sampled.

In the mixed trial the effects of a *P. leucotricha* infection in combination with a plant health protecting product application on the root-associated microbiota was studied. Therefore, three different treatment groups were sampled at three different timepoints (Fig. III-1). The treatment groups consisted of the inoculated treated (IT) group, which received a PHPP treatment, followed by pathogen infection with *P. leucotricha* and a second PHPP treatment after infection; the inoculated untreated (IU) group with just a *P. leucotricha* infection and the non-inoculated untreated control (NC) group without treatments. The IT group received the PHPP treatment prior inoculation to analyze

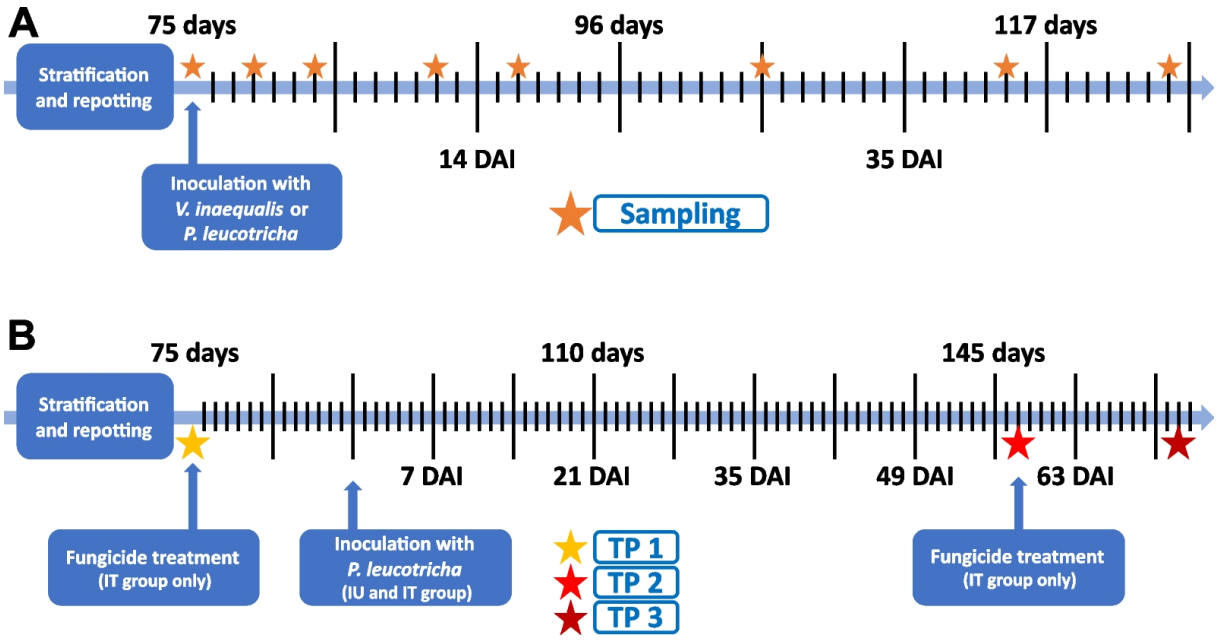

Fig. III-1: Timeline of the temporal (**A**) and mixed trial (**B**) with inoculation, fungicide application and sampling dates (TP) of apple saplings being indicated. Timelines are labelled with plant age on top and days after infection (DAI) below. The temporal trial consisted of *V. inaequalis* or *P. leucotricha* infected plants and a control treatment without infection. The mixed trial included a treatment with *P. leucotricha* infection without fungicide treatment (inoculated untreated, IU), a treatment with *P. leucotricha* infection and fungicide treatment (inoculated treated, IT), and a non-inoculated untreated control (NC).

whether a treatment only with a PHPP would cause application effects. At timepoint 1 (TP1), when the apple plants were 75 days old, the systemic product Aliette WG 80H (80% fosetyl-aluminum; 3.0 kg ha^{-1} in 600 l ha^{-1} water) (Bayer AG, Germany) was applied to the IT group, while water was applied to the IU and NC group. After two weeks, plants of the IU and IT group were inoculated with P. leucotricha as described above, while water was applied to plants of the NC group. After an additional 58 days, at timepoint 2 (TP2), when disease symptoms were prominent, a second Aliette application was given to the IT group, while water was again applied to the IU and NC group. Twelve replicate samples of the IT and IU group each were taken at TP1 (75-day old plants, 14 days prior inoculation), TP2 (147-day old plants, 58 DAI), and two weeks after TP2 at timepoint 3 (TP3; 161-day old plants, 72 DAI), while the NC group was only sampled at TP3 (Fig. III-1).

2.4 Disease documentation and sample collection

In both trials, disease severity (DS) was visually assessed over time on a 0-5 scale (0 = showing no signs of infection, 1 = having a single leaf with a single lesion, 2 = having either two leaves with multiple lesions or multiple leaves having a single lesion, 3 = having at least two leaves with large scale lesions, 4 = having one leaf entirely covered with mycelium, 5 = having multiple leaves entirely covered with mycelium and with leaves close to senescence). Sampling was performed by loosening the soil, carefully pulling out the entire root system and shaking the plant gently until all excess soil was removed. The root system was cut above the root crown and collected in 50-ml falcon tubes. It was immediately stored on ice and frozen at -80 °C within four hours after sampling. The root samples were further processed to obtain the loosely and tightly root-associated microorganisms as described by Becker et al. (2022). Briefly, excess soil was removed by gently shaking the root, and the root placed in 50-ml falcon tubes with 45 ml of 0.2 mM CaCl2 solution. The samples were vortexed 3 x 30 seconds and left 10 minutes for sedimentation. The root material (representing the T-compartment) was taken out, freeze dried and ground using a mixer mill. The suspension (representing the L-compartment) was centrifuged, and the pellet freeze dried and homogenized by vortexing.

2.5 DNA extraction, 16S rRNA gene targeted amplicon sequencing and sequence data analysis

Soil and root material underwent DNA extraction and 16S rRNA gene targeted PCR as described by Becker et al. (2022). In brief, DNA was extracted using the NucleoSpin Soil DNA extraction kit (Macherey Nagel, Düren, Germany) and the 16S rRNA gene was amplified using a nested LNA PCR protocol with the primer set 799f-1193r (V5 - V7 region). Library preparation and sequencing was performed by Novogene (Cambridge, UK) on a NovaSeq 6000 system (Illumina, San Diego, CA) and generated paired-end reads (2 × 250 bp). All following steps were done separately for the two trials. The raw Illumina sequence reads were processed using a custom bash script with Cutadapt version 3.2 to demultiplex the samples (Martin 2011). Primer removal and further processing was done with QIIME2 version 2021.04 (Bolyen et al. 2019). Paired reads were merged with max. 20 allowed differences in the overlapping region for the merging step and max. 1 expected error, quality filtered using the default

settings and denoised using deblur with reads trimmed to 350 bp length and a minimum read number of 50 (Amir et al. 2017). All further data processing steps were performed similar as described in Becker et al. (2022). Total read numbers after quality filtering, mean number of reads per sample and number of samples remaining after quality filtering are shown in Suppl. Table VIII-1.

2.6 Statistical analyses

Statistical analyses were performed within the QIIME2 environment and in R (Bolyen et al. 2019; R Core Team 2021). Disease severity based on a 0-5 rating was analyzed using Kruskal-Wallis non-parametric tests, followed by Dunn's post-hoc test. Differences in alpha diversity were assessed by richness (ACE) and diversity (Shannon and Inverse Simpson) using a feature table rarefied to 8,000 reads per sample. In the temporal trial, generalized least squares models were used with each diversity index as the dependent variable and treatment and timepoint as explanatory variables. The timepoint was used to adjust the temporal autocorrelation. In the mixed trial linear regression was used with the timepoint and treatment grouped and used as explanatory variable (e.g., TP1 – IU). This was done because the control was only sampled at the third timepoint. Pairwise comparisons were performed using estimated marginal means in the "emmeans" package. Differences in the bacterial community composition were determined using the q2-plugin "DEICODE" (Martino et al. 2019) and visualized either as principal coordinate analysis (PCoA) plot for the temporal trial or as constrained analysis of principal coordinates (CAP) plot for the mixed trial, where the analysis was constrained by the variables treatment, timepoint and disease severity. Statistical differences were calculated using a form of permutational multivariate analysis of variance (PERMANOVA) on the DEICODE distance matrices with 999 permutations, followed by pairwise comparisons with Benjamini-Hochberg correction for multiple testing, resulting in adjusted *p*-values (p_{adj}) with a strict significance threshold of $p_{adj} \leq 0.01$. As the order of factors entered into the PERMANOVA formula influences the outcome in an unbalanced design such as ours, the order of factors in the PERMANOVA formula was varied to identify the model explaining variation best. For the temporal trial, the factors treatment, timepoint, disease severity, number of leaves, plant height and relevant interactions were included in the model to identify factors explaining variance. The best fitting models are shown in the results. In addition,

analyses of similarities (ANOSIM) were performed to validate PERMANOVA findings. In the mixed trial, the treatment and timepoint variables were grouped and used as explanatory variable, similar as done for alpha diversity analysis. Homogeneity of dispersions between treatments at the individual timepoints was assessed in the temporal trial using permutational analysis of multivariate dispersions (PERMDISP) via the "betadisper" function with 999 permutations. Pairwise differential abundance analysis at phylum and genus level was performed using ANCOM-BC with detection for structural zeros turned off (Lin and Peddada 2020). In both trials, conservative variance estimates of the test statistic were used and *p*-values were adjusted using Holm's correction with alpha = 0.1.

3. Results

3.1 Temporal trial

Disease development caused by both pathogens, *V. inaequalis* and *P. leucotricha*, advanced similarly over time. Symptoms became evident twelve days after inoculation (DAI) and disease severity (DS) rose sharply and significantly during the first 28 DAI (Fig. III-2). While the mean DS of *V. inaequalis* inoculated plants plateaued afterwards at a level slightly below three, the DS of *P. leucotricha* inoculated plants increased further and caused most plants to wither at 40 DAI, when all remaining plants had to be sampled.

Community compositional analysis showed a dominance of *Proteobacteria* and clear differences between the microbiota of the L- and T-compartment, with *Proteobacteria* being even more pronounced in the T- than the L-compartment (Suppl. Fig. VIII-1, ANCOM-BC W = 13.6; $p_{adj} < 0.001$). Likewise, alpha diversity analysis using Shannon's diversity index showed that the diversity of the bacterial community was significantly lower in the T-compartment (4.6 ± 0.3) compared to the L-compartment (5.9 ± 0.4) (Kruskal-Wallis *p*-value ≤ 0.001). These differences justify a comparative analysis of responses to different pathogen infections over time separately in both fractions. However, the evaluation of treatment effects as well as of temporal changes on the Shannon index applying a generalized least square model revealed no significant differences in either compartment (Table III-1). Likewise, richness (ACE) and Inverse

Simpson indices remained unaffected by treatments or over time within the compartments.

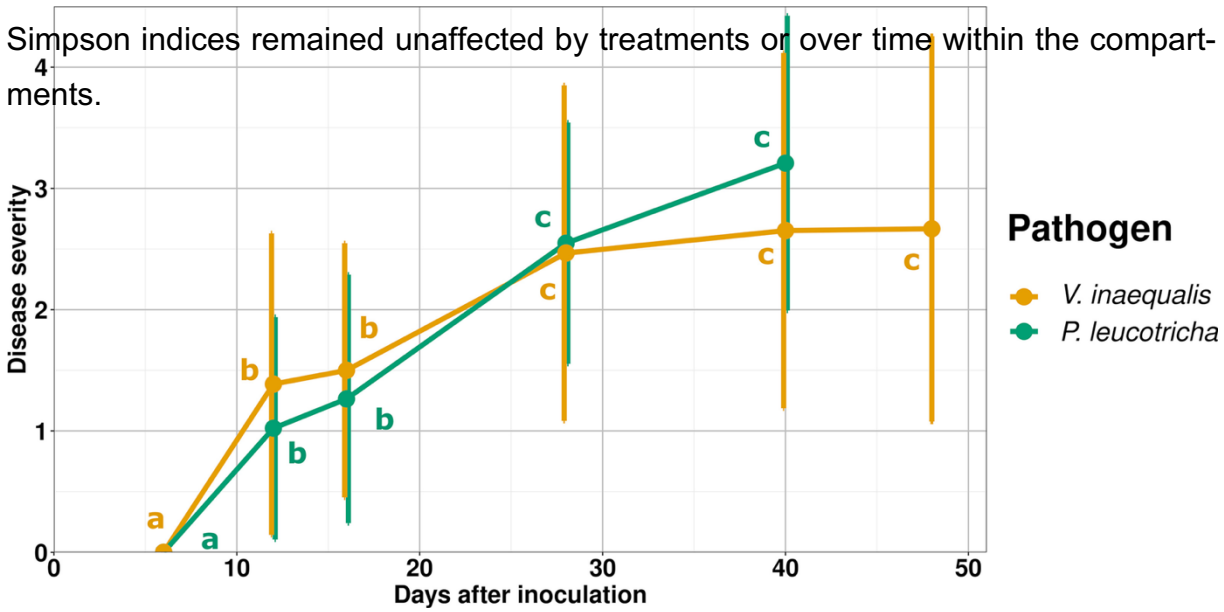

Fig. III-2: Disease severity of apple saplings infected by *V. inaequalis* or *P. leucotricha*. Disease severity was rated per plant at a 0–5 scale with 0 = healthy and 5 = multiple leaves entirely covered with mycelium and leaves close to senescence. Mean values and standard deviation are displayed based on 11–52 replicates. Significant differences in disease severity were evaluated between different timepoints based on Dunn's test with Benjamini–Hochberg correction for multiple testing. Lower case letters indicate differences at $p = 0.05$. DAI = days after inoculation.

Regarding beta diversity, we analyzed the relevance of different factors within the PERMANOVA framework. Besides treatment and time, we evaluated plant parameters as measures for plant development and disease severity, thus taking better into account that infected plants developed disease symptoms only at later sampling dates. Because some factors were consequently co-correlated (timepoint, number of leaves and plant height as well as treatment and disease severity), we evaluated different PERMANOVA models comparatively. Both, leaf number and height only explained a negligible part of the variation compared to timepoint and were thus left out in the final PERMANOVA model (Table III-1). This was confirmed by ANOSIM, where height and leaf number were identified to be of minor relevance (Suppl. Table VIII-2). In the final PERMANOVA model, timepoint was the strongest explanatory factor for bacterial community composition in both compartments (L: $R^2 = 0.273$; $p = 0.001$ | T: $R^2 = 0.291$; $p = 0.001$), whereas the treatment with two different pathogens caused minor differences in the T-compartment ($R^2 = 0.019$; $p = 0.048$) and none in the L-compartment (Table III-1). The succession over time can be observed in the PCoA plot, where samples are

separated along the second axis (Fig. III-3), whereas treatment-dependent responses remain invisible. The interaction of timepoint, treatment and DS were significant in both compartments, though only with relatively small R^2-values of 0.032 and 0.034 (Table III-1). As a consequence of those interactive effects, we evaluated the treatment effects at the individual timepoints specifically but found only few significant differences (Suppl. Table VIII-3). In the L-compartment, the factor treatment was significant at 40 and 48 DAI (with R^2-values of 0.144 and 0.102 and *p*-values of 0.038 and 0.043, respectively), whereas the factor DS was significant at 48 DAI, explaining a rather large part of the variation (R^2 = 0.432; *p* = 0.017). In the T-compartment, PERMANOVA

Table III-1: Variation in the root-associated bacterial community of apple saplings in dependence on pathogen infection, over time and by other variables. The differences in alpha and beta diversity are summarized for the L- and T-compartment. Effect sizes in beta diversity were assessed by PERMANOVA based on DEICODE distance matrices, while differences in Shannon diversity were analyzed based on generalized least square models (GLS). Significant results ($p < 0.05$) are in bold.

Compartment	Variable	PERMANOVA				GLS	
		df	F.Model	R^2	*p*-value	F.Model	*p*-value
L	Timepoint (TP)	**1**	**62.251**	**0.273**	**0.001**	0.976	0.379
	Treatment	2	1.005	0.009	0.408	0.088	0.768
	Disease severity (DS)	5	0.963	0.021	0.496		
	TP * Treatment	**2**	**4.133**	**0.036**	**0.002**	2.271	0.107
	TP * DS	5	1.22	0.027	0.236		
	Treatment * DS	**6**	**2.349**	**0.062**	**0.002**		
	TP * Treatment * DS	**3**	**2.613**	**0.034**	**0.006**		
T	Timepoint	**1**	**70.770**	**0.291**	**0.001**	0.138	0.242
	Treatment	**2**	**2.268**	**0.019**	**0.048**	2.640	0.075
	Disease severity	5	1.000	0.021	0.441		
	TP * Treatment	**2**	**2.453**	**0.020**	**0.034**	1.649	0.196
	TP * DS	5	0.821	0.017	0.683		
	Treatment * DS	6	0.868	0.021	0.624		
	TP * Treatment * DS	**3**	**2.581**	**0.032**	**0.008**		

revealed significant differences related to the factor treatment only at 28 DAI (R^2 = 0.254; *p* = 0.017). Pairwise PERMANOVA however did not result in significant

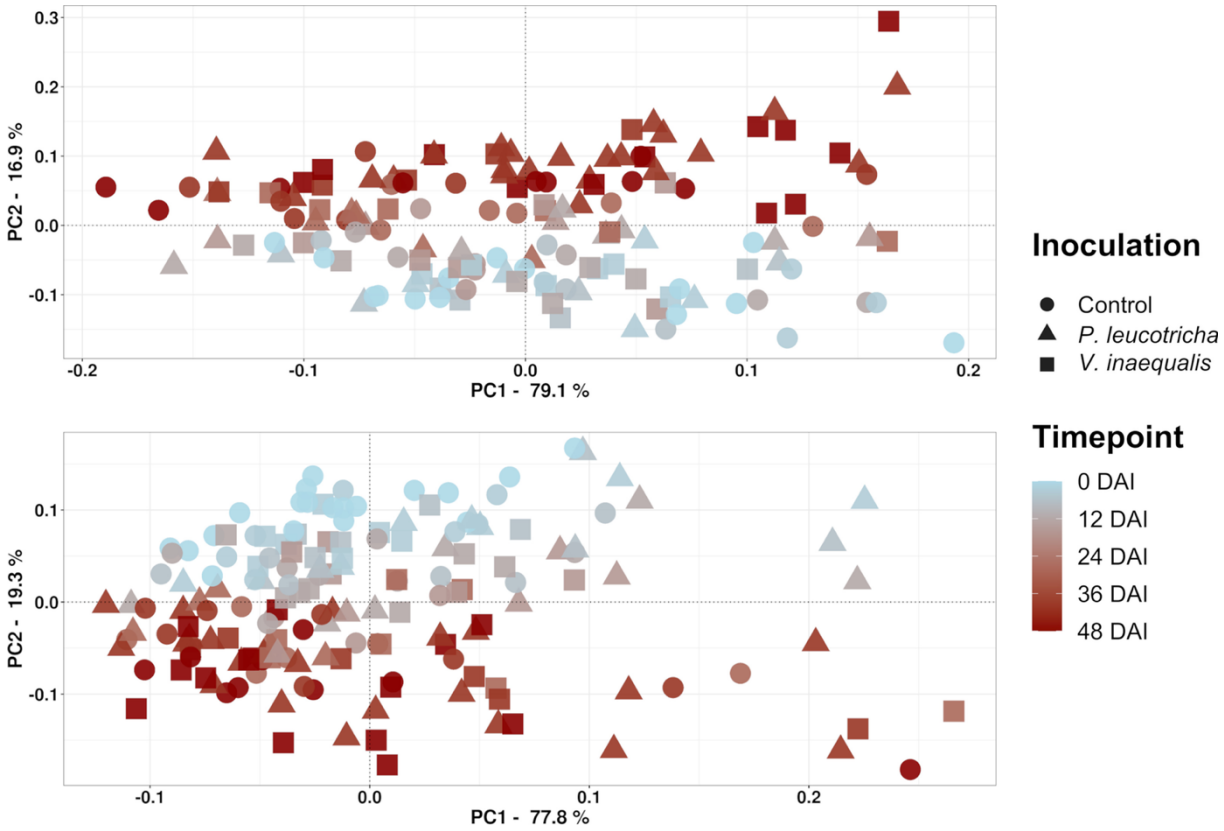

Fig. III-3: Principal Coordinate Analysis (PCoA) calculated from DEICODE distance matrices, showing variation in the root-associated bacterial community composition of differently inoculated apple saplings over time. Variation in the L-compartment (upper panel) and T-compartment (lower panel) is shown.

differences at either comparison between the respective treatments and the control. These weak treatment effects, in addition to the combined explanatory power of timepoint * treatment * DS, caused us to also evaluate more closely the temporal dynamics of each treatment separately, where treatment specific differences became more evident (Fig. III-4). The community composition of the control group did only significantly change between 0 DAI and the later timepoints at 28, 40 and 48 DAI in the T-compartment with a similar, though insignificant trend in the L-compartment (Figs. III-4 A and D). In contrast to that, both the community composition of plants inoculated with *P. leucotricha* or *V. inaequalis* shifted differently over time. The community composition of *P. leucotricha* inoculated plants did not change significantly during the first 16 DAI in either compartment, but we observed significant differences at later timepoints, when the disease severity was significantly higher. This was slightly less pronounced at 40 DAI in the T-compartment than in the L-compartment, where the community composition was significantly different to most previous timepoints (Fig. III-4 E). This shift is also clearly seen in the PCoA plots with samples taken 40 DAI clearly

shifting away from the earlier timepoints in both compartments (Fig. III-4 B). The community composition of *V. inaequalis* inoculated plants displayed differences primarily for samples taken at 40 and 48 DAI compared to samples taken at or prior 16 DAI, especially in the T-compartment (Figs. III-4 C and F). Thus, they displayed a more similar pattern to plants inoculated with *P. leucotricha* than the non-inoculated control group plants. Again, this trend was also observed in the PCoA plot, where the later timepoints shifted further away from the preceding ones than seen in the control. Besides the differences in the PCoA plot and the PERMANOVA p_{adj}-values, plants inoculated with *P. leucotricha* or *V. inaequalis* displayed larger R^2-values and thereby larger differences at the later timepoint comparisons compared to the control, evident from the heatmaps summarizing the PERMANOVA results (Fig. III-4 D-F).

We performed differential abundance analysis using ANCOM-BC for the three individual treatments between 0 DAI and 40 DAI (Suppl. Fig. VIII-2), as in particular the pathogen treated samples shifted significantly away at this timepoint (Fig. III-4). Several genera were significantly differentially abundant in one or even both pathogen treatments. However, pathogen-specific enrichments of taxa were not commonly observed, and similar trends were mostly seen in the respective pathogen treatment as well as in the control treatment, suggesting that the pathogen-infection merely enforced the enrichment of these taxa in the rhizosphere.

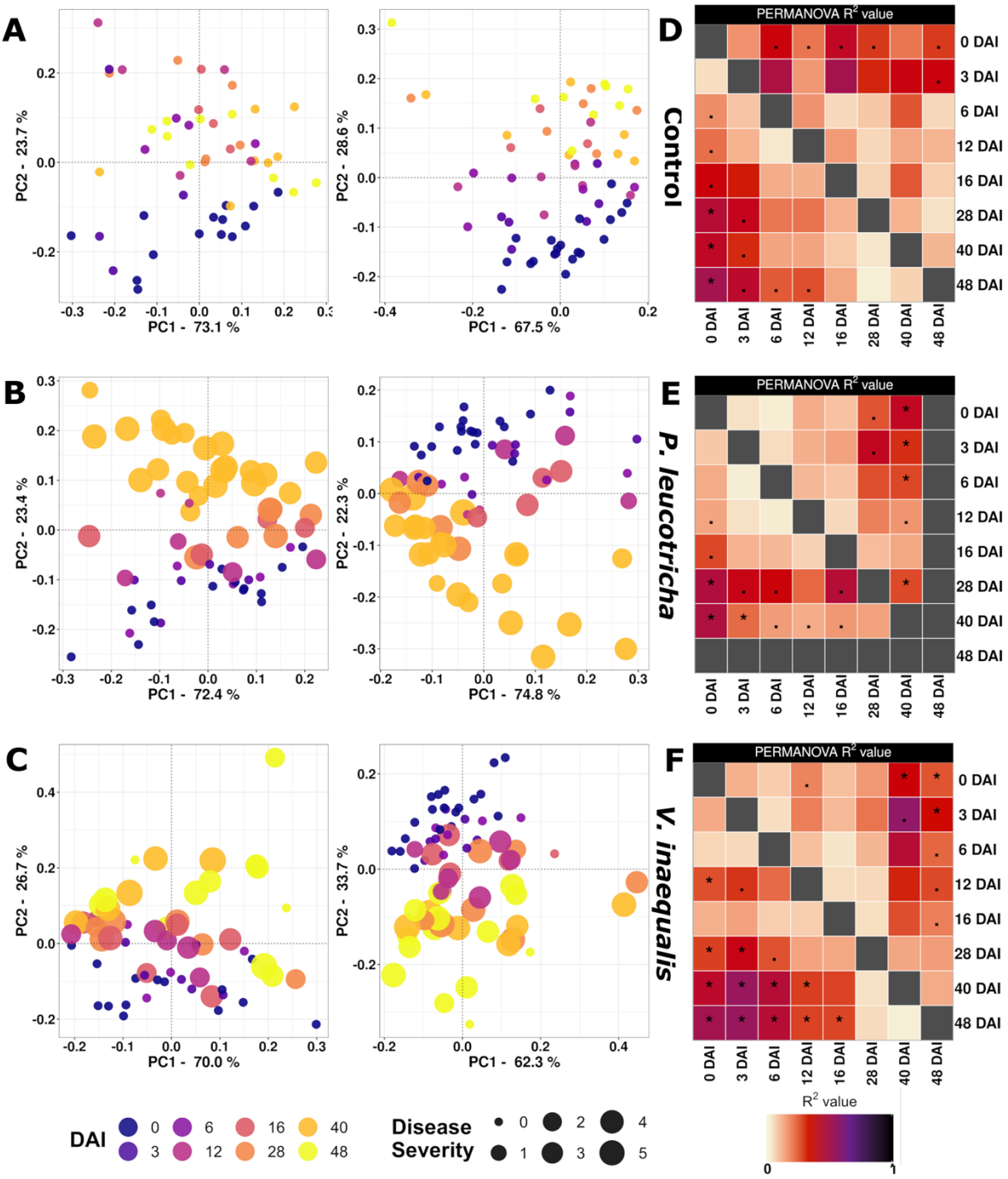

Fig. III-4: Temporal dynamics in the root-associated bacterial community composition of differently inoculated apple saplings. **A**-**C** Principal Coordinate Analysis (PCoA) based on DEICODE distance matrices, showing variation in the L-compartment (left) and T-compartment (right). **A** Untreated control plants. **B** *P. leucotricha* inoculated plants. **C** *V. inaequalis* inoculated plants. A color code illustrates the different sampling timepoints, point size indicates disease severity based on a 0–5 scale with 0 = plant with healthy leaves and 5 = plant having multiple leaves entirely covered with mycelium and with leaves close to senescence. **D**–**F** PERMANOVA results for pairwise comparisons between timepoints in the three treatment groups: **D** untreated control plants, **E** *P. leucotricha* inoculated plants. **F** *V. inaequalis* inoculated plants. Results for the L-compartment (upper right side) and the T-compartment (lower left side) are shown. R^2-values are color coded and Benjamini–Hochberg adjusted *p*-values indicated by asterisks, i.e., "*" represents $p \leq 0.01$ and "." represents $0.05 \geq p > 0.01$. The significance threshold was set at $\alpha = 0.01$.

3.2 Mixed trial

As *P. leucotricha* showed a stronger disease severity compared to *V. inaequalis* in the first trial, we used *P. leucotricha* in the mixed trial. Plants in both the inoculated untreated (IU) group and inoculated treated (IT) group were similarly infected with *P. leucotricha* and showed lesions at the second timepoint (TP2) 21 days after infection, whereas plants in the non-treated control (NC) group remained healthy (Fig. III-5). At TP3, two weeks after the second PHPP application (Fig. III-1), the mean disease severity of the IT group decreased slightly to 2.2 ± 0.7, whereas the mean disease severity of the IU group increased significantly to 4.8 ± 0.5, which resulted in significant differences between all three treatment groups (Fig. III-5). This decrease was clearly seen as a reduction of the infected leaf area and inhibition of new mycelial growth. Similar to the temporal trial, community compositional analysis showed a dominance of Proteobacteria and clear differences between the bacterial communities of the L- and T-compartment (Suppl. Fig. VIII-3). Because a preliminary CAP and PERMANOVA analysis (not shown) revealed that sampling timepoint was the major explanatory variable and because we had an uneven study design, we combined the variables sampling timepoint and treatment and defined seven

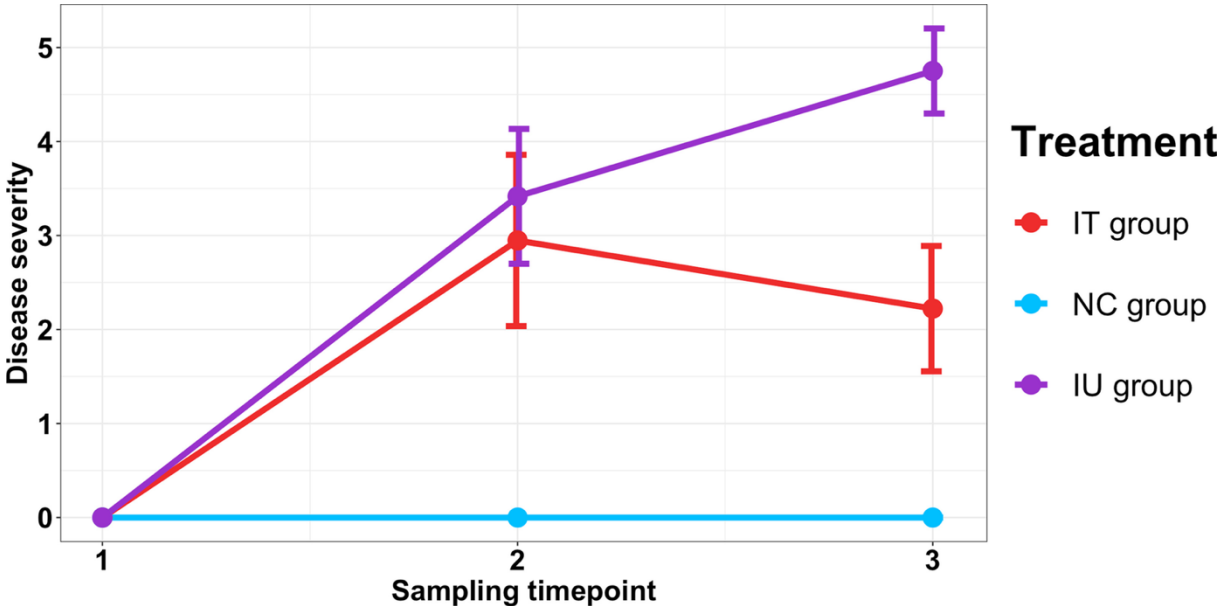

Fig. III-5: Development of disease severity over three timepoints (TP1–TP3) on *P. leucotricha* infected apple saplings. One inoculated group (IT) was treated with a synthetic fungicide at TP2, the other remained untreated (IU). Both treatments were compared to an uninoculated control group (NC). Disease severity was rated on a 0–5 scale and the mean values and standard deviation of 9–35 replicates are shown. Significant differences in disease severity between the three groups at TP2 and TP3 were assessed by Dunn's test with Benjamini–Hochberg correction for multiple testing.

categories (e.g., TP1-IU, TP1-IT, TP2-IU) for both alpha and beta diversity analysis. Significant changes in the Shannon diversity index related to the grouped variables were seen in both compartments according to linear models (L: p = 0.012 | T: p < 0.001) (Fig. III-6).

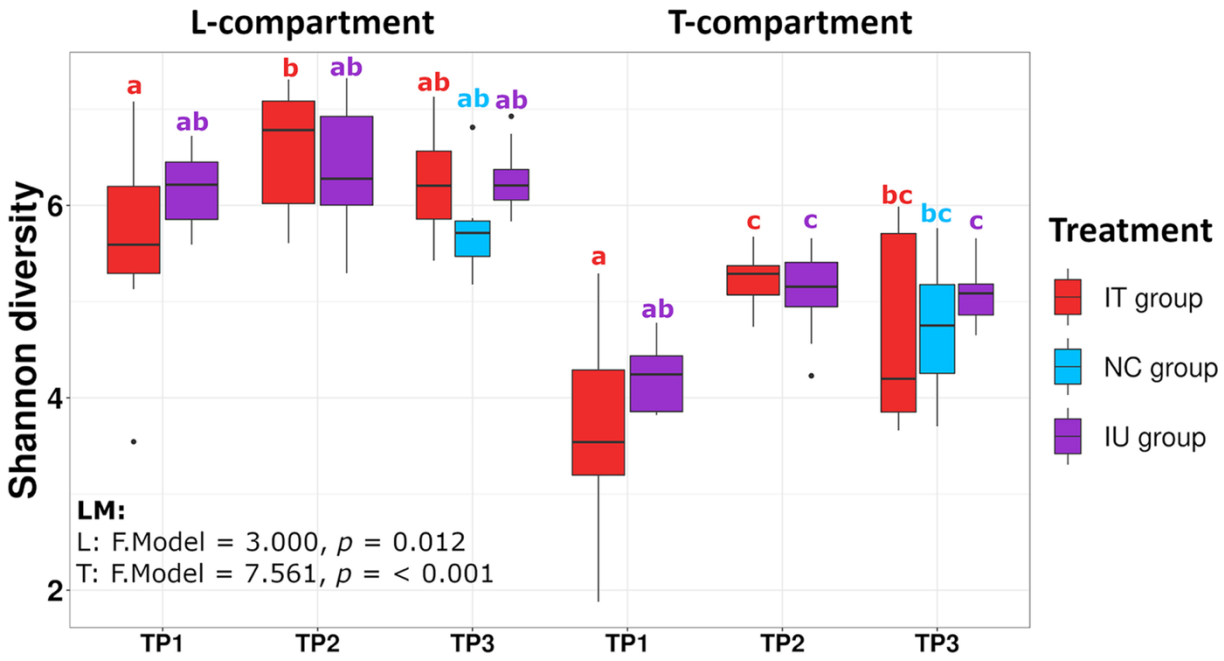

Fig. III-6: Variation in the root-associated bacterial community of apple saplings linked to treatment and sampling timepoint (TP). The variation in alpha diversity presented based on the Shannon index in the L-compartment (left panel) and T-compartment (right panel). Differences in Shannon diversity were analyzed based on linear models (LM). Different letters represent significant changes according to Tukey's HSD post hoc tests performed between all seven groups of samples.

Focusing on differences between treatments, diversity tended to be higher in the inoculated groups in the L-compartment compared to the control, but subsequent post-hoc tests revealed no significant differences between the treatments at the individual timepoints (Fig. III-6). For variation in beta diversity, PERMANOVA and CAP revealed significant differences in the bacterial community composition in both compartments by the grouped variables (Tables III-2 and III-3, Fig. III-7 and Suppl. Fig. VIII-4). Subsetting the data by time to assess the treatment effects in more detail (Table III-3) as well as displaying all pairwise comparisons in a heatmap (Fig. III-8) revealed that the different treatments were significantly different only at TP3. Here, the IU group differed significantly from the NC group in both compartments (L: R^2 = 0.195; p_{adj} = 0.004 | T: R^2 = 0.192; p_{adj} = 0.003) (Fig. III-8). The IT group however did not differ significantly from the NC group in either compartment, which can also be seen in the CAP plot of

the L-compartment, where the IT samples were more similar to those of the NC group than to those of the IT group. This was particularly true for samples with a lower DS within the IT group, which can be seen when comparing plants from TP2 to TP3 in the CAP plot (Fig. III-7). While the community composition of the IU group did not change significantly in the two weeks from TP2 to TP3 in either compartment,

Table III-2: Variation in the root-associated bacterial community of apple saplings linked to treatment and sampling timepoint (TP). Differences in beta diversity are first shown related to the combined variables treatment and timepoint (Grouped) in the L- and T-compartment. Below, treatment effects at the individual timepoints are listed. Effect sizes were assessed by PERMANOVA based on DEICODE distance matrices. Significant results ($p < 0.05$) are in bold.

Compartment	Variable		PERMANOVA			
			df	F.Model	R^2	*p*-value
L	**Grouped**		**6**	**10.044**	**0.493**	**0.001**
	TP 1	Treatment	1	1.681	0.081	0.157
	TP 2	Treatment	1	1.355	0.070	0.240
	TP 3	**Treatment**	**2**	**2.763**	**0.181**	**0.016**
T	**Grouped**		**6**	**10.085**	**0.490**	**0.001**
	TP 1	Treatment	1	1.485	0.076	0.202
	TP 2	Treatment	1	1.147	0.071	0.327
	TP 3	**Treatment**	**2**	**3.238**	**0.178**	**0.010**

Table III-3: Variation in the root-associated bacterial community of apple saplings linked to sampling timepoint (TP). Pairwise differences in beta diversity between individual timepoints in the L- and T-compartment are displayed. Effect sizes were assessed by PERMANOVA based on DEICODE distance matrices. Significant results ($p < 0.05$) are in bold.

Compartment	Variable	PERMANOVA		
		F.Model	R^2	*p*-value
L	TP1 – TP2	**15.896**	**0.290**	**0.001**
	TP2 – TP3	**4.327**	**0.086**	**0.005**
	TP1 - TP3	**26.054**	**0.357**	**0.001**
T	TP1 – TP2	**21.646**	**0.382**	**0.001**
	TP2 – TP3	**6.323**	**0.116**	**0.002**
	TP1 - TP3	**32.377**	**0.388**	**0.001**

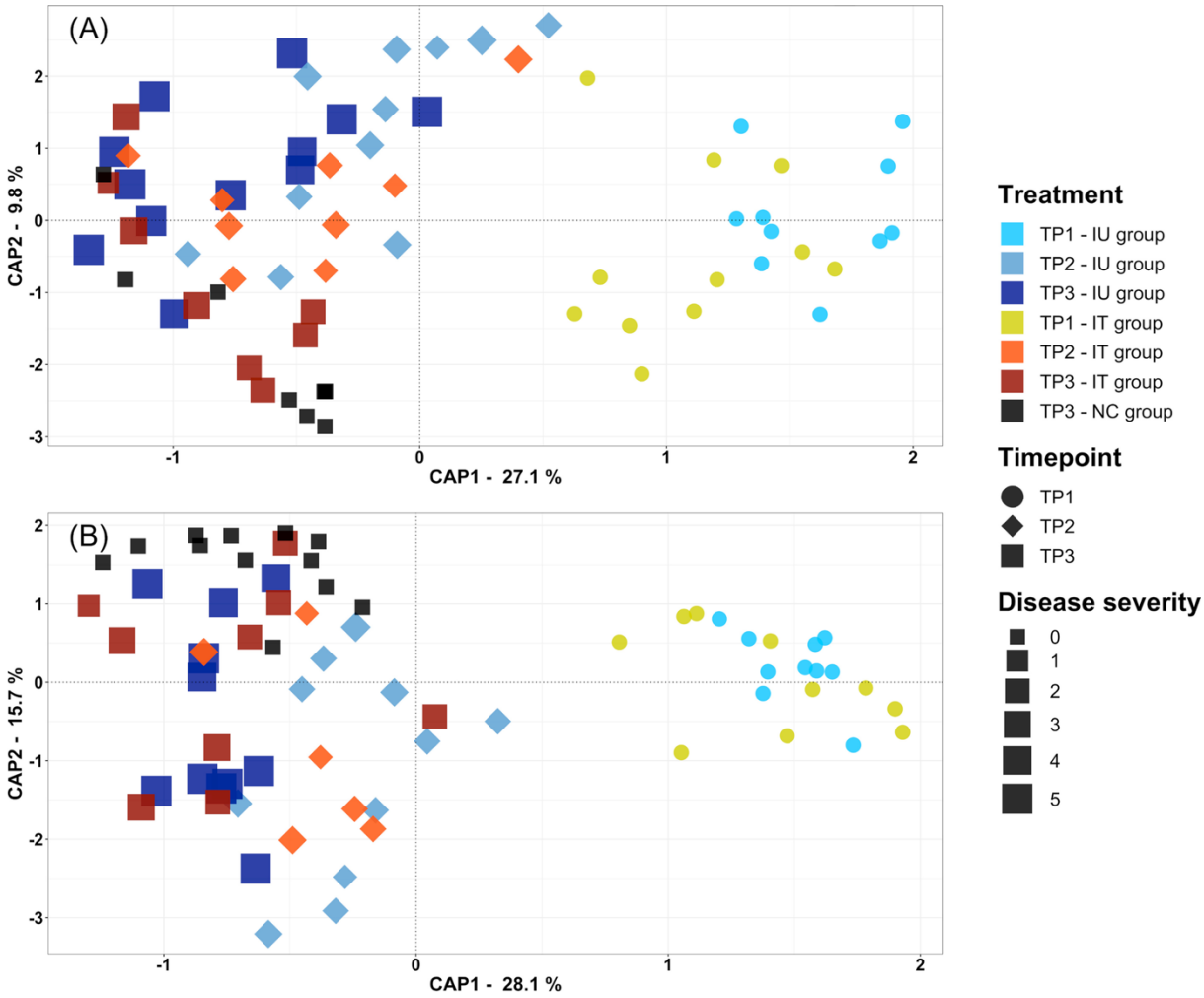

Fig. III-7: Variation in beta diversity of differently treated apple saplings at three distinct timepoints (TP) in the L-compartment (upper panel) and T-compartment (lower panel). Variation is presented based on constrained analysis of principal coordinates (CAP) using DEICODE distance matrices; it is constrained by the variables sampling timepoint, treatment and disease severity. Plants were either inoculated with *P. leucotricha* and left untreated (IU) or were additionally treated with a synthetic fungicide (IT), or they underwent a treatment with water as control (NC). The different treatments are shown in different colors, and disease severity is illustrated by different symbol sizes, rated on a 0–5 scale with 0 = healthy plants and 5 = plants having multiple leaves entirely covered with mycelium and with leaves close to senescence.

the community of the IT group samples changed significantly in the L-compartment over time (R^2 = 0.223; p_{adj} = 0.009), likely caused by samples with a smaller DS. The same trend was observed in the T-compartment; however, here the differences were not significant. The differences between treatments at TP3 were also clearly visible in the L-compartment when analyzing TP3 separately in CAP plots (Suppl. Fig. VIII-4). Likewise, the DEICODE distances of the two treatments to the control and the within control distances reflected this (Suppl. Fig. VIII-5). No differences were found between the IT group and the NC group, but the IU group differed significantly from both the IT

and NC group in the L-compartment. This trend persisted for DEICODE distances in the T-compartment; however here, the IT group differed significantly from the NC group and not the IU group.

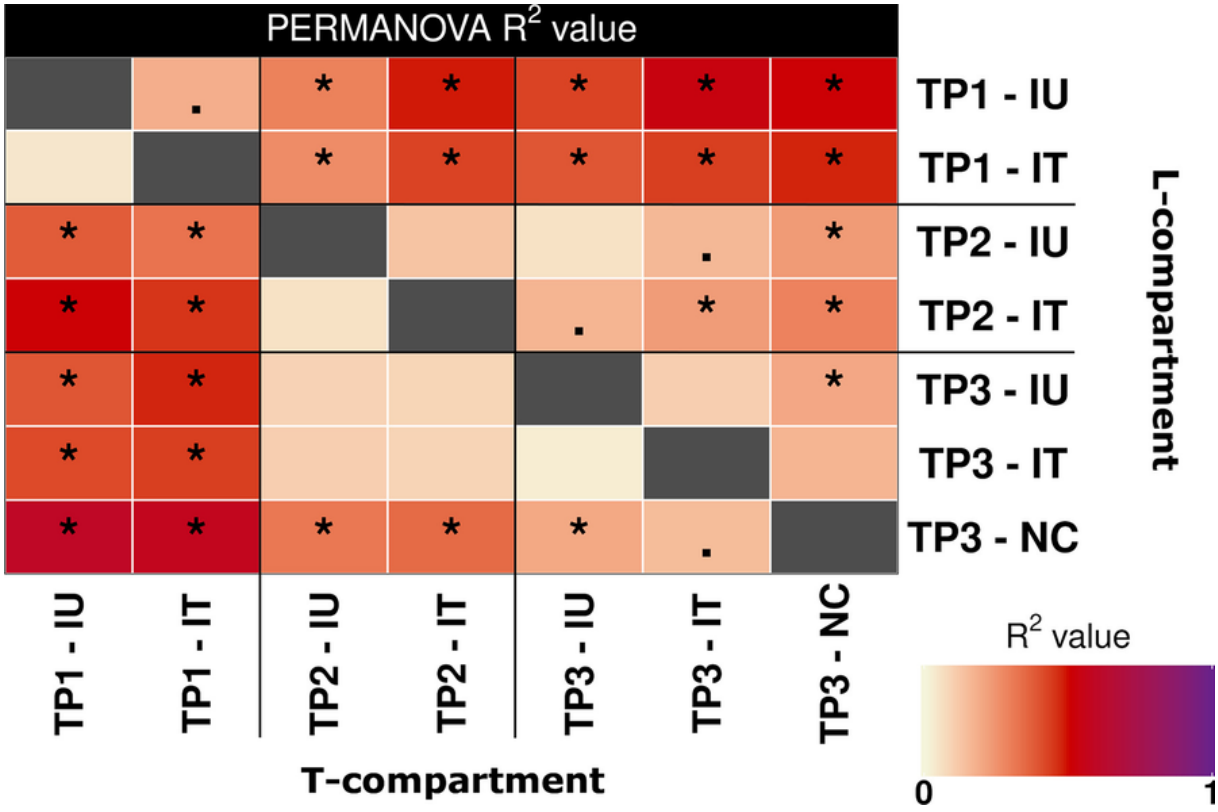

Fig. III-8: Pairwise PERMANOVA results comparing bacterial community composition in the L- and T-compartment of apple saplings at different timepoints (TP) of three differently treated groups (IU, IT, NC). R^2-values are illustrated using a color scale with the Benjamini–Hochberg adjusted *p*-values indicated by asterisks, i.e., "*" represents $p \leq 0.01$ and "." represents $0.05 \geq p > 0.01$. Results for the L-compartment are shown in the upper right side of the figure and for the T-compartment in lower left side. The significance threshold was set at $\alpha = 0.01$.

Considering the differences observed between treatments at TP3, a differential abundance analysis was performed based on ANCOM-BC to identify bacterial genera responding to the treatments at this last timepoint (Fig. III-9). In both compartments, most responsive taxa were identified between the IU and NC treatment, and additionally, IT appeared less different to NC than IU in the L-compartment. In the IU group, we observed exclusively taxa with significant increases in relative abundance compared to the NC group. In the L-compartment, several *Acidobacteriota* (*Bryobacter*, "*Candidatus* Solibacter", *Ocallatibacter*, an unclassified member of subgroup 2 in the *Acidobacteriae*), several *Firmicutes* (*Alicyclobacillus*, *Ammoniphilus*, an unclassified taxon of the

Bacilli) and *Proteobacteria* (*Devosia* and *Mizugakiibacter*) showed significant increases in relative abundance. Among these, *Devosia* and *Allicyclobacillus* were also enriched in the T-compartment, besides two further genera.

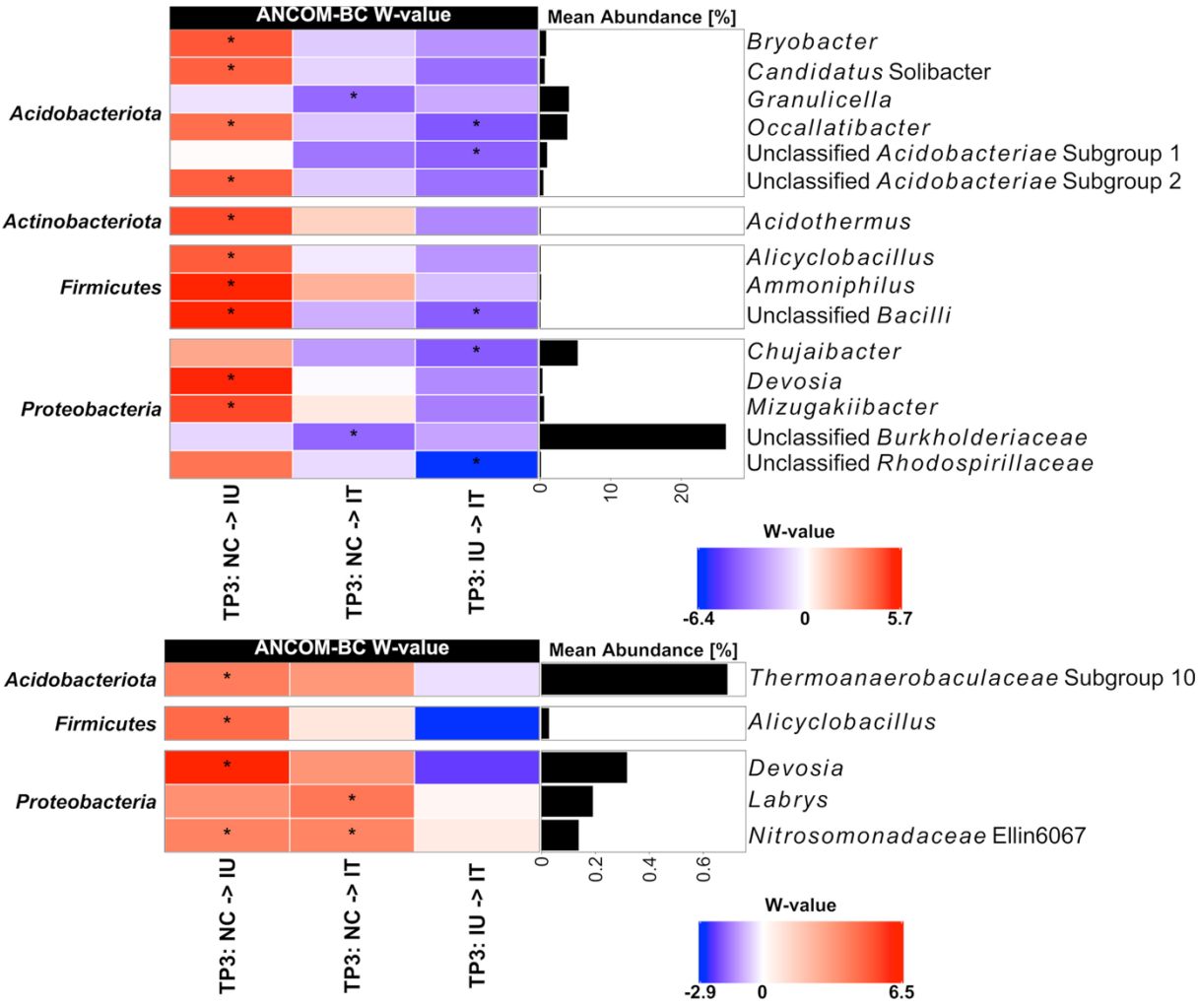

Fig. III-9: Differential abundance analysis performed at genus level by ANCOM-BC of differently treated apple saplings at the last sampling timepoint (TP3). Results are shown for the L- and T-associated bacterial communities (upper and lower panel, respectively). Plants were inoculated with *P. leucotricha* and then left untreated (IU) or treated with a synthetic fungicide (IT) or remained uninoculated and treated with water as control (NC). The heatmap shows the coefficients obtained from the ANCOM-BC log-linear model divided by their standard error (called W-value). The colour code indicates differential abundances between two treatments with red indicating enrichment in the last value of the column name. A "*" is shown if ANCOM-BC showed significant differences based on adjusted *p*-values in this comparison. In addition, the mean relative abundances of the taxa are displayed and only taxa with a mean relative abundance of > 0.1% are shown.

4. Discussion

4.1 Above ground pathogen infection causes changes in the root-associated bacterial community structure

In two separate experimental trials, we analyzed potential foliar pathogen infection induced changes over time in the root-associated bacterial community of apple plants. First with a focus on temporal dynamics, then by assessing the combined effect of pathogen infection and plant health product application. In both trials, we divided the root-associated microbiota into the L-compartment (primarily rhizosphere colonizers) and T-compartment (primarily endosphere colonizers).

Based on previous studies (Trivedi et al. 2012; Tender et al. 2016; Yang et al. 2020), we expected to observe pathogen related changes in the root-associated bacterial community. However, changes were not necessarily consistent in the literature. In this study, only small differences in alpha diversity caused by pathogen inoculation were seen. No significant changes in Shannon diversity were observed in the temporal trial, while diversity in the two pathogen treated groups of the mixed trial tended to be slightly higher in the inoculated groups compared to the untreated control group in the L-compartment (Fig. III-6). In comparison, existing studies showed no differences in alpha diversity upon above (González-Escobedo et al. 2021) or below ground pathogen infection (Kim et al. 2021), whereas one with powdery mildew in strawberry showed higher Shannon index values in the rhizosphere of healthy plants (Yang et al. 2020), and another one with *B. cinerea* leaf infection in strawberry showed a higher richness in the rhizosphere of diseased plants (Tender et al. 2016), similar to our results. A higher diversity has been hypothesized to act as an insurance for maintaining plant productivity under changing environmental conditions (Wagg et al. 2011), which was possibly also seen here under disease stress, though primarily in the rhizosphere and not in the endophytic fraction. Altered rhizodeposition, a main driver of rhizosphere assembly selection, might have been cause for this increase in diversity.

Regarding beta diversity, we observed a rather weak response to pathogen infections, whereas temporal dynamics over the observational period turned out to be more pronounced (Tables III-1 and III-2, Figs. III-3 and III-7). Especially in the temporal trial, the temporal dynamics contributed interactively with treatment-related responses to

observed differences and thus hint towards differences in the bacterial community composition (Table III-1). Direct comparisons between the two pathogen treatments with the untreated control at the individual timepoints did not result in significant differences, but the succession over time was treatment dependent. The bacterial communities of the pathogen infected plants became most distinct at the later sampling times compared to earlier timepoints and thus with increasing disease severity, while the communities of healthy plants were most distinct at the earliest timepoint (Fig. III-4). The different temporal dynamics at later timepoints of diseased plants are probably related to disease progression, whereas healthy plants developed and maintained a balanced and more stable bacterial community over time. This is supported by our findings in the mixed trial, where the differences between the inoculated untreated (IU) group and the negative control also hinted to increasing pathogen related effects on the bacterial community composition over time (Fig. III-8). Thus, the effects of an above ground pathogen infection on the root-associated microbiota are likely to increase over time as disease severity increases, especially in the L-compartment. This partially confirms our hypothesis that the root-associated bacterial community is affected by above ground pathogen infection, even though the responses remained weaker than expected.

Several studies have shown a severe impact of root pathogen infections on the rhizobacterial community composition, including changes in density, diversity and functioning. When studying systemic bacterial pathogens, one study reported that the phloem-limited bacterial Huanglongbing citrus disease caused a shift of the rhizosphere bacterial community composition towards a bulk soil-like community (Trivedi et al. 2012), whereas another with *Erwinia amylovora*, a systemic bacterial pathogen causing fireblight, only induced changes in the endosphere, not the rhizosphere (Kim et al. 2021). Our study suggests that similar processes may occur when plants are infected by pathogens that cause disease symptoms only locally above ground. This is in line with the findings of Yang et al. (2020), who found that a powdery mildew infection of strawberry influenced the richness of prokaryotic and fungal communities in rhizosphere soil slightly as well as the relative abundance of several taxa. The larger effects of root pathogens or systemically infecting pathogens appear likely, caused by the more intimate relation between the pathogens and the root-associated microbiota as part of the plant holobiont. Thus, the ability of the plant to alter its associated microbiota and even

more so to recruit a beneficial microbiota probably depends on the kind of pathogen and the level of infection.

We performed differential abundance analysis to examine if specific taxa are recruited upon pathogen infection. This revealed several taxa that increased in relative abundance at timepoint 3 in the IU group compared to the healthy control group, especially in the L-compartment. Almost all identified taxa have been shown to profit from different organic carbon compounds in the rhizosphere and are thus likely to respond to alterations in rhizodeposition. *Bryobacter* and "*Candidatus* Solibacter" have been shown to be closely related to soil carbon metabolism, as they are sensitive to labile carbon and can be influenced by the addition of straw into the soil (Yu et al. 2016; Wang et al. 2019; Li et al. 2020; Zhou et al. 2021). *Ammoniphilus*, *Mizugakiibacter*, *Acidothermus* and *Alicyclobacillus* have also been shown to utilize various plant-derived carbon compounds such as glucose, cellulose or oxalacetate (Sahin 2003; Talia et al. 2012; Liao et al. 2019; Li et al. 2020). Lastly, *Devosia* is positively correlated with soil organic carbon compounds (Chen et al. 2019; Chhetri et al. 2022). The increase in relative abundance of all these taxa indicates that the above ground pathogen infection may lead to alterations in root exudation, which then leads to changes in the rhizosphere microbial community composition. Altered root exudation upon foliar infection has already been shown in vitro for *B. cinerea* on tomato and cucumber plants, which then lead to an increase of the chemoattractive effect on the beneficial soil microbe *Trichoderma harzianum* (Lombardi et al. 2018). In our study, the increased relative abundance of the cellulolytic taxon *Acidothermus* in the L-compartment at high disease severity levels could further indicate that microbes might begin to actively hydrolyze root tissue, as the disease-stressed plant may have less capabilities to defend itself. However, the roots did not yet display symptoms of decay. The potential underlying rhizodeposition processes resulting in the observed changes in the rhizosphere microbiota deserve further studies.

Besides a mere response of the rhizosphere microbiota to altered rhizodeposition, it has been shown that plants can selectively recruit beneficial bacteria such as *Bacillus subtilis* as a "cry for help" mechanism against pathogen attack by producing specific chemical compounds and releasing them into the rhizosphere (Rudrappa et al. 2008; Jousset et al. 2011; Jousset et al. 2014; Dudenhöffer et al. 2016; Schulz-Bohm et al.

2018). The “cry for help” mechanism has so far primarily been suggested for plant infections with root pathogens such as *Phytophthora* (Solís-García et al. 2020), *Ralstonia solanacearum* (Wei et al. 2018) or *Fusarium pseudograminearum* (Liu et al. 2021b). Additionally, a downy mildew infection in *Arabidopsis* leaves led to the promotion of a beneficial bacterial consortium in the rhizosphere (Berendsen et al. 2018). In this study, we found two genera known to include strains with plant beneficial properties being increased in relative abundance in the diseased group, an unclassified member of *Bacilli*, as well as *Devosia* (Akinrinlola et al. 2018; Chhetri et al. 2022). This points to an extension of the concept to above ground infection and deserves more attention in the future.

It is remarkable how long the plants in our study maintained their preferred bacterial community even after showing clear signs of infection above ground. This is in contrast to the claim that alterations in the rhizosphere microbiota can serve as early indicator for pathogen infection (Gu et al. 2022), at least for above ground pathogens. In contrast, it is in accordance with a recent study, in which authors reported that wheat plants are capable of selecting its preferred root-associated microbiota even under stress conditions and recruit microbes with potential antagonistic activities (Yin et al. 2021). In our study, the community compositional analysis of the untreated control groups in both trials revealed high relative abundances of *Granulicella*, *Chujaibacter*, *Burkholderia-Caballeronia-Paraburkholderia*, *Acidipila*, *Bryocella*, *Occallatibacter* and unclassified members of *Burkholderiaceae* and *Acidobacteriaceae* Subgroup 1 in the L-compartment (data not shown). Several *Granulicella* species have been shown to have plant growth promoting abilities (Kielak et al. 2016) and *Chujaibacter* has been associated with nitrogen cycling reactions (Cloutier et al. 2021), thus making them typical rhizosphere colonizers. In the T-compartment some of the most prominent taxa in both trials such as *Streptomyces* or members of the family of *Comamonadaceae* have been shown to be associated root endophytes of apple before (Mahnkopp-Dirks et al. 2021; Becker et al. 2022). Thus, the soil used in this study provided a soil microbial reservoir from which the apple saplings could recruit microbes with potential benefits and taxa well-known to colonize the apple rhizosphere, as we would have expected.

4.2 Fungicide application reverts pathogen induced bacterial community compositional shifts

Aliette is a systemic PHPP with fast degradation in the soil and has likely only a limited and transient impact on the soil bacterial community composition (Fournier et al. 2020). Whereas it is primarily registered for use against oomycetes, it has been shown to decrease the disease severity of *P. leucotricha* in apples and pears (Petré et al. 2015). Even though it is a locally systemic PHPP and can be applied as protective treatment, we did not observe a protective effect in comparison to the untreated control plants when it was applied two weeks prior to the massive pathogen inoculation that followed (Fig. III-5). However, a second PHPP application after plant infection at 58 DAI decreased the disease severity of the IT group significantly in comparison to the IU group until TP3, demonstrating its curative properties. Its mode of action is still not fully understood, but it acts by inhibiting the germination process of fungal spores and the development of mycelium upon contact (Krämer 2012). Besides this direct effect, an indirect mode of action involving the promotion of plant defenses is believed to be involved.

When comparing the community composition between the different treatments, we did not see any changes in the bacterial community composition upon the first PHPP application (Table III-2). However, it was striking to observe that the composition of the IT group became in part similar to the NC group again after the second PHPP application at TP3, especially in the L-compartment, whereas the community of the IU plants did not show this development (Figs. III-7, III-8, III-9, Suppl. Figs. VIII-4 and VIII-5). Furthermore, the IT group changed significantly from TP2 to TP3, whereas the IU group did not, indicating that this change was triggered by the application of Aliette at TP2 (Fig. III-8). We consider this to be a response of the bacterial community to plant-dependent processes rather than a direct effect of Aliette, even though its active ingredient, fosetyl-aluminum, has been shown to impact the soil microbiota (Fournier et al. 2020). This was primarily observed for the soil protist community, but not for bacterial community composition. Alpha diversity was only weakly and very transiently affected, and the complexity of a bacterial co-occurrence network was only slightly decreased in that study. As we aimed to prevent a direct contact between the fungicide and the soil microbiome by covering the soil surface with felt maps, direct effects of Aliette on the rhizosphere bacterial community were unlikely to occur in this work. Thus, as

hypothesized, the observed return of the rhizosphere bacterial community from a diseased plant to that of a healthy plant was likely due to the plant regaining its ability to recruit its “healthy” root-associated microbiota with decreasing disease severity. Our observation that this change occurred apparently faster in the rhizosphere than in the endosphere could mean that the plant is quicker to readjust its microbiome in the rhizosphere by the process of rhizodeposition than in the endosphere after this kind of disturbance.

5. Conclusions

Our study demonstrates that the root-associated bacterial community of apple saplings is sensitive to plant-mediated effects resulting from above ground pathogen infections. With increasing disease severity, the two foliar pathogens *V. inaequalis* and *P. leucotricha* induced a continuous shift away from a bacterial community composition of a healthy plant. However, changes were rather subtle and without clear evidence for highly pathogen-specific responses. Genera associated with the conversion of various organic carbon compounds became enriched in the L-compartment of diseased plants with increasing disease severity, indicating that rhizodepositional processes may have changed, thereby leading to the alterations in the rhizosphere microbiota. Compared to studies with root pathogens, these disease related effects resulting from leaf pathogens on the bacterial community structure appear to be weaker and were only visible after longer inoculation periods with higher disease severity. Disease related effects on the rhizosphere microbiota appear thus to depend on both, the kind of pathogen and the disease severity. The responses to above ground pathogen infection are also likely compartment specific, as they were first noted in the tightly associated microbiota but were more pronounced at later timepoints in the loosely associated microbiota. Further, our results suggest that the curative effect of our applied PHPP fosetyl-aluminum on the root-associated microbiome is due to the plant regaining its ability to reestablish the microbiome of a healthy plant. This is apparently achieved faster in the loosely associated microbiota than in the endophytic counterpart. Based on our findings, we conclude that the impacts of pathogen infection and PHPP application on the root-associated microbiome need to be considered when developing microbiome management strategies in the context of sustainable agriculture.

IV. Effects of plant health protecting product applications on the root-associated microbiota of apple saplings and strawberries

Modified on the basis of

Maximilian Fernando Becker[1,3], Marion Deichmann[1,2], A. Michael Klueken[3] and Claudia Knief[1], 2024.

Phytobiomes Journal, ja (2024).
DOI: https://doi.org/10.1094/PBIOMES-04-24-0040-R

[1] University of Bonn, Institute of Crop Science and Resource Conservation - Molecular Biology of the Rhizosphere, Nussallee 13, 53115 Bonn

[2] University of Bonn, Institute of Crop Science and Resource Conservation - Department of Plant Nutrition, Karlrobert-Kreiten-Strasse 13, 53115 Bonn

[3] Bayer AG, Crop Science Division, Disease Control Biology, Alfred-Nobel-Str. 50, 40789 Monheim am Rhein, Germany

Author contributions:

CK, MFB and MD designed the study. MFB and MD performed the greenhouse and laboratory work, MFB did the bioinformatic and statistical analyses. MFB drafted the manuscript, CK, AMK and MFB further reviewed and edited. All authors discussed the results and agreed about the final version.

Abstract

The root-associated microbiome has been of keen research interest especially in the last decade due to the large potential for increasing plant performance. In agricultural systems, continuous applications of plant health protecting products (PHPP) are essential for obtaining high yields and quality. However, knowledge about the impact of such applications on the root-associated microbiome remains limited, especially when applied above ground. We addressed this by applying five different PHPPs from different groups, including biological agents, in two model systems, apple and strawberry, and different soils. We hypothesized that PHPP application leads to specific plant-mediated responses in the rhizosphere microbiota.

The effects of above ground applications of PHPPs on the root-associated microbiota of greenhouse-grown apple saplings and strawberry plants were studied in three experimental trials. The bacterial community structure of rhizospheric soil and endospheric root material was characterized using 16S rRNA gene amplicon sequencing. No consistent effects across trials were observed, but alpha diversity tended to be decreased after PHPP application. In some cases, shifts in community composition became evident (PERMANOVA $R^2 = 0.192$, $p = 0.001$) or increases in dispersion were observed (PERMDISP $p_{adj} = 0.040$). Movento® treatments caused in part deterministic shifts in community assembly, whereas Serenade®ASO treatments caused rather stochastic shifts. Effects were concluded to be probably transient and to disappear without continuous product application. These rather heterogenous temporary responses are in line with the concept of the ‘Anna Karenina Principle’, under which terms PHPP applications can act as mild stress factors and slightly and transiently alter the below ground bacterial community. These findings indicate that above ground PHPP applications can have product specific implications for the root-associated microbiome, which should be considered in the context of microbiome management strategies.

1. Introduction

Plant roots are colonized by complex microbial communities that play different roles in plant growth and health (Ali et al. 2017; Brader et al. 2017). Whereas some microbes remain in the rhizosphere, others have capabilities to enter the root and establish an endophytic lifestyle (Frank et al. 2017; White et al. 2019). In recent years, the overall understanding and harnessing of plant-associated microbiomes has been of keen interest to improve plant health and contribute to sustainable agriculture (reviewed in Trivedi et al. 2021; Ciancio et al. 2019; Busby et al. 2017). Microorganisms have been shown to confer fitness advantages to the plant host, including growth promotion, improved nutrient uptake and resistance to pathogens and they thus offer a possibility to reduce the need for synthetic fertilizers and pesticides (Trivedi et al. 2020; Bailly and Weisskopf 2017).

Crop pathogens and pests reduce the yield and quality of agricultural products and thus cause substantial economic losses (Michalecka et al. 2018; Carisse and Dewdney 2002; Savary et al. 2019). As a consequence, regular applications of plant health protecting products (PHPPs) are currently common practice. For example, around 350.000 tons of synthetic PHPPs were sold in Europe annually between 2011 and 2020 (Eurostat 2022). Environmental concerns, regulatory restrictions and rising pest resistances have led to an increase of biopesticides as a promising tool to minimize crop loss and simultaneously reduce the use of synthetic PHPPs (Fenibo et al. 2021; Salimi and Hamedi 2021). Biopesticides are defined as a natural product either containing microorganisms or compounds derived from living organisms including plants, nematodes and microbes that limit or reduce disease severity**.** They often work by blocking the attachment, establishment and colonization of other microbial cells via parasitism or competition.

There is growing evidence that the application of PHPPs, including synthetic compounds as well as biopesticides, can influence the root-associated microbiota (reviewed in Ramakrishnan et al. 2021). Depending on the product group and application mode, different effects on the root-associated microbiota have been observed by PHPP applications. When PHPPs were in direct contact with the microbiome, e.g. as soil or seed treatments, such as seed coatings, or in cases of systemic PHPPs, they have been shown to influence bacterial and fungal rhizosphere communities in maize,

soybean, rice, strawberry and sugar cane (Huang et al. 2021; Nettles et al. 2016; Kusstatscher et al. 2020; Deng et al. 2019; Qian et al. 2018; Chen et al. 2017). For example, the systemic herbicide haloxyfop-R-methyl, which was applied above ground, has been shown to dissipate into the rhizosphere soil upon application, where it affected bacterial richness and community structure (Liang et al. 2020; Chen et al. 2017). However, the level of impact varies according to active materials, with the soil application of a mixture of the systemic fungicides fosetyl-aluminum and propamocarb-hydrochloride having an effect on the soil microbiota, which was weak and transient (Fournier et al. 2020).

Compared with synthetic compounds, biopesticides are considered to have fewer environmental risks, but little is known about their impact on the root-associated microbiota (Samada and Tambunan 2020). While some studies using live microbial agents such as *Bacillus amyloliquefaciens* SN16-1 or *Clonostachys rosea* f. *catenulata* mainly reported transient effects on the bacterial rhizosphere communities upon addition to soil (Wan et al. 2017; Fournier et al. 2020), another study using a liquid product composed of a broad spectrum of microbes reported significant effects in bacterial community composition and relative abundance (Deng et al. 2019). In contrast to this, a biopesticide containing azadirachtin, a secondary metabolite extracted from neem seeds and leaves, exerted a negative impact on the rhizospheric microbial community, behaving in a similar way to synthetic PHPPs (Singh et al. 2015). As biopesticides and synthetic PHPPs were mostly applied directly to the soil in these studies, effects are likely to result from direct or close contact with the root-associated microbiome. However, the effects of above ground product applications and plant-mediated responses on the root-associated microbiota are currently largely unknown.

Most studies have focused on only one single PHPP, applied to a specific plant species or soil. Thus, it is unknown whether there are universal effects caused by the same PHPP, product group or application mode under different conditions on the root-associated microbiota. Furthermore, effects were mostly studied on the entire rhizosphere and/or endosphere of single plant individuals or even pooled plant material without differentiating between root compartments (i.e., root interior or exterior), different root sizes or age. However, bacterial communities differ between compartments, root sections or shift along the root axis or with root size, which is likely driven by changes in

rhizodeposition (Becker et al. 2022; Rüger et al. 2021; Keel et al. 2012; Zhalnina et al. 2018). Consequently, possible plant-mediated responses to PHPP application could lead to root compartment or section specific reactions.

Given the central role of microbes in the rhizosphere and endosphere for the plant, understanding underlying principles of responses to PHPP application as a potential stressor for the microbiome is essential. Plants and their associated microbiome have evolved several adaptive strategies to withstand different abiotic and biotic stressors. The rhizosphere microbiota shows varying degrees of change to stresses (Cloutier et al. 2021; Ely and Smets 2019; Frindte et al. 2019), including the recruitment of beneficial microbes, the so-called 'Cry-for-help'- strategy (Rizaludin et al. 2021). Whereas this process is considered a deterministic process, it has recently been proposed that external plant stressors could lead to stochastic changes in the microbial assembly (Arnault et al. 2022). These changes are thought to occur due to a transitory loss of the host capacity to regulate its microbiota and have been called the 'Anna Karenina Principle'. In a meta-analysis of 606 microbiomes to assess microbial community responses to various stressors, it has been found that stressor exposure significantly decreases alpha diversity and increases community dispersion across a range of environments and stressor types (Rocca et al. 2018). Zaneveld et al. (2017) have proposed that stochasticity produces contrasting effects depending on the severity of the perturbations. At the same time, it has been hypothesized that the more drastic the stress, the more deterministic the shift due to highly selective environmental conditions (Arnault et al. 2022). In this context, it remains unknown whether and if so, to what extent PHPP applications act as an environmental stressor that could lead to either stochastic or deterministic changes in the root-associated microbiota. The latter will hold more potential for microbiome management.

The aim of this study was to investigate the effects of above ground application of different PHPPs on the root-associated bacterial microbiota under a broad range of conditions. We hypothesized that: i) the strength of responses to PHPPs differs in different root compartments and root regions with the endosphere microbiota showing stronger responses than the one in the rhizosphere, ii) different products induce different effects on the root-associated microbiota based on their mode of action, with systemic and microbe-based products having most pronounced effects. Consequently, iii)

the application of PHPPs can lead to either deterministic or stochastic changes in the root-associated microbiota under the “cry-for-help” or ‘Anna Karina Principle’, respectively.

We chose apple (*Malus* x *domestica*) and strawberry (*Fragaria* × *ananassa*) as model plants in our study due to their economic importance and their heavy reliance on continuous PHPP applications (Damos et al. 2015; FAOSTAT 2019, 2020). For both crops, biopesticides are nowadays often used in combination with synthetic products, reducing the risk of pesticide resistance, which develop against synthetic pesticides in general use (Dara 2016; Chandler et al. 2011; Damalas and Koutroubas 2018; Ayer et al. 2021). We assessed the effects of above ground PHPP application on the bacterial communities in the rhizosphere in three different experimental trials, based on two model plants, three different soil types and partly different experimental environments to cover a broad range of conditions under which responses may occur (Table IV-1). Possible effects were analyzed comparatively in two root compartments according to the concept of Donn et al. (2015) by dividing the root-associated microbiota into loosely (L-compartment) and tightly associated (T-compartment) microorganisms. Loosely associated microorganisms occur in the rhizosphere soil and wash from root surfaces, while tightly associated microorganisms include those that remain adhered to root surfaces after washing and root endophytes. The bacterial community composition was analyzed by amplicon sequencing of the 16S rRNA marker gene.

Table IV-1: Overview of the three experimental trials and their treatments with different plant health protecting products (PHPPs).

	Temporal trial	**Concentration trial**	**Strawberry trial**
Model plant	Apple	Apple	Strawberry
Treatments	Four different PHPPs	Four different PHPPs	Five different PHPPs
Treatment concentration	Recommended dose	Recommended dose Twice the r. dose	Recommended dose Twice the r. dose
Timepoint sampled	Early: one week after final application Late: two weeks after final application	Two weeks after final application	Two weeks after final application
Root section	Pooled root system	Pooled root system	Fine roots Thick roots

2. Material and Methods

2.1 Soil substrate preparation

For the temporal trial, soil was taken from an apple orchard at the Meckenheim research station, Germany (50°37'19.7"N 6°59'48.7"E), and was collected from close proximity to the apple trees. Soil taken from a commercial apple orchard in Buxtehude, Germany (53°29'01.6"N 9°41'29.5"E), was used in the concentration trial. Soil for the strawberry trial was taken from a strawberry field in Telgte, Germany (51°58'40.1"N 7°47'56.8"E). All soils were air dried and sieved through a 2-mm mesh. For apple sapling cultivation, a growth substrate was prepared with 45 % of the soil from Meckenheim or Buxtehude, 45 % sterile silica sand and 10 % perlite. The soil for strawberry cultivation was used without further treatments. Water was added to each type of soil two days before use and the watered soil transferred into growing trays or pots.

2.2 Plant cultivation

Commercially available apple seeds (*Malus* x *domestica* Borkh., cv. Pink Lady) and strawberry plants (*Fragaria* × *ananassa*, cv. Malling Centenary) were used and cultivated according to their specific requirements. Apple seed stratification and cultivation was performed as described in Becker et al. (2023). In brief, 40-day old seedlings were transferred to 13-cm round pots containing the pre-moistured soil mixture together with 0.25 g Basacote 6 M controlled-release fertilizer (Compo Expert, Germany). Young strawberry plants with a rhizome diameter of roughly 10 mm were planted into the soil in 13-cm round pots. To each 25 l of strawberry soil, 4 g of crushed NovaTec Classic 12-8-16 fertilizer (Compo Expert, Germany) was added. Drip irrigation was used for water supply and pot positions were weekly randomized. The soil was covered with a felt mat to prevent run-off of the applied plant health protecting products into the soil.

2.3 Plant health protecting product application

A broad range of fungicidal products with different active ingredients and modes of action were chosen: Aliette® (a systemic fungicide/oomycide), Luna® Privilege (a fungicide with upward systemic movement and translaminar activity), Movento® (a systemic insecticide) and Serenade®ASO (a biological product containing a plant growth promoting *Bacillus amiloquefaciens* strain QST 713) were applied to apple saplings.

Additionally, Bactiva® (a biological product containing several plant growth promoting bacteria and beneficial fungi; see Suppl. Table IX-1) was used in the strawberry trial. The active ingredients and the application rates within each trial are listed in the supplement (Suppl. Table IX-1). Standard recommended spray rates for greenhouse applications were used in all trials (indicated with the prefix r. in the treatment nomenclature, e.g., r.Aliette). A second set of plants received twice the recommended rate, but only in the concentration and strawberry trials (double of the recommended application dose, indicated with d., e.g., d.Aliette). An exception to this were the Serenade®ASO-treated plants in these two trials, which received only the recommended application rate. Here, one set of plants was instead covered with a felt mat during application (abbreviated w felt), whereas the felt mats were removed during application for the other set (w/o felt) to assess whether stronger responses of the rhizosphere bacterial community are seen when product penetration into the soil is not fully prevented. Products were applied using a hand-held sprayer except for Bactiva®, which was applied as a drench application. For all experiments, plants treated with water served as controls. The products were applied weekly over three successive weeks on ten individual plants per treatment and samples collected either two weeks after the final application (concentration and strawberry trial) or after one and two weeks upon the final PHPP application (temporal trial). The design of each trial with total sample numbers of 190 to 480 is summarized in Suppl. Table IX-2, all treatments of a trial are specified in Suppl. Table IX-1.

2.4 Sample collection and processing

Sampling was performed by carefully extracting the entire root system of the plants from the soil by loosening the soil and carefully shaking the plant until all excess soil was removed. Then, the root system was cut above the root crown. The root system of the strawberry plants was furthermore divided into two root sections: the inner thick roots (TR) and the outer fine roots (FR) (Suppl. Fig. IX-1). This differentiation was not possible for apple saplings and therefore, the entire root system was used. The roots were collected in 50-ml falcon tubes, stored on ice and frozen at -80°C within four hours after sampling. For apple plants, height and number of leaves were determined at the sampling timepoint as proxy for possible product application induced growth responses. The further sample processing to obtain loosely and tightly root-associated

microorganisms according to the concept of Donn et al. (2015) was performed by a washing procedure as described by Becker et al. (2022). Bulk soil was also collected in all three experiments to compare the different soils to each other.

2.5 DNA extraction and 16S rRNA gene PCR

DNA extraction and 16S rRNA gene PCR were performed as described by Becker et al. (2022). In brief, DNA was extracted using the NucleoSpin® Soil DNA extraction kit (Macherey Nagel, Düren, Germany) and the 16S rRNA gene was amplified using a nested LNA PCR protocol to suppress the amplification of plant organelle derived 16S rRNA genes. The primer pair 799f-1193r with barcoded forward primer was used in the second amplification round to obtain PCR products of adequate length for sequencing. Library preparation of the PCR products from the combined and concentration trial followed by sequencing on a HiSeq system (Illumina, San Diego, CA) was performed by the Max Planck-Genome-Centre Cologne and generated paired-end reads of 2 × 250 bp. The strawberry samples were sequenced on a Novaseq system (Illumina) with 2 x 250 bp reads by Novogene (Cambridge, UK).

2.6 Sequence data analysis

The raw sequence reads of each trial were processed independently using a custom bash script with Cutadapt version 2.10 to demultiplex the samples (Martin 2011). Primer removal and further processing was done with QIIME2 version 2021.11 (Bolyen et al. 2019). The temporal and concentration trial samples were processed using DADA2 as described in Becker et al. (2022). Because Novaseq uses a different Phred score system, the strawberry trial samples were processed in a slightly different way. Paired reads were merged with max. ten allowed differences in the overlapping region for the merging step, max. one expected error and a minimum length of 350 bp. Reads were quality filtered using the default settings and denoised using deblur with reads trimmed to 370 bp length and a minimum read number of 50 (Amir et al. 2017). All further analyses were again performed as described by Becker et. al (2022). Briefly, taxonomic assignment was done using a classifier trained for the specific gene region on the SILVA 138 database, reads quality filtered and samples with less than 10,000 reads discarded. The total number of samples, the hierarchical structure of the trials, the read numbers and the number of samples remaining after quality filtering are

displayed in Suppl. Table IX-2. For most samples data of seven or more replicates were kept per treatment, the lowest was five replicates (one case).

Unless otherwise specified, statistical analyses were performed in the QIIME2 environment and in R version 4.0.2 (R Core Team 2021) using the packages “phyloseq” (McMurdie and Holmes 2013) and “microbiome" (Lahti et al. 2017). Figures were generated using the “ggplot2” package (Wickham 2016). All statistical analyses were done separately for the two root compartments. Alpha diversity was estimated by Shannon`s diversity index using a feature table rarefied to 10,000 reads per sample. The effects of the explanatory variables were assessed by linear regression using the “lm” function in the package “stats” with the Shannon index as response variable and with the different explanatory variables of the respective trials, followed by ANOVA. Pairwise comparison TukeyHSD contrasts were computed by using the “emmeans” package for the estimated marginal means of the linear models. In the temporal trial, the factors PHPP application and timepoint and their interaction were used as explanatory variables. In the concentration trial, the factors PHPP application and application mode were added as explanatory variables. The doubled application dose of the three products and the removal of the felt mat in case of Serenade®ASO were considered as analogous modifications, both leading to a possible increase in response, and were thus implemented as one explanatory variable (Application). In the strawberry trial, the factors root section and PHPP treatment and their interaction were used as explanatory variables with application mode as nested factor within PHPP treatment.

Differences in bacterial community composition were determined based on the non-rarefied dataset using the q2-plugin “DEICODE”, a form of Aitchison distance (Martino et al. 2019) and visualized in principal coordinate analysis (PCoA) plots. Statistical differences were calculated using “adonis”, a form of one-way permutational multivariate analysis of variance (PERMANOVA) with 999 permutations, followed by a pairwise PERMANOVA with Benjamini-Hochberg correction for multiple testing using the “pairwise.adonis” function, resulting in adjusted *p*-values (p_{adj}). Permutational analysis of multivariate dispersions (PERMDISP) with 999 permutations was used to test the PERMANOVA assumptions of equal variances between groups (e.g. different treatments), but also to test whether the dispersion within a group was distinct from other groups (Anderson 2006). Pairwise PERMDISP tests were performed with Benjamini-

Hochberg's correction for multiple testing. In the temporal trial, the factors PHPP application and timepoint and their interaction were used as explanatory variables. In the concentration trial, the factor PHPP application and its interaction with the application mode were used as explanatory variables, whereas the factors root section, the grouped variable of PHPP application and application mode (e.g., r.Aliette®) and their interaction were used as explanatory variables in the strawberry trial.

Phylogenetic beta diversity was estimated with the metric betaNTI weighed by abundance using the "microeco" package (Liu et al. 2021a). The same null model with random draws without replacement and 1000 iterations using the same species pool was used for each metric. In betaNTI analysis, the mean nearest phylogenetic neighbor among the individuals in two communities is calculated (Webb 2000; Stegen et al. 2012). An individual null model, where all taxa in the phylogeny had equal probability of being included in the null communities, was defined for the two root compartments separately in all trials. Within those compartments, separate models were likewise defined for the early and late timepoint in the temporal trial, and for the fine and thick roots in the strawberry trial. We then compared the observed phylogenetic beta diversities of PHPP treatments to the patterns expected under the null model. Positive betaNTI values indicate lower phylogenetic turnover than expected given the taxa turnover, meaning that turnover between the two communities occurred between closely related individuals; negative values indicate higher than expected phylogenetic turnover, meaning that turnover between the two communities occurred between distantly related individuals (Chai et al. 2016). Individual values between –2 and 2 reveal a dominance of stochastic processes, and a |β-NTI| >2 reveals the dominance of deterministic processes (Arnault et al. 2022). Furthermore, the taxonomic normalized stochasticity ratio (tNST) based on Jaccard's dissimilarity index (using the bootstrapping method with 999 randomizations) was applied to identify the bacterial community assembly processes using the "NST" package (Ning et al. 2019). Here, an index value of 0.5 serves as boundary point between more stochastic (>0.5) and more deterministic (<0.5) assembly. Like betaNTI, separate calculations were made for the compartments, the different timepoints and root sections as described above. Wilcoxon rank-sum tests were used to compare ratios of the control to the treatments as proposed by the authors (Ning et al. 2019). For both betaNTI and tNST calculations, ASV tables with a subset of 10,000 randomly chosen reads were used. Pairwise differential

abundance analysis at order and genus level was performed using ANCOM-BC without detection for structural zeros (Lin and Peddada 2020). In all trials, conservative variance estimates of the test statistic were used and *p*-values were adjusted using Holm's correction with alpha = 0.1. Only taxa with a mean relative abundance of >0.1 % are shown.

3. Results

3.1 Alpha diversity decreased sporadically upon PHPP applications

In all three trials, the effects of the different PHPP treatments on alpha diversity were assessed by linear regression of the Shannon index with ANOVA. In the temporal trial, we only observed significant differences caused by PHPPs in the bacterial community of the T-compartment, but not the L-compartment (Table IV-2). In the T-compartment, detailed pairwise comparisons of each PHPP treatment with the control revealed that only Movento® treated plants had a decreased Shannon's diversity index and only at the first timepoint (TukeyHSD *p*-value = 0.030). In the concentration trial, no significant differences in response to the PHPP treatments were found (L-compartment: F = 0.538, *p* = 0.823; T-compartment: F = 0.497, *p* = 0.853). In the strawberry trial, no conclusive trends or significant changes due to PHPP applications were detected in the T-compartment, whereas diversity decreased in the L-compartment (*p*-value = 0.005) (Fig. IV-1 B). Especially Luna® and Aliette® treated plants showed significant decreases in comparison to the control treatment (TukeyHSD *p*-values of 0.006 and 0.021, respectively) when assessed jointly over fine and thick root sections. Further, Movento® treated plants showed weak evidence for decreased diversity (TukeyHSD *p*-value of 0.064). Resolving PHPP treatment effects within the fine and thick root fraction resulted in insignificant *p*-values upon correction, but besides, we observed that the diversity was in general higher in the thick root section than in the fine root fraction (L: $p < 0.001$; T: $p = 0.003$) (Fig. IV-1).

Table IV-2: Variation in alpha diversity in the root-associated bacterial community of apple saplings due to the application of plant health protecting products in the temporal trial. Differences in Shannon`s diversity index between treatments and timepoint are reported based on linear regression analysis. Two root compartments were sampled: microbes loosely attached to the roots (L-compartment) and microbes tightly attached and inside the roots (T-compartment). Samples were taken at two different timepoints after the last application and the interaction represents the comparison of all applications at both sampling timepoints. Results with significant differences are printed in bold.

Compartment	Variable	df	F.Model	*p*-value
L	Application	4	0.276	0.893
	Timepoint	1	1.007	0.319
	Application * Timepoint	4	0.803	0.527
T	**Application**	**4**	**5.483**	**< 0.001**
	Timepoint	1	2.253	0.137
	Application * Timepoint	4	2.368	0.060

3.2 Undirected changes in the bacterial community composition

To assess possible effects of different PHPP applications on the composition of the root-associated bacterial community we analyzed the differences in composition between samples within each trial based on a form of Aitchison distance. We applied PERMANOVA to test for differences between centroids and dispersion in the community data related to PHPP treatments. To resolve whether differences in PERMANOVA were due to differences in centroids or due to dispersion effects resulting from the treatments we performed PERMDISP tests for homogeneity of dispersions. In the concentration trial, no significant effects were found for the factor PHPP application or for the factor PHPP application mode based on PERMANOVA and PERMDISP (Fig. IV-2). Only a very weak trend was observed upon pairwise comparisons of the individual treatments against the control for Luna® treated plants, which showed a slightly increased dispersion in the T-compartment in the PCoA plot (PERMDISP F = 3.722, $p = 0.036$, $p_{adj} = 0.144$; Fig. IV-2 A).

A

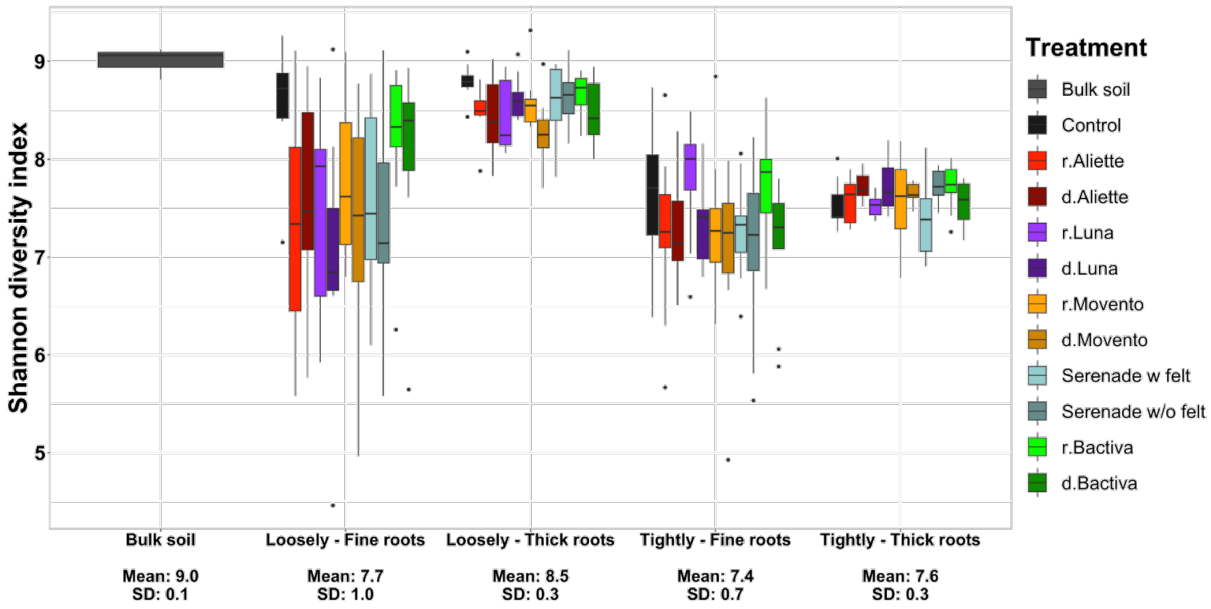

B

Compartment	Variable	df	F.Model	*p*-value
L	**PHPP treatment**	**5**	**3.447**	**0.005**
	Root section	**1**	**62.248**	**< 0.001**
	PHPP treatment * Root section	5	1.846	0.106
	PHPP treatment * Application mode	5	0.664	0.651
	PHPP treatment * Root section *Application mode	5	0.709	0.618
T	PHPP treatment	5	1.083	0.372
	Root section	**1**	**9.659**	**0.002**
	PHPP treatment * Root section	5	0.917	0.471
	PHPP treatment * Application mode	5	1.245	0.290
	PHPP treatment * Root section *Application mode	5	1.435	0.214

Fig. IV-1: Variation in alpha diversity in the root-associated bacterial community of strawberry plants upon application of different plant health protecting products (PHPPs). Boxplots show variation in Shannon`s diversity index between treatments and in comparison to bulk soil samples. Mean values and standard deviations (SD) are indicated below the figure (A). Differences in Shannon`s diversity index between treatments and in interaction with other factors are reported based on linear regression analysis (B). Two root compartments were separately analysed, representing bacteria loosely attached to the roots (L-compartment) and bacteria tightly attached to and inside the roots (T-compartment). Within the root compartments, two different root sections were considered: fine and thick roots. PHPPs were applied in two different application modes: Aliette, Luna, Movento and Bactiva were either applied at the recommended (r.) or doubled rate (d.). Serenade was applied at the recommended rate with either a felt mat (w.Serenade) covering the soil or without (w/o.Serenade). Results with significant differences are printed in bold.

A

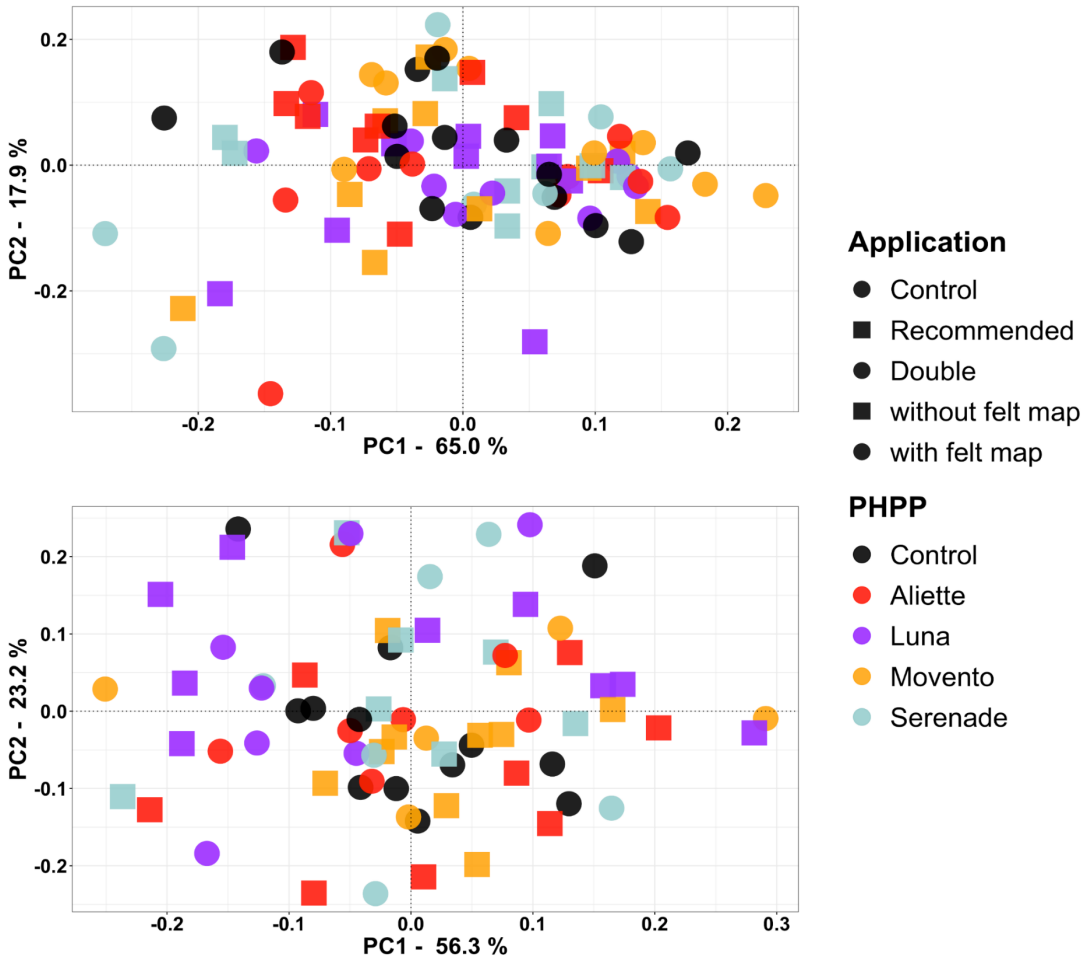

B

Compart-ment	Variable	PERMANOVA				PERMDISP	
		df	F-value	R^2	*p*-value	F-value	*p*-value
L	PHPP	4	0.840	0.038	0.618	0.631	0.642
	PHPP * Application	4	1.004	0.046	0.467	0.524	0.834
T	PHPP	4	1.276	0.071	0.207	1.571	0.192
	PHPP * Application	4	0.935	0.052	0.512	0.856	0.558

Fig. IV-2: Variation in the root-associated bacterial community of apple plants due to the application of plant health protecting products (PHPP) in the concentration trial. (A) Principal Coordinate Analysis (PCoA) based on DEICODE distance matrices. (B) Differences in community composition and dispersion assessed by PERMANOVA and PERMDISP, respectively. Responses were analysed in the two root compartments (L and T). Each PHPP was applied in two different application modes (Application). The products Aliette, Luna and Movento were either applied at the recommended rate or twice the rate. Serenade was applied at the recommended rate but in case of the "without felt mat" treatment, the felt mat covering the soil of all samples was taken off and the product was thus in direct contact with the soil.

In the temporal trial, we also found no differences due to PHPP applications in the bacterial community composition of the L-compartment (Table IV-3), but a significant effect in the community of the T-compartment (R^2 = 0.192, p = 0.001). Additionally, neither timepoint nor the interaction of timepoint with PHPP treatment caused significant effects in the L-compartment. Conversely, in the T-compartment, the PHPP treatment caused differences at both timepoints (Table IV-3), which can also be seen in the PCoA plot, where samples of Movento® and Serenade®ASO showed the most distinct clustering in comparison to the control treatment (Fig. IV-3). However, pairwise PERMANOVA revealed that the differences caused by these two treatments only differed significantly from the control at the early timepoint (Table IV-4). No significant differences were maintained between any PHPP treatment and the control at the late timepoint. PCoA indicates that the differences observed at the late timepoint were primarily due to variation between individual PHPP treatments, but not in comparison to the control (Fig. IV-3 B, lower-right panel). This was confirmed by pairwise PERMANOVA (data not shown). PERMDISP revealed similar differences in community dispersion in the T-compartment, being specific for the early timepoint (Table IV-3). These were seen for the Serenade®ASO treatment in comparison with the control (Table IV-4; p_{adj} = 0.040), but not by the Movento® treatment (p_{adj} = 1.000).

Table IV-3: Variation in the root-associated bacterial community of apple saplings due to the application of plant health protecting products (PHPP) in the temporal trial. Community compositional differences were assessed in the L- and T-compartment (Comp: L and T). PHPP effects were evaluated over both timepoints and individually at each sampling timepoint, followed by a more specific analysis in dependence on timepoint in the T-compartment (T-early and T-late). Differences were assessed by PERMANOVA and PERMDISP applied on DEICODE distances. Results with significant differences are printed in bold.

Comp. & TP	Variable	PERMANOVA				PERMDISP	
		df	F-value	R^2	*p*-value	F-value	*p*-value
L	PHPP	4	1.080	0.056	0.376	0.402	0.806
	Timepoint	1	1.187	0.015	0.332	0.0037	0.952
	PHPP * timepoint	4	0.939	0.049	0.507	0.916	0.517
T	PHPP	**4**	**4.877**	**0.192**	**0.001**	**8.774**	**< 0.001**
	Timepoint	1	0.195	0.002	0.908	0.878	0.351
	PHPP * timepoint	4	1.202	0.047	0.280	**4.708**	**< 0.001**
T-early	PHPP	**4**	**3.142**	**0.239**	**0.001**	**3.480**	**0.016**
T-late	PHPP	**4**	**2.556**	**0.216**	**0.004**	2.243	0.083

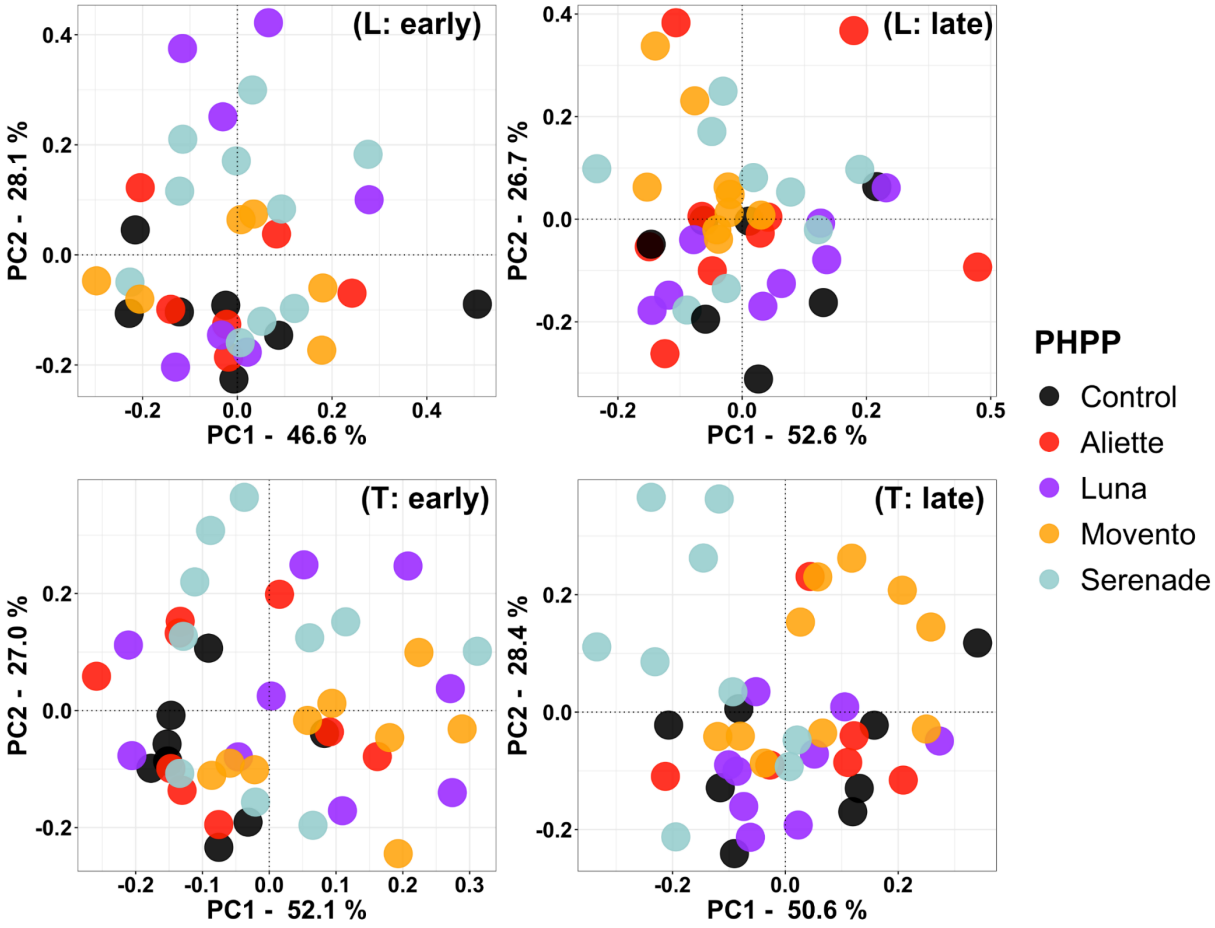

Fig. IV-3: Principal Coordinate Analysis (PCoA) based on DEICODE distance matrices showing variation in the root-associated bacterial community composition of apple plants in the temporal trial upon application of different plant health protecting products (PHPP). The individual PCoA plots display the variation in the root-associated bacterial community composition at the early and late sampling timepoint (one and two weeks after final PHPP application, respectively) in L- and T-compartments, representing the loosely (L) and tightly (T) root-associated bacteria.

This dispersion effect can also be observed in the PCoA plot, where Serenade®ASO treated samples had a higher dispersion compared to the control treatment (Fig. IV-3 B, lower-left panel). The absence of significant PERMDISP results for the Movento® treatment at the early time point in the T-compartment implies that the PERMANOVA validated differences were caused by differences between centroids and not due to altered dispersion.

In the strawberry trial, as expected, the differentiation in fine roots and thick roots was a major explanatory variable in beta diversity with PERMANOVA R^2-values of 0.341 and 0.378 in the L- and T-compartment, respectively (*p*-values = 0.001) (Fig. IV-4 A, Suppl. Fig. IX-3). Consequently, we examined a possible impact of the different PHPPs

and application modes (as grouped variable) for the root compartments and sections separately (Fig. IV-4 B, Suppl. Table IX-3). Here, we found a significant effect by PHPP application only in the fine root section of the L-compartment (R^2 = 0.157, p = 0.016). However, further pairwise PERMANOVA to compare the specific PHPP applications to the untreated control did not reveal significant differences between specific PHPP versus control treatments after p-value correction, i.e. the weak effect of d.Luna became insignificant (Table IV-5). PERMDISP applied to the larger datasets did not reveal major differences in dispersion (Suppl. Table IX-3), only some individual treatments showed significant differences in dispersion compared to the untreated control, especially in the thick root fraction of the tightly root-associated community (Suppl. Table IX-4). Almost all of these treatments showed higher dispersion in their communities than the community of the control treatment, which can be best observed in the PCoA plot of the thick roots of the T-compartment (Fig. IV-4 B, lower-right panel). Whereas the replicate control samples clustered rather closely together, the replicates of the treatments had higher dispersion due to individual outliers.

Table IV-4: Variation in the tightly root-associated bacterial community composition of apple saplings in the temporal trial due to the application of plant health protecting products (PHPP) at different sampling timepoints (TP: early and late). Pairwise PERMANOVA and PERMDISP results comparing different PHPP applications to the control group are shown. The p-values were adjusted (p_{adj}) for multiple testing using Benjamini-Hochberg correction. Results with significant differences are printed in bold.

Comp. & TP	Comparison	PERMANOVA					PERMDISP	
		df	F-value	R^2	p-value	p_{adj}	difference	p_{adj}
T-Early	Control – Aliette	1	1.571	0.095	0.203	0.203	-0.253	0.883
	Control – Luna	1	2.503	0.143	0.055	0.073	-0.553	0.267
	Control – Movento	**1**	**4.051**	**0.213**	**0.011**	**0.022**	-0.010	1.000
	Control – Serenade	**1**	**4.363**	**0.214**	**0.005**	**0.020**	**-0.782**	**0.040**
T-Late	Control – Aliette	1	0.521	0.042	0.706	0.706	0.096	0.998
	Control – Luna	1	0.948	0.059	0.475	0.633	0.432	0.559
	Control – Movento	1	1.586	0.090	0.210	0.420	0.193	0.956
	Control – Serenade	1	2.176	0.127	0.088	0.352	-0.366	0.702

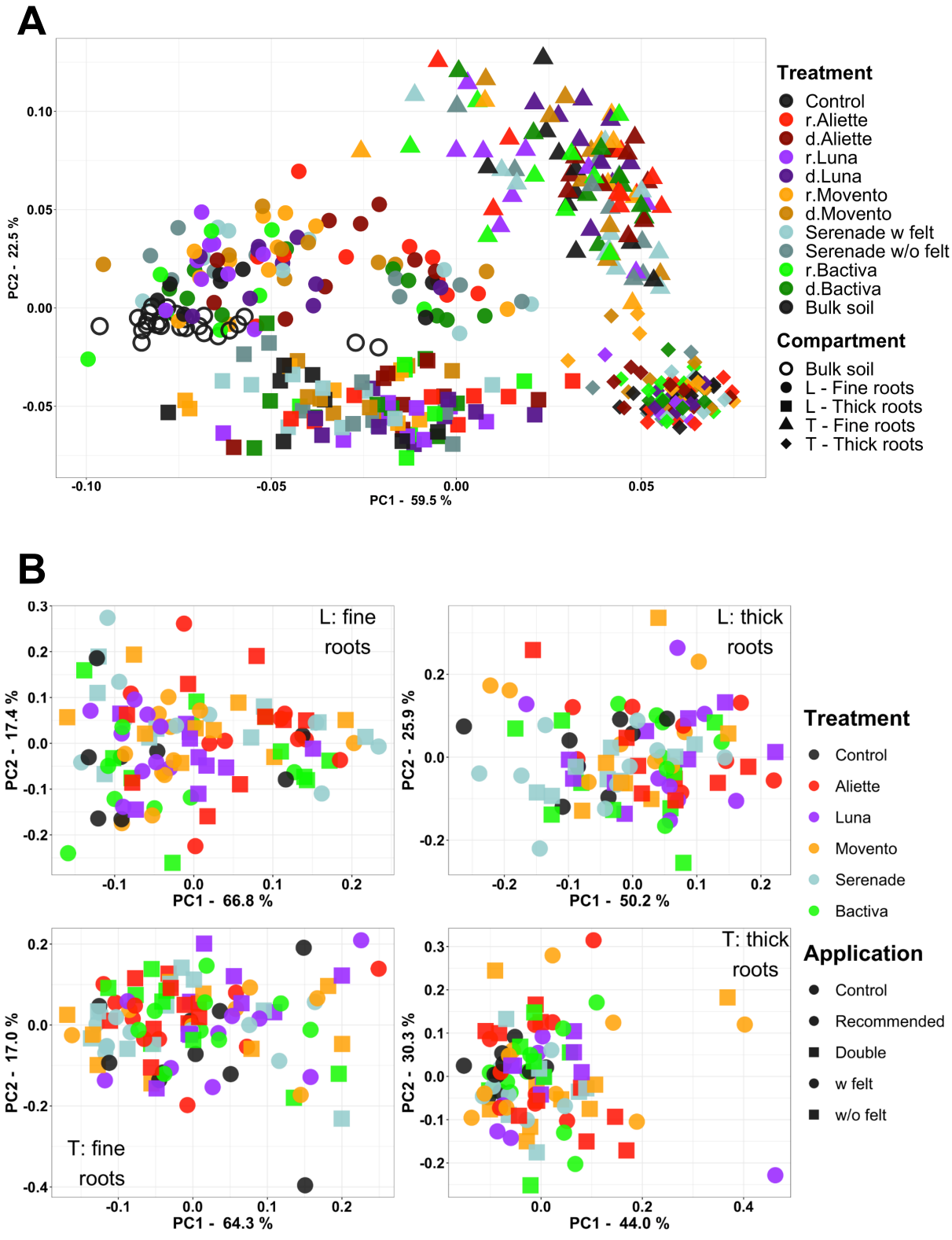

Fig. IV-4: Principal Coordinate Analysis (PCoA) based on DEICODE distance matrices showing variation in the root-associated bacterial community composition of apple plants in the temporal trial upon application of different plant health protecting products (PHPP). The individual PCoA plots display the variation in the root-associated bacterial community composition at the early and late sampling timepoint (one and two weeks after final PHPP application, respectively) in L- and T-compartments, representing the loosely (L) and tightly (T) root-associated bacteria.

Table IV-5: Results of a pairwise PERMANOVA, applied to assess differences in bacterial community composition in the L-compartment of the fine root fraction of strawberry plants upon different plant health protecting product (PHPP) applications in comparison to the control treatment. PHPPs were applied at either the recommended application rate (r) or twice the rate (d). In case of Serenade both applications were at the recommended rate but with (w) or without (w/o) a felt mat covering the soil surface. The *p*-values were adjusted (p_{adj}) for multiple testing using Benjamini-Hochberg correction. Results with significant differences are printed in bold.

Treatment	Application mode	F-value	R^2	*p*-value	p_{adj}
Aliette	r	2.426	0.132	0.076	0.184
	d	2.447	0.140	0.071	0.184
Luna	r	1.534	0.093	0.201	0.287
	d	**3.985**	**0.199**	**0.012**	0.120
Movento	r	2.457	0.126	0.054	0.184
	d	0.759	0.048	0.541	0.541
Serenade	w	0.928	0.058	0.411	0.457
	w/o	1.284	0.079	0.278	0.348
Bactiva	r	2.125	0.132	0.092	0.184
	d	1.968	0.110	0.114	0.190

3.3 Different PHPPs can cause either deterministic or stochastic changes in the microbiota assembly

To gain deeper insight into possible community responses to PHPP treatments, we quantified the relative proportion of deterministic and stochastic processes in community assembly. Therefore, we calculated the phylogenetic beta diversity based on the commonly used betaNTI metric (Suppl. Figs. IX-2 to IX-4), where a |betaNTI| <2 reveals a significant dominance of stochastic processes, whereas a |betaNTI| >2 reveals the dominance of deterministic processes. Furthermore, a betaNTI <2 indicates homogeneous selection in the community assembly process, whereas values >2 indicate variable selection. In the concentration and temporal trial, almost all betaNTI values were below the significance threshold of -2, indicating the dominance of deterministic processes and homogeneous selection, regardless of the different PHPP treatments (Suppl. Figs. IX-2 and IX-3). In the L-compartment of the concentration trial, r.Aliette and r.Luna, r.Movento and Serenade®ASO w/o felt displayed slightly lower betaNTI values compared to the control. Likewise, d.Aliette and r.Movento displayed this kind of response in the T-compartment. In contrast, betaNTI values for the Serenade®ASO treatment increased here slightly compared to the control, thus showing mostly stochastic assembly, which was also clearly seen for Serenade®ASO in the T-compartment of the temporal trial at both timepoints. Also showing a similar pattern to the

concentration trial, Movento® treated plants showed a slightly lower mean index value in the T-compartment, especially at the early timepoint. Otherwise, no changes were evident in the PHPP treatments of the temporal trial. In contrast to the concentration and temporal trial, communities in the strawberry trial were overall more often governed by stochastic processes, especially in the L-compartment of the fine roots (Suppl. Fig. IX-4). Here as well as in the T-compartment, several PHPP treatments resulted in a significant decrease in betaNTI and thus a dominance of deterministic processes compared to the control (most evident for Bactiva®, Serenade®ASO and Aliette® treatments). Thus, several treatments tended to increase deterministic assembly processes in the strawberry trial (Suppl. Fig. IX-4).

We further calculated the taxonomic normalized stochasticity ratio (tNST) based on the taxonomic turnover to analyze whether treatments caused differences in the estimated *ecological* stochasticity (Suppl. Fig. IX-5 to IX-7). Here, an index value of 0.5 serves as the boundary point between more stochastic (>0.5) and more deterministic (<0.5) assembly. In the concentration trial, Serenade®ASO w/o felt displayed a slightly higher proportion of stochasticity in the assembly process of the L-compartment compared to the control (Suppl. Fig. IX-5). In the T-compartment, d.Aliette and both Movento® concentrations caused decreased tNST values compared to the control, which fell below the boundary point and turned thus deterministic. These changes were in good agreement with the increasing determinism for these treatments seen in betaNTI analysis of the two compartments. Most striking in the temporal trial was the increase of stochasticity of the Serenade®ASO treatment and the decrease for the Movento® treatment at both timepoints in the T-compartment, likewise as observed with betaNTI. In communities of the L-compartment of the strawberry trial, the application of PHPPs also induced a decline in tNST and thus an increasing role of deterministic processes upon PHPP application (Suppl. Fig. IX-7). This was less evident in the T-compartment, where responses were more heterogenous. In the fine roots, d.Aliette and both Serenade®ASO treatments caused a decrease in stochasticity compared to the control. In the thick roots, in contrast, most PHPP treatments caused an increase in stochasticity in the communities. Overall, the results obtained for tNST were similar to the results shown for betaNTI, although some differences were more pronounced. Some PHPP treatments induced deterministic changes in the assembly process, while in most cases Serenade®ASO treatments tended to promote stochastic processes in the T-compartment.

3.3 PHPP treatments did not affect the same taxa across different trials though plants enriched similar taxa from different soils

In all three trials we used ANCOM-BC for differential abundance analysis to compare PHPP treatments to the control in the L- and T-compartment, respectively, with the aim to see whether specific taxa responded to different PHPP applications. Overall, only very few genera were significantly differentially abundant, and no genus showed a consistent response in at least two trials (Suppl. Fig. IX-8 to IX-10). Also, almost no taxa were responsive in both, the recommend and double application rate of either PHPP in either the concentration or in the strawberry trial, though similar trends were quite common. Focusing on the treatment with the clearest response in comparison to the control treatment according to PERMANOVA, i.e. the fine roots of the L-compartment in the strawberry trial, where almost 20 % of the variation was explained by the d.Luna treatment, no specific differentially abundant genus was found (Table IV-5 , Suppl. Fig. IX-10). Similarly, the Movento® treatment caused significant changes in the bacterial community composition of the T-compartment at the early timepoint in the temporal trial ($R^2 = 0.213$, $p_{adj} = 0.022$) (Table IV-4), but we only found three taxa which differed significantly from the control: *Rhizobacter,* and each an unclassified *Rhodanobacteraceae* and *Steroidobacteraceae* (Suppl. Fig. IX-9 B).

To evaluate whether the lack of consistent responses across trials was attributed to the different soils that were used, we analyzed possible soil-specific variation. The same major phyla dominated in each of the three soils, with *Proteobacteria* and *Acidobacteriota* being most prevalent (Suppl. Fig. IX-11). As expected, *Proteobacteria* increased in relative abundance from bulk soil over the L compartment to the T compartment, while *Acidobacteriota* decreased. To analyze in more detail whether similar taxa were enriched in the rhizo- and endosphere across the different trials we applied differential abundance analysis. We observed similar shifts of taxa from bulk soil to the loosely and further to the tightly associated root compartment across all trials (Suppl. Fig. IX-12). The order *Pseudomonadales* for example increased significantly in relative abundance from the bulk soil to the L-compartment and further to the T-compartment across all three trials. The orders *Streptomycetales*, *Burkholderiales*, *Caulobacterales* and *Sphingomonadales* increased in relative abundance from bulk soil to T-compartment, whereas the *Bryobacterales*, *Solibacterales*, *Gaiellales* and *Bacillales*

consistently decreased in relative abundance along this continuum in all trials. Thus, despite differences in the bulk soil and the host plant species, plants in all three trials recruited similar bacterial communities in their rhizospheres and roots.

4. Discussion

4.1 Prerequisites for comparative PHPP effect evaluation between and within different trials

We assessed the effects of above ground applied PHPPs on rhizosphere bacterial communities in three different experimental trials, covering a broad range of conditions. This likely results in the development of specific responses to PHPP applications in the individual set-ups, although we would expect some consistent responses across trials in case of strong universal effects. As a prerequisite, we analyzed community consistencies and heterogeneities between soils and trials. The three soils used in this study harbored bacterial communities with identical dominant orders, in addition to lower-abundant soil-specific orders (Suppl. Fig. IX-11). Further, a comparative analysis of differences between compartments (Suppl. Fig. IX-12) showed the enrichment of similar taxa in the root-associated compartments across the three trials. Thus, some consistent PHPP induced alterations in community composition could in principle develop across trials.

Further heterogeneity in our study was related to root regions. In the fine and thick roots of the strawberry plants, differences existed in alpha and beta diversity in the rhizosphere bacterial communities. As the thick roots had become more suberized and had less root hairs (Suppl. Fig. IX-1) they were most likely releasing less root exudates and therewith causing differences in the associated rhizosphere microbiota. Such variation between different root size categories was expected as it has likewise been shown for bacterial communities in the rhizosphere of *Brachypodium* (Kawasaki et al. 2016) and field-grown apple trees (Becker et al. 2022), and in a similar way along the root axis of maize (Rüger et al. 2021). Thus, the desired heterogeneity between and within trials was met, while maintaining consistency to enable the detection of highly universal effects.

As the effects of PHPP applications on the root-associated microbiota were our main focus, we did not put much emphasis on plant health or plant growth parameters. Nevertheless, we measured some basic parameters including plant height and number of leaves and visually assessed plant performance but did not detect differences (data not shown). Thus, specific PHPP applications did not have a visible impact on plant performance that might come along with or trigger changes in the rhizosphere microbiota related to growth.

4.2 Inconsistent and non-treatment specific responses across different experimental trials

We expected at least slight and possibly transient effects of PHPP applications on the root-associated microbiota, with some differences between the different product groups because of the mode of action of these products (Wan et al. 2017; Fournier et al. 2020). The fully systemic products (Aliette® and Movento®) were expected to have a larger impact especially on the endophytes compared to the locally systemic (Luna® Privilege) and biological products (Bactiva® and Serenade®ASO). We also expected Serenade®ASO and Bactiva®, the latter applied as drench application, to have a more pronounced effect than applying Serenade®ASO as spray application, especially when applied with a protective soil cover. However, we did not observe consistent deterministic effects of either the type of PHPP or the application mode across the trials. This was seen for both alpha and beta diversity as well as in differential abundance analyses. Most consistent across trials and treatments was a slight decrease in alpha diversity in some PHPP treatments compared to the control, especially for the systemic products Movento® (in the concentration trial and with trend in the strawberry trial) and Aliette® (strawberry trial), while we never observed a significant increase in diversity upon PHPP application. A mostly only transiently lowered alpha diversity has been reported before and our findings are thus well in line with previous studies, in which products were in direct contact with the soil or rhizosphere microbiome upon soil application (Liang et al. 2020; Qu et al. 2021; Deng et al. 2019; Wan et al. 2017; Fournier et al. 2020; Onwona-Kwakye et al. 2020). Thus, by having direct contact some PHPPs might have a filtering effect on the rhizosphere or endophytic bacterial communities.

Regarding beta diversity, we only found weak effects from Movento® and Serenade®ASO in the temporal trial at the early timepoint in the T-compartment and by

Luna® in the strawberry trial in the L-compartment of fine roots. In the concentration trial, when sampling occurred two weeks after the final application, no differences in composition or dispersion were seen for application dosage, indicating that the root-associated microbiota either did not respond or returned to a homeostatic composition after a relatively short period of time without continued PHPP application. ANCOM-BC showed that no taxa were observed to be changed consistently in at least two trials and almost no taxa were responsive in both the recommend and double application rate of either PHPP (concentration and strawberry trial). This further indicates that above ground PHPP applications have at most a weak and transient impact on the bacterial community composition, as in agreement with some previous studies (Wan et al. 2017; Fournier et al. 2020). Wan et al. (2017) reported that biopesticide applications only altered the bacterial community composition for up to ten days after application, like our study, where we observed a difference seven days after the last application, but not after 14 days, even when applying products at increased dosage in the second trial. Similarly, run-off of above ground spray applications of Serenade®ASO or drench applications of Bactiva® did not have deterministic or permanent effects on bacterial diversity or community composition, even though these contain microorganisms as active ingredient that may interact with the endogenous microbiota. Either these products did not induce changes, or alterations were of very transient nature and we did not detect them. The latter would be in line with a previous study that reported a drift back towards an unaffected microbiota profile in the interim between treatment applications in the strawberry rhizosphere (Deng et al. 2019). Thus, we could not find universal effects of PHPP applications on alpha or beta diversity across the range of conditions tested in this study. However, within specific trials PHPP applications reduced decrease alpha diversity in some cases and had in part a slight and transient effect on the root-associated microbiota without targeting specific microbes. Considering field conditions, it must be noted that no single product would be applied continuously in weekly intervals for prolonged times, even though the frequency of PHPP applications is extremely high also in the field, especially in apple and strawberry orchards, comparable to the intervals in this study. However, the number of applications of products of the same chemical class is limited in every season. Instead, products with different modes of action are used in alternation due to resistance management practices. The effects of alternating product applications remain at present unclear.

4.2 Application-related undirected changes in bacterial community composition follow the Anna Karenina Principle

In many cases a significant shift in community composition was accompanied by a significant shift in dispersion, meaning that the observed differences were not necessarily caused by consistent changes in community composition across all replicate samples, but rather by specific changes in individual samples that caused the altered dispersion within a trial (Fig. IV-3). Such apparently random responses are not well in line with the 'cry-for-help' principle but are described in the 'Anna Karenina Principle'. Ma (2020) and Zaneveld et al. (2017) applied the AKP to human and animal microbiomes, respectively, stating that certain stressors have stochastic rather than deterministic effects on community composition, because stressors reduce the ability of the host to regulate its microbial community composition. It has also recently been proposed to conceptualize plant dysbiosis as a transitory loss of the host's capacity to regulate its microbiota (Arnault et al. 2022). A hallmark of AKP effects is that the microbiological changes in dysbiotic or stressed individuals vary more in microbial community composition than in healthy individuals and that this variation can be compared using PERMDISP, which measures dispersion effects (Zaneveld et al. 2017). In our trials, such a dispersion effect was observed after product application in the temporal and to some extent in the strawberry trial. In the temporal trial we found such differences in community composition and dispersion only one week after the last application of PHPPs. Other studies investigating PHPP effects on the microbiota have not discussed a possible AKP effect, but a visual assessment of their data indicates very clearly a higher dispersion after PHPP treatment in several ordination plots (Fournier et al. 2020; Deng et al. 2019; Kusstatscher et al. 2020). In addition to the dispersion effects, we observed a transient decline in alpha diversity. A decreased diversity in stressed organisms has also been proposed as being characteristic of an AKP effect, but appears less consistent compared to the dispersion effect (Ma 2020). We did observe similar trends in this study. Thus, our partially detected alterations in the bacterial community are well in line with the AKP. That the rhizosphere microbiota may respond to above ground stresses according to the AKP is further supported by an increased dispersion in bacterial rhizosphere communities that we observed in an earlier study with comparable experimental set-up upon foliar pathogen infection of apple seedlings (Becker et al. 2023).

Another indicator for an AKP effect and stochastic rather than deterministic changes is the discrepancy between PERMANOVA and differential abundance analysis results. In case of deterministic changes, PERMANOVA would show significant effects in response to a PHPP treatment and differential abundance analysis would indicate taxa that show consistent changes in relative abundance across replicates. However, this was often not observed in our study, for example in the strawberry trial, where PERMANOVA indicated differences between the d.Luna treated and the control plants in the fine roots of the L-compartment, but no taxa were found to be differentially abundant between those two treatments. This points to rather stochastic changes in the bacterial rhizosphere community of the individual plants. Heterogenic responses between replicates due to AKP effects have also been proposed by Zaneveld et al. (2017). The authors state that even though shifts can happen, they may not rise to the level of significance, because they vary between the stressed individuals. They further state that this is enforced at more highly resolved taxonomic levels and affected by limitations in statistical power due to the need to correct for high numbers of multiple comparisons.

Besides alpha and beta diversity, Arnault et al. (2022) proposed to use betaNTI to detect a possible AKP effect. They state that an AKP effect can be detected if the non-stressed microbiota has a |betaNTI| >2 and the stressed microbiota changes to a |betaNTI| <2, therewith indicating an increase of stochasticity. We included in addition tNST, which reflects the contribution of stochastic assembly relative to deterministic assembly and thus allows for a better quantitative measure of stochasticity compared to betaNTI (Ning et al. 2019). Overall, we found that the apple root-associated microbiota was predominantly assembled by deterministic processes, identified to be homogenous according to betaNTI, whereas, the assembly of especially the fine roots of strawberries was more stochastic. Upon PHPP treatment, we found few differences and surprisingly, according to both betaNTI and tNST, stochasticity was decreased, especially in the T-compartment. It appears thus in contrast to the expectation according to Arnault et al. (2022), but Zaneveld et al. (2017) proposed different models depending on the severity of the stressor. In one of their models, the perturbation alters the microbiota deterministically, but the extent of alteration is stochastic and related to the severity of the stressor. In case of a severe stressor, the community compositions of stressed hosts would be similar to each other, whereas the community compositions

of mildly stressed hosts would display a dispersion increase. This fits with our findings and indicates that above ground PHPP applications can sometimes act as a mild stress factor. It likewise fits to the findings of a recent study, showing that bacterial communities in severely unhealthy strawberry farms with soil-borne pathogens display an increase in deterministic processes of assembly and thus properties of a severe stressor in the rhizosphere, but rather stochastic assembly of the shoot endophytes (Siegieda et al. 2024). Thus, severe stressors with deterministic responses in heavily affected plant organs appear to turn into mild stressors, triggering stochastic responses, in plant organs being less affected or more remote from locally acting stressors, as in our case.

Focusing on specific PHPPs, the application of Serenade®ASO caused an increase in dispersion and stochastic assemblies, often observed in the T-compartment, therewith following the AKP. The active ingredient of Serenade®ASO is a *Bacillus* strain and *Bacillus* spp. have been shown to form biofilms on leaves that likely play a role in their plant protective properties (Fessia et al. 2022) and to upregulate different defense mechanisms, including elicitation of induced systemic resistance (reviewed in Kloepper et al. 2004). Both biofilm formation and induction of systemic resistance may have led to the observed changes in the root-associated microbiota. In contrast, the systemic PHPP Movento® caused the most severe deterministic effect in the T-compartment shortly after its application in the temporal trial i.e., a significant shift in centroids at the early timepoint, without an increase in dispersion, as well as a few significantly differentially abundant ASVs (Suppl. Fig. IX-9 B). This is in line with our hypothesis that systemic PHPPs are more likely to cause changes in the root-associated microbiota and especially in the endophytic community than in the rhizosphere soil microbiota. These findings show that the effect of an PHPP on the root-associated microbiota depends on the compartment and on the applied PHPP, as hypothesized. Further, the example of Movento® shows that responses are not in all cases in line with the concept of AKP.

Given the current state of available studies and our results, we conclude that above ground PHPP application has only minor and transient effects on the root-associated microbiome and can lead to mild AKP effects. During application of PHPPs or at least after the first applications, they possibly act as an influencing factor on the plant, which could itself react in a way that then affects the root-associated microbial community, e.g. by changes in root exudates and thus food sources. According to our results, the

plant seems to be able to fully restore its specific root-associated microbiota after a relatively short period of time upon the last application of PHPPs.

5. Conclusions

Our study demonstrates that above ground PHPP applications can have a mild, yet transitory effect on the root-associated bacterial community of apple saplings and strawberry plants. Those effects were more likely to be caused by systemic products than by locally systemic or contact products and were often more pronounced in the endosphere than in the rhizosphere. The possible effects we observed include a lowered alpha diversity, small changes in species composition either in the form of a shift or increased dispersion in beta diversity and changes in the phylogenetic turnover. While the systemic PHPP Movento® caused rather deterministic changes in the endosphere microbiota, the biological product Serenade®ASO caused stochastic changes and an increased variability in community composition. Following the concept of the AKP, we observed that PHPP applications can act as a mild stress factor, altering the below ground bacterial community slightly and transiently. Without a continuous exposure to PHPPs, the root-associated bacterial community is likely to drift back towards the community composition profile of an untreated plant. It will be interesting to see whether fungal communities show similar responses to such PHPP treatments. Compared to studies with direct exposure of the root-associated microbiota to PHPPs, our above ground application related effects appear to be weaker. Further, effects appear to be compartment specific and to depend on the product type and its localization in the plant, soil or root-soil interface, with products directly applied into the soil having more pronounced effects. Compared to other stress factors, such as root pathogen infection, the application of PHPPs appears to be a much less severe stress factor on the root-associated microbiota. The effects of PHPPs on non-microbe sensitive marker organisms have already been thoroughly evaluated and overall, we only observed rather weak effects on the root-associated microbiome. However, in the context of microbiome management strategies, further research is required to draw recommendations for crop management practices, future PHPP development and the use of biologicals.

V. Synopsis

Modern agriculture faces numerous challenges, including plant pests, pesticide resistances, regulatory restrictions, and climate change, affecting crop yield and health. At the same time there is a need for an environmentally sustainable approach to increase yields of high quality crops due to limited resources and a continuing population growth (Ricroch et al. 2016). Thus, attaining food security while improving environmental health and resource efficiency has become one of the major challenges in the 21st century (Wang et al. 2022; United Nations 2023). Engineering the root-associated microbiome has been shown to confer fitness advantages to the plant host, including growth promotion, nutrient uptake and resistance to pathogens and thus possibly reduce the need for synthetic fertilizers and pesticides (Trivedi et al. 2020; Bailly and Weisskopf 2017). Tapping into the potential of the root-associated microbiome to improve crop health and yield through a better understanding of the processes in the root-soil interface is thus thought to be one of the most important scientific frontiers of the forthcoming decades (Wang et al. 2020b; Busby et al. 2017; Santoyo et al. 2016; White et al. 2019).

Pathogen infections, especially by fungi, remain one of the major threats to crop production and modern agriculture is currently still requiring repeated pesticide and fertilizer applications to ensure high yields and quality of agricultural products (Eurostat 2022). Due to its potential to provide a disruptive approach towards a more sustainable pest management, having a holistic understanding of the root-soil interface is crucial for its successful integration in pest management strategies. However, knowledge about the impact of both pathogen infections and pesticide applications on the root-associated microbiota, remains limited. Thus, the impact of foliar pathogen infection and above ground plant health protecting product application on the root-associated microbiota as well as above and below ground plant development was evaluated in this thesis. For this, greenhouse-grown apple saplings and fully grown orchard trees were used as model organisms. As a prerequisite, the intrinsic spatial and temporal variation of the root-associated microbiota related to root phenology and seasonal variation was assessed in fully grown trees (manuscript 1, section V.1). The tree root-associated microbiota showed spatial variation on various scales. On a smaller scale, the rhizosphere effect was observed with distinct community compositions in the

rhizosphere and endosphere. Additionally, both endosphere and rhizosphere communities shifted gradually with an increasing root size diameter. Differences at field scale were observed due to soil heterogeneities and the presence of localized soil pathogen occurrences. Both endosphere and rhizosphere communities underwent seasonal changes and displayed year-to-year variation. Similarly, spatial differences were assessed in the rhizosphere of greenhouse-grown apple saplings, as well as the temporal dynamics at early stages of apple plant development (manuscript 2 and 3). Like their fully grown counterparts, apple saplings had distinct bacterial communities in the rhizosphere and endosphere. Due to the uniformity of the root systems of apple saplings, no differentiation into root diameter categories was made for apple saplings. Significant temporal dynamics were observed only when comparing the community compositions of saplings with at least a four-week difference. Overall, this thesis contains the most comprehensive experimental comparison of spatial differences and temporal dynamics of the bacterial community composition of fully-grown trees to date.

It is known that foliar infections can induce significant effects on plant physiology, however, knowledge about their effects on the root-associated microbiota is scarce. Therefore, two economically important foliar pathogens were used to infect apple saplings and the impact on the bacterial root-associated community composition analyzed (manuscript 2, section V.2). Similarly, the effects of foliar PHPP applications on the bacterial root-associated community composition are largely unknown and therefore, PHPPs from different product classes were applied as foliar applications to apple saplings and young strawberry plants (manuscript 3, sections V.3 and V.4). Foliar pathogen infections were found to induce plant-mediated changes upon severe leaf infection in the root-associated microbiota, while foliar PHPP applications only caused minor and transient effects. Thus, above ground disturbances are reflected in the belowground microbiome. To simulate field conditions, under which foliar pathogen infections are usually treated with foliar pesticide applications, the combined effects and temporal dynamics of both pathogen infection and product application were evaluated in different root compartments of apple saplings (manuscript 2, section V.5). A curative fungicide treatment decreased disease severity and helped diseased plants regain the plant the microbiota of a healthy plant. Overall, this thesis sheds first light on the effects of agronomically extremely relevant above ground factors on the root-associated

microbiota with immense impact on microbiome management strategies in the context of sustainable agriculture.

1. Spatial and temporal variation within the root-associated microbiota

The root-soil interface is considered to be one of the most dynamic microbial hotspots with considerable impact on plant growth and health (Ali et al. 2017; Brader et al. 2017). Plants are capable of actively recruiting specific microbes from their surrounding soil, which then thrive in the rhizosphere, a process mostly driven by the plant via rhizodeposition (Beckers et al. 2017; Bulgarelli et al. 2013; Deyett and Rolshausen 2020; Zhalnina et al. 2018). Due to physiological changes of the roots with increasing age and root diameter, the composition and amount of rhizodeposits changes, potentially creating spatial variation in community composition along a root size gradient (Rüger et al. 2021; Keel et al. 2012; Zhalnina et al. 2018). Besides this spatial variation, temporal dynamics closely linked to the plant developmental stage have been shown to influence the structure of the associated microbial community of herbaceous and annual plants but not for perennials and trees. Shifts in the root-associated communities are likely to occur due to seasonal shifts in carbon allocation into the roots and the surrounding soil and due to plant litter input during autumn and winter (Bonkowski et al. 2021; Donn et al. 2015; Li et al. 2014; Maarastawi et al. 2018; Munoz-Ucros et al. 2021; Shi et al. 2015). Overall, knowledge about the spatio-temporal variation of the root-associated microbiota is currently limited, but crucial for several reasons: a holistic understanding of the complexity of the plant soil interface would allow for microbiome targeting management practices, e.g. plant defense induction. Thus, to improve the holistic understanding of plant-microbe interactions and as a prerequisite to elucidate potential above ground pathogen or PHPP application effects on the root-associated microbiota, the spatio-temporal variation of communities of both greenhouse-grown and orchard-grown apple plants was studied (manuscripts 1,2 and 3).

1.1 Bacterial communities shift between root compartments and along a root size gradient

The spatial variation was observed at two major scales: between the rhizosphere (L-compartment) and endosphere (T-compartment) and for both along a root size gradient. In field grown orchard trees, as well as greenhouse grown apple saplings and

young strawberry plants, hallmarks of the rhizosphere effect were observed, as expected. Its bottleneck effect can exemplary be seen in the decrease in alpha diversity in the endosphere compared to the rhizosphere (Figs. II-2, III-6, and IV-1). This bottleneck effect is caused by the specific selection of various dominant phyla and families. A large overlap across all trials was observed in which the same phyla and families have been either enriched or depleted in the endosphere compared to the rhizosphere. For example, in both the orchard and greenhouse trials, the *Acidobacteriota* were more prevalent in the rhizosphere compared to the endosphere, while the *Actinobacteriota* were enriched in the endosphere compared to the rhizosphere, thus pointing to a compartment specific selection process (Figs. II-1, Suppl. Fig. VII-1). Similar observations were made before for the annual crops maize, rice and wheat or *Arabidopsis* (Donn et al. 2015; Bulgarelli et al. 2013; Lundberg et al. 2012; Edwards et al. 2015; Fan et al. 2017), as well as the perennial citrus and olive trees (Fernández-González et al. 2019; Zhang et al. 2017). Overall, there is strong evidence that both apple saplings and trees, as well as strawberry plants enrich similar phyla in the endosphere, similar to previously studied model plants, further pointing towards analogous selection mechanisms. Furthermore, phylogenetic beta diversity analyses in apple saplings revealed that the deterministic assembly process is governed by homogenous selection (Suppl. Fig. IX-3 and IX-4), undermining that only selected bacterial taxa are enriched in both rhizosphere and endosphere. Taken together, the results confirm the universality of the rhizosphere effect across different plant species and any effects of above ground disturbances on the root-associated microbiota later discussed in this thesis might therefore be transferable to other plant species.

Besides the differences in root compartments, the spatial differences along a root size gradient in both compartments were analyzed and used as a proxy for root age. For fully grown orchard trees, the spatial differences were shown along a gradient with the smallest section being ≤ 1 mm and the largest ≥ 4 mm root diameter. Along this gradient, successive changes in community composition were found in both root compartments, indicating that apple trees selectively shape their bacterial communities along the root axis (Figs. II-2 and II-6). This successive change alongside this gradient was observed in the community composition but also in the enrichment of certain taxa in the root-soil interface (Fig. II-3). In the rhizosphere, the changes in the composition and quantity of rhizodeposits such as organic carbons are likely the responsible

selective driver. This can exemplary be seen by the enrichment of methylotrophs, which are associated with the conversion of organic carbon compounds in the smaller root sections. Here, especially at the root tips and in the elongation zone, the largest amount of rhizodeposits including methanol are released into the rhizosphere soil (Epron et al. 2011; Hoffland et al. 1989; Zhalnina et al. 2018; Galindo-Castañeda et al. 2024). Older root sections become suberized and are therefore less relevant compared to finer roots concerning organic carbon exudation, thus explaining the succession along the root size gradient. However, as no analysis of the composition and quantity of the rhizodeposits was done in this thesis, this direct link between rhizodeposits and changes in bacterial community composition remains speculative. In the endosphere, several genera known to contain strains being involved in biocontrol or with plant-growth promoting abilities were enriched in the root sections with a smaller diameter. Thus, apple trees specifically enrich specific taxa with certain functional characteristics in different parts of their root system depending on the root phenology. These results are particularly interesting when comparing them to the analysis of root endophytes in annuals such as maize. Here, the whole endophytic plant root system showed a homogenic bacterial community composition, which may be attributed to the young age of the maize plants and the early colonization of the endosphere by the seed microbiota (Wendel et al. 2025). The differentiation of the apple tree endosphere community by root diameter and its heterogeneity is thus likely due to the successive colonization of the endosphere by soil microbes and a root diameter dependent selection by the plant. Confirmation of the orchard study results was not possible in greenhouse grown apple saplings, as no differentiation into root size categories was possible for saplings grown in pots due to the uniformity and inextricable complexity of their root systems. However, the root system of strawberry plants could be divided into two root sections: inner thick roots and outer fine roots (Suppl. Fig. IX-1). Similar to the apple orchard trees, the communities in these root sections differed significantly from each other, although analysis of the enriched or depleted genera between those root sections regarding taxa that can be associated with specific functions in the root-soil interface is still pending (Fig. IV-4 A). Nevertheless, these findings show that root diameter has a significant impact on the bacterial community composition and can be used as an indicator for differences in root physiology. In addition, due to those differences in physiological activity of different root types, the subsequent potential differences in their root-

associated microbiota would likely have an impact on the recommended granularity of sampling methods. Currently, root samples are mostly taken either by sampling the entire root system, or by taking an undefined core with roots of unknown root size. Potential differences caused by factors only observable in specific root types or development stages would go unnoticed with those current sampling methods.

1.2 Field scale gradients and seasonal changes add to spatio-temporal variability within the root-associated microbiota

Surprisingly, in the orchard trials, there was a significantly large impact of the individual trees on the bacterial root-associated community structure (Figs. II-2, II-4 and II-6). Further spatial variability was found between and within rows, and even between adjacent trees. The variability in the L-compartment can be explained by physio-chemical differences in the soil or by the passive bacterial dispersal mechanisms in the soil (Bahram et al. 2016). Stochastic factors are also likely to play a role in the heterogeneous assembly of root-associated bacteria. A previous study has already shown that spatial variability (1-5 m) of soil microbiota was present within an apple orchard (Deakin et al. 2018), which then likely leads to differences in the assembly of root-associated bacteria. The endosphere communities also showed huge variability between tree individuals. Additionally, in single cases, high levels of the root pathogen "*Candidatus* Phytoplasma" were detected, even though no disease symptoms were visible. These observed variabilities indicate that both soil heterogeneity and symptomless pathogen infections can have an impact on the root-associated microbiota, which raises the need for sufficiently large sample sizes in future studies, even when sampling apparently uniform looking trees within the same orchard or neighboring trees is considered.

Further variation of the bacterial community composition of the orchard trees was observed over the growing season and between years. This temporal variability in both rhizosphere and endosphere was studied in detail by sampling the same orchard trees over an entire growing season. Most strikingly, sequential changes in community composition took place in both compartments with more changes occurring during spring and summer than in winter (Figs. II-4 and II-5). This was expected as the seasonal increase in photosynthetic activity results in increased rhizodeposition rates and root growth, impacting the root-associated microbiota. This has been observed in the olive tree associated microbiota as well (Epron et al. 2011; Thenappan et al. 2024). Apple

root growth in mature trees has been reported to occur unevenly during the year with a possible bimodal pattern with substantial root growth (“root flush”) around full bloom and either mid-summer or harvest (Eissenstat et al. 2006). The resulting shifts in rhizodeposit composition and quantity likely facilitated the proliferation of diverse bacterial taxa, explaining the observed rise in alpha diversity during spring and early summer across the sampled years (Fig. II-4 A). Likewise, the same processes may be the cause of the significant differences in community composition between summer and winter (Suppl. Fig. VII-6). Interestingly and in addition, annual variation was observed for the loosely associated microbial community (Fig. II-4 B and Suppl. Fig. VII-6), indicating that it does not necessarily *per se* return to a highly season-specific state after one year; an observation that was also seen in annual plants such as *Avena fatua* (Shi et al. 2015). In conclusion, both spatial and temporal variation exists within apple orchards and between individuals and needs to be considered when designing orchard trials with repeated sampling. The drivers of this variation are likely spatial and temporal changes in rhizodeposition, caused by soil and field heterogeneity, seasonal changes in photosynthetic activity, as well as root pathogen infections. Many observations found in this perennial model were also found in annual plants, pointing to analogous mechanisms between the two. Overall, this intrinsic spatio-temporal variation of orchard-grown tree root systems is in line with the first part of the first hypothesis of this thesis, stating that differences within individual orchard-grown tree root systems are likely to be related to rhizodeposition and seasonal and annual variation.

The second part of this hypothesis states that this spatio-temporal variation can also be observed in greenhouse-grown apple saplings. As mentioned above, no differentiation into different root size categories was possible for greenhouse grown apple saplings. However, when using the entire root system as a proxy for overall plant and root development, only a slow succession over several weeks was observed, mostly within the rhizosphere (Fig. III-3). It must be noted that the plants did not grow much during this period and thus the lack of more pronounced differences over time may be associated with rather small changes in plant morphology. Due to these rather small changes in the root-associated microbiota over time, effects superimposed by above ground pathogen infections or PHPP applications are more likely to be identified, even over time.

2. Above ground pathogen infection causes changes in the root-associated bacterial community structure

Pathogen infections remain one of the most significant obstacles to maintaining regular and reliable food systems, as they cause an estimated loss of around 20% to 40% of crop production (Savary et al. 2019). They decrease the yield and quality of crops by infecting various parts of the plant, including fruits, leaves, stems, and roots. The resulting changes in morphology and metabolism lead to direct and indirect effects on plant fitness and growth, thereby affecting the yield. Direct effects of e.g., leaf or root pathogens include the necrosis of infected tissue, resulting in reduced photoassimilation or nutrient uptake rates. Indirect effects include changes in plant metabolism, induction of plant defense mechanisms, and the recruitment of beneficial bacteria (Gao et al. 2021). Whether through direct or indirect effects, pathogen infections can induce local effects on the associated microbiota at the infection site, as demonstrated for e.g. root pathogens in the rhizosphere (Solís-García et al. 2020), or leaf pathogens in the phyllosphere (Li et al. 2022). In addition, there is evidence that especially root and systemic pathogens can impact the plant-associated microbiota through the modulation of plant-microbiome signaling pathways in their hosts (Liu et al. 2023). However, little is known about the interference of above ground pathogen infections with plant-microbiome signaling pathways and their effect on the root-associated microbiota. Potential factors that induce changes in plant-microbiome signaling pathways are alterations in root exudation or a stress-induced loss of control over the plant-associated microbiome. Thus, to analyze changes induced by foliar pathogen infection, the root-associated bacterial community of greenhouse-grown apple saplings was assessed over time after infection with two different pathogens (manuscript 2). Two of the most economically important foliar pathogens were used: the ascomycete fungi *Venturia inaequalis* and *Podosphaera leucotricha*, which cause apple scab and powdery mildew of apple, respectively. Infection, especially with *P. leucotricha*, led to significant disease symptoms such as mycelium cover of the entire leaf area, which ultimately induced leaf senescence. The resulting changes in plant metabolism are likely to lead to changes in the root-associated microbiota. Due to the results in the spatial analysis, the root-associated microbiota was again divided into the loosely and tightly associated microbiota.

Overall, foliar pathogen infections induced fewer changes in the root-associated microbiota than anticipated, even under strong disease pressure. Alpha diversity was slightly increased in the rhizosphere in some samples after pathogen infection. A higher diversity has been hypothesized to maintain plant productivity under changing environmental conditions (Wagg et al. 2011), which was possibly also seen here under disease stress. Alternatively, high disease pressure could lead to stress-induced loss of control over the plant-associated microbiome, resulting in the growth of opportunistic pathogenic bacteria. Changes in alpha diversity are not consistently reported in the literature with some studies (i) showing no changes in diversity upon above (González-Escobedo et al. 2021) or below ground pathogen infection (Kim et al. 2021), (ii) lower diversity upon infection (Yang et al. 2020), or (iii) an increased richness in the rhizosphere of diseased plants (Tender et al. 2016), similar to our results. In contrast, a study with symptomatic apple orchard trees has shown that using amplicon sequencing no significant differences in alpha diversity were detectable whereas a decrease was observed when using a shotgun metagenomic approach (Muñoz-Ramírez et al. 2024). Similarly, pathogen infection led to fewer differences in community composition than anticipated. In the present study, even with progressing severe disease symptoms, no significant differences were found between healthy and diseased plants when comparing them directly at individual sampling timepoints (Fig. III-3). Only when taking the temporal dynamics into account, a pathogen dependent difference in succession over time was observed. The bacterial communities of the pathogen infected plants became most distinct at the later sampling times compared to earlier timepoints and thus with increasing disease severity, whereas healthy plants developed and maintained a balanced and more stable bacterial community over time. (Fig. III-4). The same observation was made in a subsequent, similar greenhouse trial (Fig. III-8). Thus, the effects on the community of the root-associated microbiota of an above ground pathogen infection are likely to increase over time as the infection progresses. This partially confirms the hypothesis that the root-associated bacterial community is affected by above ground pathogen infection, even though the responses remained weaker than expected. When taking previous studies into account, pathogen infections appear to cause most changes locally in the infection site associated microbiota, i.e., root pathogens in the rhizosphere and foliar pathogens in the endosphere. Further, these previously reported locally induced changes by root or systemic pathogens were

more pronounced compared to remote (i.e. foliar) infection sites described in this study. This larger effect is likely caused by the proximity and a more intimate relation between the pathogens and locally associated microbiota as part of the plant holobiont. Thus, the ability of the plant to alter its associated microbiota and even more so to recruit a beneficial microbiota likely does depend on the kind of pathogen and the level of infection and does not come along with prominent changes in the root microbiota. However, though the kind of pathogen had a pronounced effect, this is likely more related to disease severity, as *P. leucotricha* caused more damage to the plants than *V. inaequalis*. Overall, these results support the initial hypothesis that the plant mediated responses have a temporal dynamic in dependence on disease severity.

Differential abundance analysis was used to determine whether specific taxa, especially potential plant beneficial taxa, were recruited upon pathogen infection. Indeed, several taxa were increased in relative abundance between severely infected and healthy plants, especially in the rhizosphere (Fig. III-9). Two genera known to include strains with plant beneficial properties showed an increased relative abundance in the diseased group, an unclassified member of *Bacilli*, as well as *Devosia* (Akinrinlola et al. 2018; Chhetri et al. 2022). However, most of the identified taxa have been shown to benefit from different organic carbon compounds in the rhizosphere and are thus likely to respond to alterations in rhizodeposition. For example, *Bryobacter* and "*Candidatus* Solibacter" have been shown to be closely related to soil carbon metabolism (Yu et al. 2016; Wang et al. 2019; Li et al. 2020; Zhou et al. 2021), while *Ammoniphilus*, *Mizugakiibacter*, *Acidothermus* and *Alicyclobacillus* have been shown to utilize various plant-derived carbon compounds such as glucose, cellulose or oxalacetate (Sahin 2003; Talia et al. 2012; Liao et al. 2019; Li et al. 2020). In addition, the cellulolytic taxon *Acidothermus* was increased in relative abundance in the rhizosphere at high disease severity levels, indicating that microbes might begin to actively hydrolyze root tissue. The increase in alpha diversity, succession in community composition and increase in relative abundance of taxa associated with the conversion of plant-derived carbon compounds in the rhizosphere is likely due to differences in plant defense levels and root exudation, caused by changes in plant metabolism. With progressing disease severity, the plant likely loses its ability to maintain its preferred microbiome in the rhizosphere, potentially leading to an increase of opportunistic pathogenic or even

cellulolytic bacteria from the surrounding soil. These findings deserve further attention in future studies.

A field trial with consistent pathogen inoculations was technically not feasible and thus, naturally occurring infection events were monitored over two years. Unfortunately, the two sampling years (2018 and 2019) provided unfavorable weather conditions for foliar pathogens and thus disease levels were relatively low. However, single incidences with high levels of below ground pathogen infection were observed in the spatio-temporal variation orchard trial (manuscript 1). Here, the root pathogen "*Candidatus* Phytoplasma" could reach up to 24.4% in relative abundance, yet no above ground signs of infection were visible at the sampling date. Due to the dominance of this pathogen according to its relative abundance, the infected trees had a significantly different community composition compared to healthy trees. Furthermore, it is conceivable that the pathogen infection led to a restructuring of the native community in infected trees, as seen in previous studies (Bulgari et al. 2014; Trivedi et al. 2012; Trivedi et al. 2016). Taken together, this suggests that the impact on the root-associated microbiota through the infection with a root pathogen was much larger than the impact of a foliar infection, leading to the conclusion that pathogen infections cause most changes in the local infection site associated microbiota, as outlined above.

3. Above ground plant health protecting product applications lead to inconsistent and non-treatment specific responses in the root-associated microbiota

The use of plant health protecting products is essential in agriculture as they help control pests, diseases, and weeds that can significantly reduce crop yields and quality. By effectively managing these threats, PHPPs contribute to increased agricultural productivity and food security, ensuring a stable supply of food for a growing population. The effects of PHPP application on biodiversity, soil health and the plant-associated microbiome have become of increasing interest over the last few decades (Zhou et al. 2025). Two recent comprehensive reviews have highlighted that PHPP applications can potentially have hugely varying effects on the plant associated microbial communities (Ramakrishnan et al. 2021; Yu et al. 2023). The effects on the root-associated microbiota largely depend on numerous factors, for example on the kind of product (e.g., whether it is a fungicide, herbicide, insecticide, biological product, etc.), the mode of action and the chemical properties of the active ingredient, or whether it is applied

directly into the soil. While some applications led to no significant effects in the community composition in a previous study (Fournier et al. 2020), some products caused minor and transient effects on the microbial abundance and community structure. Some applications, however, caused significant alterations in the composition of the root-associated microbiota, also with varying effect degrees (Huang et al. 2021; Nettles et al. 2016; Kusstatscher et al. 2020; Deng et al. 2019; Qian et al. 2018; Chen et al. 2017). In some cases, the induction of organic acid secretion and other root responses have also been observed, which is considered a major mechanism by which the plant modulates its associated microbiota (Wen et al. 2020; Qu et al. 2021). Overall, PHPP application can lead to varying effects without being consistent and predictable. It is imperative to note that almost all current studies have analyzed the effects of direct PHPP amendment into the soil or as seed treatment, disregarding potential plant mediated effects on the root-associated microbiome upon remote, i.e. above ground PHPP application. In addition, previous studies have mostly investigated single products under a defined single set of conditions, disregarding variation by external factors such as host, sampling time or soil and root type. Thus, the effects of above ground applications of various plant health protecting products were studied with the two model systems apple and strawberry in trials with varying experimental conditions. Soils from two apple orchards and a strawberry farm were used for the apple and strawberry pot trials, respectively. Additionally, the root system of strawberry plants was divided into fine and thick roots and analyzed separately to account for differences in root exudation between root types. Different concentrations of up to five products with different modes of action were used. They included two fully systemic (Aliette and Movento) and a locally systemic product (Luna Privilege) from different chemical groups that can target either phytopathogenic fungi, nematodes or insect pests, as well as products containing living microbes (Bactiva and Serenade). Based on the previous literature, the fully systemic products were expected to have a larger impact especially on the endophytes compared to the locally systemic or biological products.

Overall, no consistent deterministic effect of either PHPP application or application mode was observed across the different trials. The same product applied to different soils did not change the root-associated microbiota in a deterministic way, neither did the various products applied to the same soil. Additionally, no similar trends were observed after application in both apple saplings and strawberries, as well as between

the two root types of strawberry plants. Alpha and beta diversity indices, as well as differential abundance analyses were used to compare the different treatments, resulting in only few treatments showing significant changes compared to the untreated control (Figs. III-7, IV-1 A, IV-2 A, IV-3, IV-4). No increase in alpha diversity was observed after any application. In contrast, diversity decreased in the rhizosphere of the strawberry plants after application with the systemic products Movento and Aliette, confirming previous studies that reported a transiently lowered diversity when PHPPs were in direct contact with the soil or rhizosphere microbiome (Liang et al. 2020; Qu et al. 2021; Deng et al. 2019; Wan et al. 2017; Fournier et al. 2020; Onwona-Kwakye et al. 2020). It also gives evidence to the hypothesis that different products have different effects on the root-associated microbiota with the systemic products having a more pronounced effect. Similarly to the alpha diversity results, only a few comparisons between treatments and the control showed significant differences in community composition using PERMANOVA and PCA on the beta diversity: a weak impact on the endophytic bacterial community composition was observed after application with the systemic product Movento and the biological product Serenade. Those effects were only observed one week after the final of three weekly applications but not anymore after two weeks after the final application. It is thus likely that without a continuous application of products, the composition of the root-associated microbiota returns quickly to that of an untreated profile. This kind of transient effect, even upon direct exposure of the microbiota to PHPPs, has been shown before (Wan et al. 2017; Fournier et al. 2020). Wan et al. (2017) reported that biopesticide applications altered the bacterial community composition only up to ten days after application, similar to our study, where we observed a difference up to seven days after the last application, but not after 14 days, even when applying products at increased dosage. Differential abundance analysis also showed that no taxa were consistently enriched or depleted in (i) at least two trials, (ii) at different dose concentrations tested or (iii) in the different strawberry root types sampled. These results further indicate that above ground PHPP applications, even at twice the recommended concentration rate, have no significant persistent deterministic impact on the bacterial community composition, corroborating previous studies (Fournier et al. 2020; Wan et al. 2017). As outlined above, this thesis is the first study that analysed plant mediated effects of PHPP application with respect to external factors such as host, sampling time as well as soil and root type. Though effects were

overall weaker than anticipated, they are in line with the initial hypothesis, that those weak and transient effects were indeed product and compartment specific and should be considered in the context of microbiome management strategies. In this context, the results from this thesis justify further research to draw recommendations for crop management practices, future PHPP development and the use of biologicals.

4. Application-related undirected changes in bacterial community composition follow the Anna Karenina Principle

Though PHPP applications did not result in deterministic changes in bacterial community composition, they often led to an increase in dispersion of the community composition. This increase in dispersion was caused by specific changes of the individual replicates, resulting in more diverse compositions within each treatment group. These findings are well in line with the 'Anna Karenina Principle' (AKP). This principle states that certain stressors have stochastic rather than deterministic effects on community composition because these stressors reduce the ability of the host to regulate its microbial community composition (Zaneveld et al. 2017). It has already been applied in human and animal microbiomes and has recently been proposed to conceptualize plant dysbiosis as a transitory loss of host capacity to regulate its microbiota (Ma 2020; Zaneveld et al. 2017; Arnault et al. 2022). It is possible that the repeated application of certain PHPPs to young plants can induce a minor stress that led to those rather undirected and stochastic changes in the root-associated microbiota. There are various indications that these application-related changes were indeed within the AKP framework: (i) the increase in dispersion can be measured using PERMDISP, which showed significantly increased dispersions after applications in both strawberry and apple associated communities. An increase in dispersion was also be observed in other studies investigating potential PHPP effects (Fournier et al. 2020; Deng et al. 2019; Kusstatscher et al. 2020). While those did not investigate potential AKP effects, a visual assessment of ordination plots indicates a higher dispersion of replicate samples after PHPP applications. (ii) Another proposed characteristic of the AKP effect is a decreased alpha diversity, which was also observed in numerous cases after product application e.g. in the strawberry trial. (iii) The discrepancy between the PERMANOVA results and the differential abundance analyses are another indication that PHPP causes stochastic rather than deterministic changes. The lack of significantly enriched

or depleted taxa, even under significantly different community compositions between treatments and control, further points to AKP effects (Zaneveld et al. 2017). (iv) In addition to the already mentioned indicators, Arnault et al. (2022) also proposed to use betaNTI to detect a possible AKP effect. The betaNTI is an index used to measure the phylogenetic turnover between pairs of communities and can be used to indicate whether communities assemblies occurred more stochastically or deterministically (Chai et al. 2016). Besides betaNTI, the indices betaNRI and tNST have been used to examine the full phylogenetic turnover and to estimate the ecological stochasticity, respectively (Stegen et al. 2012; Ning et al. 2019). Though only a few comparisons showed minor but statistically significant differences in those indices, stochasticity was surprisingly decreased after PHPP applications in those comparisons. However, these results would still be in line with one of the three different AKP models proposed by Zaneveld et al. (2017). Under this proposed model, the perturbation (the PHPP application) alters the microbiome deterministically, but the extent of the alteration is stochastic, depending on the severity of the stressor. In the case of a severe stressor, the community compositions of stressed hosts would be similar to each other, whereas the community compositions of mildly stressed hosts would display a dispersion increase. The increase in dispersion (shown by PERMDISP) with deterministic changes (shown by betaNTI and tNST) suggests that above ground PHPP application can sometimes act as a mild stress factor under the concept of AKP. Within this study and out of the products tested, the two systemic products Aliette and Movento displayed the highest impact on the root-associated microbiota, specifically in the endosphere. These results further support the hypothesis that the systemic products have a more pronounced effect on the root-associated microbiota. However, it remains unclear whether this impact was due to a plant mediated signal or whether this impact was due to the direct contact of the product with the local microbiota due to the systemic distribution of the products from shoot system to the roots. The observation that the endosphere showed more pronounced effects compared to the rhizosphere would support this. In contrast to the potential effect caused by its systemic distribution, Aliette has also been shown to induce plant defenses, which might be another driver of the deterministic changes in the endosphere (Petré et al. 2015). Thus, further research is needed to answer this question. Nevertheless, these results are in line with previous studies that have provided evidence for deterministic changes in community composition due to direct

effects of pesticide applications into the soil or onto seeds (Nettles et al. 2016; Huang et al. 2021). In conclusion, above ground PHPP applications can have a minor but transient effect on the root-associated microbiome and lead to mild AKP effects. During their application, they can potentially act as an influence factor on the plant, which can in some cases mildly and transiently affect the plant's ability to maintain a stable root-associated microbiome community. Without continuous application the plant is quickly able to fully restore its homeostatic root-associated microbiome. Furthermore, no differences in plant morphological and physiological characteristics were observed, suggesting that PHPP application and the observed mild AKP effects have no negative impacts on plant health.

5. Fungicide application reverts pathogen induced bacterial community compositional shifts

In agricultural systems, plant health protecting products are either applied preventatively or as a curative measurement after pathogen infection. So far within this thesis, only the individual effects, i.e. presence of PHPPs or pathogens, have been analyzed, discounting their potential combined effect when both affect the plant simultaneously, as would be expected under field conditions. Thus, the last part of this thesis combines the experiences and results from the previous trials and focusses on the combined effect of both on the root-associated microbiota. As previously described, above ground pathogen infections have been shown to lead to increasing plant mediated effects in the rhizosphere with progressing disease severity, likely resulting in the plant losing its ability to maintain its preferred microbiome. PHPP applications on the other hand have been shown to lead to small and undirected changes in the root-associated bacterial community. A combined occurrence of pathogen pressure and product stress might increase the overall stress on the plant, leading to an even more distinct root-associated microbiota of infected, PHPP treated plants. In contrast, the curative application of a PHPP application might reduce the infection impact to some extent, resulting in a microbiota profile more similar to that of a healthy plant. To test this hypothesis, greenhouse-grown apple saplings were first treated with a preventative fungicide treatment, as often done under field conditions, later inoculated with *P. leucotricha* and treated again curatively with a fungicide when disease symptoms were moderately severe and expected to cause changes in the root-associated microbiota. The systemic

fungicide Aliette was used here, as it has been shown to decrease the disease severity of *P. leucotricha* in apples (Petré et al. 2015) while inducing weak transient changes in the root-associated microbiota, as outlined above (Fournier et al. 2020). The microbial communities of treated plants were compared to those of healthy control plants and to those of infected plants which did not receive any product application.

As expected, a single preventative application did not cause any significant changes in the root-associated microbiota. However, and most strikingly, the curative application caused a shift in the root-associated microbiota of diseased plants towards a profile similar to the one of healthy and untreated plants, as hypothesized. This shift was pronounced more in the rhizosphere than in the endosphere. This is particularly interesting, as the rhizosphere microbiota was more affected by the external stress factor compared to that of the endosphere in the first pathogen inoculation trial as well. Though those changes occurred more easily after the external stress, the plant is also quick to readjust its microbiome, likely by the process of rhizodeposition. However, as outlined above, the quantity and composition of rhizodeposits were not analyzed in this thesis, and thus this remains speculative but deserves further attention. Interestingly, the reversion to the profile of a healthy plant was possible with the dead fungal mycelium still being present on and inside the leaf tissue, suggesting that not the presence of a pathogen *per se* is the stressor leading to changes in the microbiota, but rather suggests that unfavorable physiological sink-source relationship and/or plant immune responses triggered at distal infection sites by a living pathogen are the major driving force for changes of the root-associated microbiota Alleviating the disease pressure and thereby reducing the stress from pathogen infection likely helps the plant regain its ability to modulate the rhizospheric bacterial community and return it to a more preferable profile. This is supported by tNST analysis, which shows that the curative Aliette treatment caused an increase in the deterministic assembly process (Suppl. Fig. X-1).

Overall, it is well conceivable that infections with foliar pathogens are a larger stress factor compared to the application of PHPPs, especially in the context of the AKP. While the largest differences were found to be between the infected but untreated samples to the healthy samples (thus infection being a severe stressor), a single PHPP application led to a significant decrease in disease severity and subsequently caused the microbiota to return to a healthy state. Considering the AKP effect to be transitory

loss of the host capacity to regulate its microbiota, relieving the disease stress had a larger effect than the mild stress from the PHPP application itself. Overall, these results support the model of AKP effects instead of the ‘cry-for-help’ principle, in which the plant specifically recruits beneficial microbes to overcome certain stress effects, which would then lead to deterministic changes in the root-associated microbiome. Under this principle, deterministic changes in community composition would be displayed in significant changes in community composition (using PERMANOVA), significant changes in relative abundance of specific taxa (using differential abundance analysis), as well a shift towards a deterministic community assembly (using tNST, Suppl. Fig. X-1) .

These results are particularly interesting in the context of good agricultural practice. The use of PHPPs has been a subject of ongoing discussion due to its extensive use in industrial agriculture and due to environmental concerns. Concerns include undesired effects on soil health, leaching of products into groundwater and long-lasting contamination of agricultural soils with pesticide residues (Larramendy and Soloneski 2019; Walder et al. 2022). In contrast, crop protection through the means of PHPP applications significantly increases yield and thus leads to various environmental benefits. Through the increased yield, less agricultural area, labor and energy is needed for the same amount of calories (La Cruz et al. 2023). The development of new PHPPs with high curative potential and their correct use under disease stress and within the context of an integrated pest management is thereby likely helping the plant to maintain its preferred bacterial community in both the rhizo- and endosphere, therewith possibly contributing to yield stability and minimizing certain environmental detrimental effects. However, neither yield nor crop quality were determined in this thesis and thus the observation that a curative PHPP application helped the plant regain an unimpaired root-associated microbiota profile is not yet directly linked to increased yield and crop quality. To fill this knowledge gap, further research is needed and justified.

VI. Publication bibliography

Ahmed, A.; Hasnain, S. (2014): Auxins as One of the Factors of Plant Growth Improvement by Plant Growth Promoting Rhizobacteria. In *Pol J Microbiol* 63 (3), Article 10.33073/pjm-2014-035, pp. 261–266. DOI: 10.33073/pjm-2014-035.

Akinrinlola, R. J.; Yuen, G. Y.; Drijber, R. A.; Adesemoye, A. O. (2018): Evaluation of *Bacillus s*trains for plant growth promotion and predictability of efficacy by in-vitro physiological traits. In *Int. J. Microbiol.* 2018, p. 5686874. DOI: 10.1155/2018/5686874.

Alcaraz, L. D.; Peimbert, M.; Barajas, H. R.; Dorantes-Acosta, A. E.; Bowman, J. L.; Arteaga-Vázquez, M. A. (2018): *Marchantia* liverworts as a proxy to plants' basal microbiomes. In *Sci. Rep.* 8 (1), p. 12712. DOI: 10.1038/s41598-018-31168-0.

Ali, M. A.; Naveed, M.; Mustafa, A.; Abbas, A. (2017): The good, the bad, and the ugly of rhizosphere microbiome. In : Probiotics and Plant Health: Springer, Singapore, pp. 253–290. Available online at https://link.springer.com/chapter/10.1007/978-981-10-3473-2_11.

Amir, A.; McDonald, D. et al. (2017): Deblur rapidly resolves single-nucleotide community sequence patterns. In *mSystems* 2 (2). DOI: 10.1128/msystems.00191-16.

Amos, B.; Walters, D. T. (2006): Maize root biomass and net rhizodeposited carbon: an analysis of the literature. In *Soil Sci. Soc. Am. J.* 70 (5), pp. 1489–1503. DOI: 10.2136/sssaj2005.0216.

Anderson, M. J. (2006): Distance-based tests for homogeneity of multivariate dispersions. In *Biometrics* 62 (1), pp. 245–253. DOI: 10.1111/j.1541-0420.2005.00440.x.

Araujo, R.; Dunlap, C.; Barnett, S.; Franco, C. M. M. (2019): Decoding wheat endosphere-rhizosphere microbiomes in *Rhizoctonia solani*-infested soils challenged by *Streptomyces* biocontrol agents. In *Front. Plant Sci.* 10, p. 1038. DOI: 10.3389/fpls.2019.01038.

Arnault, G.; Mony, C.; Vandenkoornhuyse, P. (2022): Plant microbiota dysbiosis and the Anna Karenina Principle. In *Trends Plant Sci.* DOI: 10.1016/j.tplants.2022.08.012.

Ayer, K. M.; Strickland, D. A.; Choi, M.; Cox, K. D. (2021): Optimizing the integration of a biopesticide (*Bacillus subtilis* QST 713) with a single-site fungicide (Benzovindiflupyr) to reduce reliance on synthetic multisite fungicides (Captan and Mancozeb) for management of apple scab. In *Plant Dis.* 105 (11), pp. 3545–3553. DOI: 10.1094/PDIS-02-21-0426-RE.

Backer, R. G. M.; Saeed, W.; Seguin, P.; Smith, D. L. (2017): Root traits and nitrogen fertilizer recovery efficiency of corn grown in biochar-amended soil under greenhouse conditions. In *Plant Soil* 415 (1-2), pp. 465–477. DOI: 10.1007/s11104-017-3180-6.

Badri, D. V.; Vivanco, J. M. (2009): Regulation and function of root exudates. In *Plant Cell Environ.* 32 (6), pp. 666–681. DOI: 10.1111/j.1365-3040.2009.01926.x.

Bahram, M.; Kohout, P.; Anslan, S.; Harend, H.; Abarenkov, K.; Tedersoo, L. (2016): Stochastic distribution of small soil eukaryotes resulting from high dispersal and drift in a local environment. In *ISME J.* 10 (4), pp. 885–896. DOI: 10.1038/ismej.2015.164.

Bailly, A.; Weisskopf, L. (2017): Mining the volatilomes of plant-associated microbiota for new biocontrol solutions. In *Front. Microbiol.* 8, p. 1638. DOI: 10.3389/fmicb.2017.01638.

Bais, H. P.; Weir, T. L.; Perry, L. G.; Gilroy, S.; Vivanco, J. M. (2006): The role of root exudates in rhizosphere interactions with plants and other organisms. In *Annu. Rev. Plant Biol.* 57, pp. 233–266. DOI: 10.1146/annurev.arplant.57.032905.105159.

Becker, M. F.; Hellmann, M.; Knief, C. (2022): Spatio-temporal variation in the root-associated microbiota of orchard-grown apple trees. In *Environ. Microbiomes* 17 (1), p. 31. DOI: 10.1186/s40793-022-00427-z.

Becker, M. F.; Klueken, A. M.; Knief, C. (2023): Effects of above ground pathogen infection and fungicide application on the root-associated microbiota of apple saplings. In *Environ. Microbiome* 18 (1), p. 43. DOI: 10.1186/s40793-023-00502-z.

Beckers, B.; Beeck, M. op de; Weyens, N.; Boerjan, W.; Vangronsveld, J. (2017): Structural variability and niche differentiation in the rhizosphere and endosphere bacterial microbiome of field-grown poplar trees. In *Microbiome* 5 (1), p. 25. DOI: 10.1186/s40168-017-0241-2.

Beckers, B.; Beeck, M. op de; Weyens, N.; van Acker, R.; van Montagu, M.; Boerjan, W.; Vangronsveld, J. (2016): Lignin engineering in field-grown poplar trees affects the endosphere bacterial microbiome. In *PNAS* 113 (8), pp. 2312–2317. DOI: 10.1073/pnas.1523264113.

Berendsen, R. L.; Pieterse, C. M. J.; Bakker, P. A. H. M. (2012): The rhizosphere microbiome and plant health. In *Trends Plant Sci.* 17 (8), pp. 478–486. DOI: 10.1016/j.tplants.2012.04.001.

Berendsen, R. L.; Vismans, G. et al. (2018): Disease-induced assemblage of a plant-beneficial bacterial consortium. In *ISME J.* 12 (6), pp. 1496–1507. DOI: 10.1038/s41396-018-0093-1.

Berg, G.; Smalla, K. (2009): Plant species and soil type cooperatively shape the structure and function of microbial communities in the rhizosphere. In *FEMS Microbiol. Ecol.* 68 (1), pp. 1–13. DOI: 10.1111/j.1574-6941.2009.00654.x.

Berrie, A. M.; Xu, X. M. (2003): Managing apple scab (*Venturia inaequalis*) and powdery mildew (*Podosphaera leucotricha*) using Adem™. In *Int. J. Pest Manag* 49 (3), pp. 243–249. DOI: 10.1080/0967087031000101089.

Birch, A. N. E.; Begg, G. S.; Squire, G. R. (2011): How agro-ecological research helps to address food security issues under new IPM and pesticide reduction policies for global crop production systems. In *J. Exp. Bot.* 62 (10), pp. 3251–3261. DOI: 10.1093/jxb/err064.

Blakemore, R. (2018): Non-Flat Earth Recalibrated for Terrain and Topsoil. In *Soil Syst.* 2 (4), p. 64. DOI: 10.3390/soilsystems2040064.

Blaustein, R. A.; Lorca, G. L.; Meyer, J. L.; Gonzalez, C. F.; Teplitski, M. (2017): Defining the Core Citrus Leaf- and Root-Associated Microbiota: Factors Associated with Community Structure and Implications for Managing Huanglongbing (Citrus Greening) Disease. In *Appl. Environ. Microbiol.* 83 (11). DOI: 10.1128/AEM.00210-17.

Bokulich, Nicholas A.; Dillon, Matthew; Bolyen, Evan; Kaehler, Benjamin D.; Huttley, Gavin A.; Caporaso, J. Gregory (2018): q2-sample-classifier: machine-learning tools for microbiome classification and regression.

Bolyen, E.; Rideout, J. R. et al. (2019): Reproducible, interactive, scalable and extensible microbiome data science using QIIME 2. In *Nat. Biotechnol.* 37 (8), pp. 852–857. DOI: 10.1038/s41587-019-0209-9.

Bonkowski, M.; Tarkka, M. et al. (2021): Spatiotemporal dynamics of maize (*Zea mays* L.) root growth and its potential consequences for the assembly of the rhizosphere microbiota. In *Front. Microbiol.* 12, p. 619499. DOI: 10.3389/fmicb.2021.619499.

Bowen, J. K.; Mesarich, C. H.; Bus, V. G. M.; Beresford, R. M.; Plummer, K. M.; Templeton, M. D. (2011): *Venturia inaequalis*: the causal agent of apple scab. In *Mol. Plant Pathol* 12 (2), pp. 105–122. DOI: 10.1111/j.1364-3703.2010.00656.x.

Brader, G.; Compant, S.; Vescio, K.; Mitter, B.; Trognitz, F.; Ma, L.-J.; Sessitsch, A. (2017): Ecology and genomic insights into plant-pathogenic and plant-nonpathogenic endophytes. In *Annu. Rev. Phytopathol.* 55, pp. 61–83. DOI: 10.1146/annurev-phyto-080516-035641.

Bulgarelli, D.; Rott, M. et al. (2012): Revealing structure and assembly cues for *Arabidopsis* root-inhabiting bacterial microbiota. In *Nature* 488 (7409), p. 91.

Bulgarelli, D.; Schlaeppi, K.; Spaepen, S.; van Themaat, E. V. L.; Schulze-Lefert, P. (2013): Structure and functions of the bacterial microbiota of plants. In *Annu. Rev. Plant Biol.* 64, pp. 807–838. DOI: 10.1146/annurev-arplant-050312-120106.

Bulgari, D.; Bozkurt, A. I.; Casati, P.; Çağlayan, K.; Quaglino, F.; Bianco, P. A. (2012): Endophytic bacterial community living in roots of healthy and '*Candidatus* Phytoplasma mali'-infected apple (*Malus domestica*, Borkh.) trees. In *Antonie Van Leeuwenhoek* 102 (4), pp. 677–687. DOI: 10.1007/s10482-012-9766-3.

Bulgari, D.; Casati, P.; Quaglino, F.; Bianco, P. A. (2014): Endophytic bacterial community of grapevine leaves influenced by sampling date and phytoplasma infection process. In *BMC Microbiol.* 14 (1), p. 198. DOI: 10.1186/1471-2180-14-198.

Busby, P. E.; Soman, C. et al. (2017): Research priorities for harnessing plant microbiomes in sustainable agriculture. In *PLoS Biol.* 15 (3), e2001793. DOI: 10.1371/journal.pbio.2001793.

Busi, R.; Vila-Aiub, M. M. et al. (2013): Herbicide-resistant weeds: from research and knowledge to future needs. In *Evolutionary applications* 6 (8), pp. 1218–1221. DOI: 10.1111/eva.12098.

Callahan, B. J.; McMurdie, P. J.; Rosen, M. J.; Han, A. W.; Johnson, A. J. A.; Holmes, S. P. (2016): DADA2: High-resolution sample inference from Illumina amplicon data. In *Nat. Methods* 13 (7), pp. 581–583. DOI: 10.1038/nmeth.3869.

Caputo, F.; Nicoletti, F.; Picione, F. D. L.; Manici, L. M. (2015): Rhizospheric changes of fungal and bacterial communities in relation to soil health of multi-generation apple orchards. In *Biol. Control* 88, pp. 8–17. DOI: 10.1016/j.biocontrol.2015.04.019.

Carisse, O.; Bernier, J. (2002): Effect of environmental factors on growth, pycnidial production and spore germination of *Microsphaeropsis* isolates with biocontrol potential against apple scab. In *Mycol. Res.* 106 (12), pp. 1455–1462. DOI: 10.1017/S0953756202006858.

Carisse, O.; Dewdney, M. (2002): A review of non-fungicidal approaches for the control of apple scab. In *Phytoprotection* 83 (1), pp. 1–29. DOI: 10.7202/706226ar.

Carrión, V. J.; Perez-Jaramillo, J. et al. (2019): Pathogen-induced activation of disease-suppressive functions in the endophytic root microbiome. In *Science* 366 (6465), pp. 606–612. DOI: 10.1126/science.aaw9285.

Chai, Y.; Yue, M. et al. (2016): Patterns of taxonomic, phylogenetic diversity during a long-term succession of forest on the Loess Plateau, China: insights into assembly process. In *Sci. Rep.* 6, p. 27087. DOI: 10.1038/srep27087.

Chandler, D.; Bailey, A. S.; Tatchell, G. M.; Davidson, G.; Greaves, J.; Grant, W. P. (2011): The development, regulation and use of biopesticides for integrated pest management. In *Philos. Trans. R. Soc. Lond. B. Biol. Sci.* 366 (1573), pp. 1987–1998. DOI: 10.1098/rstb.2010.0390.

Chaparro, J. M.; Badri, D. V.; Vivanco, J. M. (2014): Rhizosphere microbiome assemblage is affected by plant development. In *ISME J.* 8 (4), pp. 790–803. DOI: 10.1038/ismej.2013.196.

Chapelle, E.; Mendes, R.; Bakker, P. A. H. M.; Raaijmakers, J. M. (2016): Fungal invasion of the rhizosphere microbiome. In *ISME J.* 10 (1), pp. 265–268. DOI: 10.1038/ismej.2015.82.

Chen, S.; Li, X.; Lavoie, M.; Jin, Y.; Xu, J.; Fu, Z.; Qian, H. (2017): Diclofop-methyl affects microbial rhizosphere community and induces systemic acquired resistance in rice. In *J. Environ. Sci.* 51, pp. 352–360. DOI: 10.1016/j.jes.2016.06.027.

Chen, S.; Waghmode, T. R.; Sun, R.; Kuramae, E. E.; Hu, C.; Liu, B. (2019): Root-associated microbiomes of wheat under the combined effect of plant development and nitrogen fertilization. In *Microbiome* 7 (1), p. 136. DOI: 10.1186/s40168-019-0750-2.

Chhetri, G.; Kim, I.; Kang, M.; Kim, J.; So, Y.; Seo, T. (2022): *Devosia rhizoryzae* sp. nov., and *Devosia oryziradicis* sp. nov., novel plant growth promoting members of the genus *Devosia*, isolated from the rhizosphere of rice plants. In *J. Microbiol.* 60 (1), pp. 1–10. DOI: 10.1007/s12275-022-1474-8.

Ciancio, A.; Pieterse, C. M. J.; Mercado-Blanco, J. (2019): Editorial: Harnessing useful rhizosphere microorganisms for pathogen and pest biocontrol - Second Edition. In *Front. Microbiol.* 10, p. 1935. DOI: 10.3389/fmicb.2019.01935.

Cloutier, M.; Chatterjee, D.; Elango, D.; Cui, J.; Bruns, M. A.; Chopra, S. (2021): Sorghum root flavonoid chemistry, cultivar, and frost stress effects on rhizosphere bacteria and fungi. In *Phytobiomes J.* 5 (1), pp. 39–50. DOI: 10.1094/PBIOMES-01-20-0013-FI.

Coenye, T.; Vandamme, P. (2003): Diversity and significance of *Burkholderia* species occupying diverse ecological niches. In *Environ. Microbiol.* 5 (9), pp. 719–729. DOI: 10.1046/j.1462-2920.2003.00471.x.

Compant, S.; Reiter, B.; Sessitsch, A.; Nowak, J.; Clément, C.; Ait Barka, E. (2005): Endophytic colonization of Vitis vinifera L. by plant growth-promoting bacterium *Burkholderia* sp. strain PsJN. In *Appl. Environ. Microbiol.* 71 (4), pp. 1685–1693. DOI: 10.1128/AEM.71.4.1685-1693.2005.

Corkley, I.; Fraaije, B.; Hawkins, N. (2022): Fungicide resistance management: Maximizing the effective life of plant protection products. In *Plant Pathol.* 71 (1), pp. 150–169. DOI: 10.1111/ppa.13467.

Costa, R.; Götz, M.; Mrotzek, N.; Lottmann, J.; Berg, G.; Smalla, K. (2006): Effects of site and plant species on rhizosphere community structure as revealed by molecular analysis of microbial guilds. In *FEMS Microbiol. Ecol.* 56 (2), pp. 236–249. DOI: 10.1111/j.1574-6941.2005.00026.x.

Cregger, M. A.; Veach, A. M.; Yang, Z. K.; Crouch, M. J.; Vilgalys, R.; Tuskan, G. A.; Schadt, C. W. (2018): The *Populus* holobiont: dissecting the effects of plant niches and genotype on the microbiome. In *Microbiome* 6 (1), p. 31. DOI: 10.1186/s40168-018-0413-8.

Damalas, C.; Koutroubas, S. (2018): Current status and recent developments in biopesticide use. In *Agriculture* 8 (1), p. 13. DOI: 10.3390/agriculture8010013.

Damos, P.; Colomar, L.-A. E.; Ioriatti, C. (2015): Integrated fruit production and pest management in Europe: the apple case study and how far we are from the original concept? In *Insects* 6 (3), pp. 626–657. DOI: 10.3390/insects6030626.

Dangl, J. L.; Jones, J. D. (2001): Plant pathogens and integrated defence responses to infection. In *Nature* 411 (6839), pp. 826–833. DOI: 10.1038/35081161.

Dara, S. K. (2016): Managing strawberry pests with chemical pesticides and non-chemical alternatives. In *Int. J. Fruit Sci.* 16 (sup1), pp. 129–141. DOI: 10.1080/15538362.2016.1195311.

Deakin, G.; Tilston, E. L.; Bennett, J.; Passey, T.; Harrison, N.; Fernández-Fernández, F.; Xu, X. (2018): Spatial structuring of soil microbial communities in commercial apple orchards. In *Appl. Soil Ecol.* DOI: 10.1016/j.apsoil.2018.05.015.

Deng, S.; Wipf, H. M.-L.; Pierroz, G.; Raab, T. K.; Khanna, R.; Coleman-Derr, D. (2019): A plant growth-promoting microbial soil amendment dynamically alters the strawberry root bacterial microbiome. In *Sci. Rep.* 9 (1), p. 17677. DOI: 10.1038/s41598-019-53623-2.

Dessaux, Y.; Grandclément, C.; Faure, D. (2016): Engineering the rhizosphere. In *Trends Plant Sci.* 21 (3), pp. 266–278. DOI: 10.1016/j.tplants.2016.01.002.

Deyett, E.; Rolshausen, P. E. (2020): Endophytic microbial assemblage in grapevine. In *FEMS Microbiol. Ecol.* 96 (5). DOI: 10.1093/femsec/fiaa053.

Dinelli, G.; Bonetti, A.; Marotti, I.; Minelli, M.; Busi, S.; Catizone, P. (2007): Root exudation of diclofop-methyl and triasulfuron from foliar-treated durum wheat and ryegrass. In *Weed Res.* 47 (1), pp. 25–33. DOI: 10.1111/j.1365-3180.2007.00549.x.

Donn, S.; Kirkegaard, J. A.; Perera, G.; Richardson, A. E.; Watt, M. (2015): Evolution of bacterial communities in the wheat crop rhizosphere. In *Environ. Microbiol.* 17 (3), pp. 610–621. DOI: 10.1111/1462-2920.12452.

Dove, N. C.; Veach, A. M.; Muchero, W.; Wahl, T.; Stegen, J. C.; Schadt, C. W.; Cregger, M. A. (2021): Assembly of the *Populus* Microbiome Is Temporally Dynamic and Determined by Selective and Stochastic Factors. In *mSphere* 6 (3), e0131620. DOI: 10.1128/msphere.01316-20.

Dudenhöffer, J.-H.; Scheu, S.; Jousset, A. (2016): Systemic enrichment of antifungal traits in the rhizosphere microbiome after pathogen attack. In *J. Ecol.* 104 (6), pp. 1566–1575. DOI: 10.1111/1365-2745.12626.

Edwards, J.; Johnson, C. et al. (2015): Structure, variation, and assembly of the root-associated microbiomes of rice. In *PNAS* 112 (8), E911-20. DOI: 10.1073/pnas.1414592112.

Eissenstat, D. M.; Bauerle, T. L.; Comas, L. H.; Lakso, A. N.; Neilsen, D.; Neilsen, G. H.; Smart, D. R. (2006): Seasonal patterns of root growth in relation to shoot phenology in grape and apple. In *Acta Hortic.* (721), pp. 21–26. DOI: 10.17660/actahortic.2006.721.1.

El-Sheikh, E.-S. A.; Li, D.; Hamed, I.; Ashour, M.-B.; Hammock, B. D. (2023): Residue Analysis and Risk Exposure Assessment of Multiple Pesticides in Tomato and Strawberry and Their Products from Markets. In *Foods (Basel, Switzerland)* 12 (10). DOI: 10.3390/foods12101936.

Ely, C. S.; Smets, B. F. (2019): Guild Composition of Root-Associated Bacteria Changes with Increased Soil Contamination. In *Microb. Ecol.* 78 (2), pp. 416–427. DOI: 10.1007/s00248-019-01326-6.

Epron, D.; Ngao, J. et al. (2011): Seasonal variations of belowground carbon transfer assessed by in situ $^{13}CO_2$ pulse labelling of trees. In *Biogeosciences* 8 (5), pp. 1153–1168. DOI: 10.5194/bg-8-1153-2011.

Eurostat (2007): The use of plant protection products in the European Union. Data 1992-2003. European Communities.

Eurostat (2022): Agri-environmental indicator - consumption of pesticides. Agriculture, forestry and fishery statistics. Available online at https://ec.europa.eu/eurostat/statistics-explained/index.php?title=Agri-environmental_indicator_-_consumption_of_pesticides#Analysis_at_EU_and_country_level, checked on 8/30/2020.

Fan, K.; Cardona, C. et al. (2017): Rhizosphere-associated bacterial network structure and spatial distribution differ significantly from bulk soil in wheat crop fields. In *Soil Biol. Biochem.* 113, pp. 275–284. DOI: 10.1016/j.soilbio.2017.06.020.

FAOSTAT (2019): Apple production in 2018; Crops/World Regions/Production Quantity. With assistance of UN Food & Agriculture Organization. Edited by Statistics Division, checked on 11/30/2020.

FAOSTAT (2020): Annual strawberry and apple production. Edited by United Nations Statistics Division. Available online at https://data.un.org/, checked on 8/29/2022.

FAOSTAT (2022): Agricultural Production Statistics. 2000–2021. Analytical Brief 60, checked on 6/29/2023.

Fenibo, E. O.; Ijoma, G. N.; Matambo, T. (2021): Biopesticides in sustainable agriculture: a critical sustainable development driver governed by green chemistry principles. In *Front. Sustain. Food Syst.* 5, Article 619058. DOI: 10.3389/fsufs.2021.619058.

Fernández-González, A. J.; Villadas, P. J.; Gómez-Lama Cabanás, C.; Valverde-Corredor, A.; Belaj, A.; Mercado-Blanco, J.; Fernández-López, M. (2019): Defining the root endosphere and rhizosphere microbiomes from the World Olive Germplasm Collection. In *Sci. Rep.* 9 (1), p. 20423. DOI: 10.1038/s41598-019-56977-9.

Fessia, A.; Barra, P.; Barros, G.; Nesci, A. (2022): Could *Bacillus* biofilms enhance the effectivity of biocontrol strategies in the phyllosphere? In *J. Appl. Microbiol.* 133 (4), pp. 2148–2166. DOI: 10.1111/jam.15596.

Fierer, N. (2017): Embracing the unknown: disentangling the complexities of the soil microbiome. In *Nat. Rev. Microbiol.* 15 (10), pp. 579–590. DOI: 10.1038/nrmicro.2017.87.

Finkel, O. M.; Castrillo, G.; Herrera Paredes, S.; Salas González, I.; Dangl, J. L. (2017): Understanding and exploiting plant beneficial microbes. In *Curr. Opin. Plant. Biol.* 38, pp. 155–163. DOI: 10.1016/j.pbi.2017.04.018.

Fournier, B.; Pereira Dos Santos, S. et al. (2020): Impact of a synthetic fungicide (fosetyl-Al and propamocarb-hydrochloride) and a biopesticide (*Clonostachys rosea*) on soil bacterial, fungal, and protist communities. In *Sci. Total Environ.* 738, p. 139635. DOI: 10.1016/j.scitotenv.2020.139635.

Fowler, D.; Steadman, C. E. et al. (2015): Effects of global change during the 21st century on the nitrogen cycle. In *Atmos. Chem. Phys.* 15 (24), pp. 13849–13893. DOI: 10.5194/acp-15-13849-2015.

Frank, A. C.; Saldierna Guzmán, J. P.; Shay, J. E. (2017): Transmission of bacterial endophytes. In *Microorganisms* 5 (4), p. 70. DOI: 10.3390/microorganisms5040070.

Franke-Whittle, I. H.; Manici, L. M.; Insam, H.; Stres, B. (2015): Rhizosphere bacteria and fungi associated with plant growth in soils of three replanted apple orchards. In *Plant Soil* 395 (1-2), pp. 317–333. DOI: 10.1007/s11104-015-2562-x.

Frindte, K.; Pape, R.; Werner, K.; Löffler, J.; Knief, C. (2019): Temperature and soil moisture control microbial community composition in an arctic-alpine ecosystem along elevational and micro-topographic gradients. In *ISME J.* 13 (8), pp. 2031–2043. DOI: 10.1038/s41396-019-0409-9.

Galindo-Castañeda, T.; Hartmann, M.; Lynch, J. P. (2024): Location: root architecture structures rhizosphere microbial associations. In *J. Exp. Bot.* 75 (2), pp. 594–604. DOI: 10.1093/jxb/erad421.

Gao, M.; Xiong, C. et al. (2021): Disease-induced changes in plant microbiome assembly and functional adaptation. In *Microbiome* 9 (1), p. 187. DOI: 10.1186/s40168-021-01138-2.

Garbeva, P.; van Elsas, J. D.; van Veen, J. A. (2008): Rhizosphere microbial community and its response to plant species and soil history. In *Plant Soil* 302 (1-2), pp. 19–32. DOI: 10.1007/s11104-007-9432-0.

German, D. P.; Chacon, S. S.; Allison, S. D. (2011): Substrate concentration and enzyme allocation can affect rates of microbial decomposition. In *Ecology* 92 (7), pp. 1471–1480. DOI: 10.1890/10-2028.1.

Glick, Bernard R. (2015): Beneficial plant-bacterial interactions. Cham, Heidelberg: Springer (Life sciences).

González-Escobedo, R.; Muñoz-Castellanos, L. N.; Muñoz-Ramirez, Z. Y.; López, C. G.; Avila-Quezada, G. D. (2021): Microbial community analysis of rhizosphere of healthy and wilted pepper (*Capsicum Annuum* L.) in an organic farming system. Preprint.

Gottel, N. R.; Castro, H. F. et al. (2011): Distinct microbial communities within the endosphere and rhizosphere of *Populus deltoides* roots across contrasting soil types. In *Appl. Environ. Microbiol.* 77 (17), pp. 5934–5944. DOI: 10.1128/AEM.05255-11.

Gu, Y.; Banerjee, S.; Dini-Andreote, F.; Xu, Y.; Shen, Q.; Jousset, A.; Wei, Z. (2022): Small changes in rhizosphere microbiome composition predict disease outcomes earlier than pathogen density variations. In *ISME J.* DOI: 10.1038/s41396-022-01290-z.

Gu, Y.; Wang, Y. et al. (2017): Long-term Fertilization Structures Bacterial and Archaeal Communities along Soil Depth Gradient in a Paddy Soil. In *Front. Microbiol.* 8, p. 1516. DOI: 10.3389/fmicb.2017.01516.

Guyonnet, J. P.; Guillemet, M. et al. (2018): Plant nutrient resource use strategies shape active rhizosphere microbiota through root exudation. In *Front. Plant Sci.* 9, p. 1662. DOI: 10.3389/fpls.2018.01662.

Hacquard, S.; Schadt, C. W. (2015): Towards a holistic understanding of the beneficial interactions across the *Populus* microbiome. In *New Phytol.* 205 (4), pp. 1424–1430. DOI: 10.1111/nph.13133.

Haichar, F. E. Z.; Marol, C. et al. (2008): Plant host habitat and root exudates shape soil bacterial community structure. In *ISME J.* 2 (12), pp. 1221–1230. DOI: 10.1038/ismej.2008.80.

Haichar, F. E. Z.; Santaella, C.; Heulin, T.; Achouak, W. (2014): Root exudates mediated interactions belowground. In *Soil Biol. Biochem.* 77, pp. 69–80. DOI: 10.1016/j.soilbio.2014.06.017.

Hakim, S.; Naqqash, T. et al. (2021): Rhizosphere Engineering with Plant Growth-Promoting Microorganisms for Agriculture and Ecological Sustainability. In *Front. Sustain. Food Syst.* 5, Article 617157. DOI: 10.3389/fsufs.2021.617157.

Hartmann, A.; Schmid, M.; van Tuinen, D.; Berg, G. (2009): Plant-driven selection of microbes. In *Plant Soil* 321 (1-2), pp. 235–257. DOI: 10.1007/s11104-008-9814-y.

Hassan, M. K.; McInroy, J. A.; Kloepper, J. W. (2019): The interactions of rhizodeposits with plant growth-promoting rhizobacteria in the rhizosphere: A review. In *Agriculture* 9 (7), p. 142.

Henry, A.; Doucette, W.; Norton, J.; Bugbee, B. (2007): Changes in crested wheatgrass root exudation caused by flood, drought, and nutrient stress. In *J. Environ. Qual.* 36 (3), pp. 904–912. DOI: 10.2134/jeq2006.0425sc.

Herridge, D. F.; Peoples, M. B.; Boddey, R. M. (2008): Global inputs of biological nitrogen fixation in agricultural systems. In *Plant Soil* 311 (1-2), pp. 1–18. DOI: 10.1007/s11104-008-9668-3.

Hiltner, L. (1904): Über neuere Erfahrungen und Probleme auf dem Gebiete der Bodenbakteriologie unter besonderer Berücksichtigung der Gründüngung und Brache. In *Arbeiten der Deutschen Landwirtschaftlichen Gesellschaft* 98, pp. 59–78.

Hoffland, E.; Findenegg, G. R.; Nelemans, J. A. (1989): Solubilization of rock phosphate by rape. In *Plant Soil* 113 (2), pp. 161–165. DOI: 10.1007/BF02280176.

Huang, W.; Lu, Y.; Chen, L.; Sun, D.; An, Y. (2021): Impact of pesticide/fertilizer mixtures on the rhizosphere microbial community of field-grown sugarcane. In *3 Biotech* 11 (5), p. 210. DOI: 10.1007/s13205-021-02770-3.

Husaini, Amjad M.; Neri, Davide (Eds.) (2016): Strawberry. Growth, development and diseases. Wallingford, Boston: CABI.

Ikenaga, M.; Sakai, M. (2014): Application of locked nucleic acid (LNA) oligonucleotide – PCR clamping technique to selectively PCR amplify the SSU rRNA genes of bacteria in investigating the plant-associated community structures. In *Microbes Environ.* 29 (3), pp. 286–295. DOI: 10.1264/jsme2.ME14061.

Issa, A.; Esmaeel, Q. et al. (2018): Impacts of *Paraburkholderia phytofirmans* Strain PsJN on Tomato (*Lycopersicon esculentum* L.) Under High Temperature. In *Front. Plant Sci.* 9, p. 1397. DOI: 10.3389/fpls.2018.01397.

Jacoby, R. P.; Kopriva, S. (2019): Metabolic niches in the rhizosphere microbiome: new tools and approaches to analyse metabolic mechanisms of plant-microbe nutrient exchange. In *J. Exp. Bot.* 70 (4), pp. 1087–1094. DOI: 10.1093/jxb/ery438.

Jari Oksanen; F. Guillaume Blanchet et al. (2019): vegan: Community Ecology Package. R package version 2.5-4. Available online at https://CRAN.R-project.org/package=vegan.

Jeschke, Peter; Krämer, Wolfgang; Schirmer, Ulrich; Witschel, Matthias (2013): Modern Methods in Crop Protection Research. 1., Auflage. Weinheim: Wiley-VCH.

Jha, G.; Thakur, K.; Thakur, P. (2009): The Venturia apple pathosystem: pathogenicity mechanisms and plant defense responses. In *J. Biomed. Biotechnol.* 2009, p. 680160. DOI: 10.1155/2009/680160.

Jiang, J.; Song, Z.; Yang, X.; Mao, Z.; Nie, X.; Guo, H.; Peng, X. (2017): Microbial community analysis of apple rhizosphere around Bohai Gulf. In *Sci. Rep.* 7 (1), p. 8918. DOI: 10.1038/s41598-017-08398-9.

Jones, D. L.; Hinsinger, P. (2008): The rhizosphere: complex by design. In *Plant Soil* 312 (1-2), pp. 1–6. DOI: 10.1007/s11104-008-9774-2.

Jones, D. L.; Nguyen, C.; Finlay, R. D. (2009): Carbon flow in the rhizosphere: carbon trading at the soil–root interface. In *Plant Soil* 321 (1-2), pp. 5–33. DOI: 10.1007/s11104-009-9925-0.

Jordan E Bisanz (2018): qiime2R: Importing QIIME2 artifacts and associated data into R sessions. Version v0.99. Available online at https://github.com/jbisanz/qiime2R.

Jousset, A.; Becker, J.; Chatterjee, S.; Karlovsky, P.; Scheu, S.; Eisenhauer, N. (2014): Biodiversity and species identity shape the antifungal activity of bacterial communities. In *Ecology* 95 (5), pp. 1184–1190. DOI: 10.1890/13-1215.1.

Jousset, A.; Rochat, L.; Lanoue, A.; Bonkowski, M.; Keel, C.; Scheu, S. (2011): Plants respond to pathogen infection by enhancing the antifungal gene expression of root-associated bacteria. In *Mol. Plant-Microbe Interact.* 24 (3), pp. 352–358. DOI: 10.1094/MPMI-09-10-0208.

Kawasaki, A.; Donn, S.; Ryan, P. R.; Mathesius, U.; Devilla, R.; Jones, A.; Watt, M. (2016): Microbiome and Exudates of the Root and Rhizosphere of *Brachypodium distachyon*, a Model for Wheat. In *PLoS One* 11 (10), e0164533. DOI: 10.1371/journal.pone.0164533.

Keel, S. G.; Campbell, C. D. et al. (2012): Allocation of carbon to fine root compounds and their residence times in a boreal forest depend on root size class and season. In *New Phytol.* 194 (4), pp. 972–981. DOI: 10.1111/j.1469-8137.2012.04120.x.

Khajuria, Y. P.; Kaul, S.; Wani, A. A.; Dhar, M. K. (2018): Genetics of resistance in apple against *Venturia inaequalis* (Wint.) Cke. In *Tree Genet. Genomes.* 14 (2). DOI: 10.1007/s11295-018-1226-4.

Kielak, A. M.; Cipriano, M. A. P.; Kuramae, E. E. (2016): Acidobacteria strains from subdivision 1 act as plant growth-promoting bacteria. In *Arch. Microbiol.* 198 (10), pp. 987–993. DOI: 10.1007/s00203-016-1260-2.

Kim, S.-H.; Cho, G.; Lee, S. in; Kim, D.-R.; Kwak, Y.-S. (2021): Comparison of bacterial community of healthy and *Erwinia amylovora* infected apples. In *Plant Pathol. J.* 37 (4), pp. 396–403. DOI: 10.5423/PPJ.NT.04.2021.0062.

Kloepper, J. W.; Ryu, C.-M.; Zhang, S. (2004): Induced Systemic Resistance and Promotion of Plant Growth by *Bacillus* spp. In *Phytopathology* 94 (11), pp. 1259–1266. DOI: 10.1094/PHYTO.2004.94.11.1259.

Kolton, M.; Frenkel, O.; Elad, Y.; Cytryn, E. (2014): Potential role of Flavobacterial gliding-motility and type IX secretion system complex in root colonization and plant defense. In *Mol. Plant-Microbe Interact.* 27 (9), pp. 1005–1013. DOI: 10.1094/MPMI-03-14-0067-R.

Krämer, Wolfgang (Ed.) (2012): Modern crop protection compounds. 2nd, rev. and enl. ed. Weinheim: [Chichester]. Available online at https://onlinelibrary.wiley.com/doi/book/10.1002/9783527644179.

Kraska, T. (2019): Niederschlaege und Temperaturen CKA 2018 (50°37'23.25160"N,6°59'25.87563"E,224.674). University of Bonn. Available online at https://www.cka.uni-bonn.de/standort/niederschlaege-und-temperaturen-cka-2018-1, updated on 3/23/2021, checked on 4/29/2021.

Kumar, A.; Dubey, A. (2020): Rhizosphere microbiome: Engineering bacterial competitiveness for enhancing crop production. In *J. Adv. Res.* 24, pp. 337–352. DOI: 10.1016/j.jare.2020.04.014.

Kusstatscher, P.; Wicaksono, W. A.; Thenappan, D. P.; Adam, E.; Müller, H.; Berg, G. (2020): Microbiome management by biological and chemical treatments in maize is linked to plant health. In *Microorganisms* 8 (10), p. 1506. DOI: 10.3390/microorganisms8101506.

La Cruz, V. Y. V. de; Tantriani; Cheng, W.; Tawaraya, K. (2023): Yield gap between organic and conventional farming systems across climate types and sub-types: A meta-analysis. In *Agricultural Systems* 211, p. 103732. DOI: 10.1016/j.agsy.2023.103732.

La Fuente Cantó, C. de; Simonin, M.; King, E.; Moulin, L.; Bennett, M. J.; Castrillo, G.; Laplaze, L. (2020): An extended root phenotype: the rhizosphere, its formation and impacts on plant fitness. In *Plant J.* 103 (3), pp. 951–964. DOI: 10.1111/tpj.14781.

Lahti, L.; Shetty, S.; Salojarvi, J. (2017): microbiome: Bioconductor.

Lang, Gregory A. (Ed.) (2019): Achieving sustainable cultivation of temperate zone tree fruits and berries. Cambridge, Philadelphia, PA: Burleigh Dodds Science Publishing (Burleigh Dodds series in agricultural science, number 54). Available online at https://www.taylorfrancis.com/books/9780429275548.

Larramendy, Marcelo L.; Soloneski, Sonia (2019): Pesticides. Use and Misuse and Their Impact in the Environment: BoD – Books on Demand.

Leroch, M.; Kretschmer, M.; Hahn, M. (2011): Fungicide Resistance Phenotypes of *Botrytis cinerea* Isolates from Commercial Vineyards in South West Germany. In *J. Phytopathol.* 159 (1), pp. 63–65. DOI: 10.1111/j.1439-0434.2010.01719.x.

Lewis, K. A.; Tzilivakis, J.; Warner, D. J.; Green, A. (2016): An international database for pesticide risk assessments and management. In *Human and Ecological Risk Assessment: An International Journal* 22 (4), pp. 1050–1064. DOI: 10.1080/10807039.2015.1133242.

Li, H.-B.; Singh, R. K.; Singh, P.; Song, Q.-Q.; Xing, Y.-X.; Yang, L.-T.; Li, Y.-R. (2017): Genetic Diversity of Nitrogen-Fixing and Plant Growth Promoting *Pseudomonas* Species Isolated from Sugarcane Rhizosphere. In *Front. Microbiol.* 8, p. 1268. DOI: 10.3389/fmicb.2017.01268.

Li, P.-D.; Zhu, Z.-R.; Zhang, Y.; Xu, J.; Wang, H.; Wang, Z.; Li, H. (2022): The phyllosphere microbiome shifts toward combating melanose pathogen. In *Microbiome* 10 (1), p. 56. DOI: 10.1186/s40168-022-01234-x.

Li, R.; Liu, J.; Li, J.; Sun, C. (2020): Straw input can parallelly influence the bacterial and chemical characteristics of maize rhizosphere. In *Environ. Pollut. Bioavailability* 32 (1), pp. 1–11. DOI: 10.1080/26395940.2019.1710260.

Li, X.; Rui, J.; Mao, Y.; Yannarell, A.; Mackie, R. (2014): Dynamics of the bacterial community structure in the rhizosphere of a maize cultivar. In *Soil Biol. Biochem.* 68, pp. 392–401. DOI: 10.1016/j.soilbio.2013.10.017.

Liang, Q.; Yan, Z.; Li, X. (2020): Influence of the herbicide haloxyfop-R-methyl on bacterial diversity in rhizosphere soil of *Spartina alterniflora*. In *Ecotoxicol. Environ. Saf.* 194, p. 110366. DOI: 10.1016/j.ecoenv.2020.110366.

Liao, H.; Li, Y.; Yao, H. (2019): Biochar amendment stimulates utilization of plant-derived carbon by soil bacteria in an intercropping system. In *Front. Microbiol.* 10, p. 1361. DOI: 10.3389/fmicb.2019.01361.

Lin, H.; Peddada, S. D. (2020): Analysis of compositions of microbiomes with bias correction. In *Nat. Commun.* 11 (1), p. 3514. DOI: 10.1038/s41467-020-17041-7.

Liu, C.; Cui, Y.; Li, X.; Yao, M. (2021a): microeco: an R package for data mining in microbial community ecology. In *FEMS Microbiol. Ecol.* 97 (2). DOI: 10.1093/femsec/fiaa255.

Liu, H.; Li, J.; Carvalhais, L. C.; Percy, C. D.; Prakash Verma, J.; Schenk, P. M.; Singh, B. K. (2021b): Evidence for the plant recruitment of beneficial microbes to suppress soil-borne pathogens. In *New Phytol.* 229 (5), pp. 2873–2885. DOI: 10.1111/nph.17057.

Liu, H.; Wang, J.; Delgado-Baquerizo, M.; Zhang, H.; Li, J.; Singh, B. K. (2023): Crop microbiome responses to pathogen colonisation regulate the host plant defence. In *Plant and Soil* 488 (1-2), pp. 393–410. DOI: 10.1007/s11104-023-05981-0.

Lombardi, N.; Vitale, S. et al. (2018): Root exudates of stressed plants stimulate and attract *Trichoderma s*oil fungi. In *Mol. Plant-Microbe Interact.* 31 (10), pp. 982–994. DOI: 10.1094/MPMI-12-17-0310-R.

Luck, J.; Spackman, M.; Freeman, A.; Tre¸bicki, P.; Griffiths, W.; Finlay, K.; Chakraborty, S. (2011): Climate change and diseases of food crops. In *Plant Pathol.* 60 (1), pp. 113–121. DOI: 10.1111/j.1365-3059.2010.02414.x.

Lumibao, C. Y.; Kimbrough, E. R.; Day, R. H.; Conner, W. H.; Krauss, K. W.; Van Bael, S. A. (2020): Divergent biotic and abiotic filtering of root endosphere and rhizosphere soil fungal communities along ecological gradients. In *FEMS Microbiol. Ecol.* 96 (7), Article fiaa124. DOI: 10.1093/femsec/fiaa124.

Lundberg, D. S.; Lebeis, S. L. et al. (2012): Defining the core *Arabidopsis thaliana* root microbiome. In *Nature* 488 (7409), pp. 86–90. DOI: 10.1038/nature11237.

Lynch, J. M.; Leij, F. de (2001): Rhizosphere. In *e LS*. DOI: 10.1038/npg.els.0000403.

Ma, X.; Mau, M.; Sharbel, T. F. (2018): Genome Editing for Global Food Security. In *Trends in Biotechnology* 36 (2), pp. 123–127. DOI: 10.1016/j.tibtech.2017.08.004.

Ma, Z. S. (2020): Testing the Anna Karenina principle in human microbiome-associated diseases. In *iScience* 23 (4), p. 101007. DOI: 10.1016/j.isci.2020.101007.

Maarastawi, S. A.; Frindte, K.; Geer, R.; Kröber, E.; Knief, C. (2018): Temporal dynamics and compartment specific rice straw degradation in bulk soil and the rhizosphere of maize. In *Soil Biol. Biochem.* 127, pp. 200–212. DOI: 10.1016/j.soilbio.2018.09.028.

Macey, M. C.; Pratscher, J.; Crombie, A. T.; Murrell, J. C. (2020): Impact of plants on the diversity and activity of methylotrophs in soil. In *Microbiome* 8 (1), p. 31. DOI: 10.1186/s40168-020-00801-4.

MacHardy, W. E. (1996): Apple scab: biology, epidemiology, and management. In *Apple scab: biology, epidemiology, and management*.

Mahnkopp-Dirks, F.; Radl, V.; Kublik, S.; Gschwendtner, S.; Schloter, M.; Winkelmann, T. (2021): Molecular barcoding reveals the genus *Streptomyces* as associated root endophytes of apple (*Malus domestica*) plants grown in soils affected by apple replant disease. In *Phytobiomes J.* 5 (2), pp. 177–189. DOI: 10.1094/PBIOMES-07-20-0053-R.

Maitra, D.; Roy, B.; Choudhury, S. S.; Mitra, A. K. (2022): Dynamics of Soil Microbiome and Its Role in Sustainable Agriculture. In Junaid Ahmad Malik (Ed.): Microbial and Biotechnological Interventions in Bioremediation and Phytoremediation. Cham: Springer, pp. 27–55.

Mao, Y.; Li, X.; Smyth, E. M.; Yannarell, A. C.; Mackie, R. I. (2014): Enrichment of specific bacterial and eukaryotic microbes in the rhizosphere of switchgrass (*Panicum virgatum* L.) through root exudates. In *Environ. Microbiol. Rep.* 6 (3), pp. 293–306. DOI: 10.1111/1758-2229.12152.

Marchand, P. A. (2023): Evolution of plant protection active substances in Europe: the disappearance of chemicals in favour of biocontrol agents. In *Environ. Sci. Pollut. Res. Int.* 30 (1), pp. 1–17. DOI: 10.1007/s11356-022-24057-7.

Martin, M. (2011): Cutadapt removes adapter sequences from high-throughput sequencing reads. In *EMBnet j.* 17 (1), p. 10. DOI: 10.14806/ej.17.1.200.

Martino, C.; Morton, J. T.; Marotz, C. A.; Thompson, L. R.; Tripathi, A.; Knight, R.; Zengler, K. (2019): A novel sparse compositional technique reveals microbial perturbations. In *mSystems* 4 (1). DOI: 10.1128/mSystems.00016-19.

Marupakula, S.; Mahmood, S.; Jernberg, J.; Nallanchakravarthula, S.; Fahad, Z. A.; Finlay, R. D. (2017): Bacterial microbiomes of individual ectomycorrhizal *Pinus sylvestris* roots are shaped by soil horizon and differentially sensitive to nitrogen addition. In *Environ. Microbiol.* 19 (11), pp. 4736–4753. DOI: 10.1111/1462-2920.13939.

Mazzola, M.; Hewavitharana, S. S.; Strauss, S. L. (2015): Brassica seed meal soil amendments transform the rhizosphere microbiome and improve apple production through resistance to pathogen reinfestation. In *Phytopathology* 105 (4), pp. 460–469. DOI: 10.1094/PHYTO-09-14-0247-R.

McIlroy, S. J.; Nielsen, P. H. (2014): The Family *Saprospiraceae*. In Eugene Rosenberg, Edward F. DeLong, Stephen Lory, Erko Stackebrandt, Fabiano Thompson (Eds.): The Prokaryotes: Other Major Lineages of Bacteria and The Archaea. Berlin, Heidelberg: Springer Science+ Business Media, pp. 863–889.

McMurdie, P. J.; Holmes, S. (2013): phyloseq. An R package for reproducible interactive analysis and graphics of microbiome census data. In *PLoS One* 8 (4), e61217. DOI: 10.1371/journal.pone.0061217.

Mendes, R.; Garbeva, P.; Raaijmakers, J. M. (2013): The rhizosphere microbiome: significance of plant beneficial, plant pathogenic, and human pathogenic microorganisms. In *FEMS Microbiol. Rev.* 37 (5), pp. 634–663. DOI: 10.1111/1574-6976.12028.

Mendes, R.; Kruijt, M. et al. (2011): Deciphering the rhizosphere microbiome for disease-suppressive bacteria. In *Science* 332 (6033), pp. 1097–1100. DOI: 10.1126/science.1203980.

Micallef, S. A.; Shiaris, M. P.; Colón-Carmona, A. (2009): Influence of *Arabidopsis thaliana* accessions on rhizobacterial communities and natural variation in root exudates. In *J. Exp. Bot.* 60 (6), pp. 1729–1742. DOI: 10.1093/jxb/erp053.

Michalecka, M.; Masny, S.; Leroy, T.; Puławska, J. (2018): Population structure of *Venturia inaequalis*, a causal agent of apple scab, in response to heterogeneous apple tree cultivation. In *BMC Evolutionary Biology* 18 (1), p. 5. DOI: 10.1186/s12862-018-1122-4.

Miliute, I.; Buzaite, O.; Gelvonauskiene, D.; Sasnauskas, A.; Stanys, V.; Baniulis, D. (2016): Plant growth promoting and antagonistic properties of endophytic bacteria isolated from domestic apple. In *Zemdirbyste* 103 (1). DOI: 10.13080/z-a.2016.103.010.

Morales-Quintana, L.; Waite, J. M.; Kalcsits, L.; Torres, C. A.; Ramos, P. (2020): Sun injury on apple fruit: Physiological, biochemical and molecular advances, and future challenges. In *Scientia Horticulturae* 260, p. 108866. DOI: 10.1016/j.scienta.2019.108866.

Muñoz-Ramírez, Z. Y.; González-Escobedo, R. et al. (2024): Exploring Microbial Rhizosphere Communities in Asymptomatic and Symptomatic Apple Trees Using Amplicon Sequencing and Shotgun Metagenomics. In *Agronomy* 14 (2), p. 357. DOI: 10.3390/agronomy14020357.

Munoz-Ucros, J.; Zwetsloot, M. J.; Cuellar-Gempeler, C.; Bauerle, T. L. (2021): Spatiotemporal patterns of rhizosphere microbiome assembly: From ecological theory to agricultural application. In *J. Appl. Ecol.* 58 (5), pp. 894–904. DOI: 10.1111/1365-2664.13850.

National Institute of Food and Agriculture (2023): Researchers Helping Protect Crops From Pests. Edited by Lori Tyler Gula. Available online at https://www.nifa.usda.gov/about-nifa/blogs/researchers-helping-protect-crops-pests, updated on 8/2/2023, checked on 8/2/2023.

Nettles, R.; Watkins, J. et al. (2016): Influence of pesticide seed treatments on rhizosphere fungal and bacterial communities and leaf fungal endophyte communities in maize and soybean. In *Appl. Soil Ecol.* 102, pp. 61–69. DOI: 10.1016/j.apsoil.2016.02.008.

Ning, D.; Deng, Y.; Tiedje, J. M.; Zhou, J. (2019): A general framework for quantitatively assessing ecological stochasticity. In *PNAS* 116 (34), pp. 16892–16898. DOI: 10.1073/pnas.1904623116.

Oerke, E.-C.; Dehne, H.-W. (2004): Safeguarding production—losses in major crops and the role of crop protection. In *Crop Protection* 23 (4), pp. 275–285. DOI: 10.1016/j.cropro.2003.10.001.

Onwona-Kwakye, M.; Plants-Paris, K.; Keita, K.; Lee, J.; van Brink, P. J. den; Hogarh, J. N.; Darkoh, C. (2020): Pesticides decrease bacterial diversity and abundance of irrigated rice fields. In *Microorganisms* 8 (3). DOI: 10.3390/microorganisms8030318.

Padhi, E. M. T.; Maharaj, N. et al. (2019): Metabolome and Microbiome Signatures in the Roots of Citrus Affected by Huanglongbing. In *Phytopathology* 109 (12), pp. 2022–2032. DOI: 10.1094/PHYTO-03-19-0103-R.

Pausch, J.; Kuzyakov, Y. (2018): Carbon input by roots into the soil: Quantification of rhizodeposition from root to ecosystem scale. In *Global change biology* 24 (1), pp. 1–12. DOI: 10.1111/gcb.13850.

Pertot, I.; Caffi, T. et al. (2017): A critical review of plant protection tools for reducing pesticide use on grapevine and new perspectives for the implementation of IPM in viticulture. In *Crop Protection* 97, pp. 70–84. DOI: 10.1016/j.cropro.2016.11.025.

Pervaiz, Z. H.; Contreras, J. et al. (2020): Root microbiome changes with root branching order and root chemistry in peach rhizosphere soil. In *Rhizosphere* 16, p. 100249. DOI: 10.1016/j.rhisph.2020.100249.

Petré, R.; Labourdette, G. et al. (2015): Fosetyl-Al (Aliette®), a plant defense enhancer with good efficacy on bacteria and on ascomycetes in apples and pears. In *Acta Hortic.* (1094), pp. 431–438. DOI: 10.17660/actahortic.2015.1094.56.

Pramanik, M. H. R.; Nagai, M.; Asao, T.; Matsui, Y. (2000): Effects of temperature and photoperiod on phytotoxic root exudates of cucumber (*Cucumis sativus*) in hydroponic culture. In *J. Chem. Ecol.* 26 (8), pp. 1953–1967. DOI: 10.1023/A:1005509110317.

Proctor, C.; He, Y. (2017): Quantifying root extracts and exudates of sedge and shrub in relation to root morphology. In *Soil Biol. Biochem.* 114, pp. 168–180. DOI: 10.1016/j.soilbio.2017.07.006.

Prosser, J. I.; Head, I. M.; Stein, L. Y. (2014): The Family *Nitrosomonadaceae*. In Eugene Rosenberg, Edward F. DeLong, Stephen Lory, Erko Stackebrandt, Fabiano Lopes Thompson (Eds.): The Prokaryotes. *Alphaproteobacteria* and *betaproteobacteria*. Fourth edition. Berlin: SpringerReference, pp. 901–918.

Qian, H.; Zhu, Y.; Chen, S.; Jin, Y.; Lavoie, M.; Ke, M.; Fu, Z. (2018): Interacting effect of diclofop-methyl on the rice rhizosphere microbiome and denitrification. In *Pestic. Biochem. Physiol.* 146, pp. 90–96. DOI: 10.1016/j.pestbp.2018.03.002.

Qu, Q.; Li, Y. et al. (2021): Effects of S-metolachlor on wheat (*Triticum aestivum* L.) seedling root exudates and the rhizosphere microbiome. In *J. Hazard. Mater.* 411, p. 125137. DOI: 10.1016/j.jhazmat.2021.125137.

Quast, C.; Pruesse, E. et al. (2013): The SILVA ribosomal RNA gene database project: improved data processing and web-based tools. In *Nucleic Acids Res.* 41 (Database issue), D590-6. DOI: 10.1093/nar/gks1219.

R Core Team (2021): R: A language and environment for statistical computing. Version 4.1.2. Vienna, Austria. Available online at http://www.R-project.org.

Rahman, M.; Mukta, J. A. et al. (2018): Chitosan biopolymer promotes yield and stimulates accumulation of antioxidants in strawberry fruit. In *PLoS One* 13 (9), e0203769. DOI: 10.1371/journal.pone.0203769.

Ramakrishnan, B.; Maddela, N. R.; Venkateswarlu, K.; Megharaj, M. (2021): Linkages between plant rhizosphere and animal gut environments: Interaction effects of pesticides with their microbiomes. In *Environ. Adv.* 5, p. 100091. DOI: 10.1016/j.envadv.2021.100091.

Raynaud, X.; Nunan, N. (2014): Spatial ecology of bacteria at the microscale in soil. In *PLoS One* 9 (1), e87217. DOI: 10.1371/journal.pone.0087217.

Riaz, U.; Murtaza, G.; Anum, W.; Samreen, T.; Sarfraz, M.; Nazir, M. Z. (2021): Plant Growth-Promoting Rhizobacteria (PGPR) as Biofertilizers and Biopesticides. In : Microbiota and Biofertilizers: Springer, Cham, pp. 181–196. Available online at https://link.springer.com/chapter/10.1007/978-3-030-48771-3_11.

Ricroch, A.; Harwood, W. et al. (2016): Challenges facing European agriculture and possible biotechnological solutions. In *Crit. Rev. Biotechnol.* 36 (5), pp. 875–883. DOI: 10.3109/07388551.2015.1055707.

Ritchie, H.; Roser, M. (2020): Agricultural production. OurWorldindata.org. Available online at https://ourworldindata.org/agricultural-production, checked on 1/25/2022.

Rizaludin, M. S.; Stopnisek, N.; Raaijmakers, J. M.; Garbeva, P. (2021): The chemistry of stress: understanding the 'cry for help' of plant roots. In *Metabolites* 11 (6). DOI: 10.3390/metabo11060357.

Rocca, J. D.; Simonin, M.; Blaszczak, J. R.; Ernakovich, J. G.; Gibbons, S. M.; Midani, F. S.; Washburne, A. D. (2018): The microbiome stress project: toward a global meta-analysis of environmental stressors and their effects on microbial communities. In *Front. Microbiol.* 9, p. 3272. DOI: 10.3389/fmicb.2018.03272.

Rudrappa, T.; Czymmek, K. J.; Paré, P. W.; Bais, H. P. (2008): Root-secreted malic acid recruits beneficial soil bacteria. In *Plant Physiol.* 148 (3), pp. 1547–1556. DOI: 10.1104/pp.108.127613.

Rüger, L.; Feng, K. et al. (2021): Assembly patterns of the rhizosphere microbiome along the longitudinal root axis of maize (*Zea mays* L.). In *Front. Microbiol.* 12, p. 614501. DOI: 10.3389/fmicb.2021.614501.

Rumberger, A.; Merwin, I. A.; Thies, J. E. (2007): Microbial community development in the rhizosphere of apple trees at a replant disease site. In *Soil Biol. Biochem.* 39 (7), pp. 1645–1654.

Ruzzi, M.; Aroca, R. (2015): Plant growth-promoting rhizobacteria act as biostimulants in horticulture. In *Scientia Horticulturae* 196, pp. 124–134. DOI: 10.1016/j.scienta.2015.08.042.

Sahin, N. (2003): Oxalotrophic bacteria. In *Res. Microbiol.* 154 (6), pp. 399–407. DOI: 10.1016/s0923-2508(03)00112-8.

Sakai, M.; Hosoda, A.; Ogura, K.; Ikenaga, M. (2014): The growth of *Steroidobacter agariperforans* sp. nov., a novel agar-degrading bacterium isolated from soil, is enhanced by the diffusible metabolites produced by bacteria belonging to *Rhizobiales*. In *Microbes Environ.* 29 (1), pp. 89–95. DOI: 10.1264/jsme2.me13169.

Salimi, F.; Hamedi, J. (2021): Biopesticides: microbes for agricultural sustainability. In Ajar Nath Yadav (Ed.): Soil Microbiomes for Sustainable Agriculture: Functional Annotation, vol. 27. Cham: Springer (Sustainable Development and Biodiversity), pp. 471–501.

Samada, L. H.; Tambunan, U. S. F. (2020): Biopesticides as promising alternatives to chemical pesticides: a review of their current and future status. In *Online J. Biol. Sci.* 20 (2), pp. 66–76. DOI: 10.3844/ojbsci.2020.66.76.

Santoyo, G.; Moreno-Hagelsieb, G.; Del Orozco-Mosqueda, M. C.; Glick, B. R. (2016): Plant growth-promoting bacterial endophytes. In *Microbiol. Res.* 183, pp. 92–99. DOI: 10.1016/j.micres.2015.11.008.

Savary, S.; Willocquet, L.; Pethybridge, S. J.; Esker, P.; McRoberts, N.; Nelson, A. (2019): The global burden of pathogens and pests on major food crops. In *Nat. Ecol. Evol.* 3 (3), pp. 430–439. DOI: 10.1038/s41559-018-0793-y.

Schmalenberger, A.; Hodge, S.; Bryant, A.; Hawkesford, M. J.; Singh, B. K.; Kertesz, M. A. (2008): The role of Variovorax and other Comamonadaceae in sulfur transformations by microbial wheat rhizosphere communities exposed to different sulfur fertilization regimes. In *Environ. Microbiol.* 10 (6), pp. 1486–1500. DOI: 10.1111/j.1462-2920.2007.01564.x.

Schmitz, L.; Yan, Z. et al. (2022): Synthetic bacterial community derived from a desert rhizosphere confers salt stress resilience to tomato in the presence of a soil microbiome. In *ISME J.* 16 (8), pp. 1907–1920. DOI: 10.1038/s41396-022-01238-3.

Schulz-Bohm, K.; Gerards, S.; Hundscheid, M.; Melenhorst, J.; Boer, W. de; Garbeva, P. (2018): Calling from distance: attraction of soil bacteria by plant root volatiles. In *ISME J.* 12 (5), pp. 1252–1262. DOI: 10.1038/s41396-017-0035-3.

Seemüller, E.; Schneider, B. (2004): '*Candidatus* Phytoplasma mali', '*Candidatus* Phytoplasma pyri' and '*Candidatus* Phytoplasma prunorum', the causal agents of apple proliferation, pear decline and European stone fruit yellows, respectively. In *Int. J. Syst. Evol. Microbiol.* 54 (4), pp. 1217–1226. DOI: 10.1099/ijs.0.02823-0.

Shi, S.; Nuccio, E. et al. (2015): Successional Trajectories of Rhizosphere Bacterial Communities over Consecutive Seasons. In *MBio* 6 (4), e00746. DOI: 10.1128/mBio.00746-15.

Siegieda, D.; Panek, J.; Frąc, M. (2024): Ecological processes of bacterial microbiome assembly in healthy and dysbiotic strawberry farms. In *BMC Plant Biol* 24 (1), p. 692. DOI: 10.1186/s12870-024-05415-8.

Simpson, D. (2018): The Economic Importance of Strawberry Crops. In : The Genomes of Rosaceous Berries and Their Wild Relatives: Springer, Cham, pp. 1–7. Available online at https://link.springer.com/chapter/10.1007/978-3-319-76020-9_1.

Singh, S.; Gupta, R.; Kumari, M.; Sharma, S. (2015): Nontarget effects of chemical pesticides and biological pesticide on rhizospheric microbial community structure and function in *Vigna radiata*. In *Environ. Sci. Pollut. Res. Int.* 22 (15), pp. 11290–11300. DOI: 10.1007/s11356-015-4341-x.

Solís-García, I. A.; Ceballos-Luna, O. et al. (2020): *Phytophthora* root rot modifies the composition of the avocado rhizosphere microbiome and increases the abundance of opportunistic fungal pathogens. In *Front. Microbiol.* 11, p. 574110. DOI: 10.3389/fmicb.2020.574110.

Spaink, Herman P.; Kondorosi, Adam; Hooykaas, Paul J. J. (1998): *Rhizobiaceae*. Molecular Biology of Model Plant-Associated Bacteria. Dordrecht: Springer Netherlands. Available online at https://ebookcentral.proquest.com/lib/gbv/detail.action?docID=3566725.

Spengler, R. N. (2019): Origins of the Apple: The Role of Megafaunal Mutualism in the Domestication of Malus and Rosaceous Trees. In *Front. Plant Sci.* 10, p. 617. DOI: 10.3389/fpls.2019.00617.

Stegen, J. C.; Lin, X.; Konopka, A. E.; Fredrickson, J. K. (2012): Stochastic and deterministic assembly processes in subsurface microbial communities. In *ISME J.* 6 (9), pp. 1653–1664. DOI: 10.1038/ismej.2012.22.

Steiner, U.; Oerke, E.-C. (2007): Localized melanization of appressoria is required for pathogenicity of *Venturia inaequalis*. In *Phytopathology* 97 (10), pp. 1222–1230. DOI: 10.1094/PHYTO-97-10-1222.

Stenberg, J. A. (2017): A Conceptual Framework for Integrated Pest Management. In *Trends Plant Sci.* 22 (9), pp. 759–769. DOI: 10.1016/j.tplants.2017.06.010.

Strange, Richard N. (2003): Introduction to Plant Pathology. 1st ed. Hoboken: John Wiley & Sons, Incorporated.

Strickland, D.; Carroll, J.; Cox, K. (2020): Apple Powdery Mildew. Edited by Cornell University and the New York State IPM Program. New York State Integrated Pest Management Program. Available online at https://ecommons.cornell.edu/bitstream/handle/1813/43120.2/apple-powdery-mildew-FS-NY-SIPM.pdf?sequence=5&isAllowed=y, checked on 6/29/2023.

Sutton, J. C. (1998): *Botrytis* fruit rot (gray mold) and blossom blight. Compendium of strawberry diseases. St. Paul: APS Press.

Sy, A.; Timmers, A. C. J.; Knief, C.; Vorholt, J. A. (2005): Methylotrophic metabolism is advantageous for *Methylobacterium extorquens* during colonization of *Medicago truncatula* under competitive conditions. In *Appl. Environ. Microbiol.* 71 (11), pp. 7245–7252. DOI: 10.1128/AEM.71.11.7245-7252.2005.

Talia, P.; Sede, S. M. et al. (2012): Biodiversity characterization of cellulolytic bacteria present on native Chaco soil by comparison of ribosomal RNA genes. In *Res. Microbiol.* 163 (3), pp. 221–232. DOI: 10.1016/j.resmic.2011.12.001.

Tender, C. de; Haegeman, A. et al. (2016): Dynamics in the strawberry rhizosphere microbiome in response to biochar and *Botrytis cinerea* leaf infection. In *Front. Microbiol.* 7, p. 2062. DOI: 10.3389/fmicb.2016.02062.

Termorshuizen, A. J. (2016): Ecology of Fungal Plant Pathogens. In *Microbiology spectrum* 4 (6). DOI: 10.1128/microbiolspec.FUNK-0013-2016.

Thenappan, D. P.; Thompson, D.; Joshi, M.; Mishra, A. K.; Joshi, V. (2024): Unraveling the Spatio-Temporal Dynamics of Soil and Root-Associated Microbiome in Texas Olive Orchards: A Comprehensive Analysis. In *Preprint in Scientific Reports*. DOI: 10.21203/rs.3.rs-4066985/v1.

Thompson, A.; Holton, R.; KC, A.; Moretti, M.; Wiman, N. (2023): 2023 Pest management guide for tree fruits. With assistance of Oregon State University Extension Service. Available online at https://catalog.extension.oregonstate.edu/sites/catalog/files/project/pdf/em8203.pdf, updated on 01.2023, checked on 3/31/2023.

Tian, P.; Razavi, B. S.; Zhang, X.; Wang, Q.; Blagodatskaya, E. (2020): Microbial growth and enzyme kinetics in rhizosphere hotspots are modulated by soil organics and nutrient availability. In *Soil Biol. Biochem.* 141, p. 107662. DOI: 10.1016/j.soilbio.2019.107662.

Tian, X.; Zhang, L.; Feng, S.; Zhao, Z.; Wang, X.; Gao, H. (2019): Transcriptome analysis of apple leaves in response to powdery mildew (*Podosphaera leucotricha*) infection. In *Int. J. Mol. Sci.* 20 (9), p. 2326. DOI: 10.3390/ijms20092326.

Trivedi, P.; He, Z.; van Nostrand, J. D.; Albrigo, G.; Zhou, J.; Wang, N. (2012): Huanglongbing alters the structure and functional diversity of microbial communities associated with citrus rhizosphere. In *ISME J.* 6 (2), pp. 363–383. DOI: 10.1038/ismej.2011.100.

Trivedi, P.; Leach, J. E.; Tringe, S. G.; Sa, T.; Singh, B. K. (2020): Plant-microbiome interactions: from community assembly to plant health. In *Nat. Rev. Microbiol.* 18 (11), pp. 607–621. DOI: 10.1038/s41579-020-0412-1.

Trivedi, P.; Mattupalli, C.; Eversole, K.; Leach, J. E. (2021): Enabling sustainable agriculture through understanding and enhancement of microbiomes. In *New Phytol.* 230 (6), pp. 2129–2147. DOI: 10.1111/nph.17319.

Trivedi, P.; Trivedi, C.; Grinyer, J.; Anderson, I. C.; Singh, B. K. (2016): Harnessing host-vector microbiome for sustainable plant disease management of phloem-limited bacteria. In *Front. Plant Sci.* 7, p. 1423. DOI: 10.3389/fpls.2016.01423.

United Nations (2023): Global Issues: Food. Available online at https://www.un.org/en/global-issues/food, checked on 12/13/2023.

Urbanietz, A.; Dunemann, F. (2005): Isolation, identification and molecular characterization of physiological races of apple powdery mildew (*Podosphaera leucotricha*). In *Plant Pathol.* 54 (2), pp. 125–133.

Uselman, S. M.; Qualls, R. G.; Thomas, R. B. (2000): Effects of increased atmospheric CO_2, temperature, and soil N availability on root exudation of dissolved organic carbon by a N-fixing tree (*Robinia pseudoacacia* L.). In *Plant Soil* 222 (1/2), pp. 191–202. DOI: 10.1023/A:1004705416108.

Vacheron, J.; Desbrosses, G. et al. (2013): Plant growth-promoting rhizobacteria and root system functioning. In *Front. Plant Sci.* 4, p. 356. DOI: 10.3389/fpls.2013.00356.

van Horn, C.; Somera, T. S.; Mazzola, M. (2021): Comparative Analysis of the Rhizosphere and Endophytic Microbiomes across Apple Rootstock Genotypes in Replant Orchard Soils. In *Phytobiomes J.* 5 (2), pp. 231–243. DOI: 10.1094/PBIOMES-08-20-0058-R.

Vandenkoornhuyse, P.; Mahé, S. et al. (2007): Active root-inhabiting microbes identified by rapid incorporation of plant-derived carbon into RNA. In *PNAS* 104 (43), pp. 16970–16975. DOI: 10.1073/pnas.0705902104.

Vries, F. T.; Wallenstein, M. D. (2017): Below-ground connections underlying above-ground food production: a framework for optimising ecological connections in the rhizosphere. In *J. Ecol.* 105 (4), pp. 913–920. DOI: 10.1111/1365-2745.12783.

Vries, F. T. de; Griffiths, R. I.; Knight, C. G.; Nicolitch, O.; Williams, A. (2020): Harnessing rhizosphere microbiomes for drought-resilient crop production. In *Science* 368 (6488), pp. 270–274. DOI: 10.1126/science.aaz5192.

Wagg, C.; Jansa, J.; Schmid, B.; van der Heijden, M. G. A. (2011): Belowground biodiversity effects of plant symbionts support aboveground productivity. In *Ecol. Lett.* 14 (10), pp. 1001–1009. DOI: 10.1111/j.1461-0248.2011.01666.x.

Walder, F.; Schmid, M. W. et al. (2022): Soil microbiome signatures are associated with pesticide residues in arable landscapes. In *Soil Biol. Biochem.* 174, p. 108830. DOI: 10.1016/j.soilbio.2022.108830.

Wan, T.; Zhao, H.; Wang, W. (2017): Effect of biocontrol agent *Bacillus amyloliquefaciens* SN16-1 and plant pathogen *Fusarium oxysporum* on tomato rhizosphere bacterial community composition. In *Biological Control* 112, pp. 1–9. DOI: 10.1016/j.biocontrol.2017.05.014.

Wang, L.; Li, J.; Yang, F.; E, Y.; Raza, W.; Huang, Q.; Shen, Q. (2017): Application of bioorganic fertilizer significantly increased apple yields and shaped bacterial community structure in orchard soil. In *Microb. Ecol.* 73 (2), pp. 404–416. DOI: 10.1007/s00248-016-0849-y.

Wang, L.; Mazzola, M. (2019): Field Evaluation of Reduced Rate Brassicaceae Seed Meal Amendment and Rootstock Genotype on the Microbiome and Control of Apple Replant Disease. In *Phytopathology* 109 (8), pp. 1378–1391. DOI: 10.1094/PHYTO-02-19-0045-R.

Wang, L.; Rengel, Z. et al. (2022): Ensuring future food security and resource sustainability: insights into the rhizosphere. In *iScience* 25 (4), p. 104168. DOI: 10.1016/j.isci.2022.104168.

Wang, X.; Wang, S.; Jiang, Y.; Zhou, J.; Han, C.; Zhu, G. (2020a): Comammox bacterial abundance, activity, and contribution in agricultural rhizosphere soils. In *Sci. Total Environ.* 727, p. 138563. DOI: 10.1016/j.scitotenv.2020.138563.

Wang, X.; Whalley, W. R.; Miller, A. J.; White, P. J.; Zhang, F.; Shen, J. (2020b): Sustainable Cropping Requires Adaptation to a Heterogeneous Rhizosphere. In *Trends Plant Sci.* 25 (12), pp. 1194–1202. DOI: 10.1016/j.tplants.2020.07.006.

Wang, Y. H.; Yu, Z. H. et al. (2019): Elevated CO^2 alters the structure of the bacterial community assimilating plant-derived carbon in the rhizosphere of soya bean. In *Eur. J. Soil Sci.* 70 (6), pp. 1212–1220. DOI: 10.1111/ejss.12817.

Webb, C. O. (2000): Exploring the phylogenetic structure of ecological communities: an example for rain forest trees. In *Am. Nat.* 156 (2), pp. 145–155. DOI: 10.1086/303378.

Weber, R. W. S.; Hahn, M. (2019): Grey mould disease of strawberry in northern Germany: causal agents, fungicide resistance and management strategies. In *Appl. Microbiol. Biotechnol.* 103 (4), pp. 1589–1597. DOI: 10.1007/s00253-018-09590-1.

Wei, G.; Li, M. et al. (2022): Temporal Dynamics of Rhizosphere Communities Across the Life Cycle of *Panax notoginseng*. In *Front. Microbiol.* 13, p. 853077. DOI: 10.3389/fmicb.2022.853077.

Wei, R.; Wang, X.; Zhang, W.; Shen, J.; Zhang, H.; Gao, Y.; Yang, L. (2020): The improved phosphorus utilization and reduced phosphorus consumption of *ppk*-expressing transgenic rice. In *Field Crops Res.* 248, p. 107715. DOI: 10.1016/j.fcr.2020.107715.

Wei, Z.; Hu, J. et al. (2018): *Ralstonia solanacearum* pathogen disrupts bacterial rhizosphere microbiome during an invasion. In *Soil Biol. Biochem.* 118, pp. 8–17. DOI: 10.1016/j.soilbio.2017.11.012.

Wen, T.; Yuan, J.; He, X.; Lin, Y.; Huang, Q.; Shen, Q. (2020): Enrichment of beneficial cucumber rhizosphere microbes mediated by organic acid secretion. In *Hortic Res* 7 (1), p. 154. DOI: 10.1038/s41438-020-00380-3.

Wen, T.; Zhao, M.; Yuan, J.; Kowalchuk, G. A.; Shen, Q. (2021): Root exudates mediate plant defense against foliar pathogens by recruiting beneficial microbes. In *Soil Ecol. Lett.* 3 (1), pp. 42–51. DOI: 10.1007/s42832-020-0057-z.

Wendel, A. S.; Bauke, S. L.; Ileperuma, J. C.; Funken, K.; Frindte, K.; Knief, C. (2025): Implications of reduced root-soil contact for microbial rhizosphere establishment and early plant growth performance. In *Soil Biol. Biochem.* 207, p. 109816. DOI: 10.1016/j.soilbio.2025.109816.

White, J. F.; Kingsley, K. L. et al. (2019): Review: Endophytic microbes and their potential applications in crop management. In *Pest. Manage. Sci.* 75 (10), pp. 2558–2565. DOI: 10.1002/ps.5527.

Wickham, Hadley (2016): ggplot2. Elegrant graphics for data analysis. Second edition. Switzerland: Springer (Use R!).

Wingate, L.; Ogée, J. et al. (2010): Photosynthetic carbon isotope discrimination and its relationship to the carbon isotope signals of stem, soil and ecosystem respiration. In *New Phytol.* 188 (2), pp. 576–589. DOI: 10.1111/j.1469-8137.2010.03384.x.

Yang, J.; Wei, S. et al. (2020): Comparison of the Rhizosphere Soil Microbial Community Structure and Diversity Between Powdery Mildew-Infected and Noninfected Strawberry Plants in a Greenhouse by High-Throughput Sequencing Technology. In *Curr. Microbiol.* 77 (8), pp. 1724–1736. DOI: 10.1007/s00284-020-01948-x.

Yilmaz, P.; Parfrey, L. W. et al. (2014): The SILVA and "All-species Living Tree Project (LTP)" taxonomic frameworks. In *Nucleic Acids Res.* 42 (Database issue), D643-8. DOI: 10.1093/nar/gkt1209.

Yin, C.; Casa Vargas, J. M.; Schlatter, D. C.; Hagerty, C. H.; Hulbert, S. H.; Paulitz, T. C. (2021): Rhizosphere community selection reveals bacteria associated with reduced root disease. In *Microbiome* 9 (1), p. 86. DOI: 10.1186/s40168-020-00997-5.

Yu, Z.; Li, Y. et al. (2016): Effectiveness of elevated CO^2 mediating bacterial communities in the soybean rhizosphere depends on genotypes. In *Agric. Ecosyst. Environ.* 231, pp. 229–232. DOI: 10.1016/j.agee.2016.06.043.

Yu, Z.; Lu, T.; Qian, H. (2023): Pesticide interference and additional effects on plant microbiomes. In *Science of The Total Environment* 888, p. 164149. DOI: 10.1016/j.scitotenv.2023.164149.

Yuan, J.; Zhao, J. et al. (2018): Root exudates drive the soil-borne legacy of aboveground pathogen infection. In *Microbiome* 6 (1), p. 156. DOI: 10.1186/s40168-018-0537-x.

Zaneveld, J. R.; McMinds, R.; Vega Thurber, R. (2017): Stress and stability: applying the Anna Karenina principle to animal microbiomes. In *Nat. Microbiol.* 2, p. 17121. DOI: 10.1038/nmicrobiol.2017.121.

Zhalnina, K.; Louie, K. B. et al. (2018): Dynamic root exudate chemistry and microbial substrate preferences drive patterns in rhizosphere microbial community assembly. In *Nat. Microbiol.* 3 (4), pp. 470–480. DOI: 10.1038/s41564-018-0129-3.

Zhang, X.; Di Zhang; Sun, W.; Wang, T. (2019): The Adaptive Mechanism of Plants to Iron Deficiency via Iron Uptake, Transport, and Homeostasis. In *Int. J. Mol. Sci.* 20 (10). DOI: 10.3390/ijms20102424.

Zhang, Y.; Xu, J.; Riera, N.; Jin, T.; Li, J.; Wang, N. (2017): Huanglongbing impairs the rhizosphere-to-rhizoplane enrichment process of the citrus root-associated microbiome. In *Microbiome* 5 (1), p. 97. DOI: 10.1186/s40168-017-0304-4.

Zhou, W.; Li, M.; Achal, V. (2025): A comprehensive review on environmental and human health impacts of chemical pesticide usage. In *Emerg. Contam.* 11 (1), p. 100410. DOI: 10.1016/j.emcon.2024.100410.

Zhou, W.; Qin, X.; Lyu, D.; Qin, S. (2021): Effect of glucose on the soil bacterial diversity and function in the rhizosphere of *Cerasus sachalinensis*. In *Hortic. Plant J.* 7 (4), pp. 307–317. DOI: 10.1016/j.hpj.2021.02.002.

VII. Appendix A

Supporting information to chapter II

DNA extraction and 16S rRNA gene PCR

DNA extractions were performed using the NucleoSpin® Soil DNA extraction kit (Macherey Nagel, Düren, Germany). For the L-compartment and bulk soil samples 400 mg of dry soil were weighed into kit-supplied 2-ml MN Bead Tubes Type A and extraction was done according to the manufacturer´s instructions. For the T-samples two 2-ml MN Bead Tubes Type A were filled up to the 1-ml mark with grounded root material per sample and processed according to instructions until step 7 in the protocol (03/2019, Rev. 08 version). At step 7, the solution of two parallel tubes per sample were successively loaded onto the NucleoSpin® Soil Column and therewith pooled. The following steps were again performed according to manufacturer´s instructions with a final elution in 50 µl of PCR-grade water. The DNA concentrations were quantified using the QuantiFluor®dsDNA System (Promega Corporation, Fitchburg, WI) according to the manufacturer´s instructions and bulk soil or L-samples were subsequently diluted to 10 ng/µl, whereas T-samples were diluted to 30 ng/µl using PCR-grade water. For bacterial community analysis, the 16S rRNA gene was amplified using an LNA PCR protocol to suppress the amplification of plant organelle derived 16S rRNA genes (Ikenaga and Sakai 2014). The bacterial genes were amplified using the modified primer set 63f-1492r, followed by a nested PCR using primer set 799f-1193r (V5 - V7 region) to obtain PCR products of adequate length for sequencing. The first PCR was performed in triplicate assays per sample. Each 11-µl reaction contained 2 µl of 5x Herculase II reaction buffer (Agilent Technologies, Santa Clara, CA), 0.91 mM MgCl2, 0.73 mg/ml BSA, 0.23 mM of dNTPs, 0.14 µM of each bacterial primer (BioTez, Berlin, Germany), 0.55 µM of each LNA primer (Qiagen, Hilden, Germany), 0.5 U of Herculase II DNA polymerase and 1 µl of DNA template. Thermal cycling conditions were: an initial denaturation at 95 °C for 2 min followed by 25 cycles of 95 °C for 20 sec, 70 °C for 20 sec (LNA primer annealing), 56 °C for 20 sec (bacterial 16S rRNA gene primer annealing), 72 °C for 45 sec and a final elongation step at 72 °C for 3 min. The obtained triplicate PCR products per sample were pooled, 10-fold diluted with PCR grade water and used as template in the second, nested PCR for sample-specific

barcoding. Each 30-µl nested PCR assay contained 6 µl of 5x Herculase II reaction buffer, 1 mM MgCl2, 0.6 mg/ml BSA, 0.25 mM dNTPs, 0.25 µM of each primer, 1.5 U of Herculase II DNA polymerase and 3 µl template DNA. The forward primer in this nested PCR contained an 8-bp sample-specific barcode (Suppl. Table VII-2), similarly as used in Frindte et al. (2019). Thermal cycling conditions were: an initial denaturation at 95 °C for 1 min followed by 10 cycles of 95 °C for 20 sec, 56 °C for 20 sec, 72 °C for 30 sec and a final elongation step at 72 °C for 2:30 min. Successful amplification was validated by agarose gel-electrophoresis. PCR products were quantified using the QuantiFluor dsDNA System on an Infinite 200 Pro plate reader (Tecan, Männedorf, Switzerland) at 490 nm excitation and 530 nm emission wavelength. Afterwards, PCR products were pooled at equimolar concentrations and purified with the HighPrep™PCR Clean-up System kit (MagBio Genomics, Gaithersburg, MD). Library preparation and sequencing on a HiSeq system (Illumina, San Diego, CA) was performed by the Max Planck-Genome-centre Cologne and generated paired-end reads (2 × 250 bp).

Suppl. Fig. VII-1: Photographs showing the root system of a fully grown commercial apple tree (top) and two rows of an apple orchard (bottom).

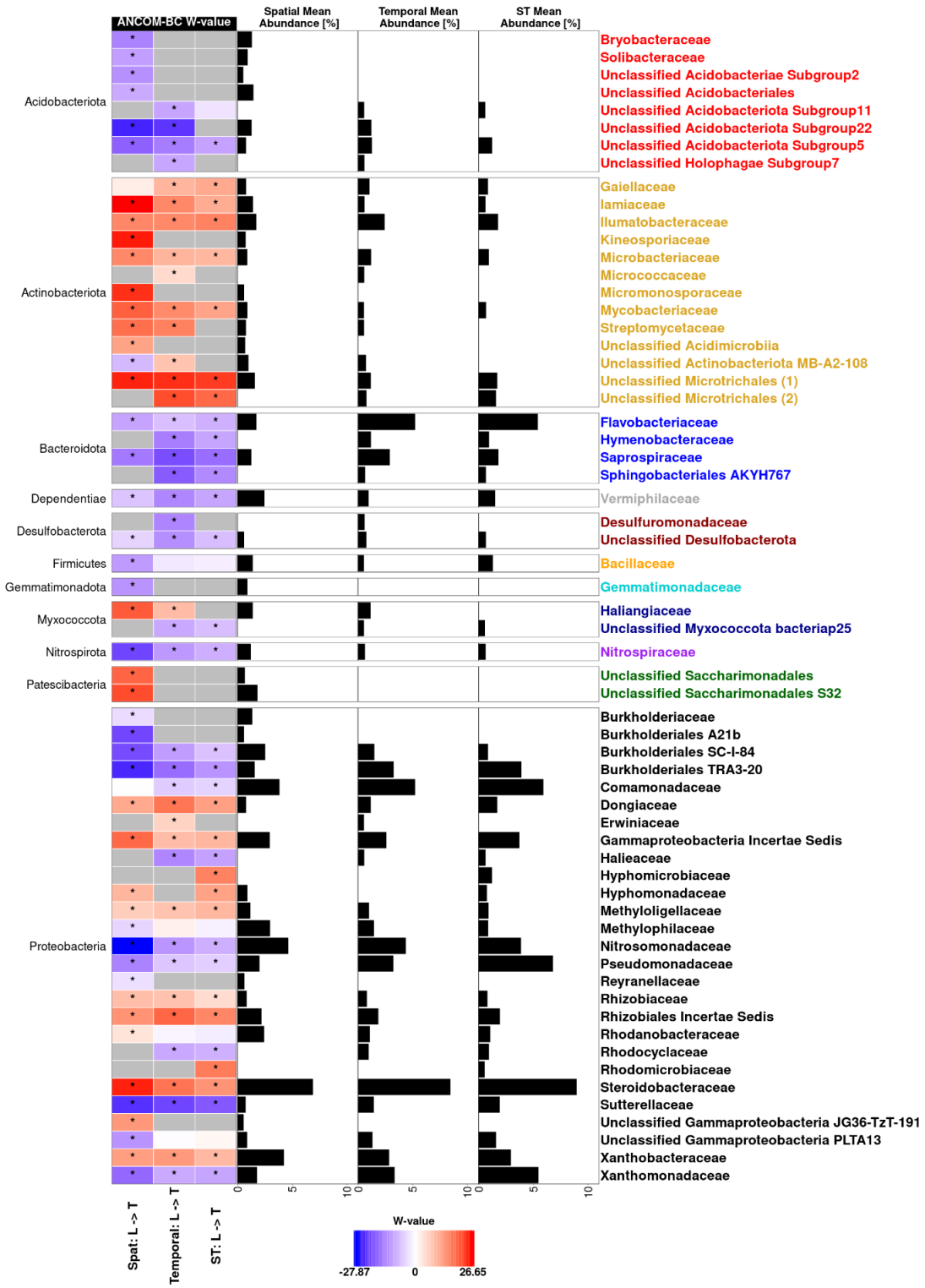

Suppl. Fig. VII-2: Differential abundance analysis of the loosely (L) and tightly (T) associated bacteria in the three experimental field trials using ANCOM-BC. The heatmap shows the coefficients obtained from the ANCOM-BC log-linear model divided by their standard error (called W-value) with red indicating enrichment in the T-compartment. A "*" is shown if ANCOM-BC showed significant differences using the adjusted *p*-value in this comparison. The mean abundance of the families in their respective trial are shown in the adjacent barplot as % and only families with mean abundances ≥ 0.5% are shown (ST refers to the spatio-temporal trial). A greyed-out field means that this family is below the 0.5% threshold in a trial. The families in the heatmap rows are separated by the phylum they belong to and displayed in different colors.

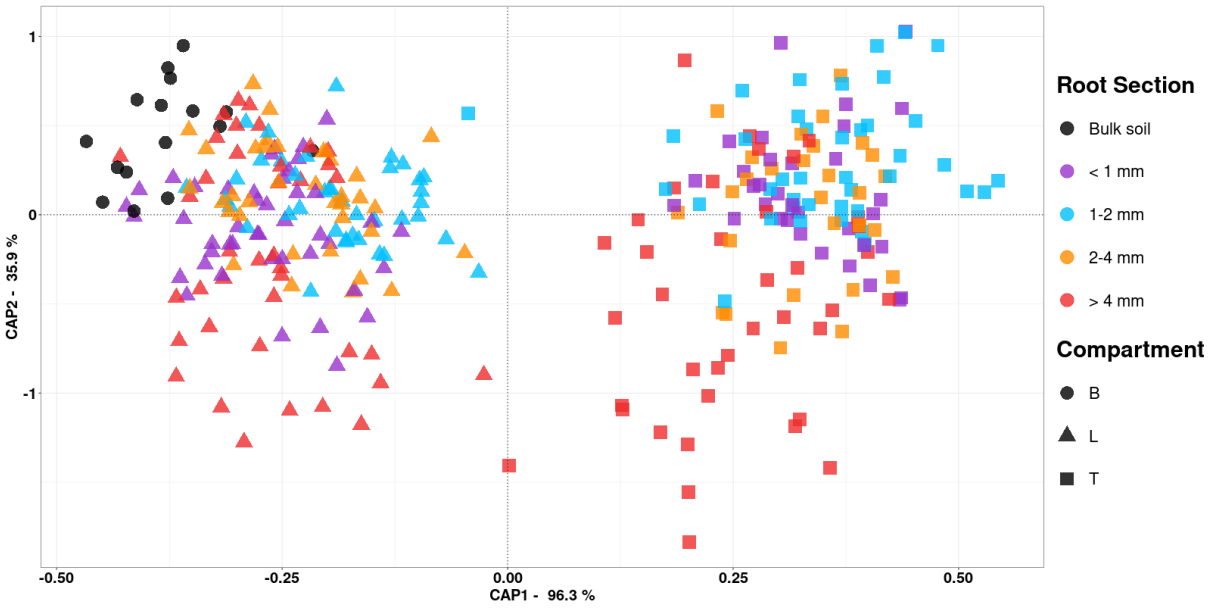

Suppl. Fig. VII-3: Root-associated bacterial community composition of the loosely (L) and tightly (T) associated bacteria in four different root size sections and the bulk soil (b) of four apple trees analyzed in the spatial trial. Constrained analysis of principal coordinates (CAP; based on DEICODE distance matrices and the variables compartment, tree and root quadrant) to assess the relevance of those variables on variation in bacterial community composition.

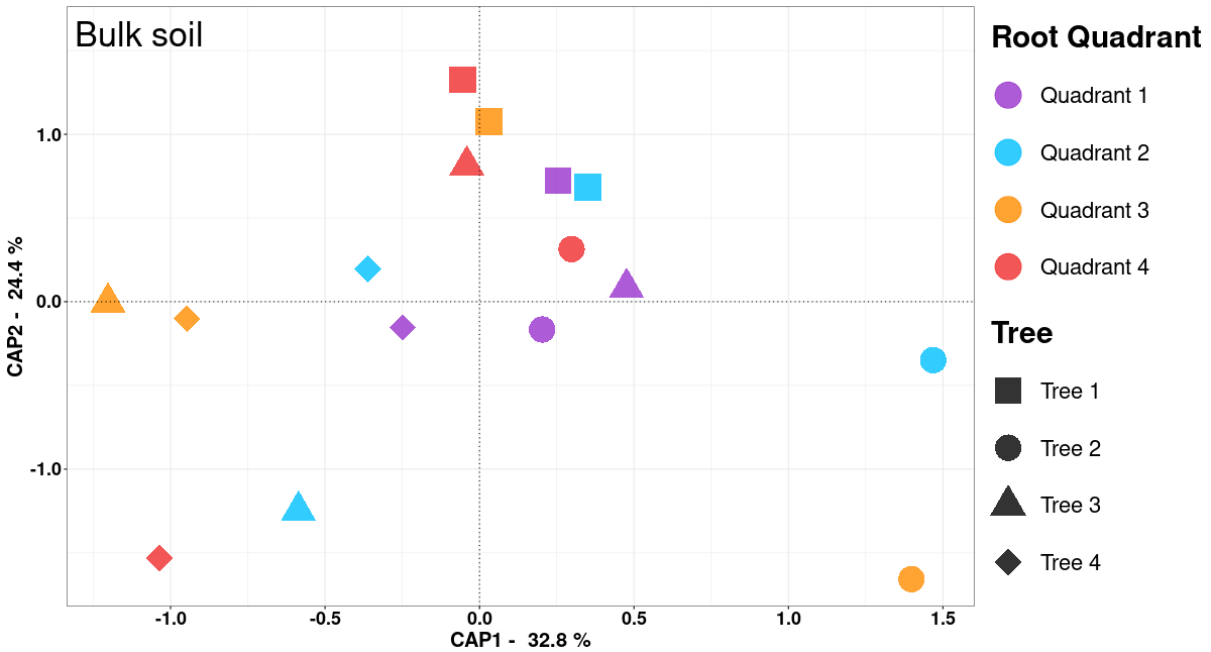

Suppl. Fig. VII-4: Root-associated bacterial community composition of bulk soil near the apple trees analyzed in the spatial trial. Constrained analysis of principal coordinates (CAP; based on DEICODE distance matrices and the variables tree and root quadrant) to assess the relevance of those variables on variation in bacterial community composition.

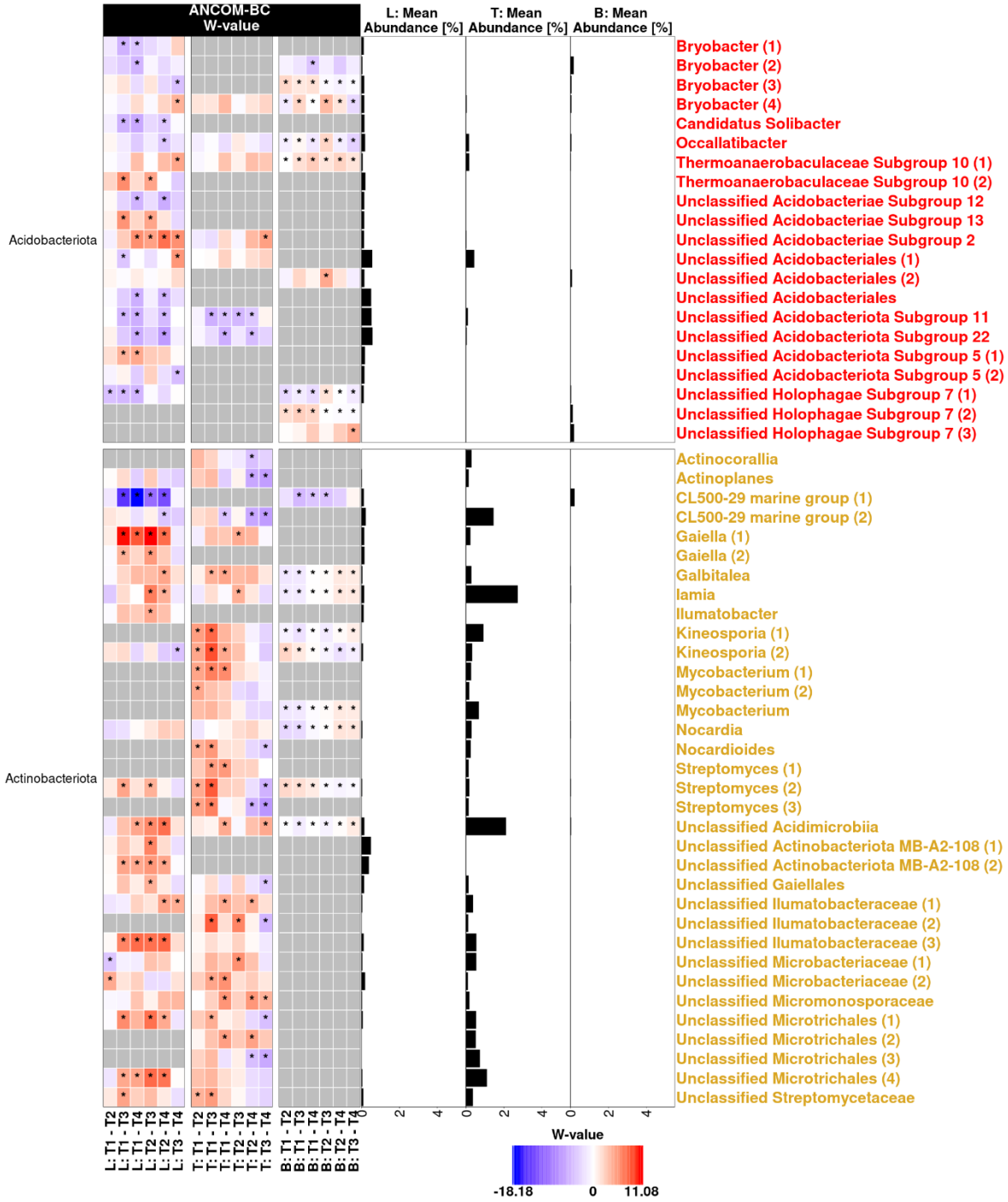

Suppl. Fig. VII-5: Part 1/4.

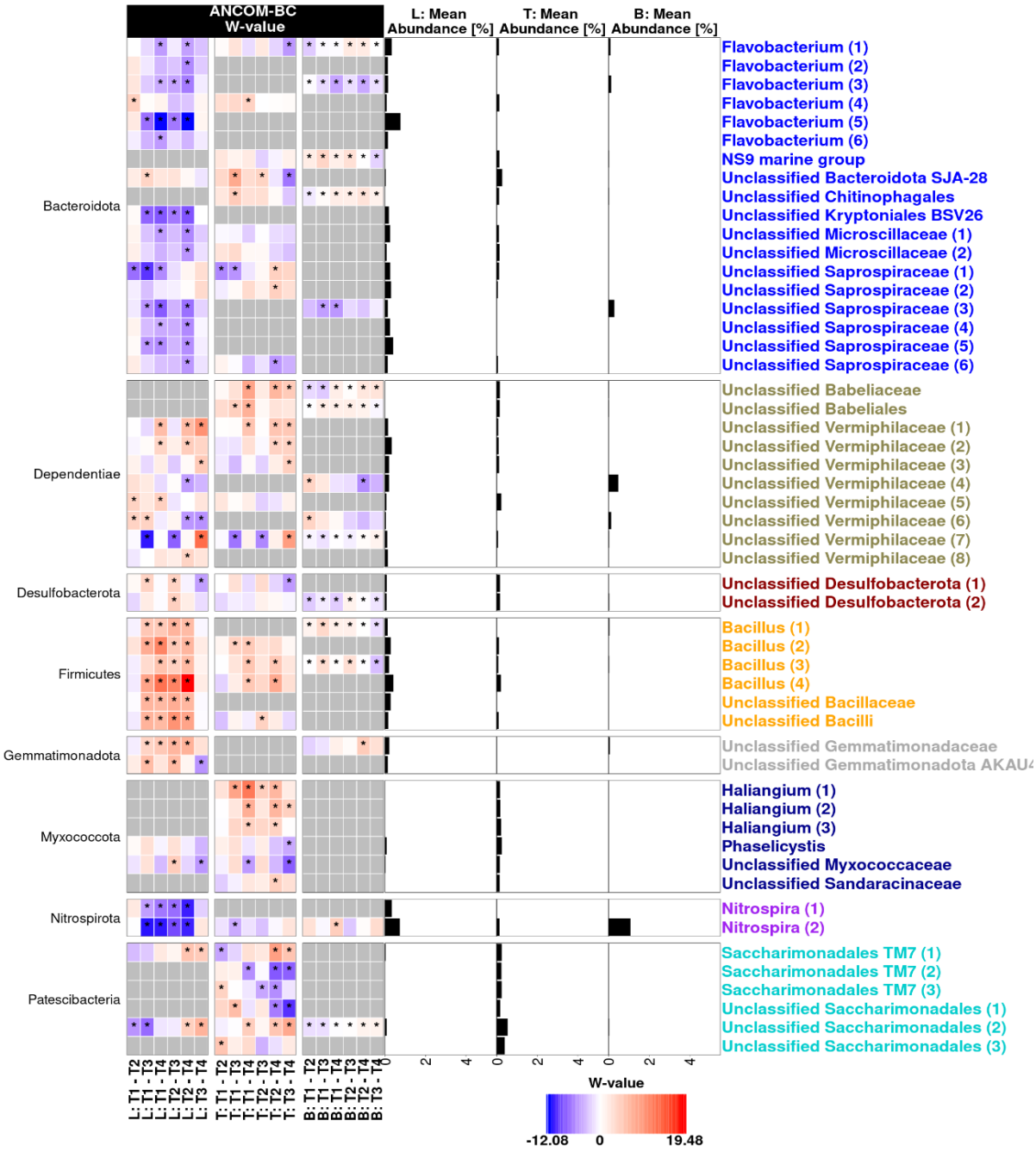

Suppl. Fig. VII-5: Part 2/4.

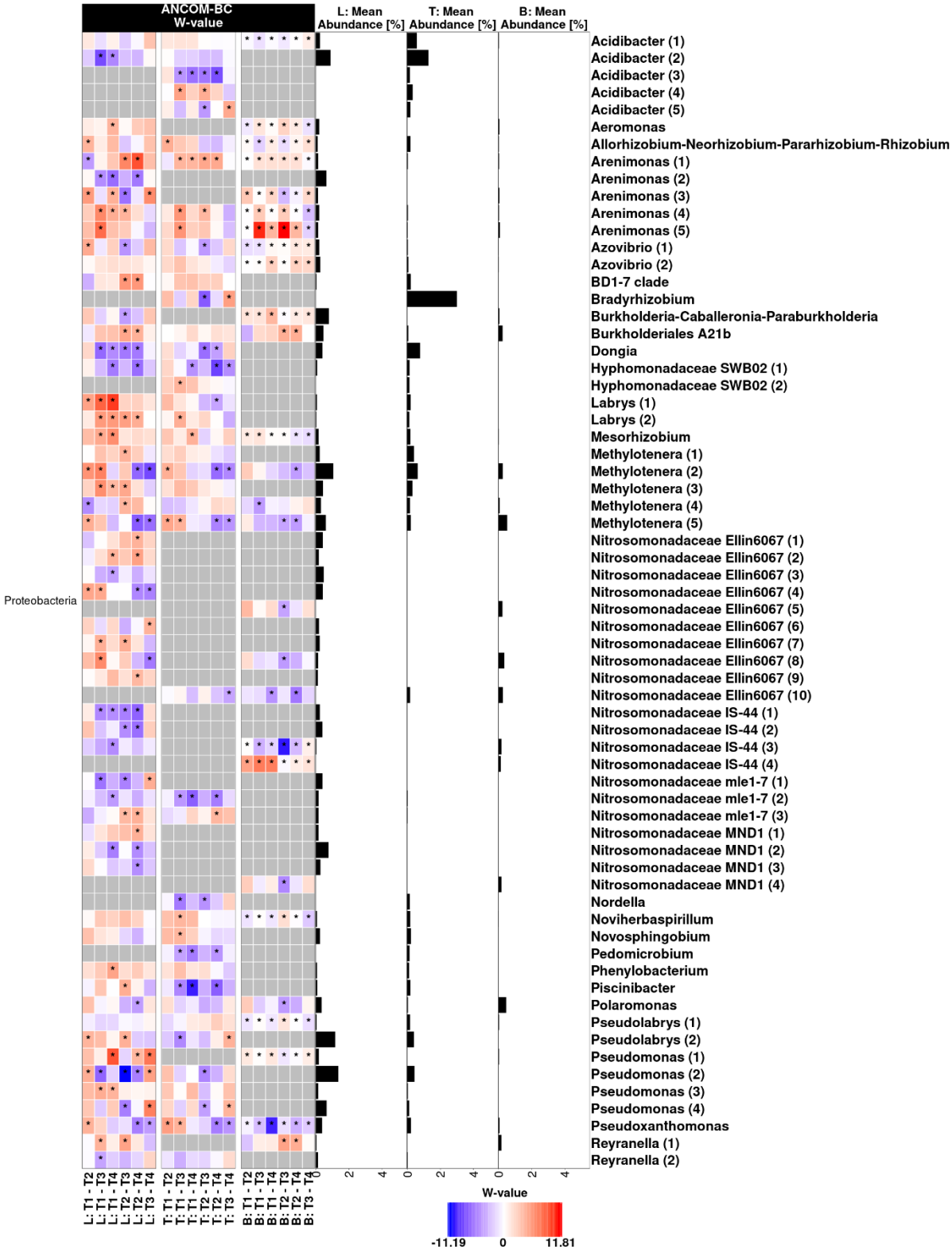

Suppl. Fig. VII-5: Part 3/4.

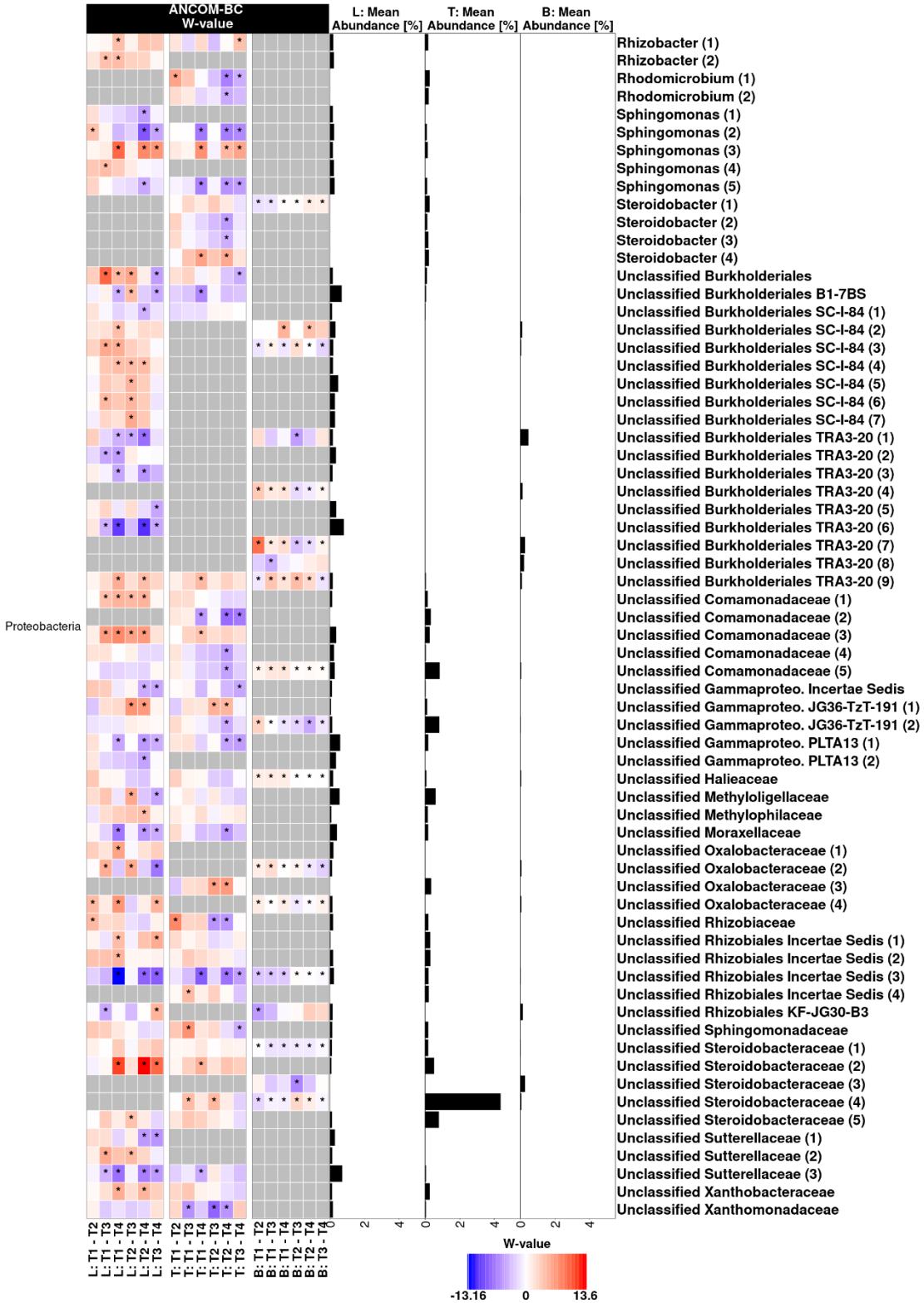

Suppl. Fig. VII-5: Part 4/4. Differential abundance analysis of the loosely (L) and tightly (T) associated bacteria and the bulk soil (b) in four different trees (T1 to T4) of the spatial trial using ANCOM-BC. The heatmap shows the coefficients obtained from the ANCOM-BC log-linear model divided by their standard error (called W-value). A "*" is shown if ANCOM-BC showed significant differences using the adjusted *p*-value in this comparison. The colour code indicates differential abundances between two samples with red indicating enrichment in the larger root sections. A grey colour indicates that this ASV was not detected in the respective compartment. The mean relative abundance of the ASVs in the entire compartment is shown as % and ASVs with mean abundances ≥0.1% in either compartment are displayed. The ASVs in the rows of the heatmap are separated according to phylum.

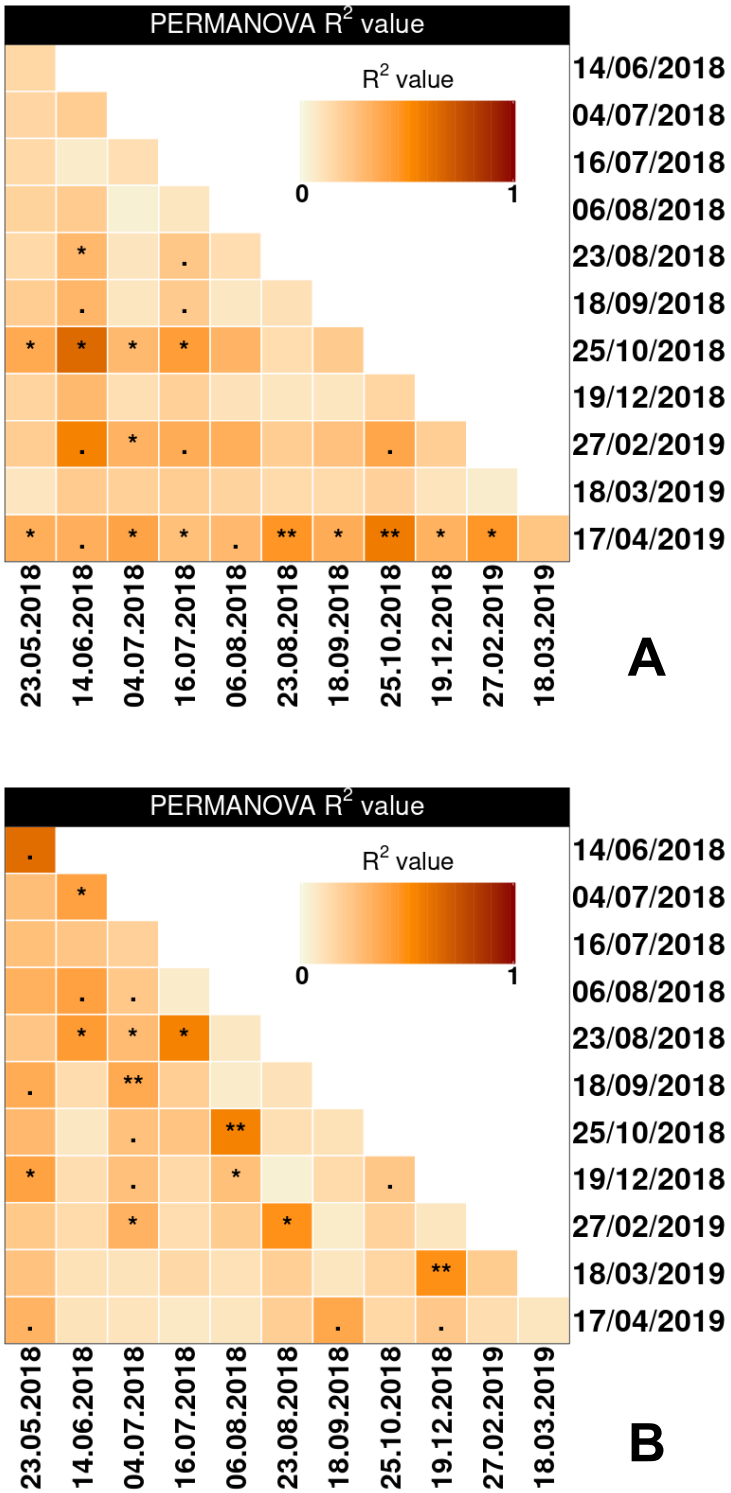

Suppl. Fig. VII-6: Pairwise PERMANOVA for comparison of timepoints in the temporal trial in the L- and T-compartment in the upper (**A**) and lower (**B**) panel, respectively. The colour codes for the R^2-value and `.` indicates a *p*-value between 0.05 and 0.1, `*` indicates a *p*-value between 0.01 and 0.05, `**` a *p*-value between 0.01 and 0.001. The adjusted *p*-values using Benjamini-Hochberg correction for multiple testing are not displayed as they were all non-significant.

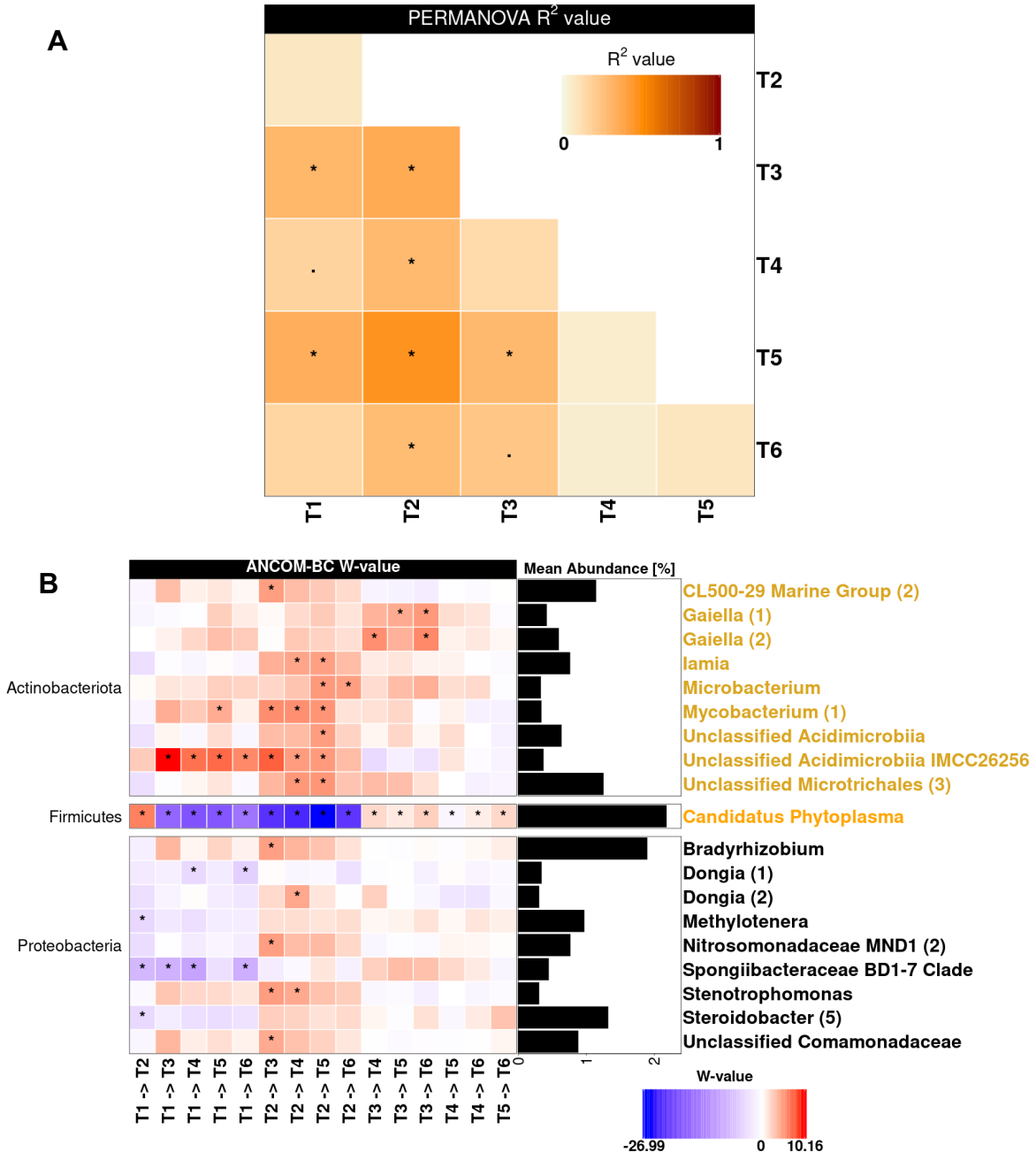

Suppl. Fig. VII-7: Comparison of the T-compartment of six tree individuals in the temporal trial. Trees 1 to 3 and trees 4 to 6 were standing adjacently in separate opposite rows. (**A**) Pairwise PERMANOVA with *p*-values adjusted using Benjamini-Hochberg correction for multiple testing. The colour codes for the R^2-value and `.` indicates a p_{adj}-value between 0.05 and 0.1, `*` indicates a p_{adj}-value between 0.01 and 0.05. (**B**) Differentially abundant ASVs identified by ANCOM-BC. The heatmap shows the coefficients obtained from the ANCOM-BC log-linear model divided by their standard error (called W-value). A "*" is shown if ANCOM-BC showed significant differences using the p_{adj}-value in this comparison. The colour code indicates differential abundances between two samples with red indicating enrichment in the tree with the higher identifier number. The mean relative abundance of the ASVs in the T- compartment is shown as % and ASVs with mean abundances ≥ 0.3% are displayed. The ASVs in the rows of the heatmap are separated according to phylum.

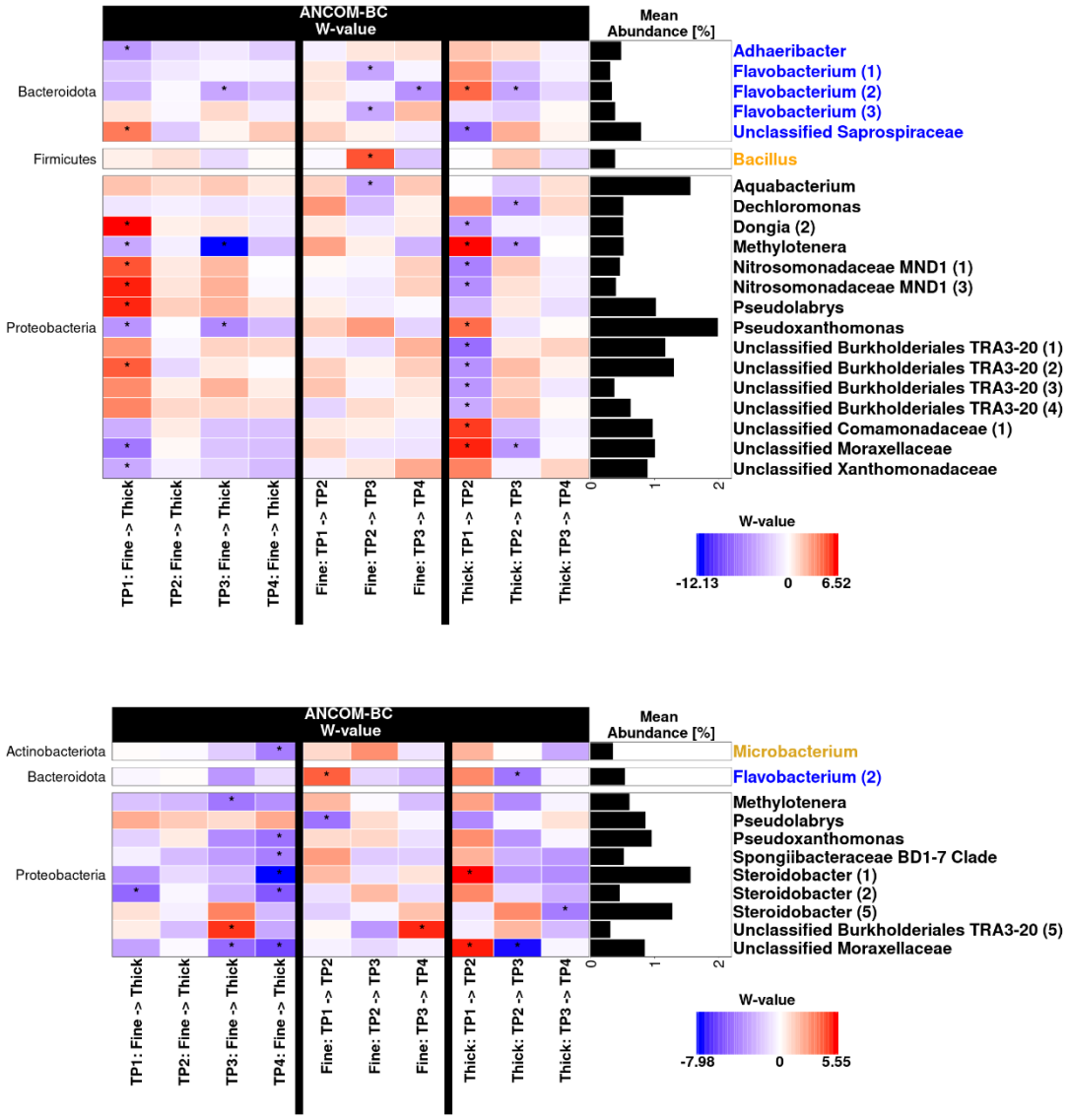

Suppl. Fig. VII-8: Differentially abundant ASVs in the L- and T-compartment (upper and lower panel, respectively) for two different root size sections at four different timepoints according to ANCOM-BC. Fine roots had a diameter between 1 and 3 mm and thick roots between 3 and 6 mm. Samples were taken at four timepoints (TP1: 21.03.2019; TP2: 15.04.2019; TP3: 05.06.2019 and TP4: 20.08.2019). The first four columns compare the fine to the thick roots at each timepoint, the next three the different timepoints in the fine roots and the last three columns compare the thick roots at each timepoint. The heatmap shows the coefficients obtained from the ANCOM-BC log-linear model divided by their standard error (called W-value). The colour code indicates differential abundances between two factors with red indicating enrichment in the second mentioned factor. A "*" is shown if ANCOM-BC showed significant differences using p_{adj}-values in this comparison. The mean abundance of the ASVs in the entire compartment is shown as % and only ASVs with mean abundances ≥ 0.3% are shown.

Suppl. Table VII-1: The sampling timepoints of the temporal trial (left) and the spatio-temporal (ST) trial (right).

Temporal trial		
Timepoint 1	23.05.2018	Spring
Timepoint 2	14.06.2018	Summer
Timepoint 3	04.07.2018	
Timepoint 4	16.07.2018	
Timepoint 5	06.08.2018	
Timepoint 6	23.08.2018	
Timepoint 7	18.09.2018	Autumn
Timepoint 8	25.10.2018	
Timepoint 9	19.12.2018	Winter
Timepoint 10	27.02.2019	
Timepoint 11	18.03.2019	
Timepoint 12	17.04.2019	Spring

ST trial		
Timepoint 1	21.03.2019	Spring
Timepoint 2	15.04.2019	
Timepoint 3	05.06.2019	Summer
Timepoint 4	20.08.2019	

Suppl. Table VII-2: Sequences of barcoded forward primers targeting the 16S rRNA gene. Primers include a barcode (8 bp) and the primer sequence itself. The reverse primer was not modified.

Name	Barcode + Primer 799f
799f-BC1	AACACCTA AAC MGG ATT AGA TAC CCK G
799f-BC2	ACGTAGCT AAC MGG ATT AGA TAC CCK G
799f-BC3	ATATAGGA AAC MGG ATT AGA TAC CCK G
799f-BC4	CACAGTTG AAC MGG ATT AGA TAC CCK G
799f-BC5	CCTACAAC AAC MGG ATT AGA TAC CCK G
799f-BC6	CGTCGGCT AAC MGG ATT AGA TAC CCK G
799f-BC7	GACGTCAA AAC MGG ATT AGA TAC CCK G
799f-BC8	GCGTTTCG AAC MGG ATT AGA TAC CCK G
799f-BC9	GGTCTGAC AAC MGG ATT AGA TAC CCK G
799f-BC10	GTTTCACT AAC MGG ATT AGA TAC CCK G
799f-BC11	TCCAGCCT AAC MGG ATT AGA TAC CCK G
799f-BC12	TGCGGTTA AAC MGG ATT AGA TAC CCK G
799f-BC13	GCAGCCTC AAC MGG ATT AGA TAC CCK G
799f-BC14	GGCGAGGA AAC MGG ATT AGA TAC CCK G
799f-BC15	GTGGGATA AAC MGG ATT AGA TAC CCK G
799f-BC16	TATCTCCG AAC MGG ATT AGA TAC CCK G
799f-BC17	ACTAACTG AAC MGG ATT AGA TAC CCK G
799f-BC18	ATCCTATT AAC MGG ATT AGA TAC CCK G
799f-BC19	CACGTGTT AAC MGG ATT AGA TAC CCK G
799f-BC20	CCTTTACA AAC MGG ATT AGA TAC CCK G
799f-BC21	CTAGATTC AAC MGG ATT AGA TAC CCK G
799f-BC22	GAGAACTC AAC MGG ATT AGA TAC CCK G
799f-BC23	GCTCAGTT AAC MGG ATT AGA TAC CCK G
799f-BC24	GTACTTGC AAC MGG ATT AGA TAC CCK G
799f-BC25	TACGAATC AAC MGG ATT AGA TAC CCK G
799f-BC26	TCCTACTA AAC MGG ATT AGA TAC CCK G
799f-BC27	TGGTCTTC AAC MGG ATT AGA TAC CCK G
799f-BC28	AACCGTGT AAC MGG ATT AGA TAC CCK G
799f-BC29	GGTCCTTG AAC MGG ATT AGA TAC CCK G
799f-BC30	GTTGTCCC AAC MGG ATT AGA TAC CCK G
799f-BC31	TCATTAGG AAC MGG ATT AGA TAC CCK G
799f-BC32	TGATCCGA AAC MGG ATT AGA TAC CCK G
799f-BC33	ATCGCCAG AAC MGG ATT AGA TAC CCK G
799f-BC34	CAGGAGGC AAC MGG ATT AGA TAC CCK G
799f-BC35	CGAACTGT AAC MGG ATT AGA TAC CCK G
799f-BC36	CTAGTCAT AAC MGG ATT AGA TAC CCK G
799f-BC37	GAGTTAAC AAC MGG ATT AGA TAC CCK G
799f-BC38	GCTGGCGA AAC MGG ATT AGA TAC CCK G
799f-BC39	GTAGAGCT AAC MGG ATT AGA TAC CCK G
799f-BC40	TACTGCGC AAC MGG ATT AGA TAC CCK G
799f-BC41	TCGCGTAC AAC MGG ATT AGA TAC CCK G
799f-BC42	TGTAGGTC AAC MGG ATT AGA TAC CCK G
799f-BC43	AAGCGGTC AAC MGG ATT AGA TAC CCK G
799f-BC44	ACTCTAAG AAC MGG ATT AGA TAC CCK G
799f-BC45	TGAGAGTG AAC MGG ATT AGA TAC CCK G
799f-BC46	TTCTGATG AAC MGG ATT AGA TAC CCK G
799f-BC47	ACAGTGCA AAC MGG ATT AGA TAC CCK G
799f-BC48	AGTAGTGG AAC MGG ATT AGA TAC CCK G

Suppl. Table VIII-3. The hierarchies in each of the trials with the number of samples. Total read number after quality filtering, mean number of reads per sample and the number of samples remaining after quality filtering.

Trial	Hierarchical structure	Number of samples	Total number of reads	Mean number of reads / sample	Samples remaining after quality filtering
Spatial trial	4 trees x 4 quadrants x 4 size classes x 3 pseudo-replications x 2 compartments	384 root associated samples	11.494.965	36.725	297 samples
	4 trees x 4 quadrants	16 bulk soil samples			16 samples
Temporal trial	6 trees x 12 time points x 2 compartments	144 root associated samples	4.248.425	37.932	112 samples
Combined trial	9 trees x 2 size classes x 4 time points x 2 compartments	144 root associated samples	3.650.109	35.785	102 samples

Suppl. Table VII-4: The ten most prominent genera in each trial with their mean relative abundance and standard deviation (SD).

		Class	Order	Family	Genus	Mean	SD
SPATIAL	L	*Gammaproteobacteria*	*Burkholderiales*	SC-I-84		4.2	1.5
		Gammaproteobacteria	*Burkholderiales*	*Nitrosomonadaceae*	Ellin6067	3.8	1.5
		Babeliae	*Babeliales*	*Vermiphilaceae*		3.1	1.4
		Gammaproteobacteria	*Pseudomonadales*	*Pseudomonadaceae*	*Pseudomonas*	3.0	2.1
		Gammaproteobacteria	*Burkholderiales*	TRA3-20		2.8	1.1
		Gammaproteobacteria	*Burkholderiales*	*Methylophilaceae*	*Methylotenera*	2.7	1.6
		Bacteroidia	*Flavobacteriales*	*Flavobacteriaceae*	*Flavobacterium*	2.5	1.5
		Acidobacteriota - Subgroup22				2.2	0.9
		Gammaproteobacteria	*Burkholderiales*	*Comamonadaceae*		2.2	1.0
		Gammaproteobacteria	*Steroidobacterales*	*Steroidobacteraceae*		2.1	1.0
	T	*Gammaproteobacteria*	*Steroidobacterales*	*Steroidobacteraceae*		10.9	3.3
		Gammaproteobacteria	Incertae Sedis	Unknown Family	*Acidibacter*	4.4	1.1
		Alphaproteobacteria	*Rhizobiales*	*Xanthobacteraceae*	*Bradyrhizobium*	3.6	0.9
		Saccharimonadia	*Saccharimonadales*	S32	TM7	3.3	1.8
		Acidimicrobiia				3.3	1.3
		Acidimicrobiia	*Microtrichales*			3.0	1.5
		Acidimicrobiia	*Microtrichales*	*Iamiaceae*	*Iamia*	2.8	1.6
		Alphaproteobacteria	*Rhizobiales*	Incertae Sedis		2.6	1.2
		Polyangia	*Haliangiales*	*Haliangiaceae*	*Haliangium*	2.3	0.8
		Gammaproteobacteria	*Burkholderiales*	*Comamonadaceae*		2.1	1.0
TEMPORAL	L	*Bacteroidia*	*Flavobacteriales*	*Flavobacteriaceae*	*Flavobacterium*	6.6	3.7
		Gammaproteobacteria	*Burkholderiales*	TRA3-20		5.1	1.6
		Bacteroidia	*Chitinophagales*	*Saprospiraceae*		4.8	1.4
		Gammaproteobacteria	*Pseudomonadales*	*Pseudomonadaceae*	*Pseudomonas*	4.1	3.9
		Gammaproteobacteria	*Burkholderiales*	*Comamonadaceae*		2.8	0.9
		Gammaproteobacteria	*Burkholderiales*	*Nitrosomonadaceae*	Ellin6067	2.8	0.6
		Gammaproteobacteria	*Burkholderiales*	*Sutterellaceae*		2.4	0.5
		Gammaproteobacteria	*Burkholderiales*	*Nitrosomonadaceae*	MND1	2.4	0.8
		Gammaproteobacteria	*Burkholderiales*	SC-I-84		2.2	0.6
		Acidobacteriota - Subgroup22				2.1	0.6
	T	*Gammaproteobacteria*	*Steroidobacterales*	*Steroidobacteraceae*	*Steroidobacter*	12.3	4.5
		Bacteroidia	*Flavobacteriales*	*Flavobacteriaceae*	*Flavobacterium*	3.7	4.2
		Gammaproteobacteria	Incertae Sedis	Unknown Family	*Acidibacter*	3.3	1.1
		Acidimicrobiia	*Microtrichales*	*Ilumatobacteraceae*	CL500-29 Marine Group	2.6	1.4
		Alphaproteobacteria	*Rhizobiales*	Incertae Sedis		2.5	1.1
		Gammaproteobacteria	*Burkholderiales*	*Comamonadaceae*		2.4	0.7
		Gammaproteobacteria	*Pseudomonadales*	*Pseudomonadaceae*	*Pseudomonas*	2.2	2.6
		Bacilli	*Acholeplasmatales*	*Acholeplasmataceae*	Candidatus *Phytoplasma*	2.2	5.1
		Acidimicrobiia	*Microtrichales*			2.2	0.9
		Alphaproteobacteria	*Rhizobiales*	*Xanthobacteraceae*	*Bradyrhizobium*	2.1	0.7
FIELD	L	*Gammaproteobacteria*	*Pseudomonadales*	*Pseudomonadaceae*	*Pseudomonas*	8.7	5.4
		Bacteroidia	*Flavobacteriales*	*Flavobacteriaceae*	*Flavobacterium*	7.3	4.2
		Gammaproteobacteria	*Burkholderiales*	TRA3-20		5.6	2.5
		Gammaproteobacteria	*Burkholderiales*	*Comamonadaceae*		3.8	2.1
		Gammaproteobacteria	*Burkholderiales*	*Sutterellaceae*		3.0	1.2
		Bacteroidia	*Chitinophagales*	*Saprospiraceae*		2.8	1.0
		Gammaproteobacteria	*Burkholderiales*	*Nitrosomonadaceae*	MND1	2.6	1.4
		Gammaproteobacteria	*Xanthomonadales*	*Xanthomonadaceae*	*Pseudoxanthomonas*	2.5	3.1
		Gammaproteobacteria	*Steroidobacterales*	*Steroidobacteraceae*		2.4	0.7
		Babeliae	*Babeliales*	*Vermiphilaceae*		2.3	1.5
	T	*Gammaproteobacteria*	*Steroidobacterales*	*Steroidobacteraceae*	*Steroidobacter*	15.7	4.7
		Gammaproteobacteria	Incertae Sedis	Unknown Family	*Acidibacter*	6.1	1.9
		Gammaproteobacteria	*Pseudomonadales*	*Pseudomonadaceae*	*Pseudomonas*	4.7	5.6
		Acidimicrobiia	*Microtrichales*			4.0	1.9
		Bacteroidia	*Flavobacteriales*	*Flavobacteriaceae*	*Flavobacterium*	3.1	3.6
		Alphaproteobacteria	*Dongiales*	*Dongiaceae*	*Dongia*	3.1	1.0
		Alphaproteobacteria	*Rhizobiales*	Incertae Sedis		2.8	0.8
		Acidimicrobiia	*Microtrichales*	*Ilumatobacteraceae*		2.4	1.1
		Alphaproteobacteria	*Rhizobiales*	*Hyphomicrobiaceae*	*Pedomicrobium*	2.4	1.0
		Alphaproteobacteria	*Rhizobiales*	*Xanthobacteraceae*	*Bradyrhizobium*	2.0	0.7

Suppl. Table VII-5: Differences in bacterial beta diversity in dependence on tree individual and root size section in the loosely (L) and tightly (T) associated root microbiota in the spatial trial. Effect sizes in beta diversity were assessed by pairwise PERMANOVA based on DEICODE distance matrices and p_{adj}-values calculated using Bonferroni's algorithm.

Compartment	Pairs	F.Model	R^2	*p*-value	p_{adj}-value
L	T1 vs T2	1.736	0.023	0.179	1.000
	T1 vs T3	37.763	0.332	0.001	0.006
	T1 vs T4	46.009	0.365	0.001	0.006
	T2 vs T3	26.828	0.266	0.001	0.006
	T2 vs T4	36.274	0.317	0.001	0.006
	T3 vs T4	6.472	0.075	0.001	0.006
	< 1 mm vs 1-2 mm	6.661	0.076	0.002	0.012
	< 1 mm vs 2-4 mm	16.862	0.178	0.001	0.006
	< 1 mm vs > 4 mm	17.485	0.178	0.001	0.006
	1-2 mm vs 2-4 mm	3.281	0.043	0.026	0.156
	1-2 mm vs > 4 mm	9.258	0.109	0.001	0.006
	2-4 mm vs > 4 mm	4.636	0.060	0.003	0.018
T	T1 vs T2	0.393	0.006	0.803	1.000
	T1 vs T3	4.321	0.060	0.008	0.048
	T1 vs T4	7.323	0.093	0.001	0.006
	T2 vs T3	3.384	0.050	0.021	0.126
	T2 vs T4	7.638	0.102	0.001	0.006
	T3 vs T4	4.986	0.066	0.002	0.012
	< 1 mm vs 1-2 mm	10.758	0.132	0.001	0.006
	< 1 mm vs 2-4 mm	23.152	0.282	0.001	0.006
	< 1 mm vs > 4 mm	32.237	0.318	0.001	0.006
	1-2 mm vs 2-4 mm	6.994	0.096	0.002	0.012
	1-2 mm vs > 4 mm	29.427	0.279	0.001	0.006
	2-4 mm vs > 4 mm	12.437	0.163	0.001	0.006

Suppl. Table VII-6: Significant differences in the apple root-associated bacterial community structure due to temporal, root size and spatial effects. The spatial effects in terms of tree-to-tree variation, longitudinal position of the tree and row of the tree were analyzed separately. Effect sizes were analyzed by PERMANOVA based on DEICODE distance matrices. Significant results are printed in bold.

Compart-ment	Input Variable	Variable	PERMANOVA		
			F.Model	R^2	*p*
L	Tree	**Timepoint**	**2.978**	**0.090**	**0.006**
		Root section	**13.681**	**0.137**	**0.001**
		Tree	**3.637**	**0.292**	**0.001**
		Timepoint * Root section	1.935	0.058	0.076
	Row	**Timepoint**	**2.215**	**0.090**	**0.017**
		Root section	**10.175**	**0.137**	**0.001**
		Row	**5.971**	**0.081**	**0.016**
		Timepoint * Root section	1.384	0.056	0.139
		Timepoint * Row	0.725	0.029	0.572
		Root section * Row	0.583	0.008	0.532
		Timepoint * Root section * Row	0.770	0.031	0.508
	Longitudinal position	**Timepoint**	**2.617**	**0.090**	**0.014**
		Root section	**12.022**	**0.137**	**0.001**
		Longitudinal position	**5.652**	**0.129**	**0.014**
		Timepoint * Root section	1.738	0.060	0.089
		Timepoint * Longitudinal position	0.760	0.052	0.619
		Root section * Longitudinal position	0.504	0.012	0.691
		Timepoint * Root section *Longitudinal position	**1.916**	**0.131**	**0.025**
T	Tree	**Timepoint**	**2.980**	**0.119**	**0.018**
		Root section	**7.259**	**0.096**	**0.001**
		Tree	**3.248**	**0.345**	**0.002**
		Timepoint * Root section	1.680	0.067	0.112
	Row	**Timepoint**	**2.010**	**0.119**	**0.043**
		Root section	**4.896**	**0.096**	**0.006**
		Row	**3.970**	**0.078**	**0.010**
		Timepoint * Root section	0.972	0.057	0.379
		Timepoint * Row	0.741	0.044	0.564
		Root section * Row	0.768	0.015	0.410
		Timepoint * Root section *Row	0.646	0.038	0.605
	Longitudinal position	Timepoint	1.739	0.119	0.068
		Root section	**4.236**	**0.096**	**0.011**
		Longitudinal position	2.040	0.093	0.308
		Timepoint * Root section	1.128	0.077	0.309
		Timepoint * Longitudinal position	0.426	0.058	0.928
		Root section * Longitudinal position	0.234	0.011	0.908
		Timepoint * Root section *Longitudinal position	0.489	0.045	0.777

VIII. Appendix B

Supporting information to chapter III

Suppl. Table VIII-1: The hierarchies in each of the trials with the number of samples. Total read number after quality filtering, mean number of reads per sample and the number of samples remaining after quality filtering.

Trial	Hierarchical structure	Number of samples	Total number of reads	Mean number of reads/sample	Samples remaining after quality filtering
Temporal trial	(8 plants x 7 timepoints x 3 treatments + 20 baseline control plants) x 2 compartments	376 root associated samples	18.193.861	58.501	311 samples
Mixed trial	(12 plants x 3 timepoints x 2 treatments + 12 untreated control plants) x 2 compartments	168 root associated samples	4.516.967	32.496	139 samples

Suppl. Table VIII-2: Differences in beta diversity of the root-associated bacterial community of apple saplings in the L- and T-compartment inoculated with two different pathogens (*V. inaequalis* or *P.leucotricha*, additionally a negative control) and sampled at different timepoints. The disease severity, the height of the plant and the number of leaves was measured at each timepoint. Effect sizes were assessed by ANOSIM based on DEICODE distance matrices. Significant results ($p < 0.05$) are printed in bold.

Factor	L-compartment		T-compartment	
	R	*p*-value	R	*p*-value
Treatment	0.007	0.209	**0.035**	**0.010**
Timepoint	**0.350**	**0.001**	**0.334**	**0.001**
Disease severity	**0.112**	**0.001**	**0.092**	**0.005**
Height	**0.109**	**0.027**	0.074	0.080
Number of leaves	0.020	0.128	**0.050**	**0.007**

Suppl. Table VIII-3: Differences in beta diversity of the root-associated bacterial community of apple saplings in the L- and T-compartment treated with two different pathogens and sampled at different timepoints (TP). Effect sizes were assessed by PERMANOVA based on DEICODE distance matrices. Significant results ($p < 0.05$) are printed in bold.

TP	Factor	L-compartment				T-compartment			
		df	R^2	F	*p*-value	df	R^2	F	*p*-value
3	Treatment	2	0.105	0.703	0.647	2	0.129	1.335	0.260
6	Treatment	2	0.022	0.114	0.975	2	0.119	0.882	0.509
12	Treatment	2	0.153	1.345	0.282	2	0.096	1.060	0.380
	DS	3	0.223	1.307	0.308	3	0.267	1.971	0.104
	Treatment * DS	1	0.057	1.009	0.375	1	0.050	1.101	0.386
16	Treatment	2	0.148	1.196	0.357	2	0.122	0.692	0.654
	DS	2	0.263	2.122	0.151	2	0.084	0.479	0.759
	Treatment * DS	1	0.091	1.474	0.241	1	0.267	1.517	0.271
28	Treatment	2	0.246	2.110	0.086	**2**	**0.254**	**2.998**	**0.017**
	DS	3	0.062	0.356	0.850	3	0.128	1.006	0.428
	Treatment * DS	1	0.052	0.891	0.419	1	0.151	3.552	0.099
40	Treatment	**2**	**0.144**	**2.721**	**0.038**	2	0.094	1.576	0.187
	DS	4	0.138	1.305	0.255	4	0.071	0.595	0.738
	Treatment * DS	1	0.033	1.239	0.310	1	0.062	1.047	0.313
48	Treatment	**1**	**0.102**	**3.268**	**0.043**	1	0.002	0.036	0.973
	DS	**4**	**0.432**	**3.467**	**0.017**	4	0.071	0.459	0.830

Suppl. Table VIII-4: Dispersion of the root-associated bacterial community of young apple plants between different treatments at different timepoints (DAI) in the L- and T-compartment. The different treatments included inoculations with either *V. inaequalis* (V) or *P. leucotricha* (L) and an uninoculated control (C). Effect sizes were assessed by PERMDISP and Tukey's test based on DEICODE distance matrices and p-values adjusted after multiple comparison. Significant results are printed in bold.

DAI	Comparison	L-compartment		T-compartment	
		Difference	p_{adj}	Difference	p_{adj}
3	L-C	-0.408	0.794	0.850	0.133
	V-C	-0.877	0.343	-0.360	0.671
	V-L	-0.469	0.691	**-1.210**	**0.025**
6	L-C	-0.049	0.997	0.704	0.222
	V-C	0.164	0.971	-0.334	0.689
	V-L	0.213	0.947	-1.039	0.066
12	L-C	0.096	0.985	0.924	0.223
	V-C	-0.451	0.726	0.059	0.993
	V-L	-0.547	0.600	-0.865	0.265
16	L-C	0.520	0.780	0.607	0.577
	V-C	0.267	0.923	-0.296	0.872
	V-L	-0.253	0.931	-0.903	0.230
28	L-C	-0.682	0.350	-0.405	0.796
	V-C	-0.180	0.925	0.139	0.968
	V-L	0.503	0.555	0.544	0.648
40	L-C	0.199	0.812	0.204	0.889
	V-C	-0.250	0.834	0.291	0.865
	V-L	-0.449	0.451	0.087	0.981
48	V-C	0.473	0.147	0.131	0.762

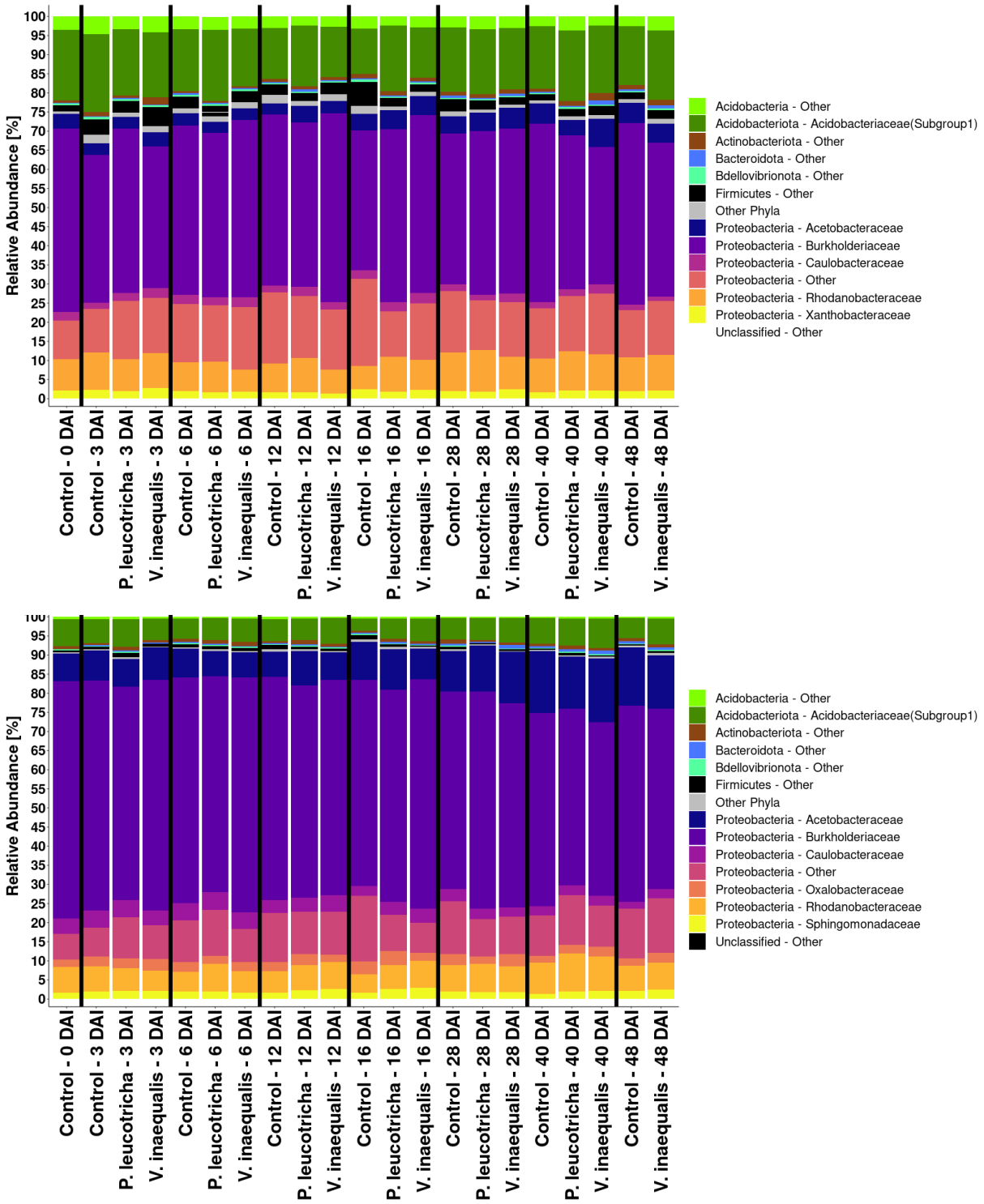

Suppl. Fig. VIII-1: Composition of the root-associated bacterial community of apple plants as revealed by 16S rRNA gene amplicon sequencing in the temporal trial. The relative abundance of bacterial families in samples from three different treatments (*P. leucotricha*, *V. inaequalis* and a negative control) sampled at different days after inoculation (DAI) in the loosely associated (L, upper panel) and tightly associated (T, lower panel) compartment is shown. Phyla and their families with < 2% relative abundance in the respective treatment were grouped as “Other”.

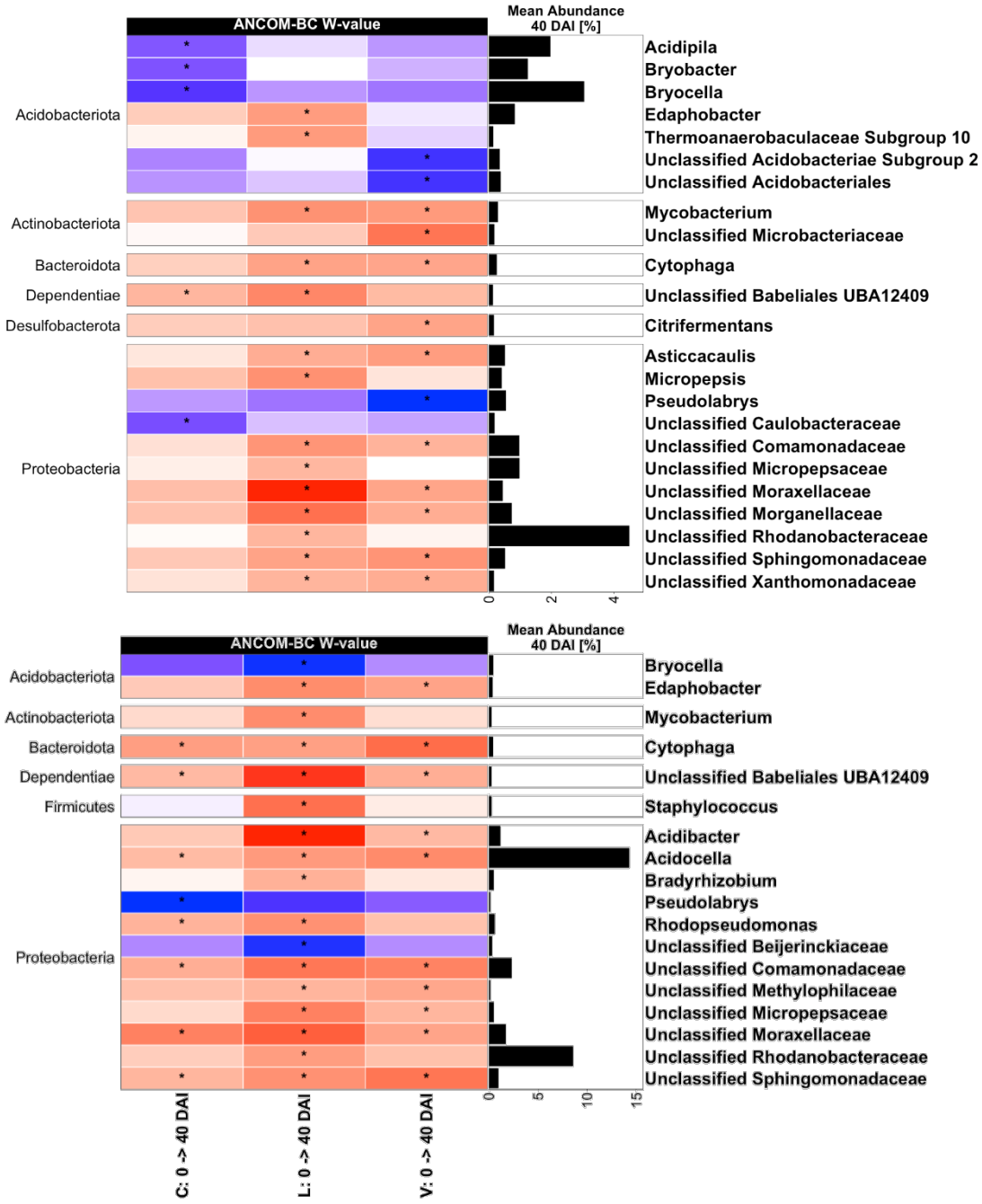

Suppl. Fig. VIII-2: Differential abundance analysis of genera in the L- and T-compartment (panel A and B, respectively) in dependence on pathogen infection 40 days after inoculation (DAI) compared to 0 DAI based on ANCOM-BC. Plants were either inoculated with *V. inaequalis* (V) or *P. leucotricha* (L) and are shown besides an uninoculated control treatment (C). The heatmap shows the coefficients obtained from the ANCOM-BC log-linear model divided by their standard error (called W-value). The colour code indicates differential abundances of genera between the two timepoints with red indicating an increase in relative abundance at 40 DAI compared to 0 DAI. A "*" is shown if ANCOM-BC showed significant differences using the adjusted *p*-value in this comparison. The mean relative abundances of the taxa are displayed at 40 DAI in percent. In the L-compartment, most identified genera of the pathogen inoculated plants belong to the phylum *Proteobacteria*, e.g., unclassified members of the *Comamonadaceae*, *Moraxellaceae*, *Morganellaceae*, *Sphingomonadaceae* and *Xanthomonadaceae*. In the control plants, several *Acidobacteriota* such as *Acidipila*, *Bryobacter* or *Bryocella* were significantly decreased in relative abundance at 40 DAI, though not in the inoculated plants. Only few observations like these were made in the T-compartment with *Edaphobacter*, *Acidibacter* and unclassified members of *Methylophilaceae* and *Micropepsaceae* being significantly increased in the inoculated plants 40 DAI, but not in the control plants.

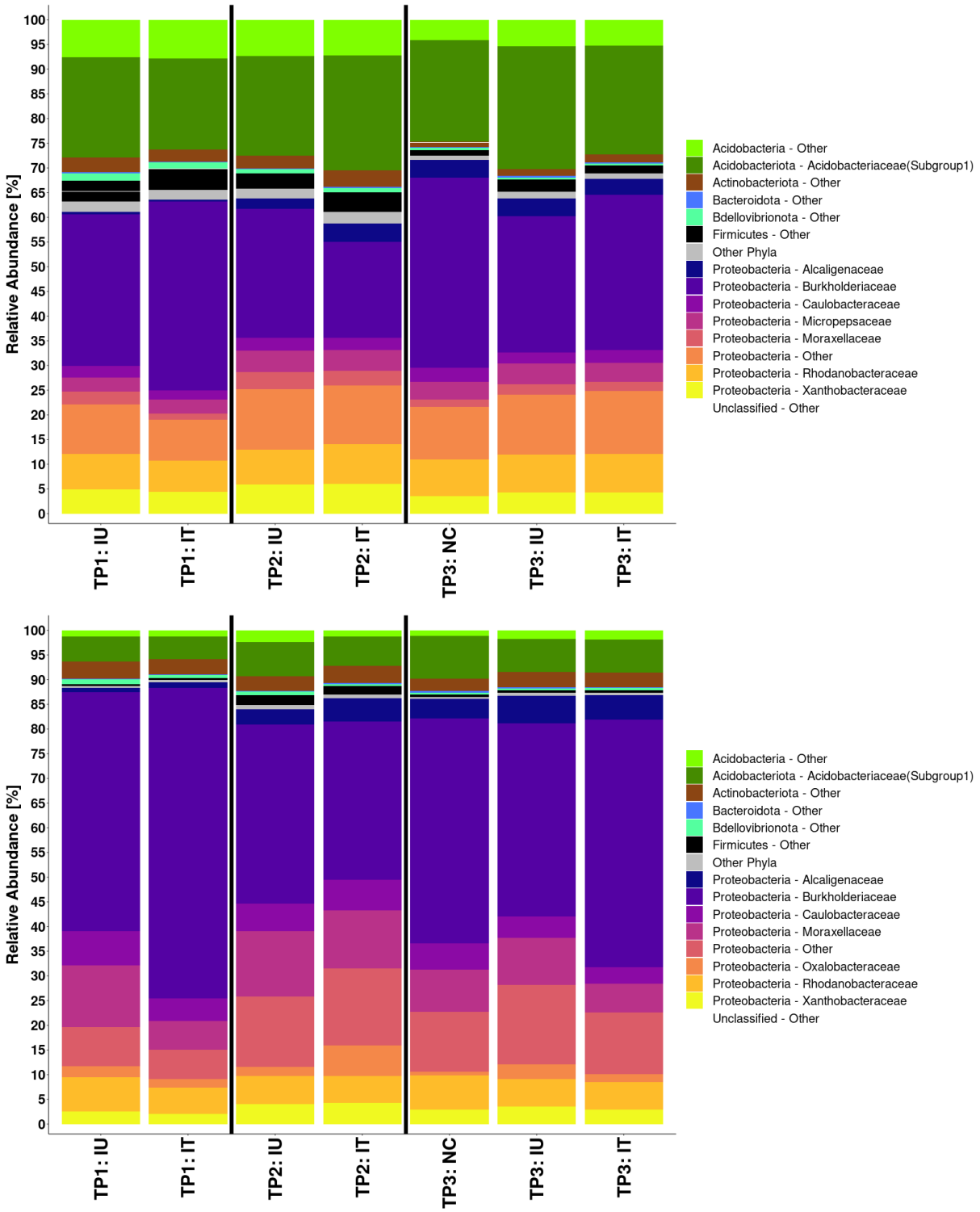

Suppl. Fig. VIII-3: Composition of the root-associated bacterial community of apple plants as revealed by 16S rRNA gene amplicon sequencing in the mixed trial. The relative abundance of bacterial families in samples from three different treatments (IU: inoculated & untreated, IT: inoculated & treated, and NC: negative control) at three different timepoints (TP) in the loosely associated (L, upper panel) and tightly associated (T, lower panel) compartment is shown. Phyla and their families with < 2% relative abundance in the respective treatment were grouped as “Other”.

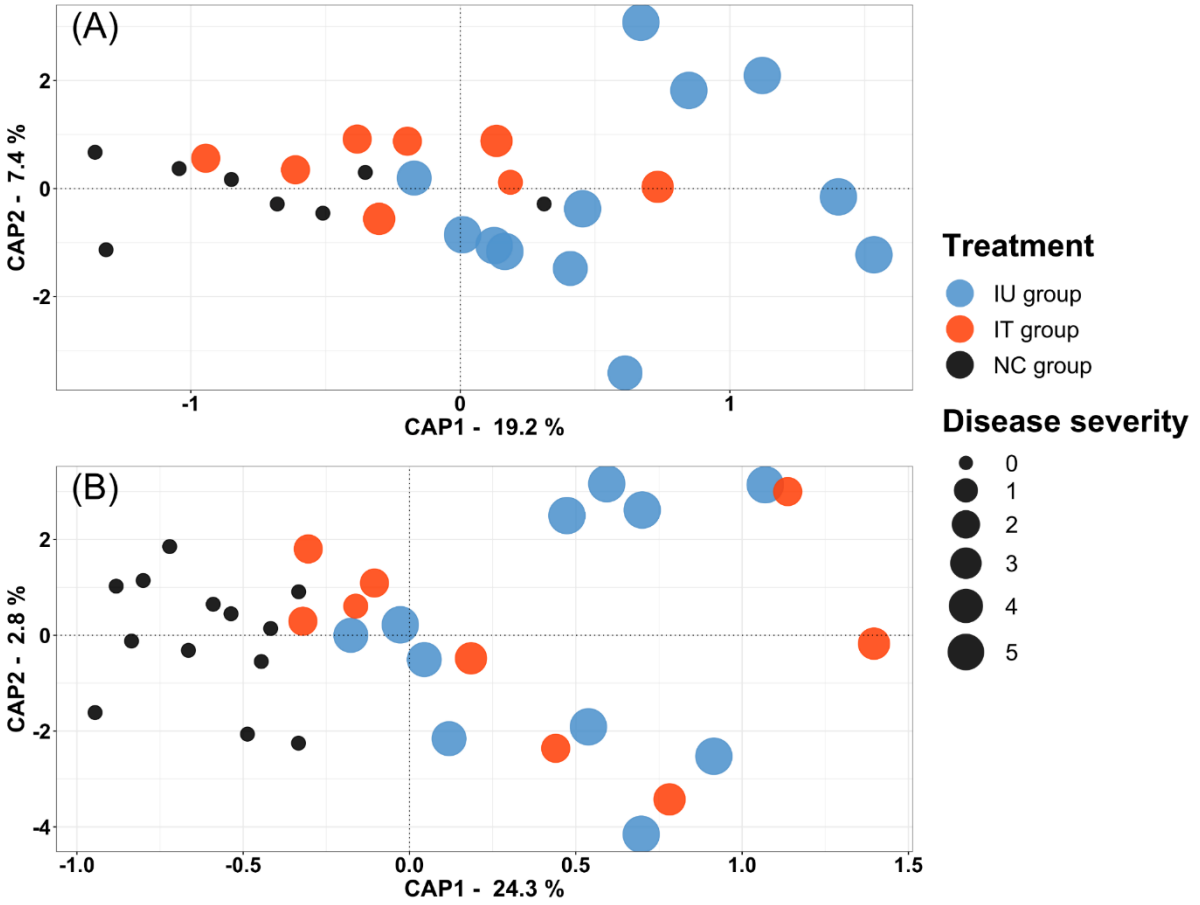

Suppl. Fig. VIII-4: Variation in beta diversity of differently treated apple saplings at timepoint (TP) 3 in the L-compartment (**A**) and T-compartment (**B**). Variation is presented based on constrained analysis of principal coordinates (CAP) using DEICODE distance matrices; it is constrained by the variables treatment and disease severity. Plants were either inoculated with *P. leucotricha* and left untreated (IU) or were additionally treated with a synthetic fungicide (IT), or they underwent a treatment with water as control (NC). The different treatments are shown in different colours, and disease severity is illustrated by different symbol sizes, rated on a 0-5 scale with 0 = healthy plants and 5 = plants having multiple leaves entirely covered with mycelium and with leaves close to senescence.

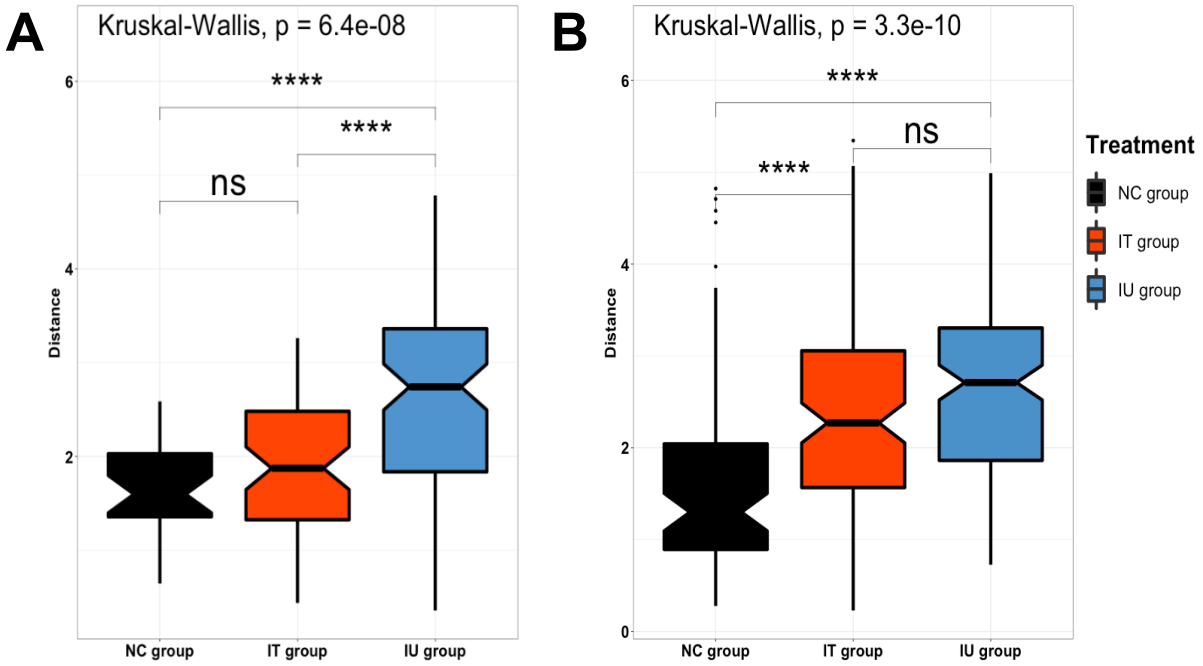

Suppl. Fig. VIII-5: Boxplots showing the differences between two different treatments (IT and IU) to an untreated control group (NC group) for the (**A**) L-compartment and (**B**) T-compartment at TP3 based on DEICODE distances. Significant differences were calculated with pairwise Kruskal-Wallis tests ("****" = *p*-value of < 0.001, ns = non-significant).

IX. Appendix C

Supporting information to chapter IV

Suppl. Table IX-1: Table of the used plant health protecting products with their active ingredients, the standard field application rate and applied concentrations.

Trial	Active Ingredient	Product	Field rate	Concentration
Temporal	Aliette WG 80	Fosetyl-Aluminium	3.0 kg/ha in 600 l/ha water	0.3 g in 100 ml/m²
	Serenade ASO	*Bacillus amyloliquefaciens* strain QST 713	4.0 l/ha in 600 l/ha water	0.40 ml in 100 ml/m²
	Movento 240 SC	Spirotetramat	0.3 l/ha in 600 l/ha water	0.03 ml in 100 ml/m²
	Luna Privilege SC 500	Fluopyram	0.5 l/ha in 600 l/ha water	0.05 ml in 100 ml/m²
	Water	negative control	600 l/ha	100 ml/m²
Concentration	Aliette WG 80	Fosetyl-Aluminium	3.0 kg/ha in 600 l/ha water	0.3 g in 100 ml/m²
				0.6 g in 100 ml/m²
	Serenade ASO	*Bacillus amyloliquefaciens* strain QST 713	4.0 l/ha in 600 l/ha water	0.40 ml in 100 ml/m²
				as above, but no felt map
	Movento 240 SC	Spirotetramat	0.3 l/ha in 600 l/ha water	0.03 ml in 100 ml/m²
				0.06 ml in 100 ml/m²
	Luna Privilege SC 500	Fluopyram	0.5 l/ha in 600 l/ha water	0.05 ml in 100 ml/m²
				0.10 ml in 100 ml/m²
	Water	negative control	600 l/ha	100 ml/m²
Strawberry	Aliette WG 80	Fosetyl-Aluminium	10 kg/ha in 1000 l/ha	1 g in 100 ml/m²
				2 g in 100 ml/m²
	Serenade ASO	*Bacillus amyloliquefaciens* strain QST 713	8 l/ha in 1000 l/ha	0,80 ml in 100 ml/m²
				as above, but no felt map
	Movento 240 SC	Spirotetramat	0.3 l/ha in 1000 l/ha	0,03 ml in 100 ml/m²
				0,06 ml in 100 ml/m²
	Luna Privilege SC 500	Fluopyram	0.5 l/ha in 1000l/ha	0,05 ml in 100 ml/m²
				0,10 ml in 100 ml/m²
	Bactiva®	Rhizobacteria and *Trichoderma*	2 kg/ha at 75.000 plants/ha	27 mg/plant
				54 mg/plant
	Water	negative control	1000 l/ha	100 ml/m²

Suppl. Fig. IX-1: Separation into fine (right) and thick (left) roots of the strawberry root system.

Suppl. Table X-2. The hierarchies in each of the trials with the number of samples. Total read number, mean number of reads per sample and the number of samples remaining after quality filtering.

Trial	Hierarchical structure	Number of samples	Total number of reads	Mean number of reads/sample	Samples remaining after quality filtering
Temporal trial	10 plants x 5 treatments x 2 sampling dates x 2 compartments	200 root associated samples	6.513.594	39.476	165 samples
Concentration trial	(10 plants x 4 treatments x 2 application modes + 15 untreated control plants) x 2 compartments	190 root associated samples	6.744.793	41.893	161 samples
Strawberry trial	10 plants x 6 treatments x 2 application modes x 2 root fractions x 2 compartments	480 root associated samples	20.309.793	52.345	388 samples

Suppl. Table IX-3: Compositional variation in the root associated bacterial communities in the strawberry trial due to the application of different plant health protecting products (PHPP) and their different modes of application. The evaluation was performed independently for both root compartments (Comp.: loosely (L) and tightly (T) fraction). The significant influence of the different root sections (fine and thick roots) resulted in further data subsetting. Five different products were applied, each with two different application modes, and those treatments were grouped as "PHPP Application". Differences in composition and dispersion were assessed by PERMANOVA and PERMDISP, respectively, applied to DEICODE distance matrices. Results with significant differences are printed in bold.

			PERMANOVA				PERMDISP	
Comp.	Root section	Variable	df	F.model	R^2	*p*-value	F-value	*p*-value
L	Together	**Root section (RS)**	**1**	**85.103**	**0.296**	**0.001**	3.077	0.081
		PHPP Application	**10**	**2.143**	**0.074**	**0.003**	0.671	0.750
		RS * PHPP Application	10	0.939	0.033	0.588		
	Fine	**PHPP Application**	**10**	**1.693**	**0.157**	**0.016**	1.031	0.425
	Thick	PHPP Application	10	1.383	0.146	0.096	0.435	0.925
T	Together	**Root section (RS)**	**1**	**85.047**	**0.313**	**0.001**	**5.573**	**0.019**
		PHPP Application	10	0.982	0.036	0.523	1.145	0.331
		RS * PHPP Application	10	0.504	0.019	0.993		
	Fine	PHPP Application	10	0.942	0.092	0.556	0.694	0.728
	Thick	PHPP Application	10	0.978	0.110	0.522	1.238	0.280

Suppl. Table IX-4: Table of pairwise PERMDISP results comparing different product applications in the strawberry trial. PHPP application occurred at the recommended application rate (r) and twice the rate (d) in comparison to a control group in the L- and T-compartment (Comp.) in different root sections (RS): fine roots (FR) or thick roots (TR). In case of Serenade both applications were at the recommended rate but with (w) or without (w/o) a felt mat covering the soil surface. Results with significant differences are printed in bold.

Comp.		Aliette		Luna		Movento		Serenade		Bactiva	
RS		r	d	r	d	r	d	w	w/o	r	d
L-FR	*p*-value	0.408	0.183	0.192	**0.018**	0.054	0.853	0.611	0.638	0.094	0.362
	p_{adj}	0.583	0.384	0.384	0.180	0.270	0.853	0.709	0.709	0.313	0.583
L-TR	*p*-value	0.736	0.787	0.951	0.848	0.687	0.746	0.390	0.765	0.514	0.765
	p_{adj}	0.942	0.942	0.951	0.942	0.942	0.942	0.942	0.942	0.942	0.942
T-FR	*p*-value	0.665	**0.006**	0.468	0.231	0.466	0.944	0.244	0.556	0.153	0.829
	p_{adj}	0.831	0.060	0.780	0.610	0.780	0.944	0.610	0.794	0.610	0.921
T-TR	*p*-value	**0.003**	**0.004**	**0.009**	0.597	**0.038**	**0.051**	0.236	**0.044**	0.189	0.052
	p_{adj}	**0.020**	**0.020**	**0.030**	0.597	0.074	0.074	0.262	0.074	0.236	0.074

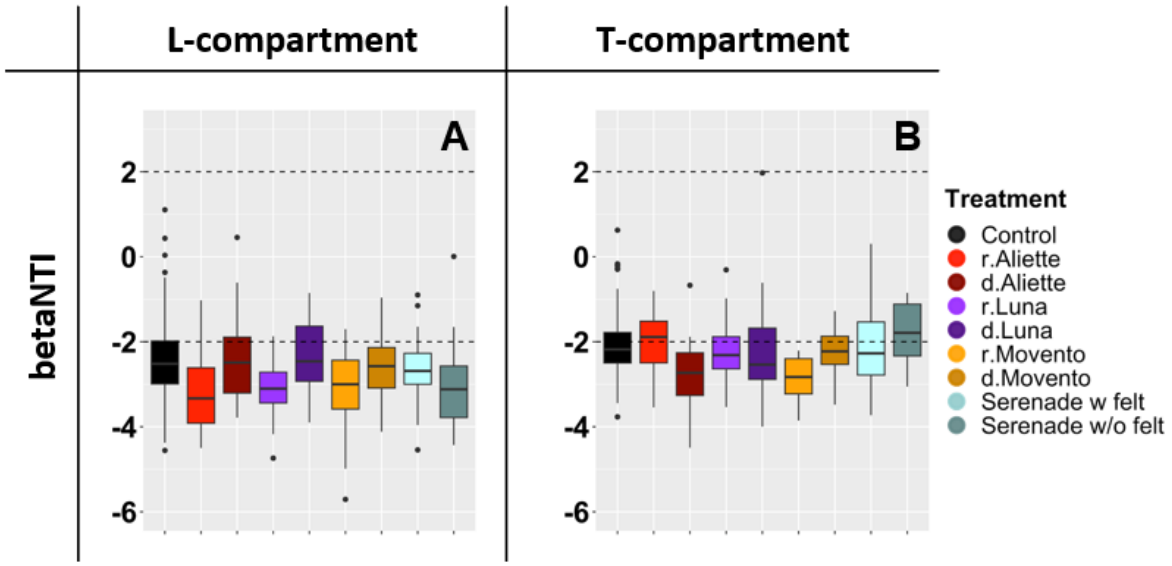

Suppl. Fig. IX - 2: Patterns of the beta Nearest Taxon Index (betaNTI) in the concentration trial. Patterns between different treatments (**A**) in the L-compartment and (**B**) the T-compartment are shown. Specifically, a betaNTI or betaNRI between –2 and 2 reveals dominance of stochastic processes, whereas |betaNRI| or |betaNTI| >2 reveals the significant dominance of deterministic processes. The products Aliette, Luna and Movento were either applied at the recommended rate (r) or twice the rate (double: d). Serenade was applied at the recommended rate but with (w felt) or without a felt mat (w/o felt) to cover the soil.

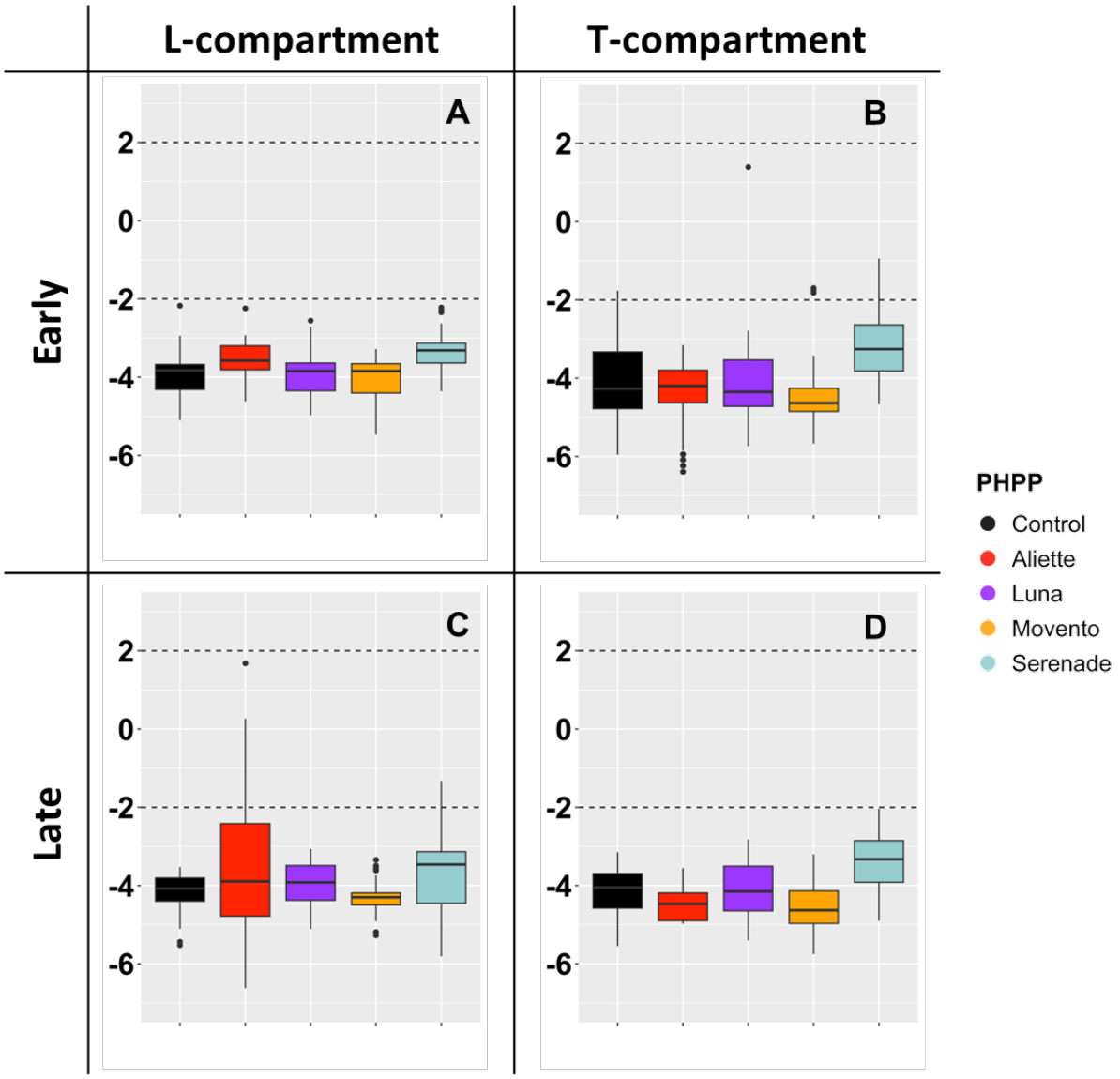

Suppl. Fig. IX - 3: Patterns of beta Nearest Taxon Index (betaNTI) in the bacterial community of the temporal trial upon different plant health protecting product (PHPP) treatments in the L-compartment (**A** and **C**) and the T-compartment (**B** and **D**) at two different timepoints (early and late).

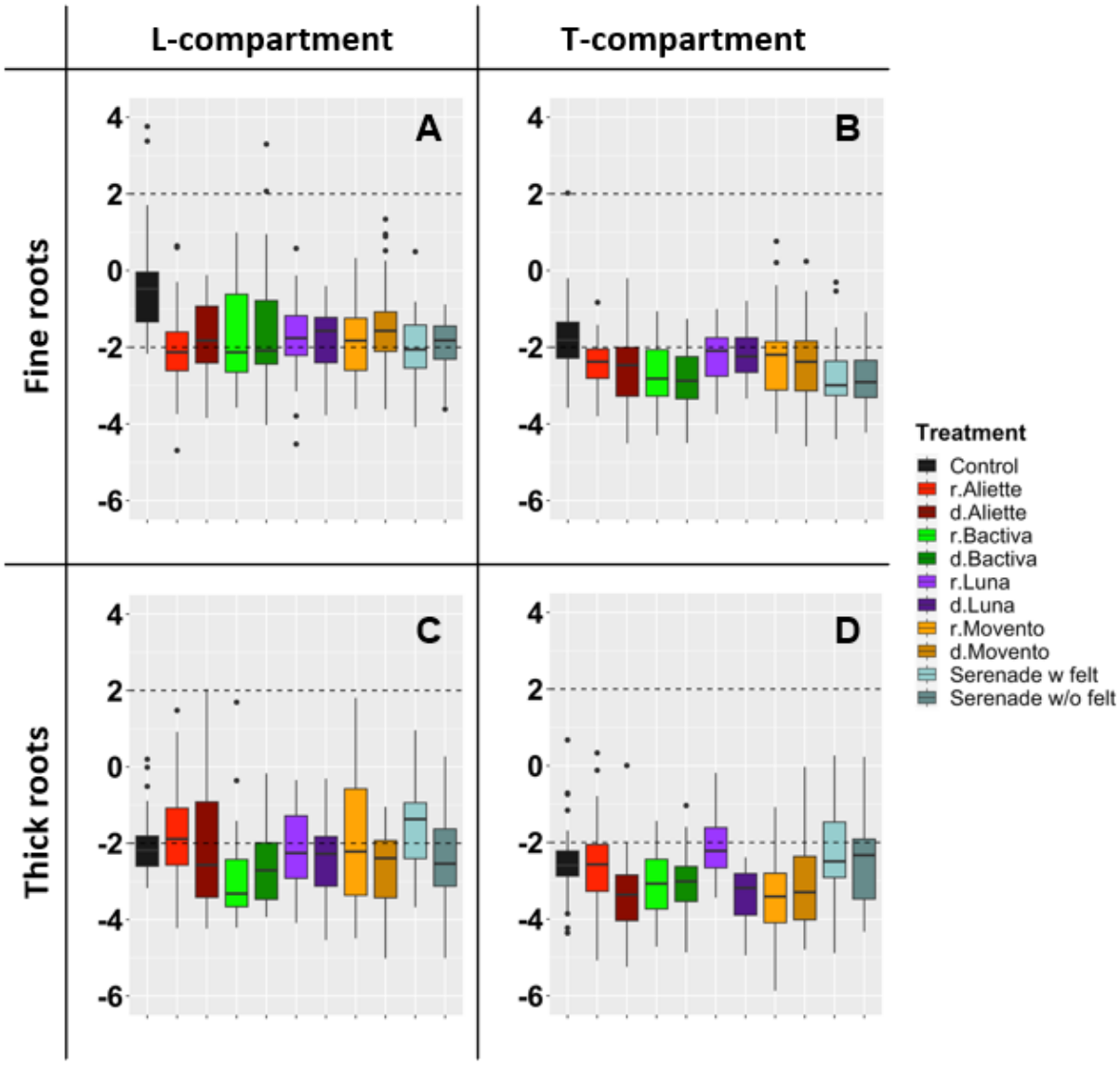

Suppl. Fig. IX - 4: Patterns of beta Nearest Taxon Index (betaNTI a,b) and beta Net Relatedness Index (betaNRI c,d) in the concentration trial. Patterns between different treatments in the L-compartment (a and c) and the T-compartment (b and d) are shown. Specifically, a betaNTI/betaNRI between –2 and 2 reveals a dominance of stochastic processes whereas |betaNRI| / |betaNTI| >2 reveals the significant dominance of deterministic processes. The products Aliette, Luna and Movento were either applied at the recommended rate (r) or twice the rate (double: d). Serenade was applied at the recommended rate but with (w felt) or without a felt map (w/o felt) to cover the soil.

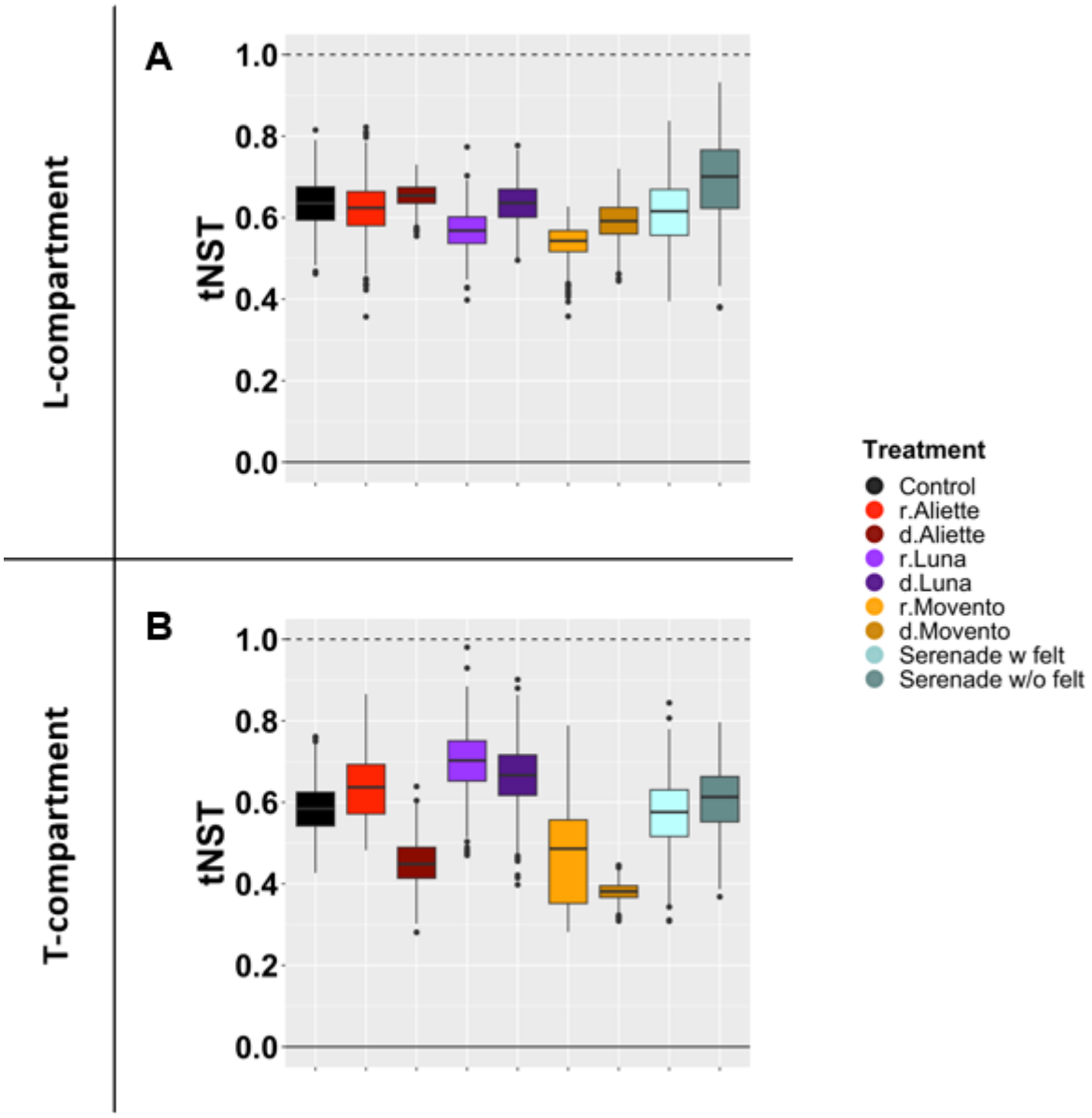

Suppl. Fig. IX - 5: Community assembly process measurements by taxonomic normalized stochasticity ratios (tNST) based on Jaccard's distance in the concentration trial. Ratios for bacterial communities upon different PHPP treatments in the L-compartment (**A**) and the T-compartment (**B**) are shown. The products Aliette, Luna and Movento were either applied at the recommended rate (r) or twice the rate (double: d). Serenade was applied at the recommended rate but with (w felt) or without a felt mat (w/o felt) to cover the soil.

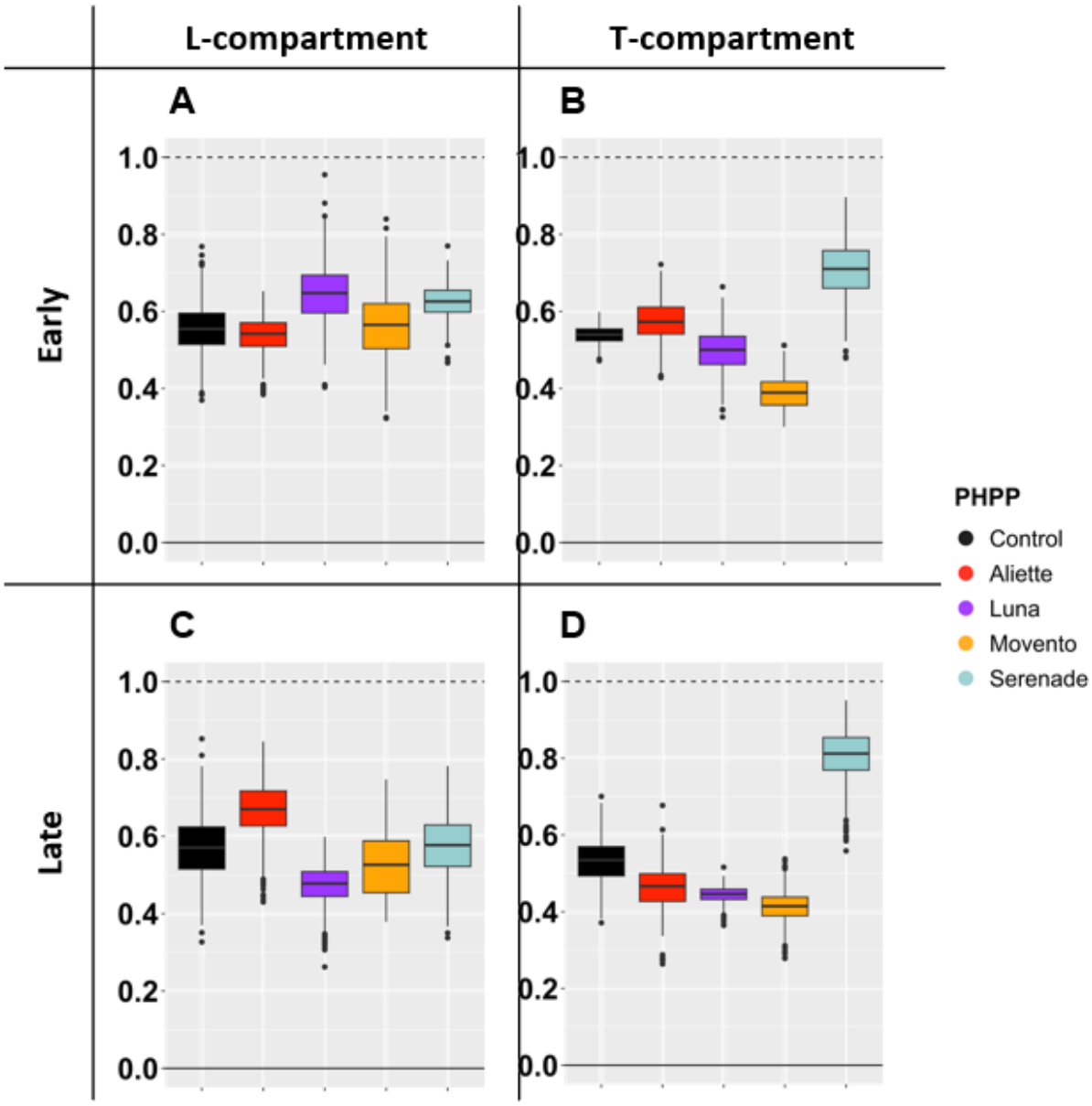

Suppl. Fig. IX - 6: Community assembly process measurements by taxonomic normalized stochasticity ratios (tNST) based on Jaccard's distance in the temporal trial. Ratios for bacterial communities upon different PHPP treatments in the L-compartment (**A** and **C**) and the T-compartment (**B** and **D**) at two different sampling timepoints (early and late) are shown.

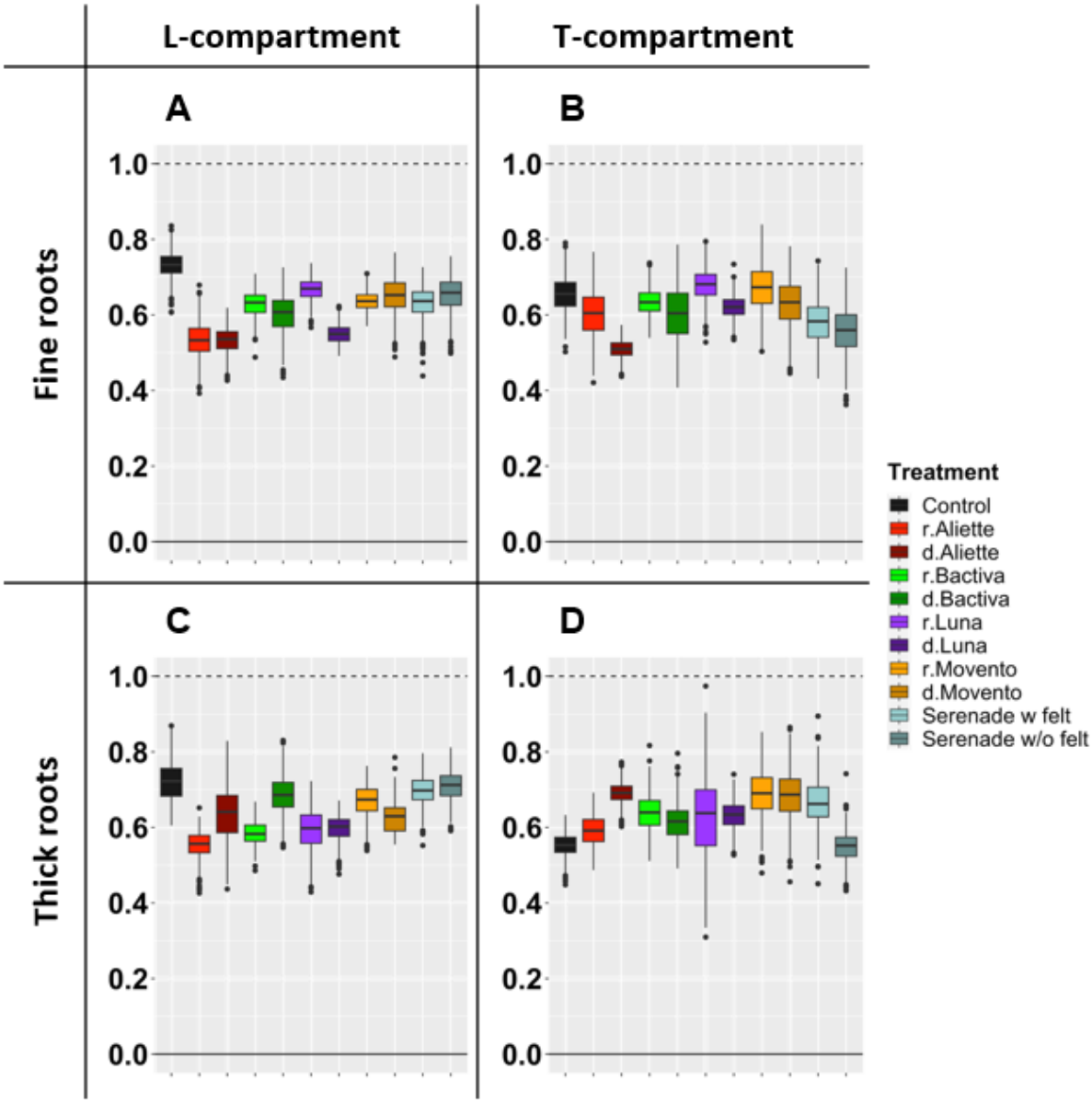

Suppl. Fig. IX - 7: Community assembly process measurements by taxonomic normalized stochasticity ratios (tNST) based on Jaccard's distance in the strawberry trial. Ratios for bacterial communities upon different PHPP treatments in the L-compartment (**A** and **C**) and the T-compartment (**B** and **D**) in two different root sections (fine and thick roots) are shown. The products Aliette, Bactiva, Luna and Movento were either applied at the recommended rate (r) or twice the rate (double: d). Serenade was applied at the recommended rate but with (w felt) or without a felt mat (w/o felt) to cover the soil.

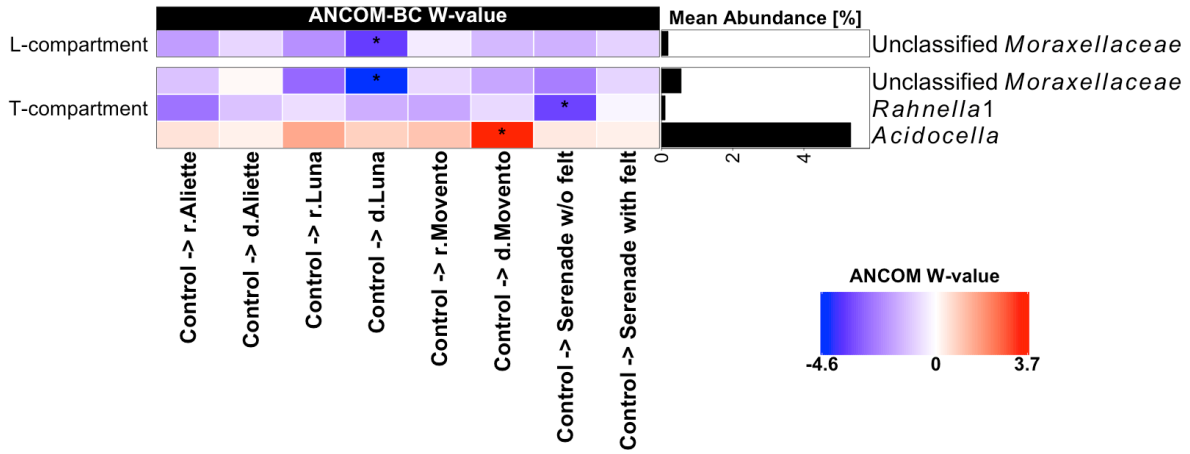

Suppl. Fig. IX - 8: Differential abundance analysis of bacterial communities in the L- and T-compartment of PHPP treated apple plants versus control plants in the concentration trial using ANCOM-BC at genus level resolution. Plants were treated with one of four different plant health protecting products with different application modes or water as control. The products Aliette, Luna and Movento were either applied at the recommended rate (r.) or twice the rate (d.). Serenade was applied at the recommended rate, but in case of the "w/o felt" treatment the felt mat covering the soil of all samples was taken off and the product was thus in direct contact with the soil. Individual models were calculated for each compartment (L and T). The heatmap shows the coefficients obtained from the ANCOM-BC log-linear model divided by their standard error (called W-value). The colour code indicates differential abundances between a treatment and control with red indicating enrichment in the last value of the column name (i.e. the respective PHPP treatment). A "*" is shown if ANCOM-BC showed significant differences using the adjusted *p*-value in this comparison ($p_{adj} < 0.05$). The mean relative abundances of the taxa across all treatments but in their respective compartment are shown in the right horizontal barplot in percent. linear model divided by their standard error (called W-value). The colour code indicates differential abundances between a treatment and control with red indicating enrichment in the last value of the column name (i.e. the respective PHPP treatment). A "*" is shown if ANCOM-BC showed significant differences using the adjusted *p*-value in this comparison ($p_{adj} < 0.05$). The mean relative abundances of the taxa across all treatments but in their respective compartment are shown in the right horizontal barplot in percent.

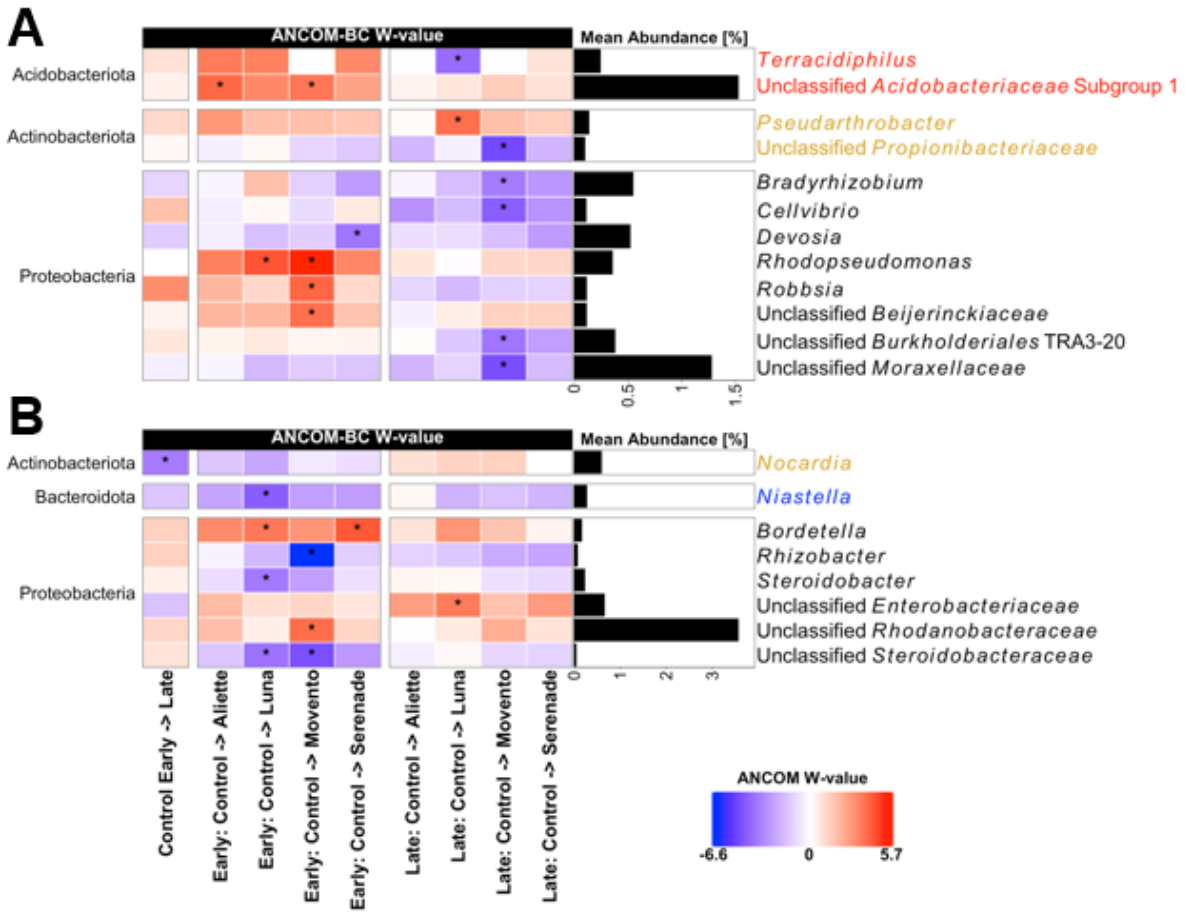

Suppl. Fig. IX - 9: Differential abundance analysis of bacterial communities in the L- and T-compartment (**A** and **B**, respectively) of PHPP treated young apple plants at two different timepoints in the temporal trial using ANCOM-BC at genus level resolution. Plants were treated with one of four different plant health protecting products or water as control and sampled either one (early) or two weeks (late) after the last PHPP application. The heatmap shows the coefficients obtained from the ANCOM-BC log-linear model divided by their standard error (called W-value). The colour code indicates differential abundances between two compartments with red indicating enrichment as given at the last position in the column name. A "*" is shown if ANCOM-BC showed significant differences using the adjusted *p*-value in this comparison ($p_{adj} < 0.05$). The mean relative abundances of the taxa across all treatments is shown in the right horizontal barplot in percent.

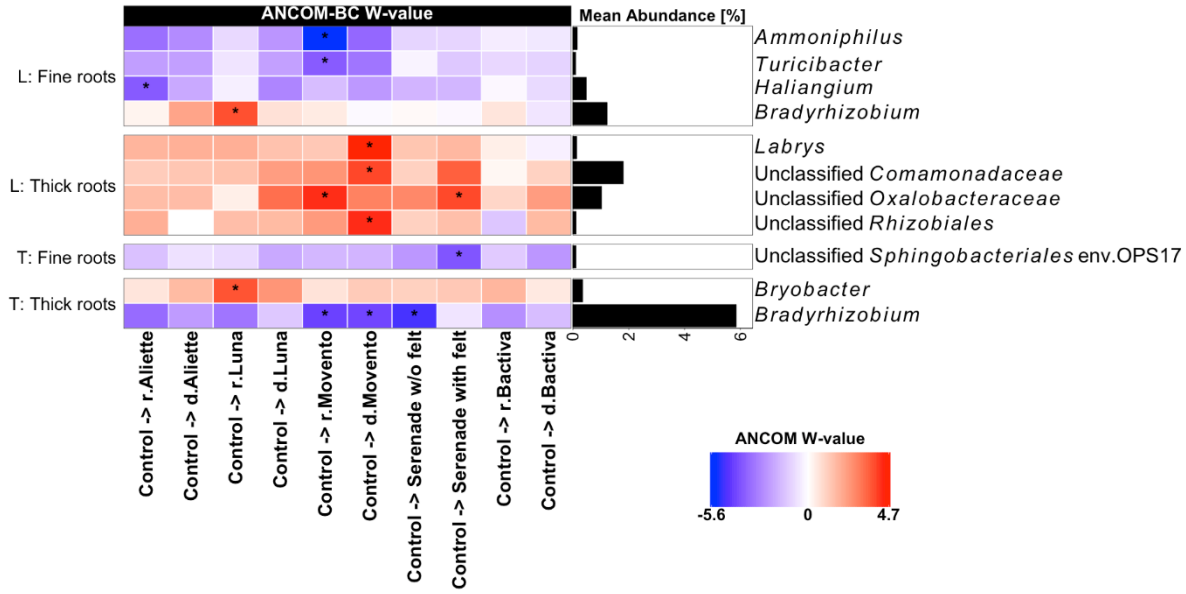

Suppl. Fig. IX - 10: Differential abundance analysis of bacterial communities in the L- and T-compartment of PHPP treated young strawberry plants at genus level using ANCOM-BC. The root system was divided into fine and thick roots. Plants were treated with one of five different plant health protecting products with different application modes or water as control. The products Aliette, Luna Movento and Bactiva were either applied at the recommended rate (r.) or twice the rate (d.). Serenade was applied at the recommended rate but in case of the "w/o felt" treatment, the felt mat covering the soil of all samples was taken off before product application and the product was thus in direct contact with the soil. Individual models were calculated for each compartment and root type. The heatmap shows the coefficients obtained from the ANCOM-BC log-linear model divided by their standard error (called W-value). The colour code indicates differential abundances between respective PHPP treatments and control with red indicating enrichment in PHPP treated plants. A "*" is shown if ANCOM-BC showed significant differences using the adjusted *p*-value in this comparison ($p_{adj} < 0.05$). The mean relative abundances of the taxa across all treatments is shown in the right horizontal barplot in percent. Scaling of colour code and relative abundance is adjusted for each plot independently.

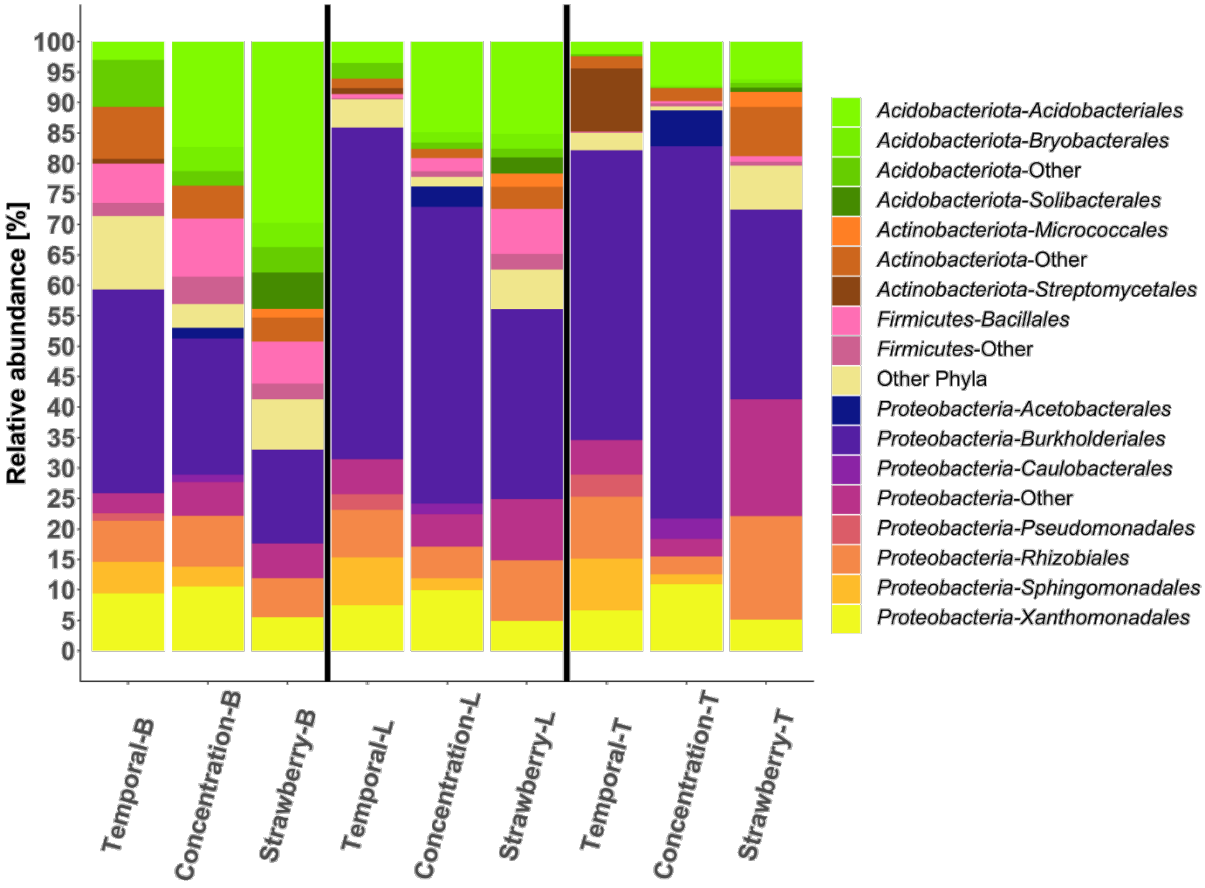

Suppl. Fig. IX - 11: Relative abundance of bacterial orders in samples from three different greenhouse trials (Temporal, Concentration, and Strawberry) in the bulk soil (B), loosely associated (L) and tightly associated (T) compartment. Phyla and their orders with < 2 % relative abundance in the respective trial were grouped as “Other”.

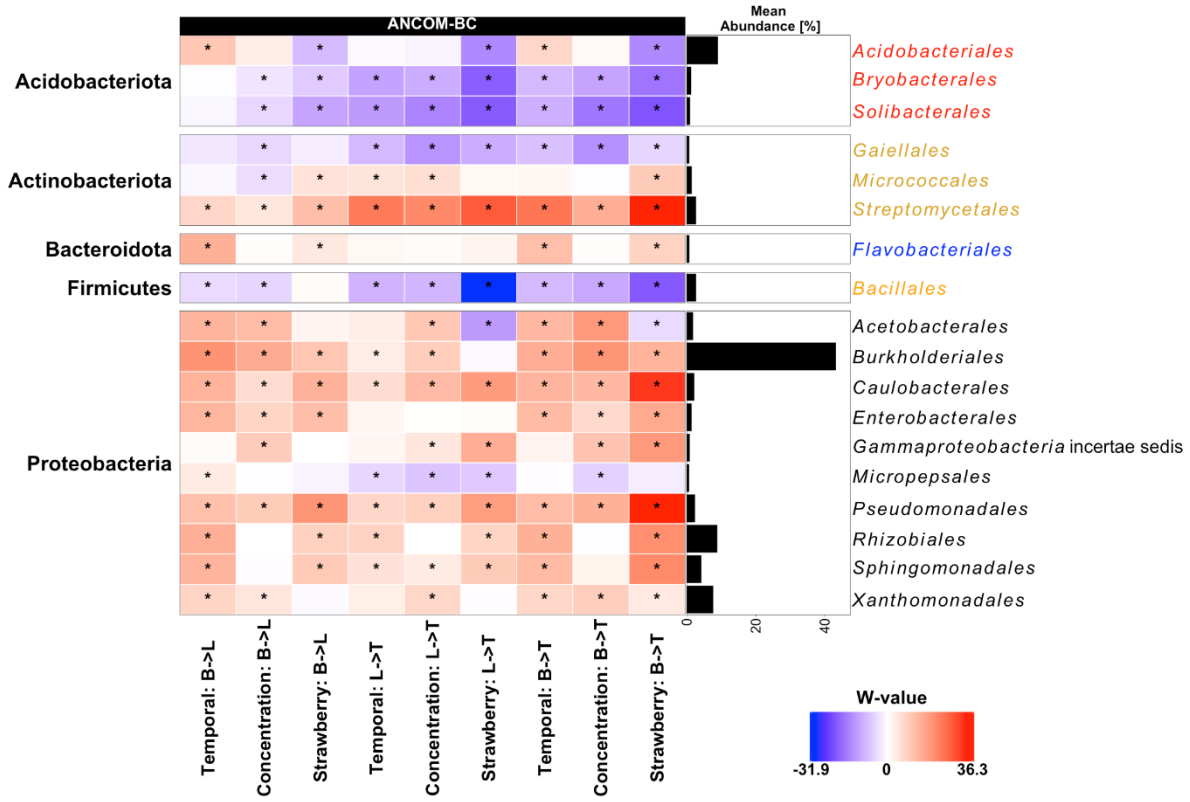

Suppl. Fig. IX - 12: Differential abundance analysis of bacterial orders obtained from bulk soil (B) and root compartments with loosely (L) and tightly (T) associated bacteria in the three experimental trials (Temporal, Concentration, Strawberry) using ANCOM-BC. The heatmap shows the coefficients obtained from the ANCOM-BC log-linear model divided by their standard error (called W-value). The colour code indicates differential abundances between two compartments with red indicating enrichment in the last value of the column name. A "*" is shown if ANCOM-BC showed significant differences using the adjusted *p*-value in this comparison ($p_{adj} < 0.05$). The mean abundance of the orders over all trials is shown in the adjacent barplot in percent and only orders with an overall mean abundance ≥ 0.5 % are shown. The orders in the heatmap rows are sorted and separated by the phylum they belong to and are displayed in different colours.

X. Appendix D

Supporting information to the synopsis

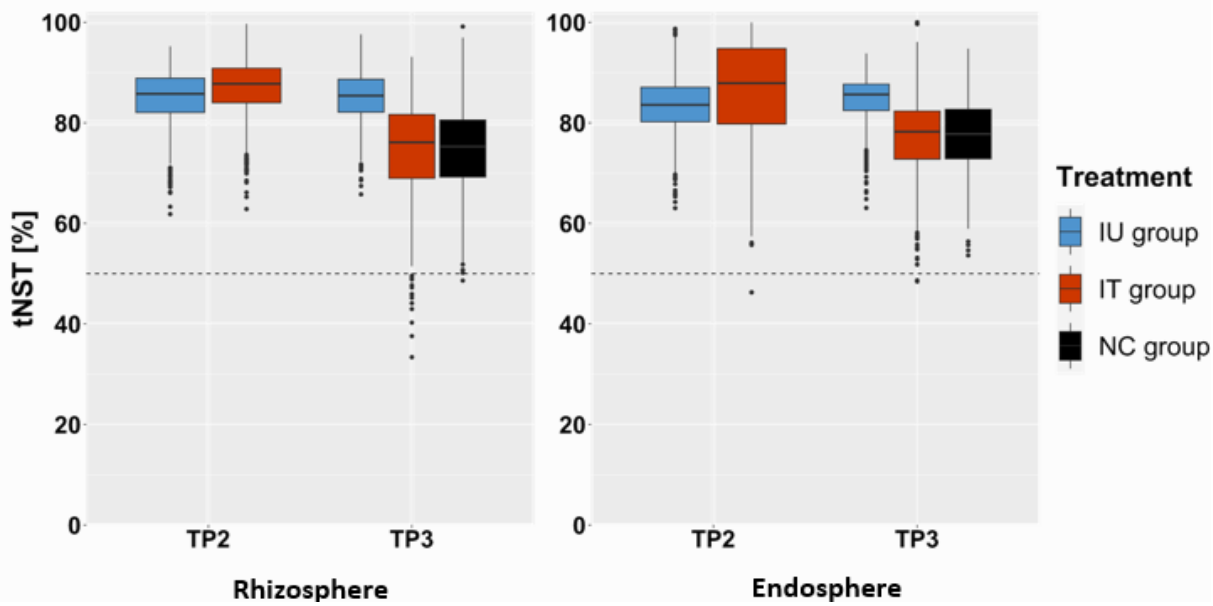

Suppl. Fig. X - 1: Community assembly process measurements by taxonomic normalized stochasticity ratios (tNST) based on Jaccard's distance in the combined trial. Ratios for bacterial communities upon different treatments in the rhizosphere and endosphere are shown. The IT group received a preventative treatment with the fungicide Aliette. After two weeks, both the IU and IT group received an inoculation with the foliar pathogen *P. leucotricha*. When disease symptoms became severe, the IT group received a curative Aliette application. The NC group was treated with water instead of a fungicide application or pathogen suspension.

Danksagung

An erster Stelle möchte ich mich ganz herzlichst bei meiner Doktormutter und Mentorin Frau Prof. Dr. Claudia Knief bedanken, die mir die Gelegenheit gegeben hat diese Dissertation anzufertigen. Ich danke dir für die vielen, äußerst wertvollen Gespräche und die ganze Arbeit, die du in dieses Projekt investiert hast! Du hattest immer eine offene Tür und ich konnte mich jederzeit mit Fragen an dich wenden. Auch nach meinem Ausscheiden aus der Arbeitsgruppe schätze ich weiterhin die offenen und inspirierenden Diskussionen!

An nächster Stelle bedanke ich mich bei Frau PD. Dr. Ulrike Steiner für die Übernahme des Postens als Zweitgutachterin für meine Dissertation und bereits für die frühe Förderung während meines Masterstudiums. Auch Herrn Prof. Dr. Michael Schloter danke ich herzlich für die Übernahme des Postens als weiteren Gutachters, Herrn Prof. Dr. Frank Hochholdinger für die Übernahme des Postens als fachnahes Mitglied meiner Prüfungskommission, sowie Herrn Prof. Dr. Wulf Amelung für die Übernahme des Prüfungsvorsitzes.

Ein ganz besonderer Dank geht an die gesamte Arbeitsgruppe, mit der man sowohl sehr gut zusammenarbeiten konnte, aber auch einfach mal beim Mittagessen rumalbern konnte! Heraushebend möchte ich mich an der Stelle bei Dr. Wiebke Sickel, Marion Deichmann, Janina Zierul und Sina Schultes bedanken. Hervorheben möchte ich ebenfalls das Mentoring und die außerordentliche Unterstützung durch Dr. A. Michael Klüken und Dr. Jochen Kleemann, die beide sehr prägend für meine wissenschaftliche Laufbahn sind.

Aber auch allen anderen die mich bei dieser Arbeit tatkräftig unterstützt haben möchte ich natürlich danken. Dazu gehören die Bobos, sowie die MitarbeiterInnen der Dienstleistungsplattform für Pflanzenversuche und des Campus Klein-Altendorf. Nicht zuletzt möchte ich meiner Familie und Freunden danken, die mir stets in jeder Lebenslage eine große Unterstützung sind.